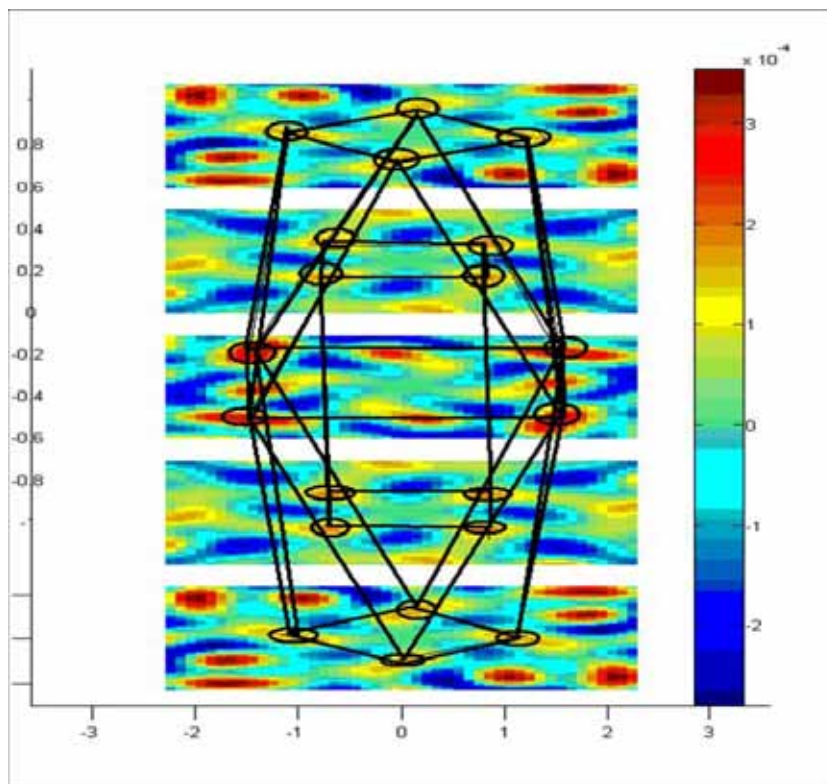BUDAPEST NEUTRON CENTRE

PROGRESS REPORT

ON THE
ACTIVITIES
AT THE

BUDAPEST RESEARCH REACTOR
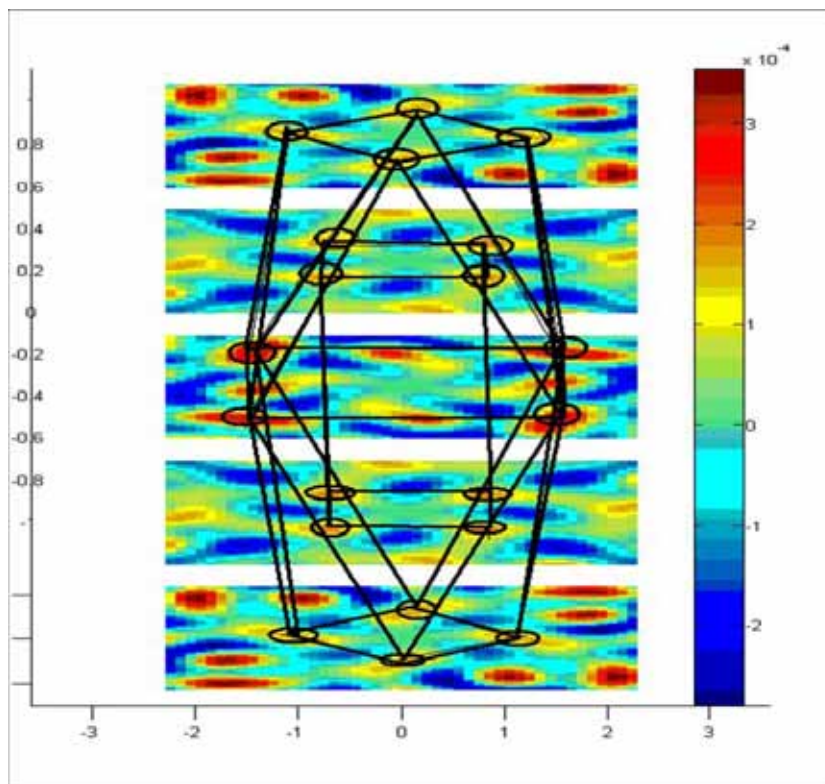

2006 - 2007

March 2009

PROGRESS REPORT

ON THE
ACTIVITIES
AT THE

BUDAPEST RESEARCH REACTOR

2006 – 2007

March 2009

Budapest Neutron Centre
Progress report 2006-2007
Edited by M. Makai, L. Rosta
Budapest, January 2005-01-21

Postal address and contact persons:

KFKI Atomic Energy Research Institute
1525 Budapest 114, POB 49, Hungary
Dr. Mihály MAKAI
Phone: 36-1-392-2296
Fax: 36-1-395-9293
e-mail: makai@aeki.kfki.hu

Institute of Isotope and Surface Chemistry
1525 Budapest 114, POB 49, Hungary
Dr. Tamás BELGYA
Phone: 36-1-392-2539
Fax: 36-1-392-2584
e-mail: belgya@iki.kfki.hu

KFKI Solide State Physics Research Institute
1525 Budapest 114, BOB 49, Hungary
Dr. László ROSTA
Phone: 36-1-392-2296
Fax: 36-1-395-9293
e-mail:rosta@szfki.hu

Location:

Budapest Research Reactor
1121 Budapest, Konkoly Thege út 29-33
KFKI, Bld, 10.

Cover page figure:
 Holographic measurement on ammonium-chloride (NH_4Cl) single crystal at the 8th channel of BRR The first application of the angular integrated elastic scattering, as a novel tool for structural studies. Reconstructed hologram of the NH4Cl single crystal

CONTENTS

PREFACE

In 2006-07 the Budapest Research Reactor was operated according to the planned normal regime, resuming 15 ten-day cycles i.e. total 3500 hours of functioning each year. The BNC facilities – a suit of reactor irradiation equipment, thermal neutron beam instruments and cold neutron spectrometers in the neutron guide hall – are open for the international user community. Research proposals can be submitted twice a year, an international selection panel takes care of the review of the proposals. This panel meets ones a year, the proposals are, however, evaluated after the submission by the panel members and even "fast-track" processing of proposals is possible thanks to the electronic communication. BNC was involved in the EU FP6 Neutron and Muon Integrated Infrastructure Initiative (NMI3) access programme providing the possibility for many experiments, which have been performed by EU partner users. Thus BNC services are available for researchers both from member states and associated states of the European Community. A table showing the experimental stations is given in the Appendix. The call for proposals including the conditions how one can make use of the EC travel support is regularly advertised in the journal Neutron News and on the web (www.bnc.hu). The web site of BNC offers also the possibility of reading reports on BNC activities, e.g. the present Progress Report.

Some highlights from the neutron beam experimental results can be cited here referring to the resume of the closing meeting of the NMI3 project in June 2008. In four sections independent European experts were asked to select the most interesting experiments out of the nearly 1000 measurements performed at the 9 neutron centres within the FP6 period (presentations are available on the www.neutron-eu.net/nmi3 page). A quarter of these highlight experiments were performed at the Budapest Research Reactor, just to mention a few of them: Residual stress determination in a gas turbine wheel (Italian group), PGAA analysis of archeological bronze fragments for the Marche region (Italy), Chemical analysis of high-pressure metamorphic rocks of geological relevance (Hungarian group), Nanoglobule stability in C-S-H gel in Portland cement (Czech group), Network structure of borosilicate glasses for uranium storage (Hungarian-Rumanian collaboration), Crystal and magnetic structure of bismuth manganites (Bulgarian group), Structure and swelling behavior of hydrophilic epoxy networks investigated by SANS (Czech group). This few examples also show that BNC plays a role of a regional hub for neutron beam experiments, and also tells about the growing interest and competence in applied materials science in the Central European countries.

The instrument development programme was progressed, mostly thanks to a domestic project (named Large International Projects, with Hungarian acronym NAP) financed by the Hungarian Innovation Fund (through the National Office of Research and Technology). A consortium of four institutes of the Hungarian Academy of Sciences (3 of them BNC members) was selected for support. Within this NAP project the installation of a new reflectometer was started (now is being commissioned) and the upgrade of the PGAA stations has been performed together with a substantial improvement of the guide system. Considerable progress has been made also for the improvement of sample conditioning; the measurement infrastructure was also improved, a sample preparation laboratory and new user offices were equipped.

In the first part of this volume a selection of topics and highlights on the research avtivity is presented. This booklet gives also the description of our experimental stations. BNC organised several workshops, schools and meetings, a summary report is also included in this issue. A list of publications concerning this two years activity is also attached.

Budapest, June 2009

János Gadó
Chairman of the BNC Board of Directors

1. BUDAPEST RESEARCH REACTOR

Sándor Tőzsér

The Budapest Research Reactor (BRR) is a tank-type reactor, moderated and cooled by light water. The reactor, which went critical in 1959, is of Soviet origin. The initial thermal power was 2 MW. The first upgrade took place in 1967 when the power was increased from 2 MW to 5 MW, using a new type of fuel and a beryllium reflector. A full-scale reactor reconstruction and upgrade project began in 1986, following 27 years of operation since initial criticality. The upgraded 10 MW reactor received the operation license in November 1993. In line with Hungarian safety regulations a periodic safety review (PSR) was conducted in 2002-2003, as a result of which the operation license was renewed in November 2003, that is now valid until further notice.

The BRR site, the Reactor Hall and the Control Room are presented in the photos can bee seen below.

1: Reactor Building with the Control Room being on the 2nd floor | 2: Reactor Hall | 3: Engine Room with air filters of the Air Ventilation System |
4: Secondary Pump Room | 5: Cooling Towers | 6: Auxiliary Building accommodating the Diesel Generators and Compressed Air System | 7:
Building of the Liquid Waste Storage Facilities (under the foreground area two storage tanks are accommodated | 8: AFR-pool Service Hall (with
solid waste storage wells in the foreground area) | 9: CNS's Measuring Hall | 10: TOF's Measuring Hall

Bird's eye view of the BRR site

Panorama view of Reactor Hall   *Control Room*

Main technical data

Reactor type:................................... Light-water cooled and moderated tank-type reactor with beryllium reflector

Fuel: .... VVR-SM(-M2) with 36 % ^{235}U initial enrichment

Core geometry: .... Hexagonal (height: 600 mm; □ 1000 mm)

Equilibrium core:............................... 227 fuel assemblies (in single equivalent)

Control: .... • 3 safety rods (B4C); • 14 shim rods (B4C); • 1 automatic (fine) rod (SS)

Nominal thermal power: .... 10 MW

Mean power density in the core: .... 61.2 kW/litre

Neutron flux density in the core:..... − $2.5 * 10^{14}$ n/cm^{2}s (thermal in the flux trap)

− $1 * 10^{14}$ n/cm^{2}s (approx. max. fast flux in the fast channel)

Spent Nuclear Fuel Shipment

The year of 2008 was a dominant period in the life of the BRR. Under the Russian Research Reactor Fuel Return (RRRFR) Program of the U.S. DOE National Nuclear Security Administration's Global Threat Reduction Initiative, spent nuclear fuel (SNF) containing high enriched uranium (HEU) is repatriated to the Russian Federation from various research reactors in Eastern Europe and Asia. As part of this program, a project was developed to support the repatriation of SNF from the BRR facility to the Russian Federation. In the frame of this program the BRR site was modified to make the AFR-pool facility possible to accommodate and serve the shipping casks.

The first part of the shipment, which contained all the fuel that had been irradiated before September 2005, was carried out successfully in 2008. Under a continuous surveillance of IAEA and EURATOM safeguards inspectors, the loading works of 16 VPVR/M Skoda transport casks were carried out within a two-month period in 2008's summer, then the shipment convoy consisting of 8 trucks left BRR's site at midnight of 15th of September 2008 for its 6 week journey, arriving on 22 of October at the shipment's final destination (the Mayak facility in Chelyabinsk, Russian Federation).

The inventory summary contained he 1st shipment can be seen in the Table below.

Table 1.Inventory summary of the 1ˢᵗ NSF sipment

Summary	LEU	HEU	Total
Number of Fuel Assemblies	82	716	798
S/D-mass U	102.27 kg	130.26 kg	232.50 kg
S/D-mass Pu	0.25 kg	1.29 kg	1.54 kg
S/D-mass ^{235}U	7.86 kg	26.50 kg	34.37 kg
Heat	28.28 W	657.91 W	708.19 W
Activity	2.66 10^{14} Bq	6.39 10^{15} Bq	6.66 10^{15} Bq
Total mass	**288.44 kg**	**1407.19 kg**	**1695.63 kg**

Core conversion from HEU to LEU

As a consequential commitment of the RRRFR program, the BRR has to change the fuel from HEU to low enriched uranium (LEU). These 'core conversion preparation activities' have been running since 2007 and according to the schedule the reactor is to start operation with LEU in the second half of 2009. The core conversion will be completed through four or five mixed cores containing HEU and LEU fuel and will be finished in the middle of 2012.

Operation in 2008

Due to this repatriation project and some prudence approach concerned the existing HEU fuel in stock the BRR has been operating in a decreased operation scenario since the second part of 2008. The operation time record (scheduled and performed) and the operation cycles performed in 2008 are shown below.

Operation time record   *Operation cycles in 2008*

Utilization

Since its initial criticality, the BRR has been utilized as a neutron source for research and various industrial and health care applications. Irradiations are performed in vertical channels (the reactor has now more than 40 channels, that can be used for isotope production and material testing) whereas physical experiments are carried out at the horizontal neutron beam ports. The reactor has ten beam ports (eight radial and two tangential) and nearly all of them are constantly in use. There are a total of thirteen so called 'larger scale experimental facilities' installed at the BRR's beam ports. The utilization matters are coordinated and managed by the Budapest Neutron Centre, which is a consortium founded by four academic institutions in 1993. Under the guidance of the BNC the 13 measuring sites opened a possibility of operating the BRR as a regional centre. In promoting that activity, the European Framework Programs helped substantially. In 2008 within the scope of the European Union FP-6 research program, the NMI3 international co-operation made possible for hundreds of users to carry out their research plans partly or entirely at the BRR.

Accommodation to the changing word – East European Research Reactor Initiative (EERRI)

While the reactor has been fulfilling its traditional mission duties since its first criticality, the operating environment – especially financial, safety, and security requirements – as well as user and public demands, have significantly changed in recent years. Thus, perceiving these changing demands a research reactor coalition was launched under the name of EERRI by the initiation of BRR. The exploratory meeting was held in Budapest, Hungary on January 28-29, 2008 at the invitation of the KFKI Atomic Energy Research Institute (AEKI). This coalition original was founded by 5 reactors but by the end of 2008 it has 8 research and education/training reactors with two observers institutions (see table below).

Strategic goals of the coalition is: to offer improved services for the user communities which will prepare themselves for the time of using leading-edge European facilities based on the synergy effect of the existing facilities participating in the coalition. Areas of Cooperation and Collaboration are: (1) education and training; (2) neutron beam application, (3) isotope production, and finally (4) irradiation of fuel and materials/PIE.

Summarizing the first year activities of the EERRI coalition, a formalized and regular dialogue among the RR operators can be mentioned as the most important achievement. Beyond the sharing of information, a kind of joint thinking and planning has been started since the first meeting. It is expected that this process will strengthen and mature.

List of EERRI's members

Country	Organization	Reactor	Satus	Specific EERRI duties
Austria	TU Vienna	TRIGA 250 kW	EERRI member	Coordinator on training activities
Czech Republic	NRI Rez	LWR-15 10 MW	EERRI member	Coordinator fuel and material irradiation and PIE
Czech Republic	CTU Prague	VR-1 (1 kW)	EERRI member	–
Hungary	AEKI	BRR 10 MW	EERRI member	General coordination of EERRI matters Coordinator on neutron scattering and beam application
Hungary	TU Budapest	100 kW	EERRI member	–
Poland	IAE Swierk	MARIA 30 MW	EERRI member	Coordinator on isotope production
Romania	ICN Pitesti	TRIGA 14 MW	EERRI member	–
Slovenia	JSI Ljubjana	TRIGA 250 kW	EERRI member	–
Austria	IAEA	–	Observer	Organizational issues
Serbia	Vinca Institute	–	Observer	

2. RESULTS OF RESEARCH ACTIVITIES

(Highlights)

2.1 THE ROLES OF SUBSURFACE CARBON AND HYDROGEN IN PALLADIUM-CATALYZED ALKYNE HYDROGENATION

D. Teschner[1], J. Borsodi[1,2], A. Wootsch[2], Zs. Révay[2], M. Hävecker[1], A. Knop-Gericke[1], S. D.Jackson[3], R. Schlögl[1]

[1]Fritz-Haber-Institut der Max-Planck-Gesellschaft, Faradayweg 4-6, D-14195 Berlin, Germany.
[2]MTA Izotópkutató Intézet, Pf. 77, 1525 Budapest.
[3]WestCHEM, Department of Chemistry, University of Glasgow, Glasgow G128QQ, Scotland, UK.

The investigation of the surface and the composition of catalysts during a reaction has been an important issue for chemists for many years. In a recent paper published in Science, methods are presented which are suitable to examine in situ the properties of palladium catalysts during the hydrogenation of hydrocarbon compounds having triple bonds, i.e. during the catalytic reaction.

High-pressure in situ X-ray Photoelectron Spectroscopy (XPS) was developed at the Fritz Haber Institute in Berlin, enabling measurements in the presence of gas mixtures with pressure of 1–10 mbar instead of ultra-high vacuum. The method is used to determine the chemical composition and the oxidation states of the components at the surface and near-surface layers of the catalysts during the reactions.

One of the world-leading Prompt Gamma Activation Analysis (PGAA) facilities can be found at the Budapest Neutron Center, and is operated by the Institute of Isotopes. The analytical procedure developed by Hungarian scientists makes it possible to get analytical information from the whole depth of thick samples, such as chemical reactors, thanks to the deep penetration of the irradiating neutrons and the emitted gamma radiation. The prompt gamma radiation produced in neutron capture is characteristic, i.e. its energy identifies the chemical element, and its intensity is proportional to the amount of the element. Contrary to traditional neutron activation analysis, in principle each isotope of every element can be investigated using PGAA. For some elements, extremely high sensitivities can be achieved with the spectrometer at Budapest. In this experiment, for instance, the irradiated part of the reactor tube was about half a gram, while the hydrogen in the palladium catalyst was only 50 micrograms. The chemical reaction was followed by a gas chromatograph and a mass spectrometer.

With the help of the two in situ methods it was possible to find correlations between the activities of the catalysts, the selectivity of the catalytic reaction, and their near-surface and bulk compositions. According to the XPS results, during the selective partial hydrogenation of alkynes to alkenes (compounds with carbon-carbon triple bonds to those with double bonds), the adsorbed alkyne molecules are fragmented, forming atomic carbon in the near-surface layers of the metal. This inhibits the bulk hydrogen in the metal to take part in the surface reactions. In this case the H to Pd bulk molar ratio is low: 0.1–0.3. During total hydrogenation the amount of carbon found in the palladium lattice is negligible, and the catalyst has the form of palladium hydride, i.e. the molar ratio is close to unity.

According to the PGAA measurements the H to Pd ratio is surprisingly high, 0.72, when the selective partial hydrogenation is performed just after total hydrogenation. This can be explained with the formation of the subsurface Pd-C layer, which separates the bulk and the surface reactions. Though the bulk palladium hydride is present, its total-hydrogenating effect does not occur. Thus the hydrogen content of the catalyst depends not only on the composition of the gas mixture, but also on the recent history of the catalyst.

Another interesting effect was found during the experiments: the spontaneous adiabatic selectivity fluctuation

between the single and double bond products, which is accompanied by fluctuation of the temperature. This can be explained with the repeated build-up and disappearance of the Pd-C layer separating the bulk palladium hydride from the surface processes. During the formation of this layer the reaction changes from the very exothermic total hydrogenation to selective partial hydrogenation. In the case of an adiabatic reaction, this results in a decrease of the temperature. This reduces the fragmentation of the adsorbed alkyne molecules and the diffusion rate of carbon, which helps the diffusion of hydrogen into the metal lattice. Thus the separation of the bulk phase spontaneously disappears, which turns the reaction into total hydrogenation again, causing an increase in temperature, and the cycle starts again.

In summary the investigations have shown that the surface and the bulk processes affect the selectivity of the palladium catalysts together in the selective alkyne hydrogenation. The near-surface and the bulk parts are separated by a palladium-carbon layer, whose spontaneous appearance and disappearance can cause a fluctuation in the selectivity of the catalytic reaction.

2.2 LOCA SIMULATION IN SCWR MODEL BY DYNAMIC NEUTRON RADIOGRAPHY

Márton Balaskó, László Horváth, Ákos Horváth, Péter Tóth

Instruments

Below we present a novel application of the dynamic neutron radiography technique, the investigation of supercritical water. We studied the loss of coolant accident (LOCA) in a supercritical water cooled reactor (SCWR). The investigation was carried out on the Dynamic Radiography Station of the Budapest Research Reactor. Neutron radiation having passed through the object under investigation is converted into light, by a scintillator screen. The light is detected by a low light level television camera. Radiography images are displayed on a monitor, stored by S-VHS and DVD recorders and for further analysis, a QUANTEL image processor system is used, data are processed by a Sapphire 5.05 software. For the quantitative repetition of the events, an extraordinary measuring frame was designed and built in house. Its functional model is shown in Fig. 1. The well equipped measuring frame is available for the wide range investigation of the supercritical water phenomena including the loss-of-coolant type accident also. It has a water cooled double Peltier block
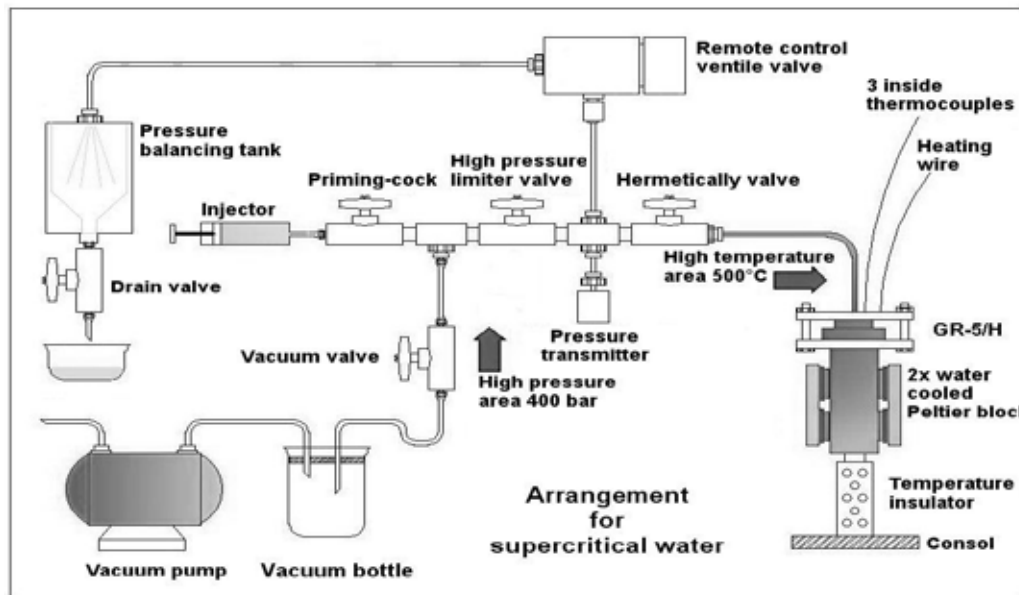

Figure 1. Functional model of the measuring frame

to freeze the water during the evacuation of the sample holder above the water level. After the evacuation the hermetical valve is closed and the water injected in the high pressure area. This area contains a pressure transmitter for measuring the pressure when the temperature have been increased above 200 °C and the hermetically valve has opened. Naturally the Peltier block is moved away before the heating procedure is started. Another important element is situated in the high pressure area this is a remote control ventilating valve which is able to stabilize the pressure independently from the temperature. This valve is designed for modelling the conditions of a loss-of-coolant type accident. The measuring frame is able to collect the escaped vapor after the condensation in the pressure balancing tank.

The supercritical-water-cooled reactor is planned to work at high temperature and high pressure above the thermodynamic critical point of water (T_c ~ 374 °C, P_c ~ 221 bar, ρ_c ~ 0,32 g/cm^3). For the quantitative repetition of the events an completely new measuring frame was designed and built in house. The dynamic neutron radiography is available to study the behavior of the water from the room temperature to the supercritical state at high temperature and at high pressure. A special sample holder (GR-5H8t) has been

developed. It has 8 inside -, 2 outside termo-couples to measure the temperature and an impulse tube to measure the pressure. The inside termo-couples are supported by six spacer discs.

Developments and applications

The rigorous requirements (high temperature > 400 °C, high pressure > 22 MPa) of the super critical water demands special sample holders. The main view points of the design work has been to apply solid and corrosion resistant materials. We have made stress analysis of our sample family for the safety of the measurements. The goal of this investigation was to calculate the three axial equivalent stresses, in accordance with the energetic theory of strength (Huber-Mises-Hencky theory, thick wall pipe).

The sample holder was made of GR5 type titanium alloy. The application of the titanium alloy gave double advantages. The first was a thinner wall thickness which resulted in a better quality of radiography picture because of the higher strength allowed. The second was that the total macroscopic cross section of the titanium is only almost the half of that of the steel or rust-proof materials. This also improved the quality of neutron radiography picture. The sample holder applied a flange style fixing of the plug system with 8 x M8 screws. It has 7 mm wall thickness and it contains of a hole with 20 mm diameter. The GR-5H sample holder was equipped by a full-length thermo-coax heating wire. The inside temperature distribution was measured by eight (T1,...T8) "K" type thermo-coax thermocouples of the GR-5H8t plug from the upper part to down its arrangement is shown in Fig. 2. These thermo-couples were supported by six pieces spacer discs. Their diameters were 18 mm with a 10 mm whole in the middle. They are made of rust-proof material. The outside temperature of the GR-5H were measured by two "J" type thermocouples on up and down (T9 and T10). The sample holder was taken in a cylinder form temperature reflector. It is made from aluminium. Its diameter is 90 mm, its length is 150 mm and its wall thickness is 0,3 mm. The temperature increasing procedure was ˜ 60 minutes from room temperature to 500 °C. Fig. 3. shows the GR-5H sample holder with 13 cm^3 water, at 25 °C. In the further we could used the advantage of the shadding (SH) method for the easier identification of the events. This was composed by QUANTEL video picture processor. The first of all the DNR picture of the empty sample holder was exposed at room temperature and stored in the memory. Later this picture was subtracted from the actual exposed picture. The temperature of the sample holder was increased step by step. The water level increased slowly and hardly changing the density of the water vapor area above the water level until 200 °C. Above this temperature the water level continued its increasing and the density of the water vapor area began to go on increasing. Above 330 °C the water level began to reduce, and the density of the water vapor area was increased. Above 374°C the water disappeared and the all working area of the sample holder became homogeneous, as it is shown in Fig. 4.
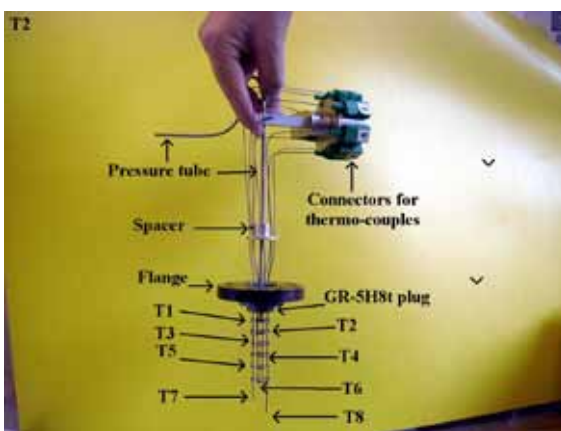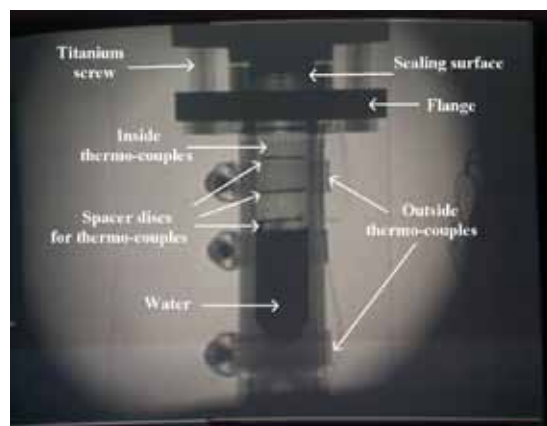

Fig.2. GR-5H8t plug with 8 thermocouples

Fig. 3. GR-5H sample holder at 25 oC

This is the supercritical state of the water. The next step was the preliminary modelling of the loss-of-coolant type accident. The ventilation valve was used five times. In the first case the opening time of the valve was 1 sec. In the second case the opening time of the valve was 5 sec. After these events all ventilation procedures were followed by a dramatic change of the pressure and an oscillation of the temperatures. In the next three cases the opening times were 10 sec. A crucial change was observable after the last ventilation procedure that the pressure stayed on zero as it is visible in Fig.5. because the density of the working area of the sample holder is brighter than in Fig.4. Additionally, the
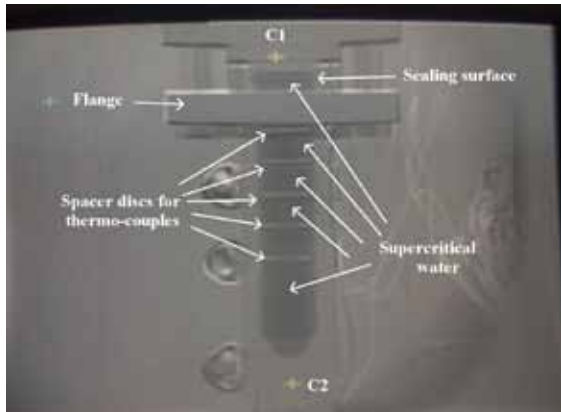

Figure 4. Supercritical state of the water
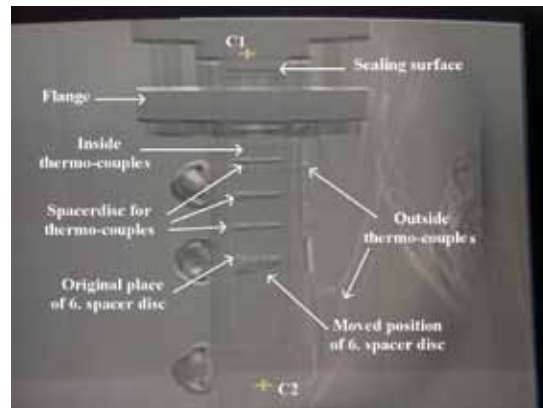in the working area of   the sample holder

Figure 5. Empty sample holder after the
ventilation procedures

lowest spacer disc is moved away by the strong streaming of the water. The horizontal black and white lines were generated by the thermal expansion on the SH pictures.

2.3. CONDENSED MATTER RESEARCH BY NEUTRON SPECTROSCOPY

L. Rosta, L. Almásy, L. Cser, I. Füzesy, J. Füzi, T. Kun, A. Len, M. Markó, A. Meiszterics, F. Mezei, G. Nagy, J. Orbán, E. Rétfalvi, L. Riecsánszky, Zs. Sánta, N. Székely, Gy. Török, T. Veres

Research Institute for Solid State Physics and Optics, Neutron Spectroscopy Department

Nanoscale structural and dynamical features of condensed matter and materials with industrial relevance are in the focus of the scientific activity of our Department. A considerable effort of our team is also devoted to development of neutron scattering techniques and neutron optics research (e.g. detector developments, focusing and polarizing optics). Organization and co-ordination of international relations at BNC level is also in the scope of our activity. The Hungarian membership to ILL in the context of the Central European Neutron Initiative (CENI, co-operation with AU, CZ, HU, SK) is managed also by our Department. Collaboration projects have been running, for example with the Joint Institute for Nuclear Research (Dubna) and the Kurchatov Institute Russian Research Center. The Hungarian Government is committed to host the European Spallation Source (ESS), the future world leading neutron source centre – our team has a major expert contribution to the preparation of this project.

Condensed matter properties

Neutron diffraction and inelastic scattering techniques are applied to investigate short and medium range ordering, nanoscale structure and atomic/molecular interactions in metals, alloys and composites, as well as in soft and liquid materials (solvents, suspensions gels, ferroliquids, micelles etc). A few examples are described below.

Structure of liquid matter – aqueous solutions. The structure and properties of aqueous tetramethylurea (TMU) solutions, as well as the intermolecular interactions in their solutions,
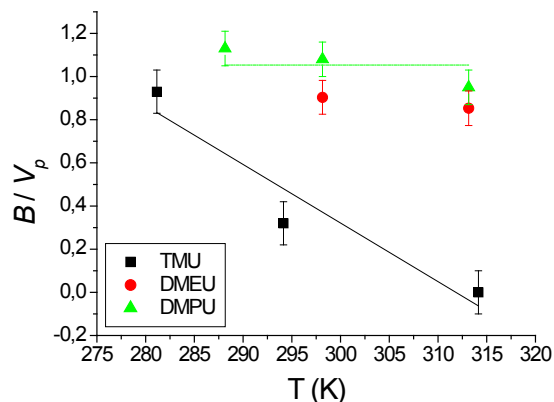

Fig.1. Temperature dependence of the dimensionless second osmotic virial coefficient (B/Vp) for the solutions of TMU, DMEU and DMPU in D_2O.

were widely studied by different experi mental and theoretical techniques. The special interest is attributed to the mainly hydrophobic character of the hydration due to the four methyl groups on the nitrogen atoms. Our previous studies indicated significant hydrophobic interaction between TMU molecules which becomes more attractive at higher temperatures. We extended our study to some TMU derivatives. Small angle neutron scattering (SANS) studies of the solutions of N,N-dimethylelthyleneurea (DMEU) in heavy water

(D$_2$O) and N,N-dimethylpropyleneurea (DMPU) in D$_2$O were carried out as a function of concentration and temperature. The DMEU represents the cyclic analogue of TMU, it contains instead of two methyl groups an ethylene group, and thus has a ring structure. The DMPU is the homologue of DMEU, it has a propylene group in the ring, instead of an ethylene group. Comparing the results obtained for the solutions of DMEU and DMPU with those previously reported for TMU conclusions can be drawn about how the structural differences between these molecules affect the intermolecular interactions.

Following the temperature and concentration dependence of the second osmotic virial coefficient (B/Vp) calculated from SANS results, the character of the interactions between the solute molecules can be estimated. If the values of B/Vp are more and more negative with increasing temperature, the pair interaction between the molecules becomes stronger. The hydrophobic interaction is stronger at higher temperatures. We compared the B/Vp values obtained for DMEU and DMPU solutions with those for TMU (Fig.1). In sharp contrast with the values for TMU solutions, the second osmotic virial coefficients of DMEU and DMPU are constant (within the experimental precision) with increasing temperature. Such behavior may suggest that the attractive DMEU-DMEU, and DMPU-DMPU interactions, in their aqueous solutions, is not of the hydrophobic type.

Structure of soft condensed matter – starch. Over 2/3-s of the global starch industry is directed towards the explotation of starch for non-food applications, the remaining third represents billions of tonnes per year used for obtaining food products. A key issue in the development of modern processed foods is to be able to specify the rate and extent of starch digestion that will be of benefit to human health and fitness. To characterize the physical and chemical properties and structure of starch solutions between different experimental conditions three type of starches have been studied by SANS: potato, wheat and maize starch. The samples were produced by different techniques; different temperature and pressure values were used for obtaining solutions, suspensions and gels. The starch granule structure is modelled as a finite number of lamellae: crystalline regions and amorphous regions, embedded in a background region. By treating the results obtained from SANS measurements the structure of granules could be compared within the three type of starches.The most pronounced change was observed in case of suspensions which were produced at ambient temperature and measured in-situ at different concentrations and temperatures.The wheat starch granules broke, while in the wheat suspension considerable lamellae structured fragments were present. The wheat starch gels showed different lamellae thickness at different temperatures. While the 0.2-2% concentrated wheat and maize samples showed no temperature and concentration dependence, the potato starch solutions structure changes significantly with the concentration.

Structure of biological matter – model membranes. Lipid vesicles in dilute dispersion of model lipid POPC have been studied by small-angle neutron scattering. The dispersions were prepared by extrusion through filters of different pore sizes. The experimental data were treated by a newly developed model, which allowed us to determine the proportions of different kinds of vesicles, unilamellar and multilamellar, of up to four bilayers, and determine their structural and hydration parameters. For the first time, the structural change of the hydration parameters in function of the vesicle radii has been characterized for unilamellar, and for multilamellar vesicles as well.

Neutron optics - 1. A new mathematical method was applied to the neutron holography data obtained on the PbCd alloy. This method allowed the direct observation of the distance between the Cd nucleus and the Pb nuclei occupying the surrounding first four neighboring shell. The inter-atomic distances were determined with picometer accuracy. They show a non-monotonic shift of the atomic positions due to the Cd atom. In order to interpret the data obtained the Friedel oscillation model was involved. The result is shown on the Figure below.

2. The first neutron holographic image was obtained by the use of the dedicated instrument installed at the 8th horizontal channel of the Budapest Research Reactor. For the sample an NH_4Cl single crystal was chosen.

The result is illustrated in the following figures (left is the simulation image, on the right hand side is the image reconstructed from the measurement). It was shown that the internal source approach of neutron holography according to our expectation is feasible even at the medium power reactor. We have found the first two neighbouring shells of H atoms, the first shell contains the first N neighbours, and the second shell contains the first H neighbours.

Applied research with neutrons – irradiation damage of reactor components. Damaged control rods of the WWR-M10 Budapest research reactor were measured by SANS. The measured 3 control rods were: K1 (ZfK VA58), K5 (ZfK VA53), Non-used (ZfK VA77). The characteristics were as follows. Chemical composition: AlMgSi (Mg(0.9), Si(0.7), Cu(0.1), Mn(0.1), Fe(0.4), Zn(0.2), Ti(0.2) % in Al matrix) rod filled with B4C powder. Size: the diameter is 27mm and the total length is 786mm. Preparation: pulling and homogenization on high temperature (550 0C). Gamma activity: on surface (measurement time June of 2005) K5 : 26mSv/h, K1:260mSv/h. We have measured 19 points on the long of the rod. The distance between the measured points is 20mm. We turned the rod with 900 to measure all side of the rod. The rod was covered with thin Al foil to avoid the measuring place from the possible radioactive fall out.

The above figures show the rod on the sample stage of the SANS instrument, SANS spectra recorded alongside the rod and the integrated intensity distribution as a function of the momentum transfer for the different positions of the rod (right). A clear correlation of the irradiation damage (the SANS curves reveal the pore structure evolution in the alloy material) is followed along the rod as a function of the flux distribution in the height of the reactor core.

ESS Hungary project. According to the Hungarian national R&D strategy, ESS is considered as a flagship facility among the investment provisions. The government initiated the process of establishing the case to host ESS in Hungary. The Hungarian bid relates to the project laid down in the EU Roadmap. The ESS is a 5 MW spallation neutron source with initially 22 instruments, 1.3 GeV protons from a linear accelerator impinge on a heavy metal target to produce Long Pulse (ms) neutrons. The highest priority new project of European neutron scattering since the early nineties, ESS will be the world's leading neutron source, providing the highest neutron intensity (in several cases up to two orders of magnitude higher peak flux than current leading facilities) and novel instrumentation as a unique tool for research into structure, characterisation, functions and dynamics of matter. Together with complementary capabilities provided by synchrotron sources, NMR, muons and e.g. electron microscopy this will provide Europe with a full range of the most advanced tools for research into matter. This Long Pulse facility (the concept of this technique was proposed and elaborated by F. Mezei) is well suited to the majority of instrumental requirements and significantly cheaper than the currently used or built short pulse facilities. The neutron science expertise of the ESS Hungary project is provided by our team.

3, DETAILED RESULTS

(Experimental Reports)

Experiment title

SANS study of dilute aqueous solutions of tetramethylurea.

Proposal No.
SANS
Local contact
L.Almasy

Principal proposer
László Almásy
Experimental team
Noémi Székely, Adél Len, László Almásy

Date of Experiment
May-Jun 2006
Date of Report
February 2009

Objectives

Aqueous solutions of tetramethylurea (TMU) have been widely studied in the last two decades by various physico-chemical methods. The specific interest in this system is motivated by the mainly hydrophobic character of hydration of the TMU, caused by the presence of the four methyl groups in the molecule. From a structural point of view, the main question of interest is the way of caging of the large hydrophobic TMU molecules into the water network, and the spatial distribution of the molecules of the two components. In some of the recent studies the TMU has been suggested to aggregate in dilute solutions, while in other studies the hydrogen bond network strengthening of the water surrounding the TMU has been considered to be responsible to the highly non-ideal behavior of TMU – water mixtures. The aim of the present study was to give more information on the structure of dilute solutions.

Results

SANS measurements were performed on solutions of TMU (Aldrich, 99.5% purity) in D_2O (purity 99.4%). Four mixtures were measured in the concentration range 0.0125 - 0.025 mole fractions of TMU. The samples were filled in 2 mm thick quartz cuvettes and thermostated at temperatures 10, 25 and 40°C with an accuracy of 0.5°C.

Mean neutron wavelength of 3.9Å and sample - detector distance 1.3 m were used, covering the scattering vector range q = 0.08 – 0.45Å^{-1}. Average exposition time per sample was four hours, at one temperature. The experimental scattering curves have been corrected for scattering from the empty cell and room background and scaled in absolute units using the incoherent scattering of light water. All curves exhibit increased scattering at forward direction, and for all samples the scattering is stronger at higher temperatures (Fig. 1).

The SANS measurements showed that these mixtures are spatially inhomogeneous in the studied concentration range (TMU mole fraction range 0.0125 – 0.025), pointing to an effective attractive interaction between the TMU molecules. The temperature dependence of this interaction suggests its hydrophobic character.

The scattering curves are adequately described by the Ornstein–Zernike structure factor, which corresponds to a mixture with statistical concentration fluctuations.

From the experimental data, the concentration fluctuations and the Kirkwood–Buff integrals have been calculated, and the association of TMU molecules in dilute aqueous solutions have been quantitatively characterized. For all studied concentrations, the magnitudes of the fluctuations and the Kirkwood–Buff integrals point to the enhancement of water-water and solute-solute interactions.

References

L. Almásy, A. Len, N.K. Székely, J. Plestil: Solute aggregation in dilute aqueous solutions of tetramethylurea. *Fluid Phase Equilibria 257: 114-119, 2007*

Objectives

We studied the effect of cholesterol and beta-sitosterol on structural parameters of bilayers composed of egg yolk phosphatidylcholine (EYPC).

Results

Cholesterol is ubiquitos constituent of mammalian membranes, beta-sitosterol is one of the sterols contained in plant membranes. Dietary beta-sitosterol is benefitial for human healt. We compared the effect of these two sterols on the EYPC bilayer.

Unilamellar liposomes composed of EYPC were prepared in the presence of 0-44.4 mol% of cholesterol or 0-41 mol% of beta sitosterol. SANS experiments were performed using two SDD (1.3 and 5.6 m) at 25 °C.

Bilayer structure was determined from SANS curve using a 3T model described by Kučerka et al. [1]. We have found that lipid bilayers thickness d_{TOT} increased linearly with increasing mol% of sterols. Both sterols influenced the bilayer thickness in the same manner in the range of experimental error

Fig. 1: SANS curve for unilamellar liposomes of EYPC+33.3 mol% of cholesterol together with the best fit.

Fig. 2: Dependence of bilayer thickness d_{TOT} (A), area per unit cell A_{UC} (B) and number of water molecules N_W (C) on the amount of sterols.

. Sterols also increased the surface per unit cell A_{UC} (EYPC+fraction of sterol) at the lipid-water interface and number of water molecules in unit cell in the polar region. We were able to evaluate the partial area of EYPC, cholesterol and beta-sitosterol at the lipid-water interface (0.641±0.010, 0.224±0.015 and 0.275±0.023 nm^2, respectively) according to Edholm and Nagle [2]. We suppose that larger partial area of beta-sitosterol in comparison with cholesterol is caused by bulkier side chain of beta-sitosterol. The partial areas of EYPC and both sterols do not depend on the concentration of sterol in the bilayer. This means that neither cholesterol nor beta-sitosterol have a condensing effect on the lipid-water interface.

References

[1] N.Kucerka, J.F.Nagle, S.E.Feller, P.Balgavy, Models to analyze small-angle neutron scattering from unilamellar lipid vesicles, Physical Review E 69 (2004) 051903

[2] O.Edholm, J.F.Nagle, Areas of molecules in membranes consisting of mixtures, Biophys. J. 89 (2005) 1827-1832

[3] Knaapila, M.; Garamus, V. M.; Almásy, L.; Pang, J. S.; Forster, M.; Gutacker, A.; Scherf, U.; Monkman, A. P.Fractal aggregates of polyfluorene-polyaniline triblock copolymer in solution state, Journal of Physical Chemistry B; 2008 112(51) 16415-16421

Objectives

We have studied nanoscale structure and solvent-induced phase behaviour of linear side chain poly(9,9-dialkylfluorene)s (PFs) as a function of side chain length and solvent quality. We have also studied aggregates of polyfluorene-polyaniline triblock copolymers. Main experimental methods have been small-angle neutron scattering (SANS), small- and wide-angle X-ray scattering (SAXS/WAXS) and optical spectroscopy. These methods have been complemented by NMR.

Results

In poor solvent methylcyclohexane PFs are largely planarized and form sheetlike aggregates that are joined together via crystalline nodes, forming thus a higher level network-type structure (see Fig. 1). The sheet formation depends on the side chain length and is possible if the number of side chain beads (n) is 6-9. Their internal structure reveals an "odd-even" effect so that the sheets are smaller and thicker for n=7,9 and larger and thinner for n=6,8. In better solvent toluene PFs may not be planarized but they still form rather similar architecture for low side chain length (n=6-7).

In diverse liquid media, polyfluorene-polyaniline triblock copolymer forms a dispersion where dispersed particles show a fractal interface. In this interface the polymers are joint together via polyaniline rich domains while polyfluorene block is dissolved down to the molecular level.
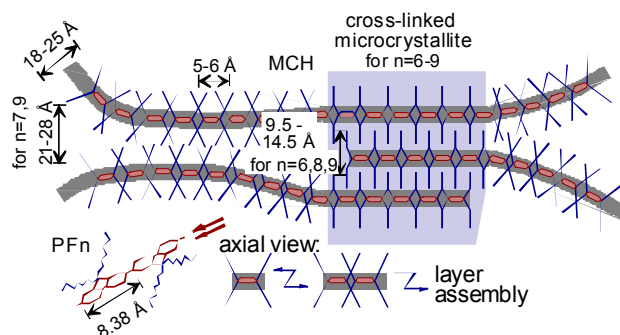

Fig.1.Idealized picture of the structural levels of poly(9,9-dialkylfluorene)s (PF) in methylcyclohexane (MCH) solutions. Here n refers to the number of side chain beads (CH2 units).

Future prospects

We are currently working on more complicated polyfluorene block copolymers and polyfluorene - mixtures with carbon nanomaterials.

References

Knaapila, M.; Dias, F. B.; Garamus; Almásy, L.; Torkkeli, M.; Leppänen, K.; Galbrecht, F.; Preis, E.; Burrows, H. D.; Scherf, U.; Monkman, A. P **Influence of side chain length on the self-assembly of hairy-rod poly(9,9-dialkylfluorene)s in the poor solvent methylcyclohexane**. *Macromolecules;* **2007** 40(26) 9398-9405.

Knaapila, M.; Almásy, L.; Garamus, V. M.; Ramos, M. L.; Justino, L. L. G.; Galbrecht, F.; Preis, E.; Scherf, U.; Burrows, H. D.; Monkman, A. P. **An effect of side chain length on the solution structure of poly(9,9-dialkylfluorene)s in toluene,** *Polymer;* **2008** 49(8) 2033-2038.

B N C Experimental Report	Experiment title **Behaviour of mono-carboxylic acids in a non-polar solvent studied by SANS**	Proposal No. SANS Local contact L.Almasy
Principal proposer V.I.Petrenko, FLNP, Joint Institute for Nuclear Research, Dubna, Russia Experimental team M.V.Avdeev, L.Almasy, L.Rosta		Date of Experiment Jan 2007 Date of Report Apr 2007

Objectives

The behaviour of mono-carboxylic acids in a non-polar solvent was analyzed to conclude about the reasons for different stabilization properties of non-saturated and saturated acids in ferrofluids. Small-angle neutron scattering (SANS) was used to obtain structure parameters of the acids in the solution and their dependence on the concentration [1].

Results

Solutions of oleic (OA), stearic (SA) and myristic (MA) acids in d-benzene over the concentration range of 1-25 vol. % were investigated. The weak scattering from single acid molecules (Fig.1,a,b) was analyzed in terms of the forward scattering intensity and radius of gyration as a function of the surfactant concentration. In the cases of OA and MA solutions the corresponding graphs (Fig.1,c,d) reveal the negative second virial coefficient, which points to the repulsion between the acid molecules. However, the values of the dimensionless analogue of this coefficient $B = -2.2$ (for OA) and $B = -2.0$ (for MA) are larger than $B = -8$ for the case of hard spheres. This fact suggests that in the pair potential for the interaction between the acid molecules the attractive component plays an important role. The behaviour of OA and MA is rather close from the interaction viewpoint, since the corresponding B-values do not differ much. For SA the attractive component is higher than the repulsive one; this results in a positive B and a shift of the transition into the liquid crystalline state (because of molecule anisotropy) towards smaller concentrations. This fact correlates with worse stabilization properties of SA in ferrofluids compared to OA and MA.
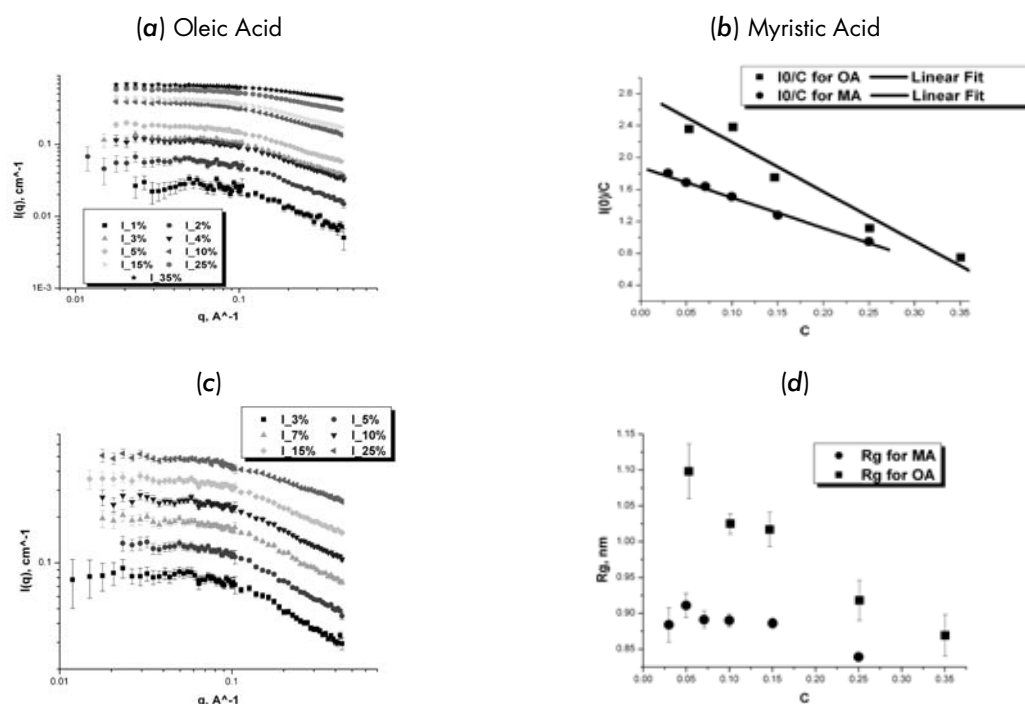
(a) Oleic Acid

(b) Myristic Acid

(c)

(d)

Fig.1. Experimental SANS curves for various volume fractions of the acids (a, b) and obtained forward scattering intensity referred to one acid concentration (c) and radius of gyration (d) vs. acid volume fraction, C. The negative slope of the data in the graphs (c, d) points to the repulsion between molecules.

References

[1] V.I.Petrenko, M.V.Avdeev, L.Almásy, L.A.Bulavin, V.L.Aksenov, L.Rosta, V.M.Garamus, J. Col. Surf. A 337 (2009) 91-95.

B N C Experimental Report	*Experiment title* **Effect of surfactant excess in non-polar ferrofluids by small-angle neutron scattering**	*Proposal No.* SANS *Local contact* L.Almasy
Principal proposer V.I.Petrenko, FLNP, Joint Institute for Nuclear Research, Dubna, Russia *Experimental team* M.V.Avdeev, L.Rosta		*Date of Experiment* June 2006 *Date of Report* Nov 2006

Objectives

The excess of free surfactants in the bulk liquid base of ferrofluids affects strongly the stability of these systems. In the given work we studied the influence of the surfactant excess on the ferrofluid microstructure revealed by means of small-angle neutron scattering (SANS) [1].

Results

The structure of a classical non-polar ferrofluid (1 vol. % of magnetite covered by a single layer of oleic acid in d-benzene) with various excess of free oleic acid (OA) was analyzed. The initial fluid was provided by the Laboratory of Magnetic Fluids, CFATR, Timisoara, Romania. The experimental curves for different volume fractions of free OA in the solution are presented in Fig.1. For OA excess higher than 25 vol. % the ferrofluids demonstrated sharp coagulation. Below this value the influence of the surfactant excess on the stability of ferrofluids was insignificant; neither particle aggregation nor surfactant agglomeration was observed. Nevertheless, the concentration dependences of the forward scattered intensity and radius of gyration for free acid molecules in the system showed a difference in the character of interaction between them as compared to pure benzene solutions (Fig.2). Namely, a significant increase in the attraction is observed, which can be related to the loss of ferrofluid stability at high excess of the acid.

Fig.1. SANS curves for ferrofluids with various excess values of OA. Solid lines correspond to model calculations (independent core-shell particles plus Guinier regime for free OA acids).
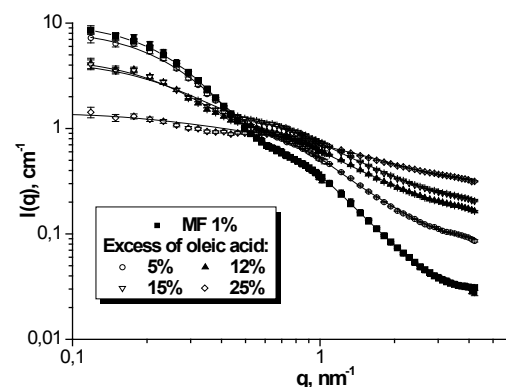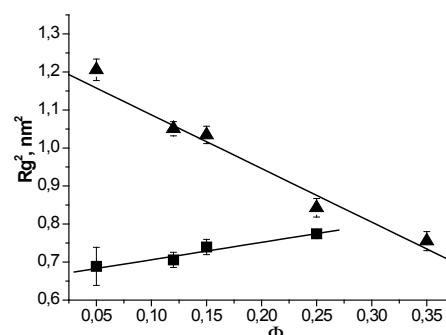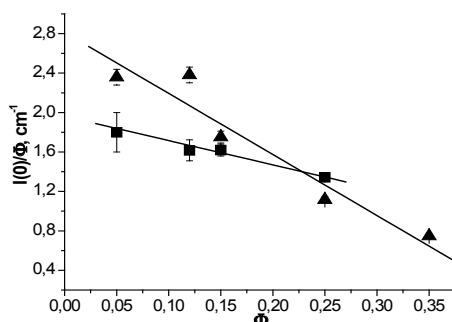
Fig.2. Normalized forward scattered intensity (*a*) and apparent radius of gyration (*b*) vs. OA volume fraction for solutions of OA in d-benzene (triangle) and in ferrofluids (square). Solid lines show linear fits.

References

[1]. V.I.Petrenko, M.V.Avdeev, V.L.Aksenov, L.A.Bulavin, L.Rosta, Solid State Phenomena 152-153 (2009) 198-201.

B N C	Experiment title	Proposal No.
Experimental Report	**SANS study of the elastomers filled with inorganic nanoparticles**	SANS *Local contact* **Noémi Székely**
Principal proposer: **Ivan Krakovský** *Experimental team:* **Ivan Krakovský, Noémi Székely**		*Date(s) of Exper.* 1-4 Dec 2006 *Date of Report* Dec 2006

Objectives *(Aim of the research in some sentences)*

Elastomers filled with inorganic particles of nanometer size represent systems of growing importance in the preparation of advanced materials for nanotechnology. Inorganic nanoparticles can be prepared in situ in elastomeric matrix in a number of ways allowing to control the size and geometrical form of the particles. For technological applications it is very important to have an information about the size, shape and space arrangement of the nanoparticles in the matrix. SANS suits very well to this purpose. In the project proposed, epoxy networks filled with CuO particles in situ will be prepared and studied by SANS. The results will be analysed in combination with data provided by other phys.-chem. methods. More details about the structure and properties of the systems suggested will be obtained.

Results

(Description of concrete results, understandable also for non-experts of the field. Insert, if possible, a typical figure)

A series of hydrophilic epoxy networks was prepared by reaction of on α,ω-diamino terminated POP/POE/POP copolymer Jeffamine ED2003 (number average of molar mass: $\overline{M_n}$ = 2000 g/mol) with diglycidyl ether of Bisphenol A propoxylate (PDGEBA). Hydrophilicity of the networks was controlled by initial stoichiometric ratio of reactive groups (amino and epoxy), r = $2[NH_2]_0/[E]_0$ = 1.00 (EP1), 1.12 (EP2), 1.25 (EP3) and 1.50 (EP4). Nanophase separated structure of these networks has been recently revealed by SANS.

Figure 1. Illustration of the preparation procedure on the network EP1 filled with CuO particles.

The networks were filled with inorganic particles of CuO via precipitation of $CuSO_4$ dissolved in swollen hydrogels by KOH as illustrated in Fig.1.

The dry epoxy networks filled with CuO were subjected to SANS. Neutron scattering properties of Cu differ very much from the remaining elements present in the system, therefore SANS patterns shown in Fig. 2 reflect the space distribution of CuO particles precipitated in the environment of epoxy network. Scattering intensity is very high in small q-region and decays monotonically with increasing magnitude of the scattering vector q. Coherent part of intensity scales approximately as $q^{-3.6}$ which corresponds to the scattering by surface fractals with surface fractal dimension d_s = 6 – 3.6 = 2.4. This parameter does not change with cross linking density. Somewhat higher scattering intensity found for filled network EP4 is due to higher swelling degree and consequently higher amount of precipitated CuO.

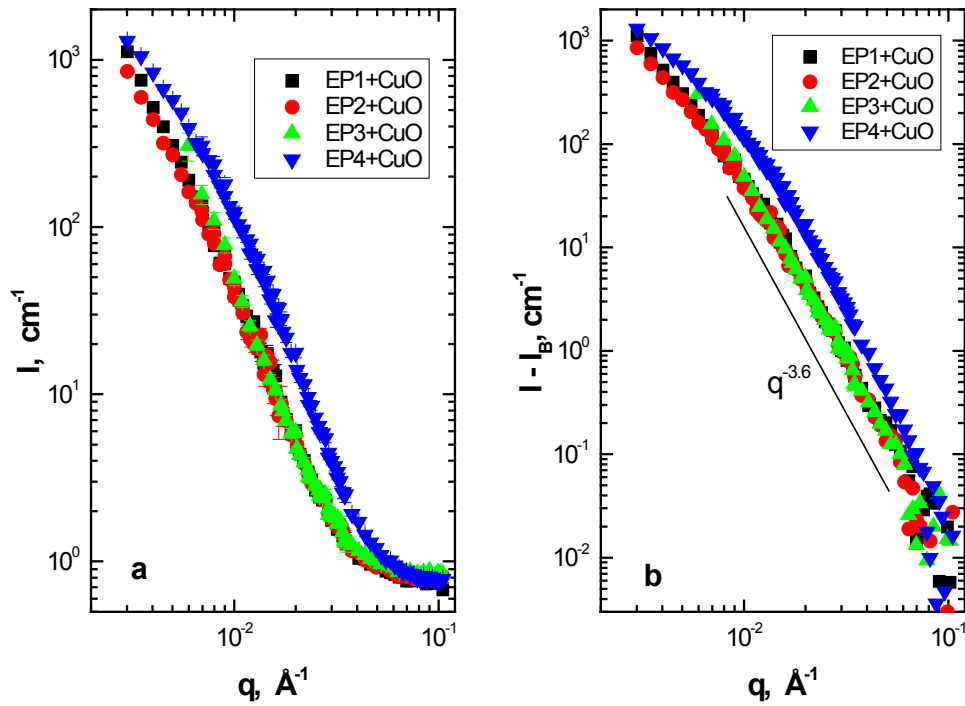*Figure 2. SANS scattering patterns (scattering intensity I vs. magnitude of scattering vector q) obtained from the polymer nanocomposites filled with CuO: a) total scattering, b) coherent scattering.*
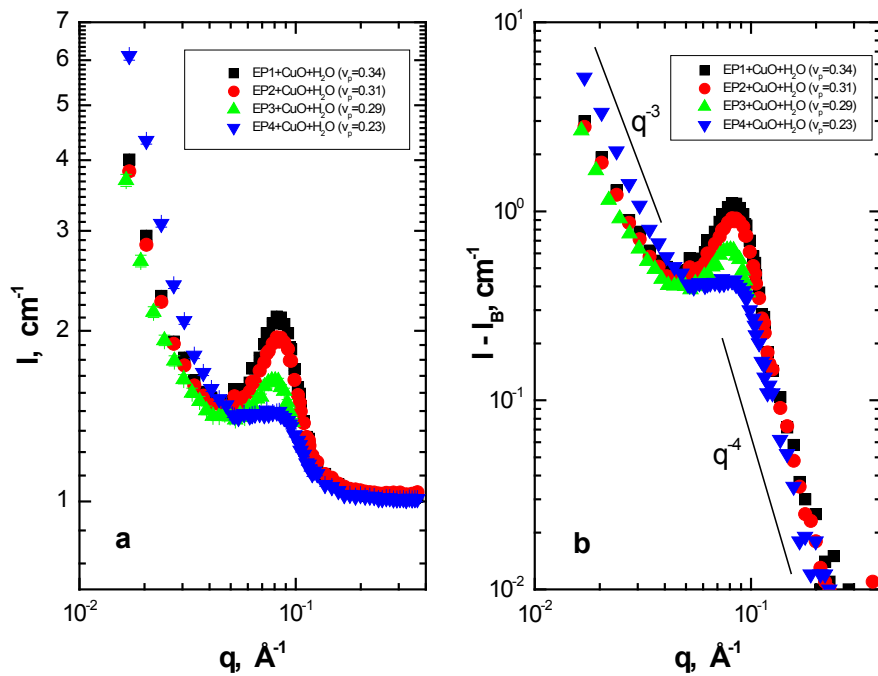

Figure 3. SANS scattering patterns from polymer nanocomposites after swelling with water: a) total scattering, b) coherent scattering. Volume fraction of nanocomposite in swollen state (vp) is also given.

The networks filled were also swollen in H_2O and subjected to SANS to investigate the effect of swelling on the structure of CuO fractal aggregates (see Fig. 3). Swelling causes a some drop of the scattering intensity and formation of distinct scattering maximum at $q_{max} \approx 0.08$ Å^{-1} corresponding to the Bragg distance $D_B = 2\varpi/q_{max} \approx 80$ Å. In high q-region scattering intensity scales as q^{-4} which corresponds to small CuO particles with compact surface formed by breakdown of fractal aggregates due to swelling of the system. The size of the CuO particles can be estimated roughly as $D_B/2 \approx 40$ Å which is in good agreement with an estimate from scanning electron microscopy (see Fig. 4).
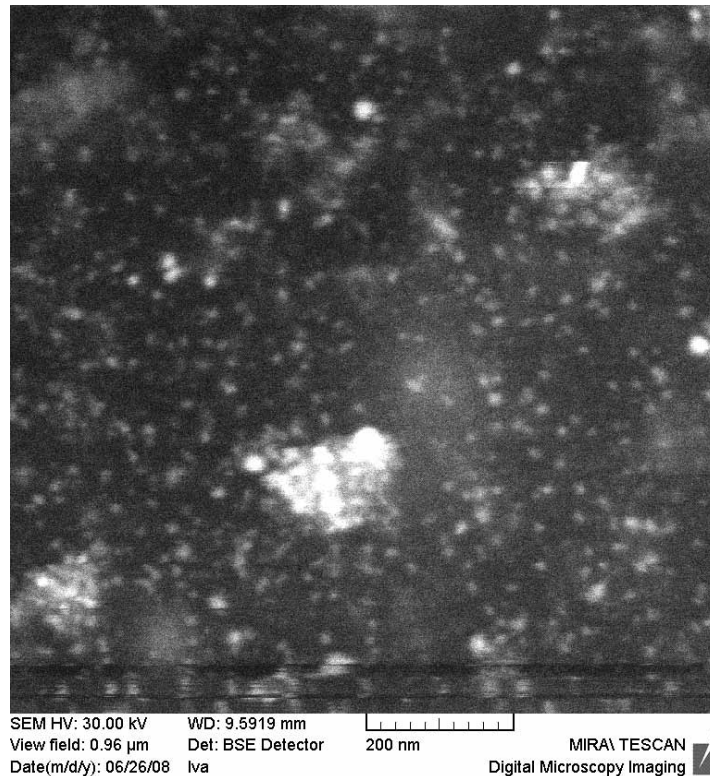
Figure 4 Scanning *electron micrograph of the surface of fracture of EP2 filled with CuO particles.*

References (Published or accepted papers, research reports, conference lectures, seminars etc.)
[1] Krakovský I., Székely N., Pleštil J.: *Structure and properties of nanocomposites filled with inorganic particles*, Proceedings of the 10th Pacific Polymer Conference, Dec. 2007, Kobe, Japan
[2] N. Székely, I. Krakovský: Eur. Polym. J., in print

B N C **Experimental Report**	Experiment title **SANS study of the aggregation of C10E7 non-ionic surfactant in its solutions with heavy water**	Proposal No. SANS Local contact Noémi Székely
Principal proposer: Aldona Rajewska, Institute of Atomic Energy, 05-400 Swierk-Otwock, Poland Experimental team: Aldona Rajewska, Noémi Székely		Date(s) of Exper. 28 April – 4 May, 2007 Date of Report 18.07.2007

## Objectives *(Aim of the research in some sentences)*

The aim of this experiment was to investigate the aggregation of C_iE_j type non-ionic surfactant (heptylethylene glycol monodecyl ether, $C_{10}E_7$, CMC=0.96mM) in D_2O solution using SANS. The notation C_iE_j indicates the number of carbon atoms in the hydrophobic alkyl chain (*i*) and the number of ethylene oxide units (*j*) in the head group. The molecular arrangement is convenient as the hydrophobic nature of the surfactant can be adjusted by changing the ratio of *i* to *j* in the surfactant molecule. This experiment was the continuation of a series of measurements on homologous C_iE_j type surfactant solutions performed at SANS instruments operating in other neutron centres. The influence of the head and tail of the surfactant molecule on its aggregation in aqueous solution has been investigated with special interest to its concentration and temperature dependence.

Results *(Description of concrete results, understandable also for non-experts of the field. Insert, if possible, a typical figure)*

The following $C_{10}E_7$ concentrations 0.17%, 0.5%, 1% were measured at 10°C, 15°C, 20°C, 25°C, 30° and 35°C. The temperature was kept constant with an accuracy of ±0.5°C. The measurements were made in the momentum transfer, **Q**, range 0.02 -0.43 $Å^{-1}$. The samples were placed in 2 mm thick quartz cells.

The $C_{10}E_7$ used in this experiment was purchased from Sigma-Aldrich and used without further purification; the D_2O was from "Prikladnaya Chimia", St. Petersburg, Russia. The micellar solutions were prepared in D_2O in order to increase the contrast between the micelles and the solvent. The scattering curves are shown in Figure 1. a. (c=0.17%), b. (c=0.5%), c. (c= 1%).

From the experimental curves one can see that the intensity of the scattered neutrons is increasing with concentration and temperature. The micelles are assumed to be cylindrical.

a.

b.
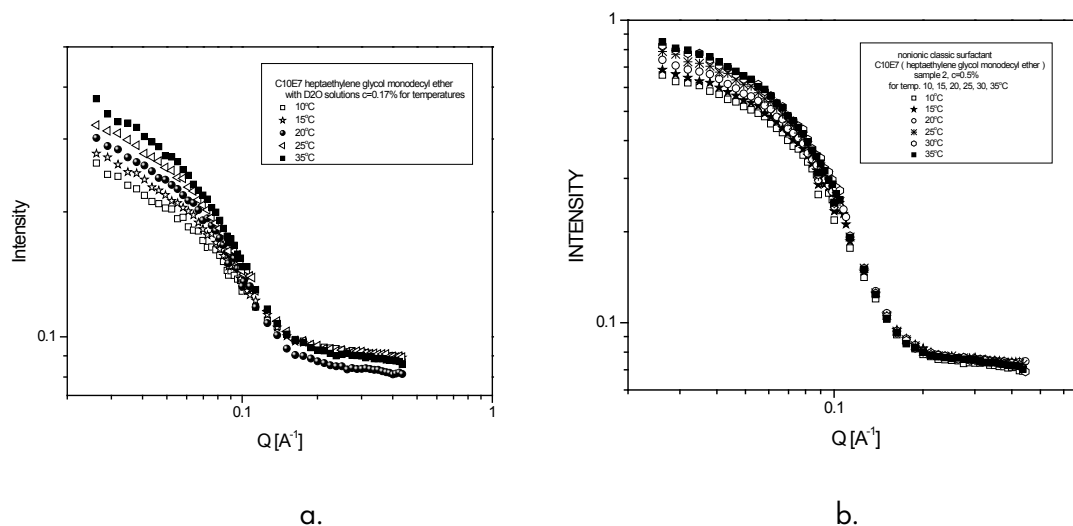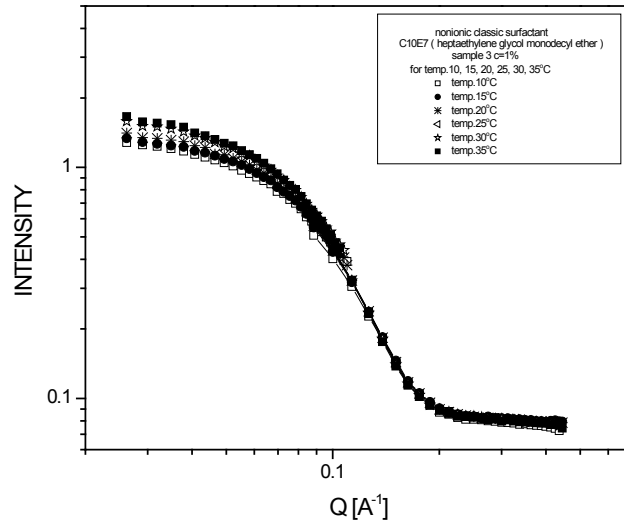
c.

Figure 1. Intensity of scattered neutrons in function of the scattering vector at concentrations: c_1=0.17% (a.) , c_2=0.5% (b.) and c_3=1% (c.). Each concentration was measured at 10°, 15°, 20°, 25°, 30° and 35°C.

Table 1. Radii of gyration for 0.17% $C_{10}E_7$–D_2O solution at three temperatures.

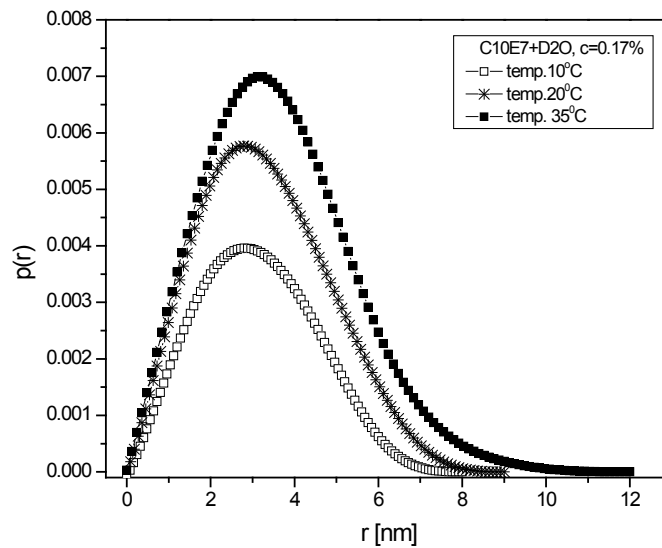| Temperature [°C]	R_g [Å]
10	24.1
20	25.6
35	25.9

Figure 2. The pair distance distribution functions determined by Indirect Fourier Transformation method for the 0.17% $C_{10}E_7$ solution at 10°, 20° and 35°C.

Future prospects *(Summary of the remaining problems to be solved, basis for the continuation of the work)*
Comparison of SANS data obtained on binary aqueous solutions of homologous C_iE_j surfactants.

Objectives

Portland cement is one of the most important and widespread material preferred by the building technology in all industrial countries. Although its binding capability in the form of hydrated solid substance has been well-known for many decades, its hydrated microstructure, among others, has not been fully explained so far. The reason is its great complexity and variability which make the research difficult. Among all hydration products of Portland cement it is the C-S-H solid gel that is especially responsible for binding quality of hydrate cement composites. The gel creates a binding matrix in which all other hydration products and sand or stone aggregates (in case of concrete) are embedded. Therefore, the microstructure of C-S-H gel is the subject of continuous interest also in our days.

It is hypothesized that the C-S-H gel consists of nanometric globules which should represent "basic building blocks" of this substance. The aim of the SANS measurements was to test the existence of the globules and analyse their stability behaviour using the ordinary Portland cement mixed at various water-to-cement (w/c) ratios.

Results

Ordinary Portland cement CEMI 42.5 R-SC of domestic provenance has been used. Three different weight-by-weight water-to-cement w/c ratios have been chosen, namely 0.4, 0.8, and 1.4. Four samples have been prepared for each of those ratios, i.e. twelve samples altogether. The cement powder was mixed with heavy water (D_2O) to facilitate further non-standard hydration conditions which could influence the stability of the C-S-H nanometric globules. In our case we should speak about C-S-D rather than about C-S-H gel but in the further text the commonly used term C-S-H will be used. After mixing the cement paste was placed into a special foil cells which ensured the sample thickness to be 0.12 mm. The cells remain open and were kept at 100% RH for 26 days. The following two days the samples were conditioned at 30% RH and then hermetically closed within their foil cells ensuring the stable 30% RH setting. After this treatment the samples were measured on the SANS diffractometre in Budapest Neutron Centre.

The SANS diffractometre was used in two configurations having identical sample-to-detector distance d=5.6 m but different wavelengths $\lambda_1 = 3.86$ Å and $\lambda_1 = 14.96$ Å. The experiments were performed at normal ambient conditions.
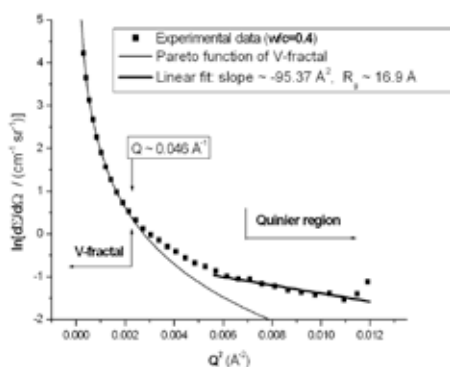
Fig. 1 Quinier plot.
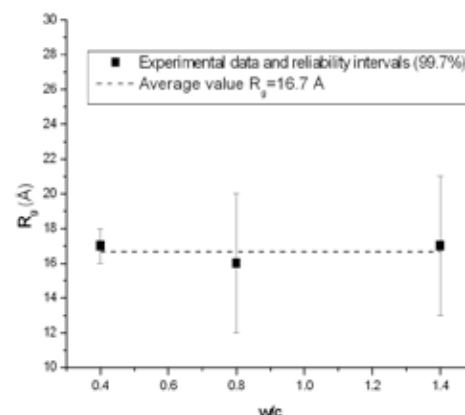
Fig. 2 Size of nanometric globules

In the performed analysis the influence of carbonation of samples have been considered, too. It was found [1 - 3] that the nanostructure of the gel undergoes essential changes when going to higher ratios w/c. In light of this fact one can ask whether also their basic "building blocks" - the nanometric globules - are subjected to similar "stormy" changes of inner structure. If the globules are really basic and inert building elements of the nanometric structure, then one can expect only negligible size changes explainable within the statistical uncertainty. To verify the behaviour of the mentioned nanometric globules, the Guinier regions of all measured scattering curves have been determined as shown in Fig. 1. The linear fits

of the Guinier regions have provided slopes from which the radii of gyration R_g have been estimated. Average values of R_g have been calculated for all the three groups of samples, i.e. w/c=0.4, 0.8, 1.4, and plotted together with their intervals of statistical reliability (99.7%) – Fig. 2. As can be seen, the changes in sizes of the globules are really small and when the overall average value of R_g is calculated (dashed line in figure 2), it does not deviated from the reliability intervals which clearly indicates the common average value $R_g \sim 17 \text{Å}$ might represent an inert size of the basic building elements for all nanometric structures of the samples investigated in the present study. The moderate differences in R_g are due to material differences rather then differences in hydration conditions. The almost constant average value of $R_g \sim 17$ Å found in the presented study of hydrated cement samples, having various w/c ratios, supports the idea that the globules of several nanometres in diameter may be the basic building elements of the nanometric structure of the C-S-H gel.

The following five points summarise the main research results:

(i) For the first time the SANS structural study has been performed with cement pastes mixed with extremely high water-to-cement ratios $w/c \rightarrow 1.4$.

(ii) Structural SANS tests have shown that dimensions of C-S-H fractals (at low RH) increase their values (their structures become more compact) with increase of w/c ratio. Higher compactness of nanometric structure should facilitate higher compressive strength of the gel but, on the contrary, higher w/c ratio guarantees lower strength because of higher capillary porosity. This paradox supports the concept that it is just the capillary porosity and not the gel porosity that governs the mechanical strength of the cement paste.

(iii) Heavy water (D_2O) for an "**ab initio**" mix of cement paste has been used to create non-standard hydration conditions to test the size steadiness of the basic building elements (nanometric globules) of the C-S-H gel.

(iv) For the first time the SANS study of structural stability of the nanometric globules of the C-S-H gel has been accomplished within an extremely wide range of w/c ratios going from 0.4 up to very high value 1.4 which is four times larger than the ratio usually used in practice (w/c ~ 0.35).

(v) In spite of non standard hydration conditions (D_2O mix, carbonation), treatment at low RH (30%), and the w/c ratio varied within an extreme range, the results have indicated high structural stability of the nanometric globules as the basic building blocks of the C-S-H structure. Their typical radius of gyration was close to 17 Å.

(vi)

References

[1] FICKER, T.; LEN, A.; CHMELIK, R.; LOVICAR, L.; MARTIŚEK, D.; NĚMEC, P.; Fracture surfaces of porous materials. *EUROPHYSICS LETTERS.* 2007. 80(6). p. 1600 - 1604. ISSN 0295-5075.

[2] FICKER, T.; LEN, A.; NĚMEC, P.; Notes on hydrated cement fractals investigated by SANS. *JOURNAL OF PHYSICS D: APPLIED PHYSICS.* 2007. 40(10). p. 4055 - 4059. ISSN 0022-3727.

[3] FICKER, T. Nanostructures of cement gel. In *PROCEEDINGS OF INTERNATIONA WORKSHOP, PHYSICAL AND AMATERIAL ENGINEERING 2008.* Prague, ČVUT. 2008. p. 19 - 22. ISBN 978-80-01-04102-4.

[4]

Future prospects

There are a lot of unsolved problems concerning the nanostructure of the C-S-H gel. For example, only little is known about the inner structure of the nanometric gel globules. Another problem is the uncertain size of fractal clusters formed from these nanoglobules. One may only guess whether the fractal structure of these clusters extends up to the micrometric scale or not. The knowledge of that would be valuable for considerations on mechanical strength of this material. All these and other topics should be a subject of a carful analysis and, therefore, further SANS measurements would be desirable.

Objectives

The investigated microturbine (see Fig. 1)is a new MEMS device for the first pioneering study of either gas or airflow sensing using the low pressure-head characteristics of axial flow. The substrate material of the microturbine is a negative photoresist composed of an epoxy resin organic solvent. The substrate containing Gamma-Butyrolactone (GLB) mixed with Triarylsulfonia and Hexafluoroantimonate in the substrate is considered for a Small Angle Neutron Scattering (SANS) investigative feasibility study, paying particular attention to molecular orientations and other micro-characteristics in connection with the mechanical properties of the microturbine. This study wished to confirm the feasibility of the SANS process for GLB on the nanoscale prior to a full materials investigation, which is expected to provide useful information to both improve the characteristics and performance of the microturbine and estimate its lifetime more accurately.
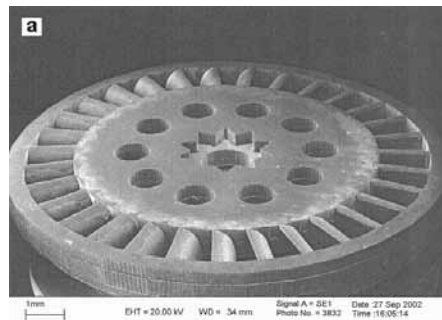
Results

The used sample to detector distance was **5.6 m** which sets the **Q** at values from **0.006 to 0.04** Å^{-1}. The two-dimensional scattering patterns were azimutally averaged, normalized to the incoming neutron flux and corrected for transmission. The 1 mm thick sample was used to correct the detector pixel's efficiency. The samples (a preform and part-finished stator) were assumed to be fabricated under the same conditions, sample 1 was a new sample, sample 2 was used during 1 year.
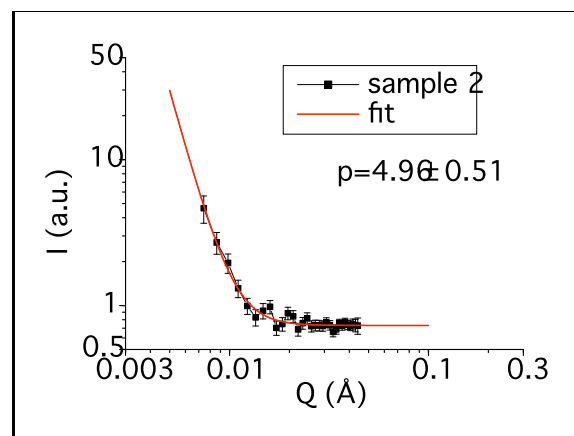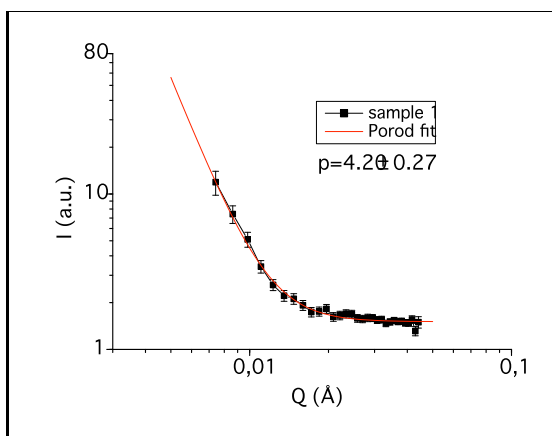
Figures 2 and 3 show the averaged, measured data points and the fitted curves. The used model was the Porod model:

$$F(Q) = \frac{B}{Q^p} + bg$$

, where **B, p** and **bg** were the fitted parameters. The parameter **B** contains the total area of the interface per unit volume of sample and the contrast factor, **bg** is the background and **p** is the Porod exponent. The

B parameter can provide information about the total scattering surface of the sample, for this a better statistic's measurement and an absolute calibration is needed. The parameter *p* has the value of *4.20 ± 0.27* for sample 1 and *4.96±0.51* for sample 2.

The Porod constant of 4.2 and 4.9 has to be treated carefully because the low count rate of the measurements and because the available Q range of the instrument. A lower Q range can be achieved at Yellow Submarine SANS instrument at the same detector position (5.6 m) and a higher wavelength at λ_{max} =23 Å. However this would mean a very low neutron flux at the sample position. A Porod constant between 3 and 4 means sharp interface between phases. Slopes larger than 4 may be obtained in cases where there are no sharp interfaces but rather a gradual transition (like a smooth composition gradient) between the phases.

The points on the graphs (Figs 2 and 3) before the fit line starts to rise are too close to the background to be considered. Thus, it is clear that measurable graphical differences would be seen if the experimental conditions could be adjusted for a better scattering statistics and lower Q values and if the samples used in the above experiment were produced under the proposed conditions of widely varying polymerization and wear. For example a furnace holder could be used to vary the curing temperature during the next round of more definitive tests.

References *(Published or accepted papers, research reports, conference lectures, seminars etc.)*

M.E. Heaton, M. Rogante, A. Len: A Feasibility Study for a SANS Investigation of a Heat Cured and Laser Machined Organic Resin Microturbine as Used for Airflow Sensing, *OPTO 2005 Dublin, International Conference on Materials-Energy-Design MED06*

Future prospects *(Summary of the remaining problems to be solved, basis for the continuation of the work)*

Using smaller values for Q in the Guinier region – equation (1)- would allow to find averaged sizes of the inhomogeneities. Also, although the SU-8 can clearly scatter the neutrons in a measurable way, the height of the error bars could be lessened if two or three microturbines were stacked together to increase thickness and hence scattering.

In order to obtain comparative results using SANS method, one of the rotors would be new while the remaining would be subjected to various durations of rotation (i.e., aged).

In addition to the finished turbines, three crosslinked preform microturbines are also proposed for SANS investigation, the first after excessive UV exposure and the remaining two after differing durations of thermal baking up to 300°C.

In a full SANS analysis particular attention would be paid to the scattering object's orientations (anisotropy in the scattering patterns), presence of globular defects due to the nucleation of the ordered phases or formation of nano-voids and other micro-characteristics connectable with the material's mechanical properties.

The contrast between the matrix and the scattering object can be changed so that the borders (surface) between new and damaged areas become invisible (transparent) for the neutrons and the interior defects (voids and cracks) become visible. Simple comparative measurements and data treatment on new and old-aged material, the media surrounding the defects could be used isolate all the different defects to be find out in the material. This could define their structural strength limits and allow them to be selected for the right mainstream applications, for example airspeed conditions or the power generation requirements for handheld devices.

B N C **Experimental Report**	*Experiment title* Small angle neutron scattering on bronze aged samples	*Proposal No.* SANS *Local contact* Adél Len
Principal proposer: Zsombor Sánta *Experimental team:* Adél Len, Zsombor Sánta		*Date(s) of Exper.* July 2006 *Date of Report* F e b r u a r y 2009

Objectives *(Aim of the research in some sentences)*

A non-destructive neutron analysis method - Small Angle Neutron Scattering (SANS) – was applied for the investigation of archaeological bronze objects. The quantitative element analysis and phase composition analysis as well as microstructure characterization of Copper and Bronze Age axes was carried out in order to gather information on their ancient fabrication (hammering or casting) technology.

Results *(Description of concrete results, understandable also for non-experts of the field. Insert, if possible, a typical figure)*

Measured points

Brass Belt buckle   Bronze Axe b110

Bronze Axe Balaton
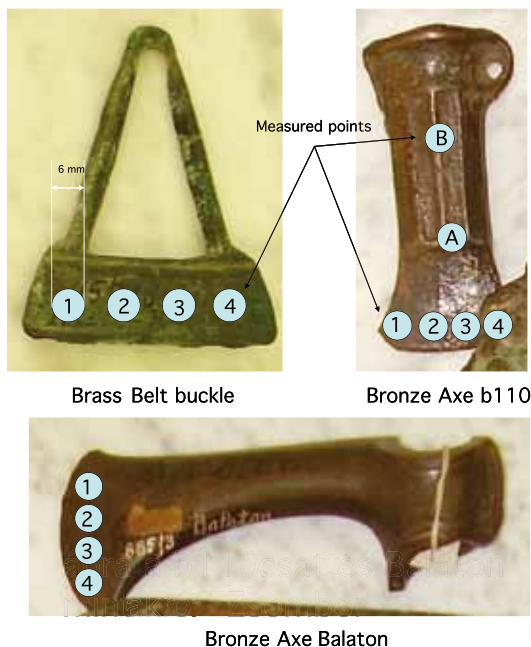
The measured archeological samples produced in the Bronze Age were studied by SANS method.

Dimensions of precipitates were measured at 4 or 6 different points on each sample and no difference was found in the dimension of precipitates compared to the original material. The size of the precipitates varies between **336 Å** and **364 Å**.

The p exponent, that gives information about the surface of the scattering particles (precipitates) was found to be dependent of the bronze and brass samples. The exponent **2.61 ÷ 2.89** found in the case of brass belt buckle represents the volume fractal exponent, and the **3.06 ÷ 3.69** exponent represents the surface fractal size.

SANS Instrument: Yellow Submarine at Buda Neutron Center

Sample – Detector distance: 5.6 m

Wavelength: 11.22 Å

q range: 0.004-0.04 Å-1

The I=f(Q) curves were fitted by the so called Guinier and Porod model. The results are listed in Table 1. The applied models are:

$$I(q) = const\, N (\Delta\rho)^2 V_p^2 e^{-\frac{R_g^2 q^2}{3}} \text{ and } I(q) = const N (\Delta\rho)^2 V_p^2 q^{-P}$$

where: **const** – instrument characteristic constant

     N – number of scattering particles

     $\Delta\rho$ – contrast term

     Vp – particle volume

     Rg – radius pf gyration

     P – Pareto exponent

Sample	p	rg (Å)
Bronz Axe b110 / 1	3,25 ± 0,06	342,70 ± 25,80
Bronz Axe b110 / 2	3,06 ± 0,08	336,23 ± 26,08
Bronz Axe b110 / 3	3,13 ± 0,08	343,80 ± 26,27
Bronz Axe b110 / 4	3,18 ± 0,05	342,40 ± 25,45
Bronz Axe b110 / A	3,54 ± 0,06	350,72 ± 22,29
Bronz Axe b110 / B	3,57 ± 0,06	347,19 ± 22,42
Brass Beltbuckle / 1	2,89 ± 0,10	354,54 ± 24,94
Brass Beltbuckle / 2	2,61 ± 0,04	352,61 ± 25,20
Brass Beltbuckle / 3	2,80 ± 0,05	361,31 ± 24,40
Brass Beltbuckle / 4	2,81 ± 0,05	364,41 ± 24,06
Bronz Axe Balaton / 1	3,69 ± 0,11	363,54 ± 23,50
Bronz Axe Balaton / 2	3,56 ± 0,11	357,79 ± 23,41
Bronz Axe Balaton / 3	3,63 ± 0,11	364,10 ± 23,62
Bronz Axe Balaton / 4	3,64 ± 0,11	357,18 ± 23,72

Brass Belt buckle
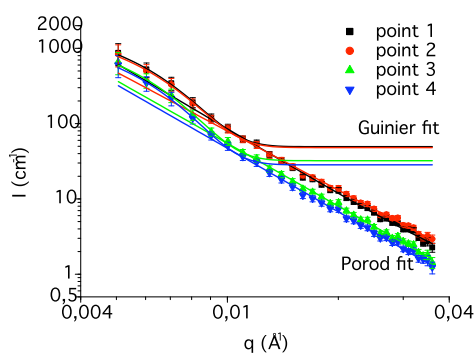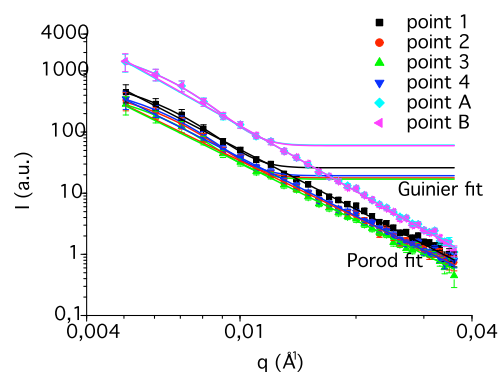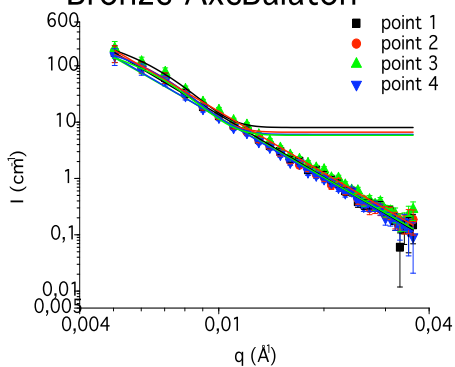
Bronze Axe b110

Bronze AxeBalaton

References *(Published or accepted papers, research reports, conference lectures, seminars etc.)*
[1] Presented at European Powder Diffraction Conference – 19-22 September 2008, Warsowia, Poland

B N C **Experimental Report**	*Experiment title* **SANS analysis of non-polar organic magnetic fluids stabilized by saturated mono-carboxylic acids**	*Proposal No.* SANS *Local contact* L.Adel
Principal proposer L.Vékás, Laboratory of Magnetic Fluids, CFATR, Romanian Academy, Timisoara Division, Romania *Experimental team* M.V.Avdeev, D.Bica, V.L.Aksenov, L.Rosta		*Date of Experiment* Jan 2006 *Date of Report* Mar 2006

Objectives

Colloidal stability of magnetic fluids (MFs), especially at a high volume fraction of magnetic nanoparticles, φ_m, is a complex issue connected with the synthesis procedure, including the nature of surfactant(s) and carrier liquids used. In this experiment we apply small-angle neutron scattering for studying the structure of ferrofluids based on decahydronaphtalene (DHN) and stabilized by various chain length molecules from a series of saturated and straight carboxylic acids, namely lauric (LA), myristic (MA), palmitic (PA) and stearic (SA) acids with C_{12}, C_{14}, C_{16}, C_{18}- tails, respectively, and compare them with the classical fluid stabilized by non-saturated oleic acid (OA) with bent C_{18}- tail.

Results

The studied ferrofluids were prepared in the Laboratory of Magnetic Fluids, CFATR, Timisoara, Romania, by the same procedure [1,2], which is standard for OA stabilization. Magnetite nanoparticles, Fe_3O_4, were obtained by the co-precipitation in aqueous solution of Fe^{2+} and Fe^{3+} ions and dispersed in DHN. Coating with single surfactant layer around magnetite particles provided sterical stabilization and ensured the maximal volume fraction of dispersed magnetite up to 10 %. In SANS experiments, samples were dissolved down to $\varphi_m \sim 1.5$ %.

The main structural difference revealed for the fluids with saturated acids as compared to the OA case concerns the size distribution function of the stabilized magnetite nanoparticles. The SANS curves are given in Fig.1. The scattering from the surfactant layer is almost matched, because the values of the mean scattering length density for the surfactants and carrier are close [3]. Also, the nuclear scattering dominates strongly over the magnetic part, which is a result of the large contrast between magnetite and carrier [3]. So, the curves in Fig.1 correspond to the nuclear scattering from magnetite. They are treated in the frame of the model of homogeneous polydisperse spheres [3]. The resulting radius distribution functions (RDFs) are shown in the inset to Fig.1. All of the saturated acids give close RDFs, which, nevertheless, differ from RDF in the case of OA stabilization. Both the mean radius and polydispersity decrease when replacing OA with saturated acids. Thus, whereas OA is proved to be highly efficient surfactant for stabilizing nanomagnetite over the wide radius interval of 1-10 nm, acids LA, MA, PA, SA stabilize partially this interval dispersing in the carrier only a fraction of smaller particles. The details of the experiment interpretation can be found in [4].
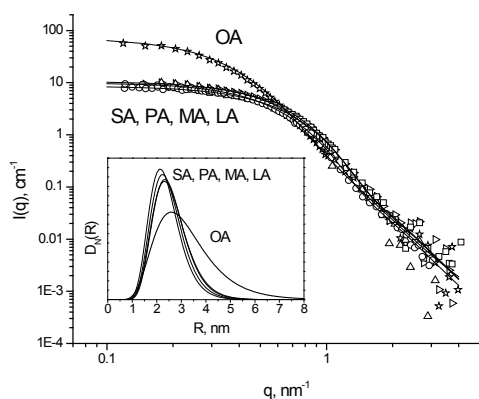
Fig.1. Experimental (points) SANS curves for MFs in DHN normalized to $\varphi_m = 1.5$ %. Lines are the results of approximation by the model of polydisperse independent spheres. The inset shows the corresponding particle size distributions of magnetite.

References

1. D.Bica: Rom. Rep. Phys. Vol. 47 (1995) 265
2. M.V.Avdeev, D.Bica, L.Vékás, et al.: J. Mag. Mag. Mater. 311 (2007) 6
3. M.V.Avdeev, V.L.Aksenov, M.Balasoiu, et al.: J. Coll. Interface Sci. 295 (2006) 100
4. M.V.Avdeev, D.Bica, L.Vékás, et al.: Solid State Phenomena 152-153 (2009) 182

Objectives *(Aim of the research in some sentences)*

The investigation of stresses in reactor control rod material in exceptionally important due to the affect of reactor safety. The measurement residual stresses in a control rod caused by incompatible internal permanent strains because they may increase the rate of damage by fatigue, creep or environmental degradation... They may be generated or modified at every stage in the component life cycle, from original material production to final disposal. Tensile residual stresses may reduce the performance or cause failure of manufactured products.

Results *(Description of concrete results, understandable also for non-experts of the field. Insert, if possible, a typical figure)*

The measurement setup on athos spectrometer
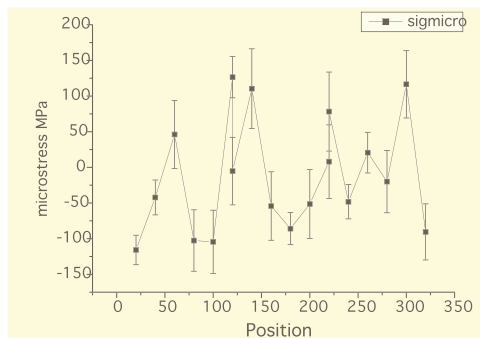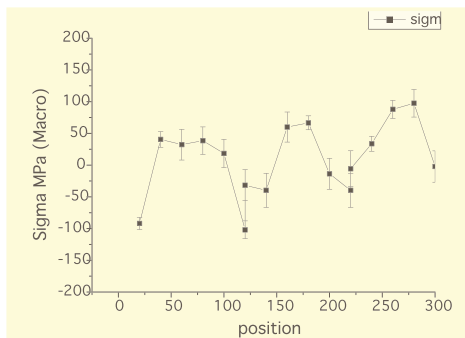
Macrostress component along the rod and microstress II component on the control rod

From the measurement clearly seen that no substantial residual stress in the investigated non radioactive control rod

That is a non destructive prove of quality of fabrication about the internal stress what can be a source of corrosion and damage.

Future prospects *(Summary of the remaining problems to be solved, basis for the continuation of the work)*

Building a proper shielding and automatic sample movement a measurement of radioactive sample is desirable.

Objectives

The aluminium control rods of research reactor of Budapest are in the core at high neutron flux and at temperature of 45oC. The vertical distribution of flux shown cosinus function along the rods, the maximum value is $2.5*1014$ n/cm2s. The investigated control rod was in the reactor for 13 years. The effect of radiation embrittelement has high safety significance for the reactor operation. The high neutron fluence causes forming of nanoscaled inhomogeneities (bubbles, precipitates, dislocation loops, etc). To observe microstructural changes in the radioactive component non-destructively small angle neutron scattering is a very good tool

Results

Measurements were performed on 19 points of the control rods along the vertical axis. Two irradiated (K1, K5) and one non-irradiated (IA) rods were compared. We observed marked difference in the character of the size distribution function of precipitates.
I
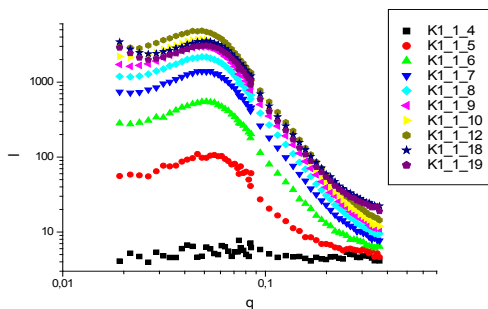
The radial summarized curves for K1 rod
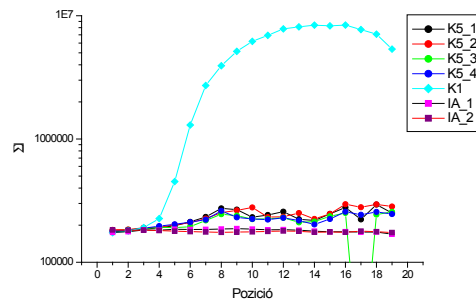
The summarized scattered intensity in the high q range for each measured points for all rod

We observed marked isotropic small angle scattering for the K1 rod and anisotropic from the others. The fitted model for the K1 rod correspond to the small interactive precipitates on the grain boundaries. This formation can be seen on the TEM pictures of the same alloys.

On the summarized scattered intensity in the high q range from the K1 rod can be seen that the sum surface of precipitates follow the vertical distribution of the reactor zone flux. The non-used rod curves is very equable, contrary to the K5 rod curves, which are fluctuated along the rod.

The anisotropic pictures from the non-used and the cracked rod shows cubic symmetry due to the preparation and using of rod. The K5 rod have more elongated and fluctuated anisotropic images, which could be from the internal stress.

References

Future prospects

Measurements of more control rods from different core position.

| **B N C** **Experimental Report**	*Experiment title* **Small angle neutron scattering study of reactor control rod**	*Proposal No.* *Local contact* Gy. Török.
Principal proposer: **E. Rétfalvi, Gy. Török, F. Gajdos, L. Rosta, S. T□zsér** *Experimental team:* **E. Rétfalvi,** Gy. Török (SzFKI)		*Date(s) of Exp.* 2006 *Date of Report* 2008

Objectives *(Aim of the research in some sentences)*

The aluminium coated B4C control rods of research reactor of Budapest are in the core at high neutron flux and at temperature of 60oC.. The investigated control rod was in the reactor for 13 years. The effect of radiation embrittelement has high safety significance for the reactor operation. The high neutron fluence causes forming of nanoscaled inhomogeneities (bubbles, precipitates, dislocation loops, etc). In order to observe microstructural changes caused non-destructively small angle neutron scattering is a very good tool.

Results *(Description of concrete results, understandable also for non-experts of the field. Insert, if possible, a typical figure)*

The SANS measurements were carried out on the irradiated radioactive rod at the „Yellow Submarine" spectrometer in the momentum transfer range between 0.1 and 3.5 nm-1. Measurements were performed on 20 points of the control rod along the vertical axis. The irradiated and non-irradiated states were compared.. We observed the vertical cosinus function distribution of flux along the rods, by amount of radiation tracks in the aluminium rod. Also we observed marked difference in the character of the size distribution function of precipitates
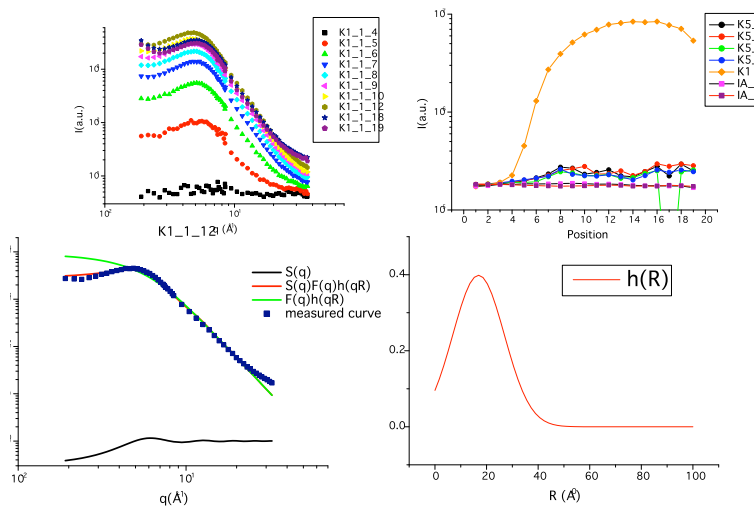
The radial summarized curves for K1 rod: The summarized scattered intensity in the high q range for each measured points for all rod

The fitted intensities according to the (1)

We fitted for the curves the following model:

Where: - F(q) - form factor for sphere

- S(q) – structure factor (hard sphere potential)

- h(R) – size distribution function (Gauss)

We used to the fit the PRIMUS small angle scattering data analysis program to analyze the size distribution of precipitates caused by irradiation

We have found that the precipitates have a relatively narrow size distribution with average diameter of 20 A. This fully agree with the other neutron irradiated aluminum alloys

Size distributions of precipitates

$I(q)=N \ F(q) \ S(q) \ h(R)$ (1)

Objectives In photosynthesis, light energy is harvested by antenna complexes, which 'funnel' the dilute photon flux for photochemistry. The excitation energy is transferred from the light harvesting complexes (LHCs) towards the photochemical reaction centers for energy conversion. In green plants, this complex process occurs in a multilamellar membrane system. The natural system is constituted by essentially identical thylakoid membranes, which - in the lateral direction - contain a large number of photosynthetic complexes and redox components.

In this project we planned to investigate small angle neutron scattering of native photosynthetic systems and those of different, artificially constructed lipid-LHCII lamellar aggregates.

Results Lamellar aggregates of LHCII, type II, loosely stacked, lipid enriched preparation were prepared from spinach leaves. For SANS measurements, the samples were suspended in D_2O-based 20 mM tricine buffer. The chlorophyll content of the samples was adjusted to about 1 mg ml^{-1}. Different amounts of these samples were added to solution of DPPC (dipalmitoyl phosphatidyl choline) multilamellar lipid vesicles to get final LHCII/DPPC mass ratios between 0 and 1/50. Samples were filled in quartz cuvettes with 2 mm optical pathlength and inserted into a thermostated sample holder. The obtained two dimensional scattering data (Fig. 1.) were radially averaged and the obtained curves (Fig.2.) were analyzed. Gauss function was fitted to the Bragg peaks originating from the multilamellar structure, and average repeat distance of the membranes was calculated. Results can be seen on Tab.1.
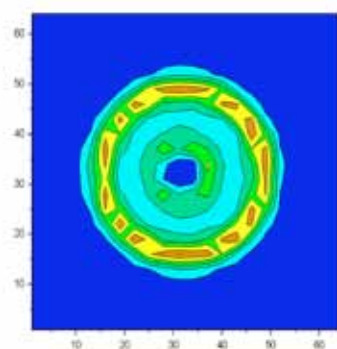
Fig. 1.
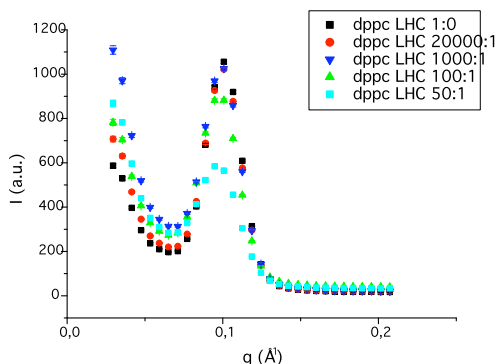
Fig. 2.

DPPC:LHCII	Repeat distance, Å
1:0	62.88 ± 0.11
20000:1	63.19 ± 0.13
1000:1	63.87 ± 0.16
100:1	64.67 ± 0.13
50:1	66.63 ± 0.04

Tab. 1.

Reference 4th European Conference on Neutron Scattering (Lund, Sweden, 2007): Nagy, Holm, Posselt, Rétfalvi, Lambrev, Kovács, Bóta, Rosta, Garab: Small angle neutron scattering of magnetically aligned natural and artificial multilamellar systems containing light-harvesting antenna complexes

Future prospects These data indicate that LHCII can be incorporated into multilamellar lipid vesicles, albeit – currently – we have only been able to achieve it at low concentrations of the complexes. Further experiments are required on lipid:LHCII macroassemblies with higher protein content, and to obtain periodic multilamellar systems similar to the native systems.

B N C **Experimental Report**	*Experiment title* **Micelle formation of dodecylbenzenesulfonic acid in aqueous solutions by small-angle neutron scattering**	*Proposal No.* SANS *Local contact* E.Retfalvi
Principal proposer V.I.Petrenko, FLNP, Joint Institute for Nuclear Research, Dubna, Russia *Experimental team* M.V.Avdeev, L.Rosta		*Date of Experiment* Nov 2007 *Date of Report* Feb 2008

Objectives

The given experiment was the continuation of the study of factors, which determine the stability of ferrofluids (fine liquid dispersions of magnetic nanoparticles coated with surfactant molecules). The goal of the present work was to study the behavior of dodecylbenzenesulfonic acid, $C_{18}H_{30}SO_3$, (DBS) in heavy water (d-water). DBS surfactant is a component of various technical ferrofluids with double stabilization [1]. The second surfactant layer in these fluids is formed due to physical adsorption under surfactant excess in the solution. Here, small-angle neutron scattering (SANS) was used to reveal the character of interaction between the surfactant molecules, as well as the structural parameters of their micelles formed in solutions (d-water) of free DBS.

Results

The experimental SANS data obtained in a wide concentration interval are given in Fig.1 together with the modeling curves. The micelle formation is observed. The model approximates simultaneously the form- and structure-factors of the micelles (program FISH). The peaks in the curves reflect the repulsive character of micelle interaction. The structure parameters of micelles including the aggregation number and surface charge density have been obtained. It has been shown that the micelles have spherical shape at low concentrations and then become ellipsoidal with increasing acid concentration. Some increase in the micelle size with the growth in the acid concentration has also been found.
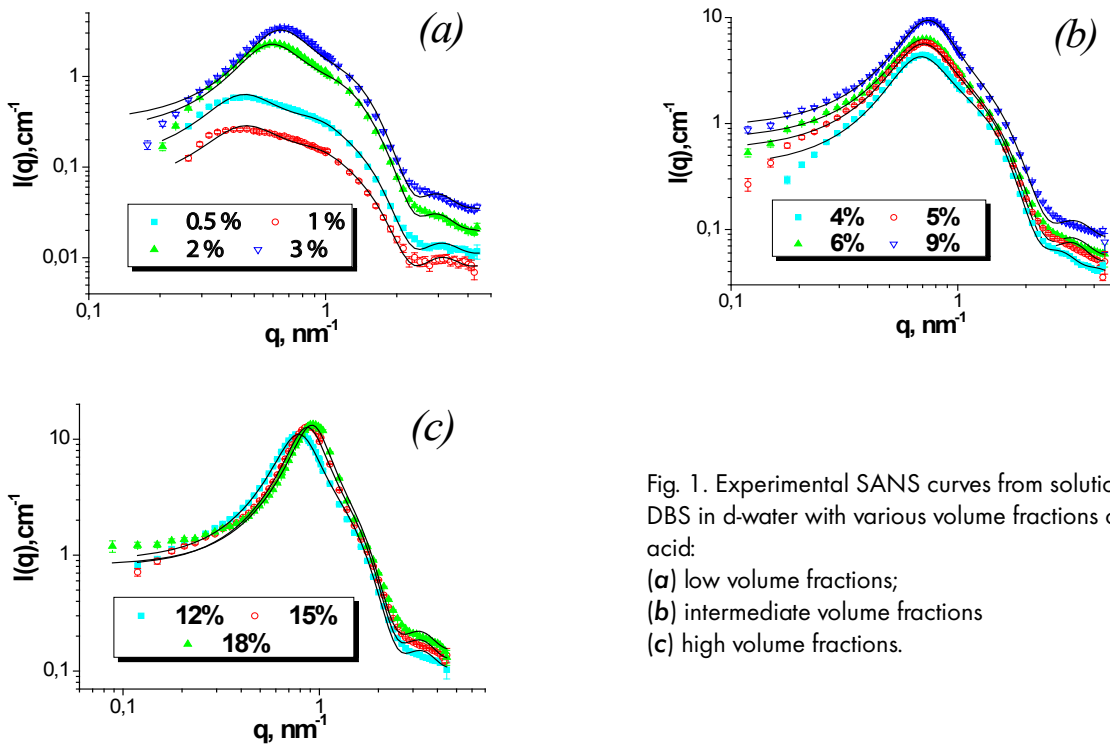
Fig. 1. Experimental SANS curves from solutions of DBS in d-water with various volume fractions of the acid:
(*a*) low volume fractions;
(*b*) intermediate volume fractions
(*c*) high volume fractions.

References

1. M.V.Avdeev, V.L.Aksenov, M.Balasoiu, et al.: J. Coll. Interface Sci. 295 (2006) 100

B N C **Experimental Report**	*Experiment title* **Structure analysis of new water-based ferrofluids by means of small-angle neutron scattering**	*Proposal No.* SANS *Local contact* L.Rosta
Principal proposer V.I.Petrenko, FLNP, Joint Institute for Nuclear Research, Dubna, Russia *Experimental team* L.Vekas, D.Bica, M.V.Avdeev		*Date of Experiment* Nov 2007 *Date of Report* Apr 2008

Objectives

The prospects of ferrofluids (fine liquid dispersions of magnetic nanoparticles coated with a surfactant layer) for medical applications are determined by the development in the synthesis of highly stable water-based samples. In the given experiment new water-based ferrofluids with magnetite or cobalt ferrite nanoparticles coated by double layer of various surfactants were investigated by means of small-angle neutron scattering (SANS). The goal of the study was to compare the structure of the fluids where different combinations of surfactants were used.

Results

Ferrofluids based on non-deuterated water (φ_m < 3 %) were synthesized in the Laboratory of Magnetic Fluids, CFATR, Timisoara, Romania, in accordance with the recently developed technique [2]. Various surfactants including dodecylbenzenesulfonic (DBS), oleic (OA), myristic (MA) and lauric (LA) acids were used in the stabilization procedures. Whereas DBS is a standard surfactant in the synthesis of technical ferrofluids, mono-carboxylic acids were probed with respect to the synthesis of biocompatible samples. The examples of the experimental SANS curves are given in Fig.1. The scattering from the surfactant layer is almost matched, because the values of the mean scattering length density for the surfactants and carrier are close. Qualitatively, the experimental curves have similar characters. Still, some difference allows us to conclude about various structural organizations of the ferrofluids. Thus, the volume distribution function, $D_V(R)$, depending on the particle radius was obtained by the indirect Fourier transform. It differs significantly from $D_V(R)$, which was expected for separate magnetic nanoparticles. The examples of the $D_V(R)$ functions found for the biocompatible samples are shown in Fig.2. They are compared with $D_V(R)$ obtained from the electron microscopy data related to single magnetite particles. One can see that in addition to separate particles (radius of about 5 nm) the large clusters (characteristic radius of 10-20 nm) are present in the systems. The fluid with double stabilization LA+LA is the closest to the distribution function $D_V(R)$ of separate particles, while the worst is the sample OA+OA [2].
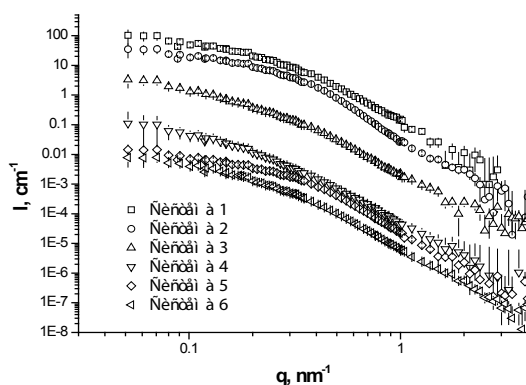
Fig.1. The experimental SANS curves for water-based ferrofluids with different combinations of surfactants. For convenient view the curves are divided by 10 (second DBS+DBS), 100 (OA+OA), 1000 (MA+MA), 10000 (LA+LA), 100000 (MA+DBS).
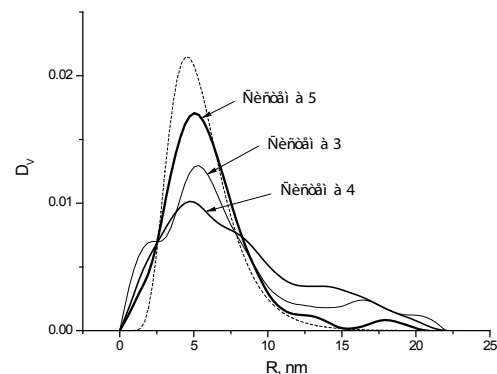
Fig.2. Found volume distribution functions (program GNOM) for biocompatible ferrofluids are compared with the electron microscopy data (EM).

References

1. D.Bica, L.Vekas, M.V.Avdeev, et al., J. Mag. Mag. Mater. 311 (2007) 17-21
2. V.I.Petrenko, V.L.Aksenov, M.V.Avdeev, L.A.Bulavin, L.Rosta, L.Vekas, V.M.Garamus, R.Willumeit, Physics of the Solid State (2008), accepted

B N C Experimental Report	*Experiment title* **Further studies on grey flint samples**	*Proposal No.* *Local contact* Zs.Kasztovszky
Principal proposer: T. Biró Katalin, András Markó – Hungarian National Museum, Hungary *Experimental team:* Zsolt Kasztovszky – Institute of Isotopes, HAS, Hungary		*Date(s) of Exp.* June 2006 *Date of Report* 09.01.27

Objectives

Provenance study of lithic raw materials is one of the key issues of prehistoric archaeology. The 'grey flint' varieties from Central Europe are standard items of prehistoric long distance trade. Flint is one of the typical 'long distance' raw materials in the Carpathian Basin, most of the sources being at a considerable distance, over hundreds of kilometres across the mountain range of the Carpathians. The only genuine flint resource in Hungary is known from Nagytevel, environs of Pápa, Transdanubia. The nearest comparable grey flint sources are located outside the arch of the Carpathians. Macroscopically similar varieties of silex include grey hornstone (chert of Triassic age) and radiolarites, fairly common all over Hungary. So far, the source identifications accomplished were mostly based on macroscopical investigations and only a few studies aimed at chemical identification of the source groups. Non-destructive PGAA studies help much in the characterisation of these raw material types.

Results

In more sequences of experiments, 19 archaeological and 26 geological flint or siliceous rock samples have been analysed from the collection of the Hungarian National Museum. Ukrainian flint samples were collected by A. Markó. Because of the very high silica content of grey flint varieties, it was possible to detect, fully and adequately, only part of the major components (TiO_2, Na_2O, and H_2O) and only a few trace elements (B, Cl, Sm and Gd). Some major components' concentrations are close to (Al_2O_3, Fe_2O_3, MnO, CaO and K_2O) or a little bit below (MgO) the detection limits, as well as traces of Sc, Eu and Nd. Basically, due to extremely high SiO_2 content flint is difficult to characterise with PGAA,. We have to state that the variation of chemical composition is small too, and the number of the comparative samples has to grow significantly, in order to achieve a more certain source identification. It is encouraging, however, that samples from the same archaeological source, assigned to the same category, tend to be the closest to each other. It has also turned out from the PCA that the most distinctive chemical components are Ti, H (or equivalently H_2O) and B, at least from those of that we are able to quantify.

References

The work was part of the OTKA K 62874 project

K. T. Biró, Zs. Kasztovszky: Further studies on grey flint samples (poster), *36th International Symposium on Archaeometry*, 2-6 May, 2006, Quebec City, Canada
Zs. Kasztovszky, K. T. Biró, A. Markó, V. Dobosi: Cold neutron prompt gamma activation analysis – a non-destructive method for characterisation of high silica content chipped stone tools and raw materials, *Archaeometry*, 2008, 50, 1, 12-29.

Future prospects

The number of samples to analyse should be increased essentially. When the source regions are properly characterised, PGA has great potentials in assigning items of long distance trade being fully non-destructive.

Objectives

Artefacts in private or museum collections that originate from Egypt or any other ancient culture are often of unknown or at least uncertain provenance. Scientific study can provide information about the elemental composition. The elemental composition can yield valuable information concerning place and time of manufacture.

These artefacts belong to the world's cultural heritage and therefore are valuable objects and should not be further damaged in any way. Destructive sampling should therefore be avoided. We decided to determine the elemental bulk composition using the non-destructive PGAA technique. Furthermore, the PGAA technique covers a fairly large volume of the object.

The objects of interest came from Egypt and the Roman Empire and were made of bronze.

Results

The first object was a shabti attributed to pharaoh Psusennes I. Surface studies already revealed that the surface was covered with a layer of cuprite and that small areas containing malachite and azurite were present. The elemental composition was measured with PGAA. The bronze shabti turned out to be typically a low tin bronze.

Comparing this composition with earlier literature results from sample taking and chemical analysis on contemporary shabti's gives us a lot of insight in early Egyptian bronze casting. Data concerning elemental composition of shabti's from the same period (app. 1000 BC) are rare. However, a few destructive studies by Clayton confirmed the absence of lead and the low concentration of tin in bronzes of this particular period. PGAA proved to be excellent technique in provenance and authenticity study of valuable artefacts. In addition to the shabti a few more Egyptian and Roman artefacts were investigated with success.

Elements	At%	w%	Rel. unc %
H	0.4	0.006	29.8
S	0.2	0.1	30.4
Cl	<det.limit		
Fe	0.6	0.5	12.5
Co	<det.limit		
Cu	96.6	95.3	0.3
Zn	<det.limit		
As	<det.limit		
Ag	<det.limit		
Sn	2.2	4.1	6.3
Sb	<det.limit		
Pb	<det.limit		
Sum	100.00	100.00	

References

Future prospects

The challenge for the future is to measure a larger series of artefacts and compare the results with those from destructive analysis performed on comparable objects. Furthermore we would like to find out if some (series of) artefacts can be attributed to ancient sources of copper or tin, thereby visualizing trade routes in classical periods.

B N C **Experimental Report**	*Experiment title* **Non-destructive Elemental Analysis of Ancient Egyptian Bronze**	*Proposal No.* BRR_169 *Local contact* Zs.Kasztovszky
Principal proposer: Stefan Blankenborg - Spark Origin B.V., Nijmegen, the Netherlands *Experimental team:* Zsolt Kasztovszky - Institute of Isotope, HAS, Hungary Stefan Blankenborg - Spark Origin B.V., Nijmegen, the Netherlands		*Date(s) of Exp.* Dec 2007 *Date of Report* 09.01.27

Objectives

The goal of this study was to investigate introduction of bronze in Egyptian art and utensils due to the import of tin from Asia. Tin containing objects are common from the start of the first millennium BC, but many objects from an earlier date lacked the presence of tin. The Egyptian empire in the second millennium BC stretched from Sudan to Syria. This study follows the route of the tin back in time, trying to investigate some ancient utensils (e.g. weapons) at the edge of empire.

Results

The PGAA measurement gave us the elemental composition of the bronze artefacts. Quite surprisingly, bronze weapons from the edge of the Egyptian Empire in Asia both consisted of only a few elements, viz. copper, tin and a few traces of others. Clearly in the second Millennium tin-bronze was already commonly used for weapons, and had replaced the arsenic copper of previous times. The tin concentration is still small; 3-6%. Except for small amounts of silver, chloride and sulfur no other elements were found. This might partly be due to the high detection limit for some of these elements.

Comparing these values with composition values of atefacts from the first Millennium BC we see that at about 1000 BC the composition is still approx. 95% Cu and 5% Sn, while from 600 BC onwards, lead is introduced.

We found no artefacts from the period 2000 BC- 200 AD consisting of copper without tin. This is a clear indication that tin was introduced at a very early stage in metal refining. A second surprise for us was the absence of arsenic in all samples, indicating replacement of arsenic by tin in the second millennium BC.

A disadvantage of PGAA is that it is not really suitable to measure trace elements, except for a few sensitive elements (e.g. Ag, Cd). However, the great strength of PGAA, i.e. non-destructive bulk measurement, predominates here and makes it an excellent tool for studying ancient metals.

References

Future prospects

B N C **Experimental Report**	*Experiment title* **The link of the Otranto Byzantine kiln to the medieval ceramics production of the Salento region (Italy)**	*Proposal No.* *Local contact* Zs.Kasztovszky
Principal proposer: Alberto Botti - Dip. Fisica, Univ. Roma TRE, Italy *Experimental team:* Alberto Botti, Armina Sodo - Dip. Fisica, Univ. Roma TRE, Italy Zsolt Kasztovszky - Institute of Isotope, HAS, Hungary		*Date(s) of Exp.* June 2007 *Date of Report* 09.01.27

Objectives

In this co-operation with the Physics Department of University of Rome TRE, we aimed to characterise archaeological ceramics from 7th-9th century, as well as clay samples with the help of PGAA. The archaeological pottery samples were excavated close to Otranto in the Apulian region of Salento, which is known as one of the few Mediterranean production centres which can be attributed to the early Medieval Ages. Remains of a Byzantine kiln have been found on the excavation site. The objectives of the research are twofold: to differentiate among the potential clay deposits which can be found in the Salento, and to define more precisely the raw material used in the Otranto kiln.

Results

The kiln products and the raw clay materials are shown on Fig., using the first and the second principal component. Samples gather in three distinct groups: in the positive region of the second component there are almost all typology of amphorae; in the negative region, data split in two clusters: a bigger one which contains the majority of the tableware (indicated in red by G5) but also some of the other typology of products, and a smaller one were again different product overlap.
Interestingly, OT1B belongs to the group of tableware, OT1C to that one of the amphorae and CUT1 B-C to the third small recognizable cluster. These results allow answering to the question: were they using different deposits?
The Figure suggests that the main clay deposits were those of Otranto, and only in very few cases they used a single deposit located in Cutrufiano Località Signorella. This confirms the hypothesis of a well standardized production which exploited preferentially local raw materials.
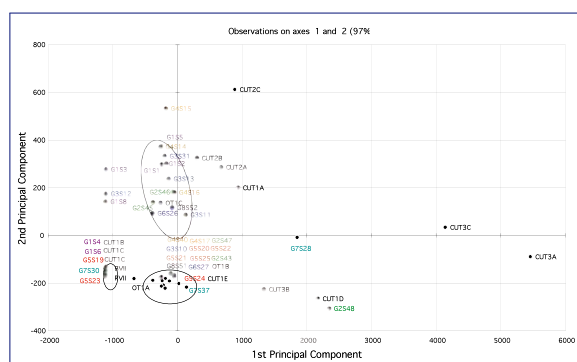
References

[1] Kasztovszky, Zs., Biró, T.K., Gherdán, K., Botti, A., Sodo, A., Sajo-Bohus, L., Applicability of Prompt Gamma Activation Analysis to the archaeometry of pottery (poster), 9th European Meeting on Ancient Ceramics, 2007, Oct. 24-27, Budapest
[2] Zs. Kasztovszky: Application of Prompt Gamma Activation Analysis to investigate archaeological ceramics, Archeometria Műhely, elektronic journal (http://www.ace.hu/am/) 2007, IV. 2 pp. 49-54.

B N C **Experimental Report**	*Experiment title* **PGAA analysis of geological silicate samples from Central Transylvania for comparison with analysis of prehistoric artefacts**	*Proposal No.* *Local contact* Zs.Kasztovszky
Principal proposer: Otis Crandell - Universitatea "1 Decembrie 1918" Alba Iulia, Romania *Experimental team:* Zsolt Kasztovszky, Veronika Szilágyi - Institute of Isotope, HAS, Hungary Otis Crandell - Universitatea "1 Decembrie 1918" Alba Iulia, Romania		*Date(s) of Exp.* May 2007 *Date of Report* 09.01.27

Objectives

The objectives of the study were to determine whether Prompt Gamma Activation Analyses (PGAA) could be successfully used to distinguish between jasper samples originating from different known geological sources, as well as matching similar jasper artefacts to sources. In this study, three macroscopically identical sources of jaspers from central and western Romania were analysed. Thus, the PGAA data for samples from three areas was compared with PGAA data obtained for five Neolithic artefacts from the Limba site (Alba county). Statistical interpretation of the elemental data was used to characterise the geological sources and to predict the origins of the five artefacts.

Results

In almost all samples, the following elements had levels above the quantification limit. Major elements: SiO_2, Fe_2O_{3t}, MnO, K_2O and H_2O. Trace elements: B, Cl, Gd. TiO_2, MgO, CaO, Na_2O and Sm were measurable in some samples. Due to the limited number of detected trace elements, this method produces inconclusive results for discriminating between jaspers from different sources.

All of the artefacts analysed received a prediction of their source but all had extremely low levels of probability of the predictions. Although with the artefacts the probability is much lower, in the 4 statistical interpretations, the same sources were usually predicted. The results of this study would suggest that most of the jasper (at least in these artefacts) was coming from the Metaliferi Mountains with only one piece potentially being of more local origin.

References

Crandell, O. N., Kasztovszky, Zs., The use of PGAA to aid in distinguishing between sources of jasper (poster), *37th International Symposium on Archaeometry*, 2008, May 12-16, Siena, Italy

Future prospects

The discrimination between different jaspers has to be made by combining macroscopic, microscopic, geochemical and geological data.

BNC Experimental Report	Experiment title **PGAA elemental analysis of Mesopotamian seals and their raw Material consisting of 'haematite'**	Proposal No. Local contact Zs.Kasztovszky
Principal proposer: Martine de Vries-Melein - VU University Amsterdam, the Netherlands *Experimental team:* Zsolt Kasztovszky, Veronika Szilágyi - Institute of Isotope, HAS, Hungary Dirk Visser - Reactor Institute Delft, TU-Delft, the Netherlands		*Date(s) of Exp.* May 2007 *Date of Report* 09.01.27

Objectives

Non-destructive PGAA of Mesopotamian stone seals made of haematite and similar minerals were proposed in order to differenciate between the objects, and to identify possible raw material sources. Indications of the type of additional inclusion material next to haematite, magnetite and goethite can be obtained, as well as trace material important for provenancing purposes. The proposed objects are material from an excavation at Selenkahiye, Tall Bazi (Syria) and unprovenanced material made available by the Allard Pierson Museum, RMO Leiden and LMU-München.

Results

As it was expected from our previous studies, with PGAA we were able to identify most of the major elemental components and a few traces. In Heamatite and Goethite besides the major Fe (51% to 69%), we have quantified H, B, Na, Mg, Al, Si, S, Cl, K, Ca, Sc, Ti, V, Cr, Mn, Fe, Co, Ni, Cu, Zn, Ba, Nd, Sm and Gd. Calcite, as it was expected can be clearly distinguished from the other two kinds, based on PGAA. On the other hand, it seems that PGAA is not capable to differentiate between Heamatite and Goethite.

	NINO 75 *Goethite*		NINO 67 *Heamatite*		NINO 55 *Calcite*	
El	**c%** el/ox	*unc* %	**c%** el/ox	*unc* %	**c%** el/ox	*unc* %
H	1.18	*1.7*	0.04	*3.6*	0.06	*2.8*
B	0.00234	*1.8*	0.00038	*3.0*	0.00046	*2.4*
C					12.3	*2.7*
Na					0.083	*7.*
Mg	0.65	*21.*			0.72	*6.*
Al	0.10	*33.*	0.12	*23.*	0.21	*6.*
Si	1.2	*6.*			2.4	*3.1*
Cl	0.046	*3.4*	0.0052	*22.*	0.065	*2.6*
K					0.09	*3.3*
Ca	0.063	*32.*	0.074	*22.*	33.4	*2.4*
Ti			0.019	*10.*	0.017	*4.*
Mn	0.060	*5.*	0.012	*15.*	0.0049	*9.*
Fe	59.8	*0.4*	69.4	*0.1*	0.14	*3.9*
Sm	0.00015	*4.0*	0.000001	*32.*	0.00002	*5.*
Gd	0.00025	*9.*	0.00002	*9.*	0.00003	*7.*
O (calc)	36.9		30.3		50.3	

References

Future prospects

The archaeological interpretation of the analytical results is in progress.

Objectives

The aim of this study to obtain basic composition data of further polished stone objects made of greenschist, amphibolite and basalt. We wish to extend our database of previous investigations, in order to perform provenance studies.

Results

After comparing the recent results with our data on metabasic rocks, we can confirm that greenschist of Felsőcsatár origin can be clearly separated from those of Bohemian Massif origin. Provenance of stone tools made of basalt can be identified as Balaton Highland – Little Hungarian Plane volcanic area. In certain cases, especially in case of very fine grained objects, PGAA helped in identification of raw materials (hornfels, quarzite, metagabbro, etc.), when it was impossible according to macroscopic investigations. The most adventageous feature of PGAA is the non-destructivity, again.

References

Future prospects

B N C Experimental Report	*Experiment title* **PGAA of Prehistoric pottery fragment and clay deposits from Vörs, Western Hungary**	*Proposal No.* *Local contact* Zs.Kasztovszky
Principal proposer: Katalin Gherdán – Eötvös University, Budapest, Hungary *Experimental team:* Zsolt Kasztovszky, Veronika Szilágyi - Institute of Isotope, HAS, Hungary Katalin Gherdán – Eötvös University, Budapest, Hungary		*Date(s) of Exp.* 2007 *Date of Report* 09.01.27

Objectives

Vörs is situated at the South-West shore of Lake Balaton (See **Map 2**). It is representative not only for the Neolithic Age, but abundant of pottery findings from various periods from Early Neolithic (6000 B.C.) up to Hungarian Conquest Period (1000 A.D.). The unique feature of this multiperiodical site serves the opportunity to perform a comparative study of various cultures. Archaeological ceramics were selected from two separated parts of the site (Vörs-Máriaasszonysziget and Vörs-Tótok dombja). One of the basic questions was if it is possible to make a distinction between the pottery of the two "sub-sites". The other question was about the potential raw materials applied for pottery making. The two candidates for the original raw material were the local clayish-sandy soils from Vörs and the clayish sediment of the closest known clay mine in Battyánpuszta.

Results

To answer these questions, the TiO_2/Al_2O_3 vs. Zr/V bivariate correlation diagram was constructed. It was not possible to separate the pottery of Vörs-Máriaasszonysziget and Vörs-Tótok dombja on geochemical basis. However, there was a group of two sherds from Vörs-Máriaasszonysziget, which diverged from the main cluster of ceramics by almost all of the incompatible elements and their ratios. This group comprises those sherds which proved to be "carbonatic sand tempered" by microscopic petrographic investigations. This feature separates them from the major part of the ceramics from Vörs which are "crushed pottery tempered". The second part of geochemical interpretation dealt with the identification of the potential raw material. It became clear that local soils nearby the archaeological site are not the proper raw material from geochemical point of view. However, clays from Battyánpuszta are quite similar to potteries – especially to the carbonate sand tempered ceramics. This fact makes it probable that the not too far clay source of Battyánpuszta could provide raw material for the ceramic manufacturing in Vörs during the Early Bronze Age.

References

B N C	*Experiment title*	*Proposal No.*
Experimental Report	**Proficiency test on Chinese porcelain reference material**	*Local contact* Zs.Kasztovszky
Principal proposer: Matthias Rossbach - IAEA *Experimental team:* Zsolt Kasztovszky, Zsolt Révay, Katalin Gméling, László Szentmiklósi - Institute of Isotope, HAS, Hungary		*Date(s) of Exp.* May 2006 *Date of Report* 09.01.27

Objectives

The International Atomic Energy Agency (IAEA) has organized a proficiency test between the participant laboratories of the CRP, entitled "Applications of nuclear analytical techniques to investigate the authenticity of art objects" A Chinese porcelain reference material has been distributed and various nuclear analytical methods (INAA, PGAA, PIXE and XRF) have been applied to determine elemental composition. The results provided by the individual laboratories, have been evaluated by the IAEA.

Results

The PGAA measurements have been repeated more times on subsamples, and the spectrumm evaluations were done by different people. The proficiency test has resulted in the following outcome: All the identified components with PGAA agreed with the reported target values, excluding Na, which we have quantified with a significant deviation from the target value. A possible explanation of this deviation is the unlucky interference of the Na 472.2 keV prompt gamma line with the irregularly wide B 477.6 keV line. This interference must be taken into correction more carefully to get the precise sodium concentration data.
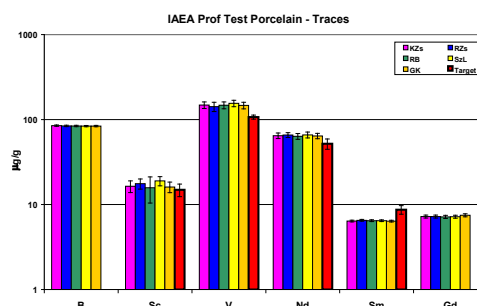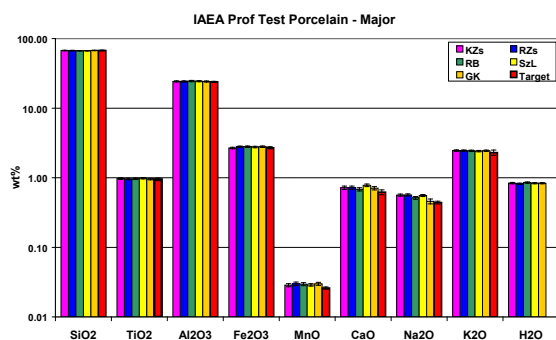
References

Report on the IAEA-CU-2006-06 proficiency test: Determination of major, minor and trace elements in ancient chinese ceramic IAEA / AL / 168

Future prospects

B N C Experimental Report	Experiment title **Application of PGAA for the studies of historic glass**	Proposal No. BRR_134_r Local contact Zs.Kasztovszky
Principal proposer: Jerzy Kunicki-Goldfinger – Institute of Nuclear Chemistry and Technology, Poland Experimental team: Zsolt Kasztovszky - Institute of Isotope, HAS, Hungary Jerzy Kunicki-Goldfinger – Institute of Nuclear Chemistry and Technology, Poland		Date(s) of Exp. Apr 2007 Date of Report 09.01.27.

Objectives

The project, as a continuation of a previous one, aimed both technological and provenance studies of historic glass artefacts, mainly of the façon-de-Venise (fdV) vessels. We also wanted to check if the seventeenth century fdV glass (and earlier ones) contained boron. The element is known to be present in certain late seventeenth century glasses in northern Europe, but till now there is no published results in regard to the element concentration in Venetian and fdV glass. The extremely low PGAA detection limit for boron (order of 0.1 ppm) provided us the possibility to answer this question. We also wished to recognize whether certain pattern of impurities would allow us to distinguish the objects of different origins.

Results

Main, minor and some trace elements including boron were measured in more than 20 historical and reference glasses. The concentration of B_2O_3 was between 0.04 and 0.06 wt. %. This is the level of naturally occurring boron in many historical glasses and the results are in agreement with data published by other researchers. No glass with boron introduced intentionally was found. Major and minor element concentrations allowed us to distinguish objects of various origins and represented various manufacturing traditions. Many impurities were identified, which have been introduced into glass batches as contaminations of certain raw materials. Their concentration also helped us to distinguish glasses of various origin and/or glasses made of raw materials of different origin.

An interpretation of the results allowed us to distinguish, among other, five groups of the façon-de-Venise (fdV) vessels: fdV cristallo like and fdV 1-4. (Fig 1) Moreover, a group of Baroque glasses as well as the following single items have been distinguished: post-medieval green bottle, 19th century stained glass, medieval stained glass. One analysed Roemer fitted to the group fdV-4.
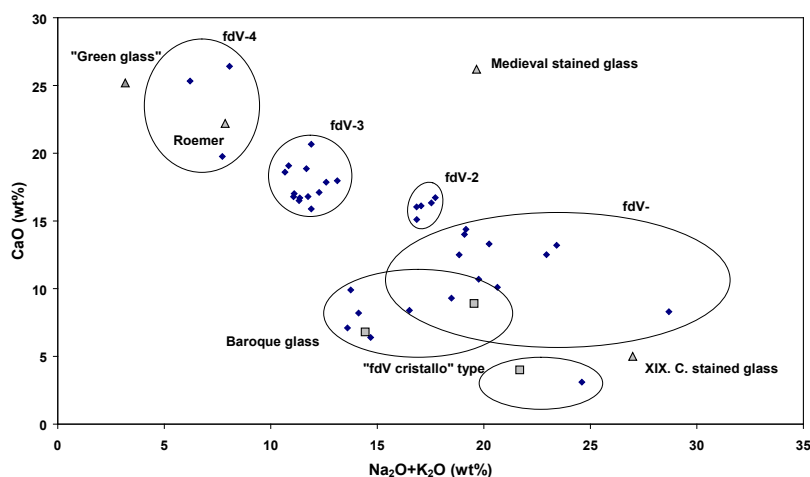
References

Kasztovszky, Zs., Kunicki-Goldfinger, J., Applicability of Prompt Gamma Activation Analysis to glass archaeometry (poster), *37th International Symposium on Archaeometry*, 2008, May 12-16, Siena, Italy

BNC Experimental Report	Experiment title **Archaeometry research of lithic raw materials for early Neolithic prehistoric communities with PGAA**	Proposal No. Local contact Zs.Kasztovszky
Principal proposer: Marcel Buric, Rajna Sosic – University of Zagreb, Croatia Experimental team: Zsolt Kasztovszky, Veronika Szilágyi – Institute of Isotope, HAS, Hungary		Date(s) of Exp. Apr 2006 - Date of Report 09.01.27

Objectives

Obsidian and radiolarite have always been a key element of prehistoric material culture. Obsidian is a favourite subject of archaeometrical studies. Radiolarite is of comparable significance, however, much less known and analysed as yet. In the earliest phase of the Neolithic, both obsidian and radiolarite are important markers of the movements of goods as well as people trading them. Their investigation may have a key role also in tracing the Neolithisation process.

There is no local obsidian on the territory of Croatia: import, however, may originate from both the Carpathian Basin and the Western Mediterranean region. The last decades of research showed the importance of radiolarites in Hungary. It is apparent, however, that there is essential local supply of various radiolarites in Croatia, too. On the other hand, there is considerable (supposed) import from the territory of Hungary. It is imperative to find objective discrimination features to define these supply zones and the border of these zones. This project runs in the frame of TéT bilateral cooperation.

Results

Both archaeological and geological samples were investigated. Obsidian from archaeological context was provided from our Croatian partners; fieldwork both in Hungary and Croatia supplied comparative geological samples.

After fieldtrips in Croatia and Hungary, we started to perform non-destructive PGAA on the obsidian and radiolarite objects. As in previous experiments, we were able to quantify most major- and some trace components. The analytical results were built in our previous database of lithic material from the Carpathian Basin and surroundings. Based on the comparision between archaeological obsidian from Croatia and archaeological and geological samples from other regions, it seems that the provenance of the objects can be determined with high probability. With radiolarite, we have only very limited results due to low number of analyses performed. We anticipate that it will be more difficult but historically equally important.

Principal Component Analysis of obsidian data
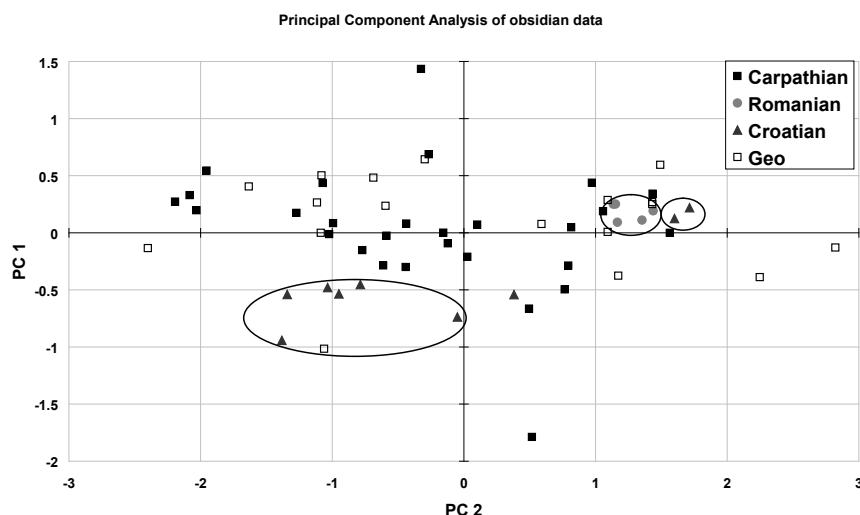
References

Future prospects

We continue to analize the collected material in order to have more precize statistical consequences.

B N C **Experimental Report**	*Experiment title* **A geochemical study of the Lower Permian volcanic rocks from the north-eastern margin of the Wolsztyn Ridge (West Poland) by means of PGAA**	*Proposal No.* *Local contact* K. Gméling Zs. Kasztovszky
Principal proposer: Dr Magdalena Pańczyk, Polish Geological Institute, Warsaw *Experimental team:* Magdalena Pańczyk, Katalin Gméling, Zsolt Kasztovszky Nuclear Research Department Institute of Isotope, Hungarian Academy of Sciences		*Date(s) of Exper.* 0 6 . 0 4 . 1 9 - 04.25. *Date of Report* 09.01.30.

Objectives

The objective of the project was to measure 35 volcanic rock samples from drill cores of Western Wielkopolska, West Poland by PGAA. Thickness of the volcanogenic formation ranges from 100 to 200 m. The lower part of the Rotligendes volcanic succession is represented by andesites, whereas the upper one by rhyolites and rhyodacites. The major aim of our measurements was to obtain the concentration of major elements and trace elements such as Nd, Sm, Gd and transition elements like V, Cr, Co. Furthermore, the concentration of B, which is an extremely important element to estimate tectonic setting. Because of non-destructive nature of PGAA, the same samples were used for later INAA measurements, as a complementary method. All the obtain results were used for the determination of the petrogenetic processes leading to the differentiation of the volcanic succession as well as for the identification of the tectonic setting.

Results

35 volcanic rock samples from andesite to rhyolites in composition were measured with PGAA. Some of the samples were powdered, while others were hand pieces from the drill cores, thus their size varied between 0.4 and 3.7 grams and the measurement time also varied between 3684 and 61202 seconds. The smallest sample was measured for two days to have enough counts in order to be evaluated effectively. The major oxides of all the samples were determined, only the MgO contents were under detection limit of the PGAA in many high-silica samples. B, Cl, Nd, Sm, and Gd were determined in all samples, but transition elements like Sc, V, Cr or Co was possible to quantify only in few samples. We measured one sample for a shorter and later for a much longer time to see, if the precision gets better or the detection limit can be decreased with the extended measurement time. We obtained the same results from both measurements, but for V, we were able to get results only from the longer measurement. The B content of the measured samples varied within wide ranges (7.7-129 µg/g). It correlates positively with the SiO_2 content of the samples, as it was expected. However, some of the high-silica samples have unexpectedly low B content, which can be a result of secondary processes, such as leaching or weathering. All the expected results of the PGAA measurements were achived and they were considered, compared and completed with previous studies and modelling. Results were published on a conference of the Mineralogical Society of Poland.

References

Pańczyk, M. (2006): Petrogenesis of the Permian volcanic rocks from the southeastern part of North Sudetic Basin (West Sudetes, Poland). Geophysical Research Abstracts, Vol. 8, 08276, 2006

Pańczyk M., (2005): XII Sesja Petrologii Polskiego Towarzystwa Mineralogicznego. Skały krystaliczne kratonu wschodnioeuropejskiego. Stary Folwark, 13-16.10.2005. Przegląd Geologiczny, 54, (2): 99-101.

Future prospects

We plan to run a bilateral academical cooperation in the future.

B N C **Experimental Report**	Experiment title Elemental analysis of limestones from quarries along the river Nile basin using Prompt Gamma Activation Analysis (PGAA)	Proposal No. BRR 131 *Local contact* Zs.Kasztovszky
Principal proposer: Emmanuel Pantos - CCLRC, Daresbury Laboratory *Experimental team:* Zsolt Kasztovszky - Institute of Isotope, HAS, Hungary Emmanuel Pantos - CCLRC, Daresbury Laboratory, UK		*Date(s) of Exp.* June 2006 *Date of Report* 09.01.27

Objectives

We proposed to analyse limestone samples from quarries along the river Nile basin by PGAA. Their mineralogical composition is known from synchrotron powder XRD and, for some of them, from neutron time-of-flight diffraction. Other properties have been studied with FTIR, SAXS and XANES as well as petrography and electron microscopy. We aim to identify some characteristic elements and to establish the nucleus of a database of elemental composition of these samples which can be compared to archaeological samples from the great pyramids at Giza, particularly the casing stones, which are reported to have come from the Tura/Mokattam quarries across the Nile, but which to-date have not been reported to have been analysed by any physical technique.

Results

Besides the major and accessory elements of C, O, Na, Si, Al, Mg, K, and Ca we have identified trace elements such as H, B, F, S, Cl, Ti, Mn, Fe, Sr, Sm and Gd, in some cases with outstanding values.

From the mineralogical and elemental compositions, the ancient samples show significant variations in marker phases, such as ankerite, quartz, gypsum, sepiolite and palygorskite. Although the sampling statistics is quite small yet, comparison with samples from quarries along the Nile, significant differences in mineralogical and elemental composition are not consistent with the Tura / Mokkatam provenance view.

Dendrogram for 2005-2006-2008 PGAA
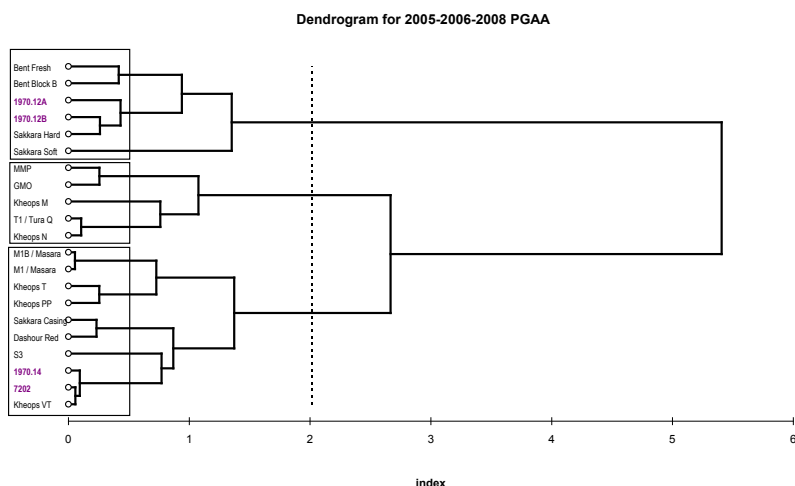
References

Pantos, M., Exell, K., Kockelmann, W., Kasztovszky, Zs., Morlidge, M., Ellis, M., Bilsborrow, B., Mineralogical characterisation of limestone from the Great Pyramids and limestone quarries along the Nile, *Synchrotron Radiation in Art and Archaeology*, 2008, October 22-24, Barcelona, Spain

Future prospects

Sampling away from the surface exposed to weathering is required. In parallel, more representative sampling of quarry limestone along the Nile valley is also needed.

B N C **Experimental Report**	*Experiment title* **Archaeometric investigations of polished stone tools and grinding stones made of basalt, greenschist and serpentinite**	*Proposal No.* *Local contact* Zs.Kasztovszky
Principal proposer: Péterdi Bálint - Geological Institute of Hungary, Budapest *Experimental team:* Zsolt Kasztovszky, Veronika Szilágyi - Institute of Isotope, HAS, Hungary		*Date(s) of Exp.* 04.2006- 02.2007 *Date of Report* 09.01.27

Objectives

Various polished stone tools and grinding stones found in Balatonőszöd and Üllő, were investigated with PGAA. The aim of this study was provenance determination, i.e. identification of possible raw material sources.

Results

The investigated stone axes, semiproducts and raw materials were made of basalt, greenschist, serpentinite, nephrite and andesite. Comparing the PGAA results with previous analysis of similar objects, we can exclude the Mecsek origin of their raw material. ICP-AES and ICP-MS results (Embey-Isztin & Dobosi) were also used for archaeometric evaluation. Based on the present analytical data, we were not able to identify the individual sources within the Balaton Highland, because of the large variability of each site's material. Good agreements between ICP and PGAA data were found.

References

Péterdi, B., Szakmány, Gy., Judik, K., Dobosi, G., Kasztovszky, Zs., Petrographical and geochemical investigation of grinding stones from Üllő 5. site, Pest County, Hungary (poster), *37th International Symposium on Archaeometry*, 2008, May 12-16, Siena, Italy

Future prospects

B N C **Experimental Report**	*Experiment title* **Archaeometric investigations of chipped stone tools made of limnoquarzite from the Tokaj hills**	*Proposal No.* *Local contact* Zs.Kasztovszky
Principal proposer: Szekszárdi Adrienn – Eötvös University, Budapest, Hungary *Experimental team:* Zsolt Kasztovszky, Veronika Szilágyi - Institute of Isotope, HAS, Hungary		*Date(s) of Exp.* 05-07. 2007 *Date of Report* 09.01.27

Objectives

The aim of this study was to differentiate between archaeological objects made of limnoquarzite and limnoopalite, found in different sites of Eperjes-Tokaj mts. Identification of raw material sources was also aimed.

Results

Six archaeological pieces and 15 geological references were analyzed with PGAA. Most of the object contain over 97 wt% SiO_2. Only three had SiO_2 < 90 wt%, one of them contained carbonates (high Ca and Mg), two were silicified vulcanites These were clearly separable from the rest. The detected B concentrations were above the Earth crust average. These values can be characteristic for the geological formation, but it requires further investigations. Although based on the PGAA results it was not possible to differenciate between objects within one geological area, but there is a chance to differenciate between rocks from various areas (Mátra mts., Sub-Carpathian area, etc.)

References

The work was part of the OTKA K 62874 project and a subject of a diploma thesis:

Szekszárdi Adrienn, ELTE Diploma thesis, 2007.

Szekszárdi Adrienn, A vizsgálati lehetőségek áttekintése a Tokaji-hegységi limnokvarciton és limnoopaliton, a pattintott kőeszközök eredetének azonositása céljából, Archeometriai Műhely, 2005 II. 4, 56-61.

Future prospects

In the frame of the above mentioned OTKA, we will extend the investigated area to other possible raw material sources of similar geological features.

B N C Experimental Report	*Experiment title* **Completing of provenance analysis of Inka Period ceramics (Paria, Bolivia) by PGAA**	*Proposal No.*
		Local contact V.Szilágyi
Principal proposer: Veronika Szilágyi		*Date(s) of Exp.* 2007
Experimental team: Zsolt Kasztovszky, Veronika Szilágyi Institute of Isotope, HAS		*Date of Report* 09.02.07

Objectives

Inka Period (A.C. 1450–1535) pottery of Paria, an Inka administrative centre (Bolivia) was chemically characterized in order to localize its raw material sources. During the excavations different archaeological types of pottery were found. A limited collection of ceramics was selected for PGAA analysis. In addition, local river sediments as potential raw materials were also investigated. Preparatory to the geochemical investigation, a comprehensive petro-mineralogical analysis of the samples was fulfilled (Szilágyi et al., 2005, 2007). The main goal of the research was to catch differences in the material of the archaeologically separated ceramics. This part of the study could provide information about the local and non-local raw materials of pottery. PGAA analysis was utilized as a completing geochemical method for special samples since other techniques (INAA, XRF) are destructive for the sample.

Results

To answer these questions, the TiO_2/SiO_2 bivariate correlation diagram is presented here. Although petrography classified the Inka Period ceramics into three main groups, geochemistry could not separate all of these groups of pottery. However, the special white ceramic type could be clearly separated from the other types by almost all of the incompatible elements and their ratios. This feature of this sample suggests its foreign origin. In addition, instead of the petrographic interpretation that local sediments were used for pottery making, it is clear from the chemical composition that a strict selection of local raw materials should be applied since the sediment samples measured by PGAA show different composition from the ceramics.

References

SZILÁGYI, V., SZAKMÁNY, Gy., GYARMATI, J., TÓTH M. (2007): Preliminary Comparative Archaeometric Results of Colonial and Inka Pottery in Paria (Oruro, Bolivia). In: Waksman, Y.S. (ed.): Archaeometric and Archaeological Approaches to Ceramics: Papers presented at EMAC'05, 8th European Meeting on Ancient Ceramics, Lyon 2005, BAR International Series 1691, 2007, pp. 195-199. (in English)

SZILÁGYI, V., SZAKMÁNY, Gy., GYARMATI, J. (2005): Inka kori kerámiák petrográfiai vizsgálatának előzetes eredményei (Paria, Bolívia). [Preliminary results of the petrographic investigation of Inka Period ceramics (Paria, Bolivia).] Archeometriai Műhely, 2005/2 (http://www.ace.hu/am/index.html). (in Hungarian)

B N C Experimental Report	*Experiment title* **Non-destructive element analysis of early English monumental Brass letters (1250- 1350 AD): provenance and dating**	*Proposal No.* *Local contact* Zs.Kasztovszky
Principal proposer: Dirk Visser - ISIS Facility, Rutherford Appleton Laboratory, Chilton, Didcot, UK *Experimental team:* Zsolt Kasztovszky - Institute of Isotope, HAS, Hungary Dirk Visser - ISIS Facility, Rutherford Appleton Laboratory, Chilton, Didcot, UK		*Date(s) of Exp.* May 2007 *Date of Report* 09.01.27

Objectives

Lombardic monumental brass letters are the earliest application of 'layton' : a CuZnSn-Pb alloy to commemorative monuments. In this study we propose to determine the elemental composition of 30 brass letters dated to the Period 1250 - 1350 AD in order to establish if standardisation applies to these objects in connection to stylistic dating and workshop provenance can be obtained.

Results

We analysed 8 monumental brass letters and three letter stops which belonged to the earliest from of written text on English monumental effigy slabs. Often these letters have no provenance anymore and can be found in musea and private collections. We studied objects from private collectors. Three very recent metaldetectorist finds where analysed within this study. The letter L found in the near vincinity of the Church of North Stoke (Oxon) has now definitely been provenanced to this church. The letter belongs to the earliest type of effigy with lettering found in England.

We analysed letters in the form of a Q, Z, L, K, P, A, D and O. The PGAA analysis shows a remarkable homogeneity over the first 6 letters as well as two letter stops; Cu: 77-74 w%, Zn: 17-12 w%, Sn: 7-5 w%, Ag ~0.5 w%. Pb was found in quantities of less than 1 w% (close to the detection limit) or maximum 4.5 w%, what results in large uncertainty of lead concentration data. The amounts of trace elements like Fe and As were also close to the DL. The PGAA measurements indicate that - within the measurements uncertainties - the manifacture of the early brass letters belonging to this group was done with a standarised alloy. The letter D and one nail have a different composition; Cu: 84 w%, little Zn: 1-6 w%, little Pb: 1-2 w% and a relative high percentage of Sn: ~ 11 w%. The letter O is an exceptional object in this series. This object is very thin < 0.5 mm in comparison to the normal 2 - 2.5 mm thickness of the other letters. The composition is also different from the other letters, with a Cu content of 66.5 w% Cu, 30 w% Zn, 3 w% Sn and Pb lower than the quantification limit. This make up of this alloy must be of a much younger period (Renaissance or later). Two or three different measurements were made at different position on the letters; the PGAA results indicate a homogenious distribution of the main alloying elements. The large uncertainty in the determination of the Pb concentration, due to the low neutron absorption cross-section for thermal or cold neutrons, does not allows to determine the mixability of the Pb metal as a non dissolvable additiv in theMedieval layton (CuZnSn alloy).

References

[1.]   Visser, D., Kasztovszky, Zs., Blair, J., Bayliss, J., Stuchfield, M. H., Badham, S., Non- destructive element analyis of medieval English brass letters (poster), *37th International Symposium on Archaeometry*, 2008, May 12-16, Siena, Italy

Future prospects

B N C Experimental Report	Experiment title **PGAI measurement of a benchmark object**	Proposal No. Local contact T. Belgya
Principal proposer: T. Belgya – Institute of Isotopes-HAS Experimental team: T. Belgya, Z. Kis, L. Szentmiklósi, Zs. Kasztovszky – Institute of Isotopes-HAS		Date(s) of Exper. Apr-Jun 2007 Date of Report 01-30-2009

Objectives

To perform a quasi 3D scanning of a simple object with known composition

Results

The first non-destructive PGAI, quasi 3D elemental compositions of a known object (an elongated benchmark sample) were measured in a grid scan.
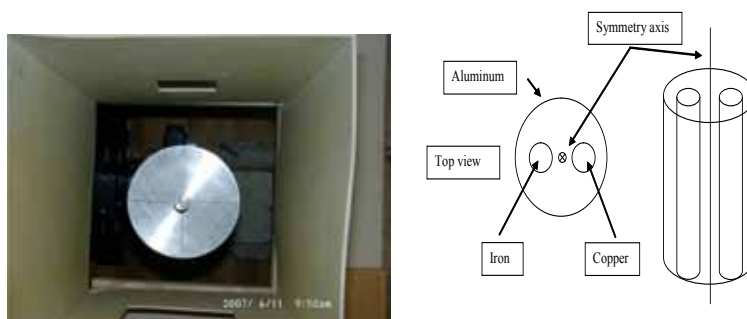
The peak areas of most intense peaks of the elements (the 1778-keV decay line of Al, the 352-keV and 278-keV prompt lines of Fe and Cu, respectively) were used to produce 2D (quasi 3D) elemental distributions of the target. The raw elemental map (left panel: map of Al cylinder, middle panel: map of Fe rod, right panel: map of Cu rod) agrees qualitatively well with the know composition of the object. This way, it is proved that the idea of the 3D elemental mapping of the interior of bulk samples is working with PGAI. As it can be seen from the panels the originally rotational symmetric objects are elongated in the X direction, which is due to the larger FWHM of the gamma collimator transmission.
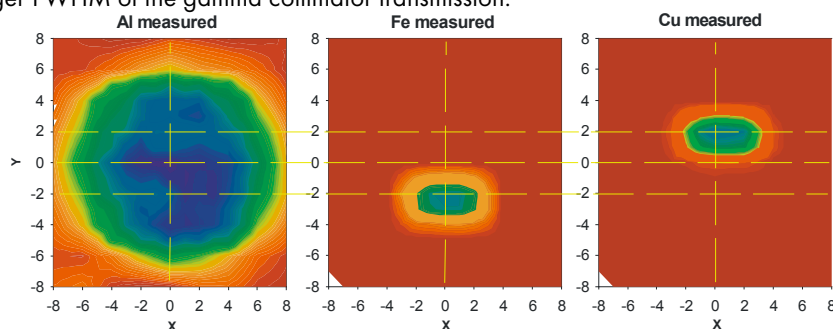
Future prospects

To improve the quality of the figures, corrections for the neutron distribution, the gamma transmission trough the collimator, the neutron scattering and the self absorption for both neutrons and gamma rays should be applied. The development of the methodology of these calculations is still in progress.

References

1. T. Belgya, Z. Kis, L. Szentmiklósi, Zs. Kasztovszky, P. Kudejova, R. Schulze, T. Materna, G. Festa, P. A. Caroppi, and the Ancient Charm Collaboration. First elemental imaging experiments on a combined PGAI and NT setup at the Budapest Research Reactor. Journal of Radioanalytical and Nuclear Chemistry, 278 (3) (2008): 751–754.

B N C **Experimental Report**	*Experiment title* **Radiography-driven PGAI measurement of complex test objects**	*Proposal No.* *Local contact* T. Belgya
Principal proposer: T. Belgya – Institute of Isotopes-HAS *Experimental team:* T. Belgya, Z. Kis, L. Szentmiklósi, Zs. Kasztovszky – Institute of Isotopes-HAS P. Kudejova, R. Schulze – University of Cologne, Cologne		*Date(s) of Exper.* Jun 2007 *Date of Report* 01-30-2009

Objectives

To perform PGAI-NR/NT measurements on complex benchmark samples with unknown composition

Results

The benchmark samples, so-called 'black boxes', produced as imitations of real archaeological objects were analyzed in the framework of the AC collaboration. The contents of the boxes were made of materials frequently occurring in an archaeological context. Measurements on only one box, the H-VI, are discussed here, while a more complete study has been published elsewhere.

The H-VI object is an iron box having four sections that contained the following materials: 1. silver lathe turnings; 2. fill, talcum; 3. fill, sand; 4. fill, iron lumps; 5. fill, salt (NaCl); Separation plates: copper sheets; Al internal cover plate (not shown). One can see the radiographic image and the positions of the neutron collimator slit (n1–n5) in the successive measurements.
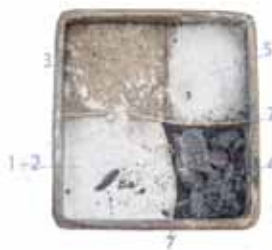
Iron was detected in all spectra, i.e. in this geometry it always comes from the front and back walls too. At point n1 (material 3), we detected a whole set of elements common in sand, such as H, B, Na, K, Cl, Al, Si, and Ti. At spot n2 (material 5), both elemental components, i.e. the sodium and the chlorine were detected. The determined molar ratio was in agreement with the expected 1:1. In quadrant 4 at spot n3 (material 4), we saw an increased counting rate in the Fe peaks, indicating an additional amount of iron within the box. At beam spot n4 silver is detected, in addition to the matrix elements H, Si. Finally the separation plates were measured (n5), and both were found to be copper.

Future prospects

These objects will drive the final development of the PGAI/NT imaging technique. Accurate PGAI-NR/NT measurements on these samples are needed for the integration of these measurements with the other imaging techniques.

References

1. Zs. Kasztovszky, Z. Kis, T. Belgya, W. Kockelmann, S. Imberti, G. Festa, A. Filabozzi, C. Andreani, A. Kirfel, K.T. Biró, K. Dúzs, Zs. Hajnal, P. Kudejova, M. Tardocchi, and the Ancient Charm Collaboration. Prompt gamma activation analysis and time of flight neutron diffraction on 'black boxes' in the 'Ancient Charm' project. Journal of Radioanalytical and Nuclear Chemistry, 278 (3) (2008): 661–664.

2. Z. Kis, T. Belgya, L. Szentmiklósi, Zs. Kasztovszky, P. Kudejová and R. Schulze. Prompt Gamma Activation Imaging on 'black boxes' in the 'ANCIENT CHARM' project. Archaeometry Workshop(1) (2008): 41-60.

3.

Objectives

The neutron capture cross section of 22Ne is important in nuclear astrophysics, because the ^{22}Ne$(\alpha, n)^{25}$Mg reaction is one of the major neutron sources for s-process nucleosynthesis. In the hydrogen burning zones of stars slightly more massive than the Sun, practically all CNO nuclei are converted into ^{14}N, because ^{14}N$(p, \gamma)^{15}$O is the slowest reaction in the CNO cycle. At the higher temperatures during the subsequent He burning, ^{22}Ne is abundantly produced by the reaction sequence ^{14}N$(\alpha, \gamma)^{18}$F$(\beta+)^{18}$O$(\alpha, \gamma)^{22}$Ne. However, the resulting ^{22}Ne abundance is not only consumed for neutron production, but represents also a potential neutron poison. For this reason, the neutron capture cross section of 22Ne plays an important role for the overall neutron balance of the s process.

Results

The thermal neutron capture cross section for the 22Ne(n,)23Ne reaction was determined using mixtures of 22Ne and CH4 gas under high pressure. With the assumption that the new decay-scheme is complete, the recently developed CIS rule method and the inverse Q-value rule yield practically the same thermal cross section of 52.7±0.7 mb, 18% larger than the previously accepted value. The influence of this result on the analysis of the stellar capture rate of 22Ne is under investigation.

Future prospects

The influence of this result on the analysis of the stellar capture rate of 22Ne is under investigation. Article in peer reviewed journal.

References

Belgya, T., E. Uberseder, D. Petrich, and F. Käppeler. Thermal neutron capture cross section of 22Ne. in 13th Int. Symp. on Capture Gamma-Ray Spectroscopy and Relatrd Topics. 2008. Cologne, Germany, 25-29 August 2008 talk

B N C **Experimental Report**	*Experiment title* **Setup of a working PGAI-NR/NT system**	*Proposal No.* *Local contact* T. Belgya
Principal proposer: T. Belgya – Institute of Isotopes-HAS *Experimental team:* T. Belgya, Z. Kis, L. Szentmiklósi, Zs. Kasztovszky – Institute of Isotopes-HAS G. Festa, L. Andreanelli, M.P. De Pascale, A. Pietropaolo – Univ. of Rome Tor Vergata, Rome P. Kudejova, R. Schulze – University of Cologne, Cologne T. Materna – Institut Laue-Langevin, Grenoble		*Date(s) of Exper.* Oct 2006-Apr 2007 *Date of Report* 01-30-2009

Objectives

To develop a sophisticated instrument capable to analyze the internal composition of complex archaeological objects by the simultaneous use of Prompt-Gamma Activation Imaging (PGAI) and Neutron Tomography (NT) which can non-destructively provide the 3D-distribution of elements in interesting regions of objects.

Results

The setup is a result of the Ancient Charm project and many consortium members contributed (design, hardware and/or software) to its realization. The schematic drawing of the PGAI-NT setup is shown. The setup is designed to accommodate a maximum 10 cm by 10 cm object horizontally, although its height can be up to 20 cm. The incident neutron beam has a cross-section of 20 mm by 20 mm, when used for neutron tomography. For PGAI, an adjustable neutron collimator was fabricated from 6Li-enriched polymer, which can make a 2-mm wide pencil beam with height of 2 to 20 mm.

As the first step, the components of the system were aligned, tested and the basic characteristics of the facility have been determined. This included the measurement of the neutron beam and gamma collimator profiles, as well as determining the resolution of the tomograph. Methods were worked out to acquire and process a large number of gamma spectra.
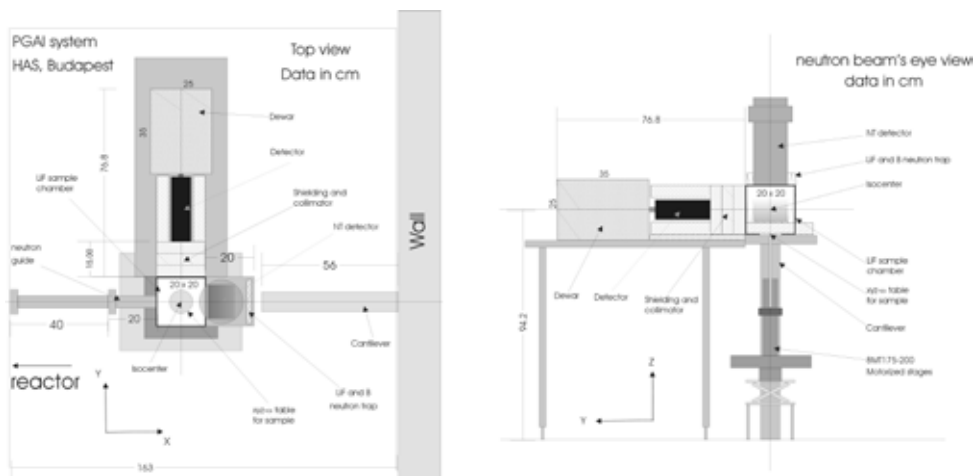
Future prospects

Installation of the PGAI-NT set up at FRM-II, Garching including the transfer of the hardware from NIPS to FRM-II and some adaptation.

References

4. T. Belgya, Z. Kis, L. Szentmiklósi, Zs. Kasztovszky, G. Festa, L. Andreanelli, M.P. De Pascale, A. Pietropaolo, P. Kudejova, R. Schulze, T. Materna, and the Ancient Charm Collaboration. *A new PGAI-NT setup at the NIPS facility of the Budapest Research Reactor.* Journal of Radioanalytical and Nuclear Chemistry, 278 (3) (2008): 713–718.

B N C **Experimental Report**	Experiment title **Determining the response function of the Budapest PGAA detector**	Proposal No. Local contact L. Szentmiklósi
Principal proposer: L. Szentmiklósi - Institute of Isotopes, HAS Experimental team: L. Szentmiklósi - Institute of Isotopes, HAS		Date(s) of Exper. Mar 2006. Date of Report 01-30-2009

Objectives

To determine the response function of the Budapest PGAA detector.

Results

The PGAA detector system consists of an n-type HPGe detector (Canberra GR 2518) and a Bismuth Germanate (BGO) guard detector arranged in a coaxial geometry. The eight main segments of the suppressor are complemented by two additional "catchers" behind the HPGe crystal. The whole detector is surrounded by a 10 cm-thick lead shielding.

The interpretation of the highly complicated elemental PGAA spectra and the prediction of the spectroscopic conditions for multi-component analytes require the accurate knowledge of the detector response function. The first step towards the characterization of our spectrometer was the accurate measurements of well known and simple gamma spectra. Unfortunately there are only a few commercially available radioactive sources for this purpose (^{109}Cd , ^{241}Am, ^{57}Co, ^{51}Cr, ^{207}Bi, ^{137}Cs, ^{54}Mn, ^{65}Zn, ^{60}Co), while some additional nuclides with short half-lives could be prepared by activation in the neutron beam (^{198}Au, ^{116m1}In, ^{127}I, ^{56}Mn, ^{24}Na, ^{52}V, ^{20}F, ^{28}Al), and could be measured with the chopped-beam technique. A few, simple PGAA spectra (H(n,γ), D(n,γ), C(n,γ), Pb(n,γ)) were also involved in the study.

The measurements were compared with Monte-Carlo simulations. For normal spectra, the agreement is already good, while for the reproduction of the Compton-suppressed spectra requires further refinements of the simulation software.
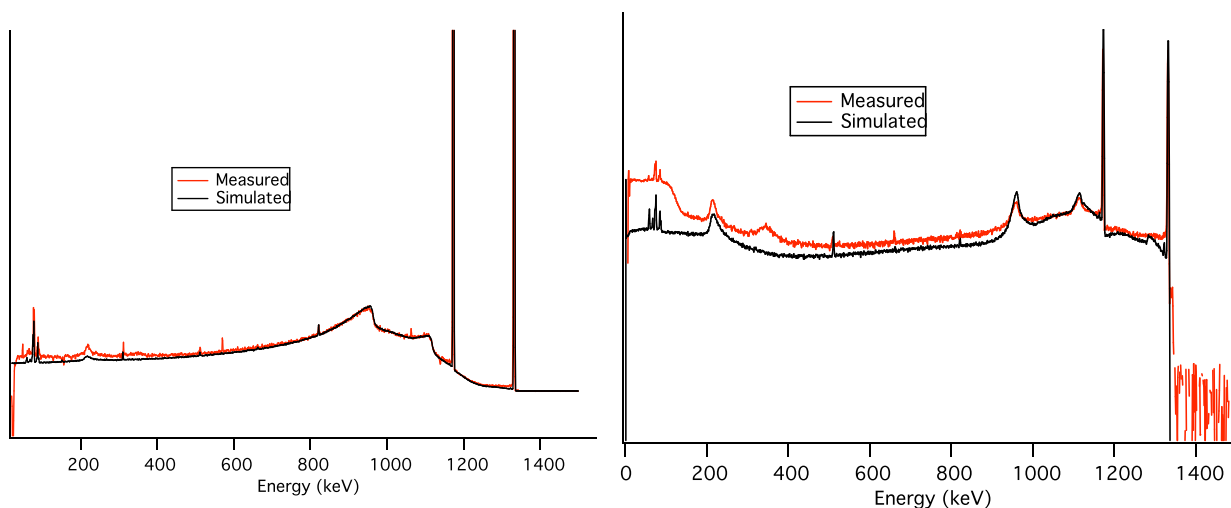
Figure 1. The measured and simulated spectra of the ^{60}Co radioactive source, in unsuppressed mode (left figure) and in Compton-suppression mode (right figure)

B N C **Experimental Report**	*Experiment title* **Cold-neutron radiography of a temperature-controlled chemical reactor**	*Proposal No.* *Local contact* L. Szentmiklósi
Principal proposer: D. Teschner, Zs. Révay- Institute of Isotopes, HAS *Experimental team:* L. Szentmiklósi, Z. Kis, A. Wootsch, J. Borsodi - Institute of Isotopes, HAS		*Date(s) of Exper.* 26-28 Apr 2007 *Date of Report* 01-30-2009

Objectives

To visualize the internal structure of an in-beam chemical reactor and ensure its proper alignment in the beam.

Results

Small-size continuous-flow reactors were placed in the isocenter of the PGAI-NT system. For this study a 20-cm-high, 10-cm-wide, cylinder-shaped aluminum house was designed and manufactured containing vertical tubes for heating or cooling. The total mass of the aluminum tank was about 1.6 kg. It contained an axial hole to accommodate reactor tubes with different inside diameters. Two radial channels were also made in the directions of the beam and the detector to eliminate the attenuation of the radiations.

The alumina-ceramic reactor tube had a length of 20 cm, a total mass of 3 g, and its inner diameter was 3 mm. Catalyst or inert material in the form of powder was loaded into the tube.

With the help of the radiography, it was possible to position the small catalysis tube to the sensitive volume of the detector and detect the signal from hydrogen, minimize the neutron-induced background and optimize the gas flow, in order to avoid the bubbling of the catalysts.

a.

c.

d.

b.
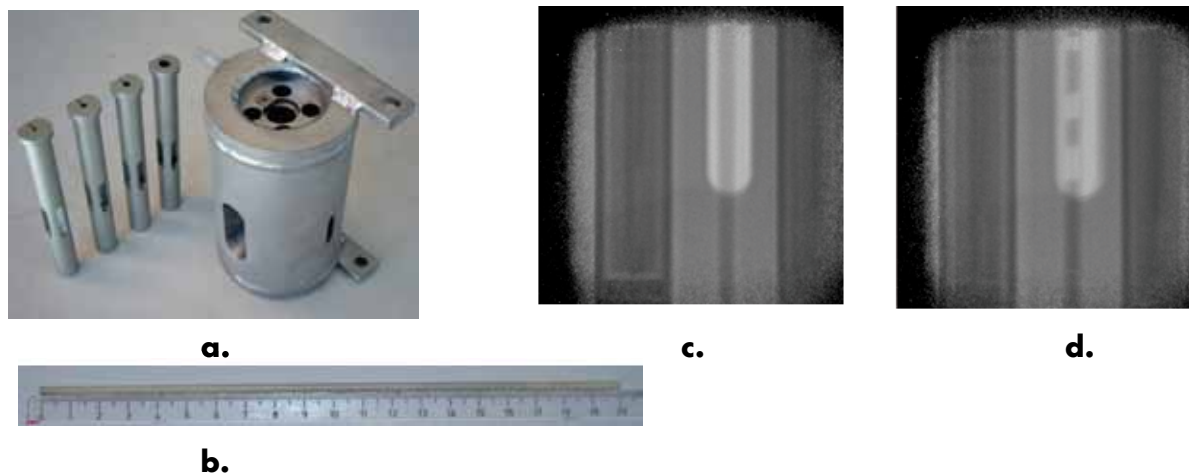
Figure1. a. photo of the pilot chemical reactor; b. the photo of the tube reactor; c. neutron radiographic image of the well-aligned cell and the tube reactor within (dark stripe in the middle); d. the bubbling of the catalysis bed at high gas flow.

Reference

Zs. Révay, T. Belgya, L. Szentmiklósi, Z. Kis, A. Wootsch, D. Teschner, M. Swoboda, and R. Schlögl, J. Borsodi, R. Zepernick, In situ determination of hydrogen inside a catalytic reactor using prompt gamma activation analysis, Anal. Chem. **80** (15) (2008) 6066-6071

B N C Experimental Report	Experiment title **Accurate relative intensities and energies of** 233**Pa**						Proposal No. Local contact L. Szentmiklósi	
Principal proposer: A. Simonits - KFKI-AEKI *Experimental team:* L. Szentmiklósi - Institute of Isotopes, HAS							*Date(s) of Exper.* May-Jun 2007 *Date of Report* 01-30-2009	

Objectives

To measure relative intensities and energies of 233Pa.

Results

Literature data of the 233Pa decay ($T_{1/2}$=26.967 days) show outliers and discrepancies in the energies and intensities of the peaks. It has significance in calibrating NAA spectra of geological samples containing 232Th.

An Al-0,82%Th sample (CBNM) with a diameter of 1 mm has been irradiated in the reactor core and was cooled for 3 weeks. Thereafter it has been measured at the PGAA and LeGe detectors of the Institute of Isotopes and on the D4 detector of the AEKI during the reactor shutdown period.

The spectra have been evaluated with Hypermet-PC or Hyperlab 2005.b, and the resulting peak positions and areas were statistically analyzed. Formulas have been derived to account for the statistical and systematic uncertainties of the measurements at different counting systems. The results are summarized as follows:

Measured Energy (keV)	Internal Unc. (keV)	External Unc. (keV)	Literature Energy (keV) [1]	Unc. [1]	Relative Intensity	Unc.	Literature Intensity [1]	Unc. [1]
75.228	0.002	0.004	75.354	0.004	1.415	0.018	1.39	0.08
86.5955	0.0014	0.0021	86.814	0.003	1.943	0.014	1.97	0.12
103.8580	0.0015	0.0012	103.971	0.009	0.825	0.007	0.87	0.03
248.308	0.007	0.003	248.5	0.5	0.057	0.001	0.059	0.0003
258.428	0.0014	0.0019	258.46	0.20	0.030	0.001	0.0039	0.0016
271.5414	0.0022	0.0024	271.48	0.08	0.330	0.001	0.328	0.012
298.747	0.014	0.016	298.89	0.20	0.122	0.005	0.035	N/A
300.1209	0.0009	0.0010	300.34	0.02	6.539	0.006	6.62	0.06
311.9050	0.0008	0.0005	312.17	0.02	38.5	0.021	38.6	0.4
340.4700	0.0008	0.0008	340.81	0.03	4.475	0.007	4.47	0.04
375.3929	0.0015	0.0015	375.45	0.04	0.679	0.002	0.679	0.008
398.4870	0.0016	0.0015	398.62	0.08	1.402	0.004	1.390	0.012
415.7534	0.0022	0.0025	415.76	0.04	1.763	0.006	1.745	0.016

Table 1. Comparison of the energy and intensity values from the present work and from Table of Radioactive Isotopes (ToRI) [1].

References

[1]   Y.A. Akovali, NDS 59,263 (1990), see also at:

http://nucleardata.nuclear.lu.se/nucleardata/toi/nuclide.asp?iZA=910233

B N C **Experimental Report**		*Experiment title* **PGAA of environmental and nutritional samples**				*Proposal No.* *Local contact* Zs. Révay	

Principal proposer: M. C. Freitas - Reactor-ITN, Technological and Nuclear Institute, Portugal *Experimental team:* Zs. Révay, L. Szentmiklósi - Institute of Isotopes, HAS	*Date(s) of Exper.* 12-19 Feb 2007. *Date of Report* 01-30-2009

Objectives

To determine the compositions of environmental and nutritional samples and compare them to NAA results.

Results

   Environmental and nutritional samples were analyzed using Compton-suppressed PGAA. Filters and barks were analyzed as sampled; the other samples were freeze-dried, ground to a powder, and put into hand-made, small Teflon bags.

Element		Teflon (blank)	Teflon (PM2.5)	Water	Lettuce	Lichen	Pinus bark	Platanus bark
H	(%)	1.46(3)	1.82(3)	0.84(5)	8.9(2)	4.11(9)	5.14(3)	5.27(5)
B		1.6(6)	2.9(5)	n.d.	41.2(2)	17.9(9)	4.11(3)	15.7(5)
C	(%)	29(5)	33(4)	n.d.	72(1)	33(10)	48(3)	43(5)
N	(%)	n.d.	n.d.	n.d.	n.d.	0.9(11)	n.d.	n.d.
O	(%)	n.d.	n.d.	n.d.	n.d.	57(7)	44(4)	43(7)
F	(%)	67(2)	63(2)	n.d.	n.d.	1.8(19)	1.4(7)	5.5(7)
Na		n.d.	n.d.	38%(2)	0.31%(6)	0.34%(10)	30(20)	170(14)
Mg	(%)	n.d.	n.d.	n.d.	1.6(12)	n.d.	n.d.	0.17(13)
Al	(%)	2.4(4)	1.3(6)	n.d.	n.d.	0.20(16)	0.64(4)	0.82(7)
Si	(%)	n.d.	n.d.	n.d.	0.4(19)	0.38(11)	0.112(5)	n.d.
P	(%)	n.d.	n.d.	n.d.	1.1(10)	n.d.	n.d.	n.d.
S		n.d.	n.d.	n.d.	0.69%(4)	0.14%(10)	320(6)	210(15)
Cl		70(12)	380(4)	55%(2)	2.75%(2)	0.31%(9)	114(4)	115(6)
K		n.d.	n.d.	2.3%(2)	11.3%(2)	0.15%(10)	350(5)	350(8)
Ca	(%)	n.d.	n.d.	4(29)	1.17(4)	1.26(10)	0.39(4)	0.68(6)
Ti		n.d.	n.d.	n.d.	140(13)	100(11)	28(11)	n.d.
V		n.d.	n.d.	n.d.	100(24)	n.d.	n.d.	n.d.
Mn		n.d.	n.d.	n.d.	n.d.	60(15)	23(10)	48(10)
Fe		n.d.	n.d.	n.d.	n.d.	0.11%(12)	500(7)	0.07%(13)
Cu		n.d.	n.d.	n.d.	n.d.	n.d.	50(20)	n.d.
Cd		0.8(17)	0.9(26)	n.d.	0.6(16)	n.d.	0.06%(19)	n.d.
Sm		n.d.	n.d.	n.d.	n.d.	0.12(18)	n.d.	n.d.
Gd		n.d.	n.d.	n.d.	n.d.	0.17(11)	n.d.	n.d.
Pb	(%)	n.d.	n.d.	n.d.	n.d.	0.8(12)	n.d.	1.1(18)
Total	(%)	99.9	99.2	100.1	100.2	100.5	99.9	99.7

Table 1. Element concentrations in environmental and nutritional matrices. All data in mg.kg^{-1} dry weight, except otherwise indicated (%); uncertainties within brackets are in %. n.d: not determined.

Reference

M. C. Freitas, Z. Révay, L. Szentmiklósi, I. Dionísio, H. M. Dung, A. M. G. Pacheco: Different methodologies in neutron activation to approach the full analysis of environmental and nutritional samples, J. Radioanal. Nucl. Chem. **278**, No.2 (2008) 381–386

B N C Experimental Report	Experiment title **Thermal neutron capture cross section of ²²Ne**	Proposal No. Local contact Zs. Révay
Principal proposer: D. Teschner – Fritz-Haber-Institut der Max-Planck-Gesellschaft, Faradayweg 4-6, D-14195 Berlin, Germany *Experimental team:* Zs. Révay, J. Borsodi, L. Szentmiklósi– Institute of Isotopes-HAS D. Teschner – Fritz-Haber-Institut der Max-Planck-Gesellschaft, Faradayweg 4-6, D-14195 Berlin, Germany		*Date(s) of Exper.* Oct. 09-14 2007 June 13-16 2006 *Date of Report* 02-27-2009

Objectives

To follow the hydrogen content of Pd catalyst bad during the catalysis.

Results

Alkynes can be selectively hydrogenated into alkenes on solid palladium catalysts. This process requires a strong modification of the near-surface region of palladium, in which carbon (from fragmented feed molecules) occupies interstitial lattice sites. In situ x-ray photoelectron spectroscopic measurements under reaction conditions indicated that much less carbon was dissolved in palladium during unselective, total hydrogenation.

Additional studies of hydrogen content using in situ prompt gamma activation analysis, which allowed us to follow the hydrogen content of palladium during catalysis, indicated that unselective hydrogenation proceeds on hydrogen-saturated b-hydride, whereas selective hydrogenation was only possible after decoupling bulk properties from the surface events. Thus, the population of subsurface sites of palladium, by either hydrogen or carbon, governs the hydrogenation events on the surface.

Pd metal (beta-hydride)   **Pd-C surface phase**

Future prospects

Further studies of catalysis using in-situ PGAA.

References

Teschner, D., J. Borsodi, A. Wootsch, Z. Revay, M. Havecker, A. Knop-Gericke, S.D. Jackson, and R. Schlogl, *The roles of subsurface carbon and hydrogen in palladium-catalyzed alkyne hydrogenation.* Science, **320**(5872), (2008) p. 86-89

Revay, Z., T. Belgya, L. Szentmiklosi, Z. Kis, A. Wootsch, D. Teschner, M. Swoboda, R. Schlogl, J. Borsodi, and R. Zepernick, *In situ determination of hydrogen inside a catalytic reactor using prompt gamma activation analysis.* Analytical Chemistry, **80**(15), (2008) p. 6066-6071

Objectives

To determine the composition of the samples

Results

Different samples from North-American excavation were examined. Many of them show the sign of extraterrestrial origin, or the formation in a cosmic catastrophe. In these series of measurements glassy carbon samples and magnetic grains were analyzed. They were irradiated in the cold neutron beam and analyzed using our standard procedure. The next Tables show their composition.

Table 1. The composition of 30 mg of glassy carbon

Elem	conc. %	Rel. biz%
H	2.54	3
B	2.65 ppm	3
C	75	2.1
N	0.14	7
O	20	8
Al	0.43	4
Si	1.85	3
Cl	151 ppm	3
K	80 ppm	10
Ca	0.29	4
Ti	330 ppm	3
Cd	0.16 ppm	12
Sm	0.14 ppm	5

Table 2. Oxide composition of magnetic grains from Morley (mass 130 mg).

Elem	Konc. %	Rel. biz%
H	4.3	2.0
B	0.013	1.9
Na	0.74	3
Al	5.5	3
Si	57.7	1.1
S	0.25	13
Cl	0.016	5
K	1.25	2.5
Ca	11.6	3
Ti	1.669	2.3
Mn	0.159	3
Fe	16.72	2.0
Ni	0.036	22
Cu	0.031	15
Cd	0.4 ppm	15
Sm	0.30 ppm	3
Gd	0.38 ppm	4

References

R. B. Firestone, A. West, J. P. Kennett, L. Becker, T. E. Bunch, Zs. Revay, P. H. Schultz, T. Belgya, D.J. Kennett, J.M. Erlandson, O.J. Dickenson, A.C. Goodyear, R.S. Harris, G.A. Howard, J.B. Kloosterman, P. Lechler, P.A. Mayewski, J. Montgomery, R. Poreda, T. Darrah, S.S.Q. Hee, A.R. Smitha, A. Stich, W. Topping, J.H. Wittke, W.S. Wolbach: *Evidence for an extraterrestrial impact 12,900 years ago that contributed to the megafaunal extinctions and the Younger Dryas cooling*, Proc. Nat. Acad. Sci. USA, 104/41 (2007) 16016.

Objectives

To determine pollutants of grafenes.

Results

Grafene is made of monoatomic planar sheets of graphite. Grafene can be regarded as an allotrope of carbon. Carbon is an ideal matrix for PGAA, as it has a low cross-section (3.8 mbarn), thus its pollutants can easily be analyzed.

This sensitive and precious material could not be measured in vacuum. To lower the background, the measurement was performed using the following setup:

40 mg of grafene was placed in 25-μm-thick Teflon foil, and it was sealed in a Teflon bag, containing helium gas. Helium does not capture neutrons, and the radiation background is much lower, than in the air. The composition was determined according the routine analytical method. The result is shown below:

Elem	Concentration wt%	Rel. unc. %
H	0.77%	13%
B	19ppm	14%
C	98.6%	0.2%
Cl	0.61%	12%

Hydrogen and chlorine are remnants from the solvents, used in the production, while boron was very likely in the original graphite.

References

B N C **Experimental Report**	**Determination of elementary composition in borosilicate glasses with PGAA spectroscopy**	*Proposal No.* PGAA- *Local contact*
Principal proposer: E. Veress *Experimental team:* M. Fábián, E. Sváb, SZFKI; E. Veress, Cluj, Romania, Zs. Révay, IKI		*Date(s) of Exp.* March 2006 *Date of Report*

Objectives

Multi-component borosilicate glasses are good candidate materials to use as isolating host media of radioactive waste materials [1]. In the last years we have undertaken neutron diffraction structure study on newly synthesized multi-component borosilicate glass system. For data treatment the elementary composition is essential, which was measured by PGAA method .

Results

For this study, we have synthesized a new series, with nominal composition of $(65-x)SiO_2 \cdot xB_2O_3 \cdot 25Na_2O \cdot 5BaO \cdot 5ZrO_2$, where x= 5, 10, 15, 20 mol%. For sample preparation a high temperature electrical furnace was used with a platinum crucible under atmospheric conditions. The raw materials used were all of p.a. grade, SiO_2, Na_2CO_3 supplied by Reactivul (Bucuresti), BaO and ZrO_2 by Merck (Darmstadt), and B_2O_3 by Sigma–Aldrich Co. (Hungary) isotopically enriched in ^{11}B (99.6%) [2]. The melt was quenched by pouring it on a stainless steel plate (for more details see [3,4]). Powder samples were prepared by powder milling of the quenched glasses in an agate mill.

The elemental compositions of the multi-component boron containing specimens were verified by prompt gamma activation analysis (PGAA) [5]. The results are given in Table 1.

Table 1. Elemental composition (at%) of the multi-component glasses measured by PGAA method. (The relative errors are indicated in brackets)

Element	Elemental composition (at%)			
	SiBxNaBaZrO			
	x=5	**x=10**	**x=15**	**x=20**
Si	19.1(1.8)	19.1(1.8)	15.24(1.8)	10.0(2.0)
B	3.69(1.0)	6.59(1.0)	9.15(0.9)	16.4(0.8)
Na	15.37(1.4)	14.3(1.5)	13.08(1.4)	11.5(1.5)
O	58.0(0.5)	58.4(0.5)	58.5(0.4)	58.9(0.3)
Ba	1.3(2.6)	1.3(2.6)	1.3(2.5)	1.05(2.6)
Zr	2.19(2.5)	2.18(2.4)	2.42(2.4)	1.92(2.7)

References

[1] K.S. Chun, S.S. Kim, C.H. Kang, *Journal of Nuclear Materials*, **298** (2001) 150.
[2] Zs. Varga, G. Surányi, N. Vajda, Zs. Stefánka, *Microchem. J.* **85** (2007) 39.
[3] M. Fábián, E. Sváb, Gy. Mészáros, L. Kőszegi, L. Temleitner, E. Veress, *Zeitschrift für Kristallographie* **23** (2006) 461.
[4] M. Fábián, E. Sváb, Gy. Mészáros, Zs. Révay, Th. Proffen, E. Veress, *J. Non- Cryst. Solids* **353** (2007) 2084.
[5] Zs. Révay, T. Belgya, G.L. Molnár, J. Radioanal. *Nucl. Chem.* **265** (2005) 261.

	Experiment title	Proposal No.
B N C **Experimental Report**	*Experiment title* **Determination of elementary composition in borosilicate waste glasses containing uranium with PGAA spectroscopy**	*Proposal No.* PGAA- *Local contact*
Principal proposer: E. Veress *Experimental team:* M. Fábián, E. Sváb, SZFKI; E. Veress, Cluj, Romania, Zs. Révay, IKI		*Date(s) of Exp.* April 2006 *Date of Report*

Objectives

Alkali borosilicate glasses are of significant current interest as suitable materials for isolating host media for radioactive waste material storage (i.e. UO_3 or PuO_2) [1]. Structural characterization of these glasses is essential for understanding of glass durability. We are motivated in the neutron diffraction structure study of multi-component borosilicate waste glasses added with uranium. For modelling of the neutron diffraction pattern the knowledge of the elemental composition of the contributing elements is essential, therefore we applied for PGAA measurements.

Results

The samples with the general composition of $70wt\%[(65-x) SiO_2 \cdot xB_2O_3 25Na_2O5BaO \cdot 5ZrO_2] +30wt\%UO_3$, where x= 5-20 mol% were prepared in a similar manner as described in our previous report (see also [2,3]). Boron was isotopically enriched in [11]B (99.6%) in order to reduce the influence of the high neutron absorption of [10]B present in natural boron.

The elementary composition of the specimen was verified by prompt gamma activation analysis, the results are tabulated in Table 1.

Table 1. Elemental composition (at%) of the multi-component glasses with uranium $70wt\%[(65-x)SiO_2 \cdot xB_2O_3 \cdot 25Na_2O \cdot 5BaO \cdot 5ZrO_2]+30wt\%UO_3$, measured by PGAA method. (The relative errors are indicated in brackets).

Element	Elemental composition (at%)			
	SiBxNaBaZrUO			
	x=5	**x=10**	**x=15**	**x=20**
Si	15.27(2)	14.4(2)	15.99(2)	11.13(2)
B	3.43(3)	5.97(2)	9.10(1)	13.7(1)
Na	12.76(2)	12.7(2)	11.8(2)	8.17(1)
O	61.05(0.5)	59.84(0.5)	55.5(0.4)	61.1(0.5)
Ba	1.34(3)	1.40(4)	1.23(4)	0.55(15)
Zr	2.81(5)	2.45(7)	2.96(6)	2.3(8)
U	3.11(2)	3.14(4)	3.3(3)	3.05(3)

References

[1] K.S. Chun, S.S. Kim, C.H. Kang, *Journal of Nuclear Materials*, **298** (2001) 150.
[2] M. Fábián, E. Sváb, Gy. Mészáros, Zs. Révay, Th. Proffen, E. Veress, *J. Non- Cryst. Solids* **353** (2007) 1941.
[3] M. Fábián, E. Sváb, Gy. Mészáros, Zs. Révay, Th. Proffen, E. Veress, *J. Non-Cryst. Solids* **353** (2007) 2084.

Objectives

Due to their diverse practical applications and fundamental scientific importance, sodium-borosilicate glasses belong to the most investigated disordered systems. In order to obtain new structural characteristics on the short- and medium range order of theses glasses we have undertaken a combined neutron-, x-ray and reverse Monte Carlo modelling study. For data treatment the elementary composition of the specimens is essential, therefore we have applied for PGAA measurements.

Results

We have synthesized by melt quench technique glassy samples with composition $(75-x)SiO_2 \cdot xB_2O_3 \cdot 25Na_2O$ where x= 5, 10, 15, 20 mol%. The raw materials used were all of p.a. grade, and boron was isotopically enriched in ^{11}B (99.6%). The melted mixture was kept at 1450° C for 2 h, during which the melt was periodically homogenized by mechanical stirring. Thereafter, the melt was cooled to the pouring temperature, 1400°C, and kept there for 30 min. Finally, it was quenched by pouring the melt on a stainless steel plate.

The elemental composition of the specimens was verified by PGAA spectroscopy using cold neutrons at the Budapest research reactor. The results are given in Table 1.

Table 1. Elemental composition (at%) of glassy $(75-x)SiO_2 \cdot xB_2O_3 \cdot 25Na_2O$ specimens. (The relative errors are indicated in brackets)

Element	Elemental composition (at%)			
	SiBxNaO			
	x=5	x=10	x=15	x=20
Si	21.01(1.7)	18.42(1.8)	15.98(1.8)	14.19(1.9)
B	4.76(1)	8.49(1)	12.1(0.9)	14.81(0.9)
Na	16.69(0.5)	15.64(1.3)	14.49(1.4)	13.56(1.4)
O	57.53(0.5)	57.43(0.5)	57.4(0.4)	57.43(0.4)

Future prospects

Neutron- and x-ray diffraction experiments on these materials are in progress.

Objectives

To determine the compositions of environmental and nutritional samples and compare them to NAA results.

Results

Environmental and nutritional samples were analyzed using Compton-suppressed PGAA. Filters and barks were analyzed as sampled; the other samples were freeze-dried, ground to a powder, and put into hand-made, small Teflon bags.

Element		Teflon (blank)	Teflon (PM2.5)	Water	Lettuce	Lichen	Pinus bark	Platanus bark
H	(%)	1.46(3)	1.82(3)	0.84(5)	8.9(2)	4.11(9)	5.14(3)	5.27(5)
B		1.6(6)	2.9(5)	n.d.	41.2(2)	17.9(9)	4.11(3)	15.7(5)
C	(%)	29(5)	33(4)	n.d.	72(1)	33(10)	48(3)	43(5)
N	(%)	n.d.	n.d.	n.d.	n.d.	0.9(11)	n.d.	n.d.
O	(%)	n.d.	n.d.	n.d.	n.d.	57(7)	44(4)	43(7)
F	(%)	67(2)	63(2)	n.d.	n.d.	1.8(19)	1.4(7)	5.5(7)
Na		n.d.	n.d.	38%(2)	0.31%(6)	0.34%(10)	30(20)	170(14)
Mg	(%)	n.d.	n.d.	n.d.	1.6(12)	n.d.	n.d.	0.17(13)
Al	(%)	2.4(4)	1.3(6)	n.d.	n.d.	0.20(16)	0.64(4)	0.82(7)
Si	(%)	n.d.	n.d.	n.d.	0.4(19)	0.38(11)	0.112(5)	n.d.
P	(%)	n.d.	n.d.	n.d.	1.1(10)	n.d.	n.d.	n.d.
S		n.d.	n.d.	n.d.	0.69%(4)	0.14%(10)	320(6)	210(15)
Cl		70(12)	380(4)	55%(2)	2.75%(2)	0.31%(9)	114(4)	115(6)
K		n.d.	n.d.	2.3%(2)	11.3%(2)	0.15%(10)	350(5)	350(8)
Ca	(%)	n.d.	n.d.	4(29)	1.17(4)	1.26(10)	0.39(4)	0.68(6)
Ti		n.d.	n.d.	n.d.	140(13)	100(11)	28(11)	n.d.
V		n.d.	n.d.	n.d.	100(24)	n.d.	n.d.	n.d.
Mn		n.d.	n.d.	n.d.	n.d.	60(15)	23(10)	48(10)
Fe		n.d.	n.d.	n.d.	n.d.	0.11%(12)	500(7)	0.07%(13)
Cu		n.d.	n.d.	n.d.	n.d.	n.d.	50(20)	n.d.
Cd		0.8(17)	0.9(26)	n.d.	0.6(16)	n.d.	0.06%(19)	n.d.
Sm		n.d.	n.d.	n.d.	n.d.	0.12(18)	n.d.	n.d.
Gd		n.d.	n.d.	n.d.	n.d.	0.17(11)	n.d.	n.d.
Pb	(%)	n.d.	n.d.	n.d.	n.d.	0.8(12)	n.d.	1.1(18)
Total	(%)	99.9	99.2	100.1	100.2	100.5	99.9	99.7

Table 1. Element concentrations in environmental and nutritional matrices. All data in mg.kg^{-1} dry weight, except otherwise indicated (%); uncertainties within brackets are in %. n.d: not determined.

Reference

B N C Experimental Report	*Experiment title* **Monitoring hydrogenation of alkynes with in situ PGAA**	*Proposal No.* *Local contact* Zs. Révay
Principal proposer: D. Teschner – Fritz-Haber-Institut der Max-Planck-Gesellschaft, Faradayweg 4-6, D-14195 Berlin, Germany *Experimental team:* Zs. Révay, J. Borsodi, L. Szentmiklósi – Institute of Isotopes-HAS D. Teschner – Fritz-Haber-Institut		*Date(s) of Exper.* Oct. 09-14 2007 June 13-16 2006 *Date of Report* 02-27-2009

Objectives

To monitor the hydrogen content inside a catalytic reactor.

Results

Alkynes can be selectively hydrogenated into alkenes on solid palladium catalysts. This process requires a strong modification of the near-surface region of palladium, in which carbon (from fragmented feed molecules) occupies interstitial lattice sites. In situ X-ray Photoelectron Spectroscopic (XPS) measurements under reaction conditions indicated that much less carbon was dissolved in palladium during unselective, total hydrogenation.

Additional studies of hydrogen content using in situ prompt gamma activation analysis, which allowed us to follow the hydrogen content of palladium during catalysis, indicated that unselective hydrogenation proceeds on hydrogen-saturated β-hydride, whereas selective hydrogenation was only possible after decoupling bulk properties from the surface events. Thus, the population of subsurface sites of palladium, by either hydrogen or carbon, governs the hydrogenation events on the surface.

Pd metal (beta-hydride)   **Pd-C surface phase**

Future prospects

Further studies of catalysis using in-situ PGAA.

References

Teschner, D., J. Borsodi, A. Wootsch, Z. Revay, M. Havecker, A. Knop-Gericke, S.D. Jackson, R. Schlogl, Science, **320** (2008) 86.

Revay, Z., T. Belgya, L. Szentmiklosi, Z. Kis, A. Wootsch, D. Teschner, M. Swoboda, R. Schlogl, J. Borsodi, and R. Zepernick, Analytical Chemistry, **80** (2008) 6066.

B N C Experimental Report	Experiment title The real operational conditions of helicopter rotor blades applying Non-DestructiveTesting (NDT) technologies in the frame of HU-AVT-01 project	Proposal No. Rad-3/06, *Local contact* M. Balaskó
Principal proposer: Maj. Zoltan Vigh, Ministry of Defence,Hungary, Lt. Col. Dr. Trivissono Giovanni and Major Dr. Dati Enrico, Italian Air Force, 1 st Division of Logistic Command,Chemical Department *Experimental team:* M. Balaskó		*Date(s) of Exp.* 03-05. 2006. *Date of Report* 10. 01. 2007.

Objectives

To combine the results of the different kinds of NDT methods to study the life conditions of helicopter rotor blades. Identification of failures gained during ultrasound testing, thermography and X-ray radiography (XR) on the reference objects by neutron radiography (NR) investigation.

Results

The special reference samples with the generated errors were produced by the Hungarian experts.

The experiments partly were performed at the Dynamic Radiography Station (DRS) of the Budapest research reactor where the necessary developmental work with respect to the size of the rotor blades were carried out. As a result the reconstructed DRS can inspect 10 m long and 0.7 m wide targets (the weight is approx. 140 kg) by NR,XR. The other NDT inspections were performed at the laboratory of Italian Air Force, 1 st Division of Logistic Command,Chemical Department.

Neutron Radiography (NR) for detecting and visualizing irregularity and defects in the composite structure. NR method is sensitive in revealing the hydrogen (water) content its distribution in the rotor blades. X-ray Radiography (XR) is a complementary and useful tool for detecting the structural integrity of the metal parts of the rotor blades. Thermographic inspection(ThI) was conducted in two ways: monolateral (camera and heater on the same side) and bilateral (camera and heater at opposite side). This method allowed to detect water ingestion, sealant and metal insertion and cut of the surface.Ultrasonic evaluation (UT), a preliminary of the pulse echo technique showed no application: the first echo and its multiple, caused by the back surface of the upper skin, masked all the other indications, and a signal from the backside of the opposite skin was not detectable. The through-transmission technique, on the other hand, allows the detection of metal and sealant insertion and was the only method to find the disbound.

Refrences

M.Balaskó,E.Svab,I.Veres,Gy.Molnár: Classification of defects in honeycomb composite structure of helicopter rotor blades, Nuc. Inst. and Method A542, issues1-3, 21 April 2005, pp. 45-51.

Future prospects

The project was finished by RTO FINAL REPORT of the HU-AVT-01 project in 2006.

B N C Experimental Report	Experiment title **Development of heated sample holders by Dynamic Neutron Radiography**	Proposal No. Rad-5/07, *Local contact* M. Balaskó
Principal propoe: Házi Gábor: MTA KFKI AEKI *Experimental team:* M. Balaskó, L.Horváth and P.Tóth		*Date(s) of Exp.* 07-09. 2006. *Date of Report* 10. 01. 2007.

Objectives

The difference kind of the heating procedures were developed on the samples regarding on the homogeneous distribution of the temperature. The useable sealing configurations were verified on the samples in normal operating mode and in "lost-off-cooling agent" mode. The visual information about the water extension and the changing of the water vapour density was served by dynamic neutron radiography (DNR).

Results

The supercritical water has an extraordinary feature. Its density is changing dramatically above 370 0C (~22 MPq).This basic event is available to study by (DNR). Four pieces sample holder were designed. The first two (KV-1 and KV-2) were made from high solidity structural steel. Both of them have 10 mm wall thickness and KV-1 contains of a 10 mm hole while KV-2 contains of 20 mm whole. They have concentric worm of screw plug system (M28 X 1,5) with metal sealing ring. The third sample holder (GR-2) was made from GR-2 type titanium alloy. Its dimensions were the similar to KV-2 but the wall thickness was 7 mm only. The application of the titanium alloy gave double advantages. The first was the higher solidity reduced the wall thickness gave better quality radiography picture. Additional the total macroscopic cross section of the titanium is the half of the iron only. It is meaning a better quality neutron radiography picture also. Later the plug system was modified to a flange style fixing with 8 X M6 screws (GR-2P). These three versions of the sample holder applied an up and down thermo-coax heating system for the good DNR visualisation of the middle part of the sample. However the gradient of the temperature distribution was a little much to the middle from the ends (50-60 0C on KV-2 and GR-2). The fourth version of the sample holder was made from GR-5 titanium alloy. Its dimensions were the similar to GR-2P but it contains a full-length thermo-coax heating system and its flange style plug system was fixed by 8 X M8 titanium screws. Its identification is GR-5H. The Fig.1. shows the picture of GR-5H and GR-2P sample holders

Figure 1. Flange style closing system on GR-5H and GR-2P sample holders

Future prospects

The work will be continued by the study of the behaviour of the supercritical water by DNR.

Objectives

We want to study the features of the supercritical water (SCW). We have to approach this task on versatile mode. Very important to know the distribution of the inside temperatures and the inside pressure to the understanding of the density changing which is measured by dynamic neutron radiography.

Results

The GR-5H sample holder was equipped by a full-length thermo-coax heating wire. Some plug constructions were designed to it to optimize for our needs. In the first version the temperature distribution inside of it was measured by three "K" type Ni- NiCr thermo-coax thermocouples on the middle from the ends (3-4 °C), this parameter outside of it was measured by three "J" type (Fe-Konst.) thermocouples on the middle from the ends (3-4 °C). It has a special inner heating coil for modelling the core of 4th generation reactor. It is the GR-5HB3t arrangement. As it is shown in the Fig. 1. by neutron radiography (NR) picture of Imaging Plate technique. The second version of the plug was designed for the scientific cognition of the inside temperature distribution of GR-5H. The temperatures were measured by eight (T1,...T8) "K" type thermo-coax thermocouples from the upper part to down. These thermo-couples were supported by six pieces spacer discs. Their diameters were 18 mm with a 10 mm whole in the middle. They are made from rust-proof material. The outside temperature of the GR-5H were measured by two "J" type thermocouples on up and down (T9 and T10). It is the GR-5H8t arrangement which is shown in Fig.2. by a Dynamic neutron radiography (DNR)picture. Both of the plugs were equipped by a pressure tube to measure the inside pressure of the arrangements.
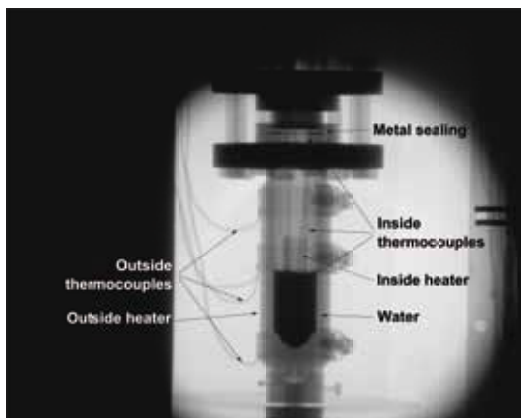
Fig.1. NR picture of GR-5HB3t
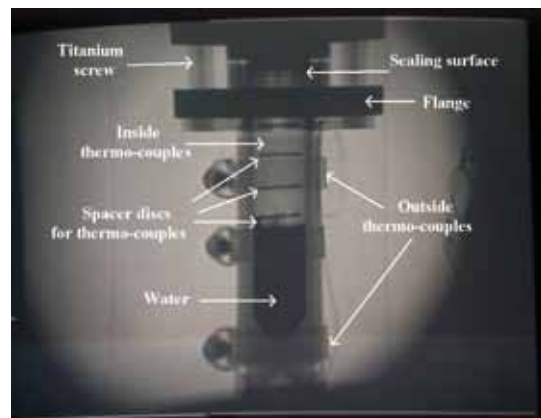
Fig. 2. DNR picture of GR-5H8t

Future prospects

The work will be continued for the repeatable measurement procedure.

Objectives

The Dynamic Neutron Radiography (DNR) gives a possibility to observe the changing of the density of the water in extreme conditions (Tc ~ 374 oC,   Pc ~ 221 bar, rc ~ 0,32 gcm3). The dynamic parameters of the changing were estimated by QUANTEL image processor.

Results

The aim of the DNR investigation was to give visual information about the behaviour of the two phases of the water in the sample holder. The first of all the DNR picture of the empty sample holder was exposed. It was very important for the high level evaluation work which is used the Shading mode subtracting this picture from the actual exposed picture. The temperature of the GR-5H was increased step by step.
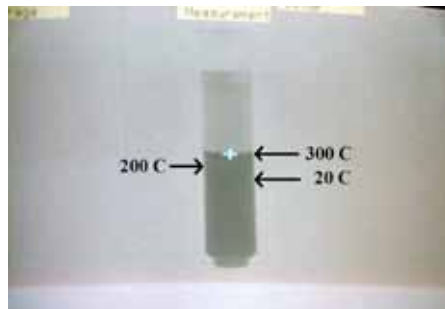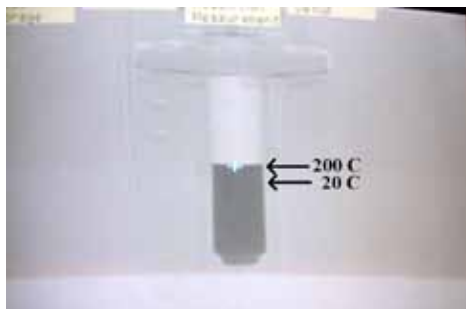
Fig. 1/a. SH picture of GR-5H at 200°C

Fig. 1/b. SH picture of GR-5H at 300°C
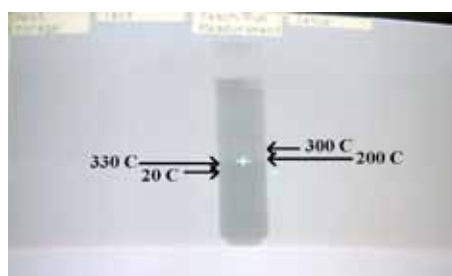
Fig. 1/c. SH picture of GR-5H above 330°C

Fig.1/d. SH picture of GR-5H at 374°C

The water level increased slowly and hardly changing the density of the water vapor area above the water level until 200 °C, as it is shown in Fig. 1/a. Above this temperature the water level continued its increasing and the density of the water vapor area began to increase on ~300 °C, as it is shown in Fig. 1/b. Above 330 °C the water level began to reduce, and the density of the water vapor area was increased, as it is shown in Fig. 1/c. At 374°C the water disappeared and the all volume of the sample became homogeneous, as it is shown in Fig. 1/d. This is the supercritical state of the water (SCW).

Future prospects

The work will be continued for the versatile measurement of the properties of SCW.

Objectives

Important task to solve the repeatable measurement conditions of the supercritical water properties.

Results

A unique equipment was designed for the repeatable conditions of the measurement procedure. The well equipped measuring frame is available for the wide range investigation of the supercritical water phenomena including the loss-of-coolant type accident also. It has a water cooled double Peltier block to freeze the water during the evacuation of the sample holder above the water level. After the evacuation the hermetical valve is closed and the water injected in the high pressure area. This area contains a pressure transmitter for measuring the pressure after the temperature is increased above 200°C and opened the hermetically valve. Naturally the Peltier block is moved away before the heating procedure is started. Another important element is situated in the high pressure area this is a remote control ventilating valve which is able to stabilize the pressure independent from the temperature. This valve is designed for modelling the conditions of a loss-of-coolant type accident. The measuring frame is able to collect the escaped vapor after the condensation in the pressure balancing tank. The functional model of the measuring frame is shown in Fig.1.
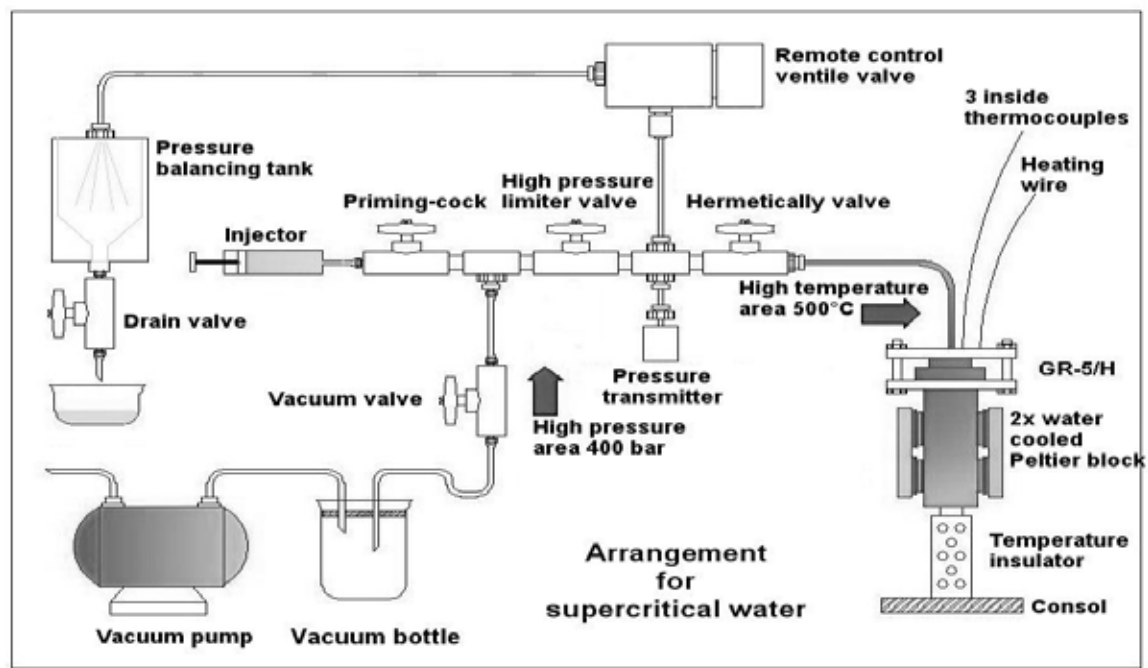
Fig. 1. Functional model of the measuring frame

Future prospects

The work will be continued to combine of the DNR measurements with other non-destructive testings.

Objectives

Above a certain wall thickness (more, then 20 mm) of the investigated sample holders, the dynamic neutron radiography (DNR) will be not able to give information about the behaviour of the super critical water (SCW). Additional two other Non-Destructive Testing (NDT) methods were used to complete the inspection technology, as vibration diagnostics (VD) and acoustic emission (AE).

Results

The effect for vibration diagnostics was detected by a 4366 type accelerometer using a 2635 type charge sensitivity preamplifier. Its audio signal was registered by one audio band of S-VHS video recorder. The acoustic emission events were detected by D9203 type sensor stored and evaluated by NEZ-220 type Defectophone unit.

Simultaneously the dynamic neutron radiography, vibration diagnostics and acoustic emission were used in the observation of the behaviour of the supercritical water. The VD and AE methods are able to give important information about the inner events of the sample holders for supercritical water. These methods were used simultaneously with DNR. They have contributed our error analysis when the water vapour escaped from the sample holder on high temperature and on high pressure. The sketch of the arrangement is shown in Fig. 1.

Future prospects

The work will be continued for the modelling of the "loss-off-coolant agent" type accident.

Fig. 1. Arrangement of the combined NDT methods

Objectives:

The goal was to determine the appearing internal stresses caused party by the surface brazed thermocouple around the brazing and partly by the enclosed water during heating on the brazed free part of the sample holder. Doing this the shift of the Fe(110) Bragg reflection has to be measured ones in the depths from the brazing surface on room temperature (RT) and once its temperature dependence on a brazed free part of the sample.

Results:

The measurements have been carried out in the above-mentioned sequence. Figure 1 shows the RT Bragg peak shift caused by the brazing. In the vicinity of the brazing not only stresses can cause the peak shift but also the penetration of the thermocouple materials into the iron can cause structure changes. It means that in the vicinity of the brazing the internal stresses cannot be calculated properly. However, further on the penetration can be neglected and the internal stresses can be calculated. The maximum stress is 18 MPa compression.

Figure 2 shows the (110) Bragg peaks measured on RT (red) and at 400 C (black). There are two effects that contribute to the peak shift. A./ The first one is the simple thermal expansion – easy to calculate and to subtract. B./ Stress caused by the increasing water pressure. The calculation gives 101 MPa tension caused by the hot water. Fortunately, this tension is below the Yield stress of iron. It means that the measurements verified the sizing of the holder and it is suitable for the additional supercritical water investigations.
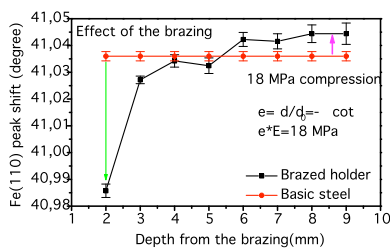
Figure 1. **Influence of the brazed thermocouple (RT). The peak shift of the (110) Bragg reflection of the steel holder. The green arrow shows the first appreciable measurement from the brazed surface (sampling volume =2x2x4 mm³).**

Figure 2. **The (110) peak position displacement caused both by the thermal expansion of the steel and the increasing pressure of the water (sampling volume =2x2x10 mm³).**

Future prospects:

Although this series of measurements qualified the steel holder, further investigations are also needed to control the effect of cyclic heating.

In the meantime titanium containers were also produced that will need similar investigations. The starting material, as reference, has been investigated already.

Reference:

The results were presented on the 7. Intern. Conf. On NDE in relation to Structure Integrity for Nuclear and Pressurized components, Yokohama, March 12-14 2009

B N C **Experimental Report**	*Experiment title* **Complex Radiography inspections for the CODEX project**	*Proposal No.* Rad-11/06, *Local contact* M. Balaskó
*Principal proposer:*Z. Hózer *MTA KFKI AEKI* *Experimental team:* M. Balaskó and L.Horváth		*Date(s) of Exp.* 11-12. 2006. *Date of Report* 01. 01. 2007.

Objectives

The complex radiography inspections were produced on the Dynamic Radiography station for the mock-up of a damaged fuel element. Where the gamma- (GR) and X-ray radiography (XR) were used to study the inner structure of the inspected, damaged CODEX sample. The energy of the gamma radiation was 8,2 MeV from the reactor and its dose rate was 8,3 Gy/h. The source of the X-ray radiation was MXR 300 type portable, industrial generator. The applied power was 275 kV and 3 mA.

Results

The CODEX sample was packed in a polivinil-chloride (PVC) tube, its diameter was 62 mm and its length was 1050 mm. The inside of the tube was filled up by artificial resin to fix the position of the sample. The radiography pictures were exposed in horizontal position of the PVC tube. A led marker system was used for the easier identification of the errors. Every 5 cm was marked by led numbers from zero to 105 cm. BAS 20 X 40 MS type imaging plate was used as detector both for gamma- and X-ray radiography. BAS 2500 type scanner was used to read the plates. The evaluation work was contributed by AIDA software. The sample was divided in three (A,B and C) bands. The "A" band was from 0 to 350 mm-, "B" band was from 320 to 670 mm and "C" band was from 670 to 1020 mm. Every band was exposed in 0º, 45º and 90º rotations. The
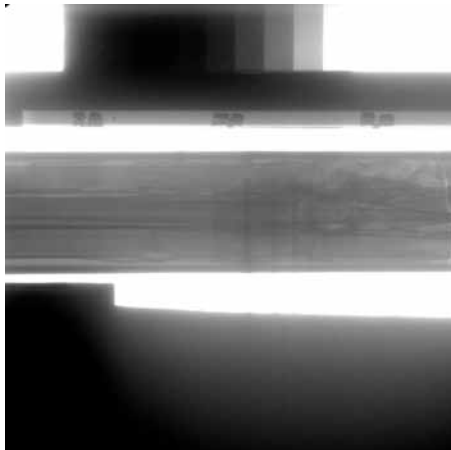
Fig.1. XR picture of the damaged sample after the experiment

Fig. 1. shows the damaged part of the fuel element mock-up after the experimental procedure. On the high resolution XR pictures were very well visible the cracks of the artificial resin in the PVC tube and the collapses of the fuel element imitations.

Future prospects

The project will be continued on the next year with another sample holder of the CODEX project.

Objectives

The X-ray radiography (XR) inspection of the damaged CODEX –CT-2 boundle was produced on the Dynamic Radiography station. Where the source of the X-ray radiation was MXR 300 type portable, industrial generator. The applied power was 275 kV and 3 mA. The focus distance was 1250 mm. The exposure time was 60 sec.

Results

The XR was used to study the inner structure of the inspected, damaged CODEX sample. It was packed in a polivinil chloride (PVC) tube, its diameter was 62 mm and its length was 1050 mm. The inside of the tube was filled up by artificial resin to fix the position of the sample. The radiography pictures were exposed in horizontal position of the PVC tube. A lead marker system was used for the easier identification of the errors. Every five centimetres was marked by lead numbers from zero to 105 cm. BAS 20 X 40 MS type imaging plate was used as detector both for XR. BAS 2500 type scanner
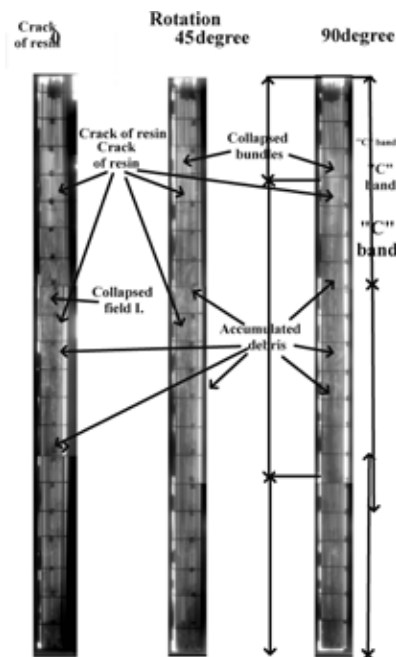
Fig. 1. The composed picture of the whole sample in 0º, 45º and 90º rotations.

was used to read the plates. The evaluation work was contributed by AIDA software. The sample was divided in three (A,B and C) bands. The "A" band was from 0 to 350 mm-, "B" band was from 350 to 650 mm and "C" band was from 650 to 1020 mm. Every band was exposed in 0º, 45º and 90º rotations.

Future prospects

The project was finished by the Final Report of CODEX-CT-2 project.

Objectives

The versatile beam radiation of the Dynamic radiography station was available to begin the experimental work for the gamma laser pump. The Super Liliput type portable, industrial X-ray generator was used as a source of the radiation.

Results

A special lead tower was designed for holding the ^{99}Tc preparation. The activation of the preparation was 0,13 TBq, decay time was 6 hours and its energy was 142 keV, the level energy of the generated electrons was 181 keV. The lead tower has a remote controlled closing system operated by pneumatically. The neutron radiography picture of the lead tower is shown in Fig. 1. The applied detector was the ND 200X250 type Imaging Plate which was processed by BAS 2500 type scanner and AIDA software. The exciting energy was served by the Super Liliput type portable, industrial X-ray generator on 140 keV; 5 mA power.
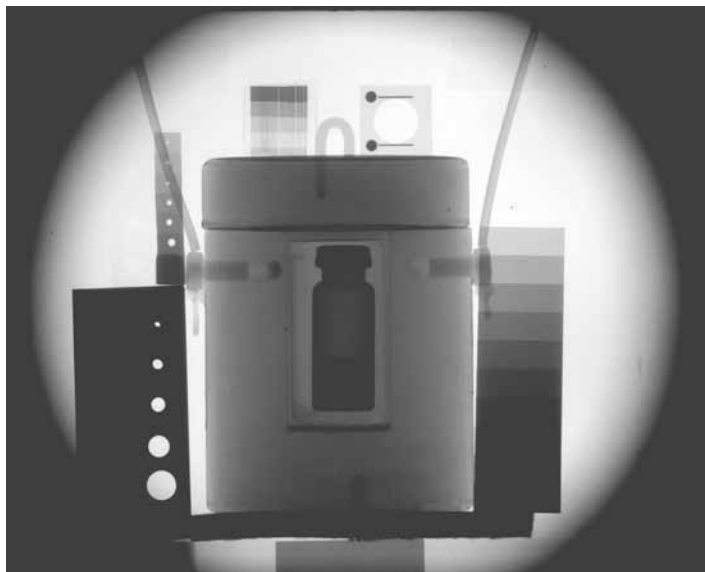
Fig.1. Neutron radiography picture of the
lead tower with the ^{99}Tc preparation

The intensity of the X-ray generator was not sufficiently to the successful measurement

Future prospects

The project was finished.

B N C Experimental Report	*Experiment title* **Complex radiography investigation of the rotor blade of Kamov – 26 type helicopter**	*Proposal No.* Rad-2/06, *Local contact* M. Balaskó
Principal proposer: Rep.szer. Kft. *Experimental team:* M. Balaskó		*Date(s) of Exp.* 02-04. 2006. *Date of Report* 10. 01. 2007.

Objectives

In order to inspect the possible defects in the rotor blade of Ka-26 helicopter combined neutron- and X-ray radiography investigations were performed at the Budapest Research Reactor. The rotor blades were about 6,5 m long, their wide were 0,25 m, therefore the radiography images were taken in several well-adjusted segments, and a special program was developed to reconstruct the entire radiographic image from the individually segmented images. Several types of defects were discovered using neutron radiation: resin-rich or starved areas at the core-honeycomb surfaces, in homogeneities in the adhesive filling and water percolation at the sealing interfaces of the honeycomb sections. The localization of structural metal parts were analysed by X-ray radiography.

Results.

Defects can be external or internal to the structure. External defects can be visually inspected, such as dimensions, finish, and warped. Internal defects were discovered by radiography techniques. The description of the measurement was very prudent regarding the dangerous nature of the radiation material testing both neutron- and X-ray radiography (NR and XR). In the schedule of the inspection the first step was an NR inspection in dry condition, the second step was the XR test. Three pieces of rotor blades were verified by this inspection technology. The simple arrangement of the 80 pictures in 2 horizontal rows and 40 vertical columns would be not enough to evaluate a whole radiography picture of the rotor blades with good quality. A method was applied to compose the precise well determined composition of the whole rotor blade surface. Its name was   Rotor Puzzle method. The Fig. 1a. and Fig. 1.b shows the XR and NR picture of the end element of a Ka-26 helicopter rotor blade. The NR picture is able to give distinguishable information about the flatter weight of the blade which is made from steel and lead.
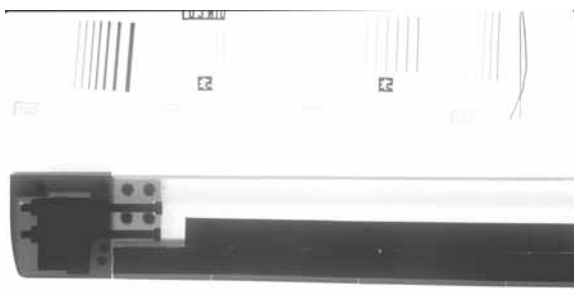
Figure 1.a.	Figure 1.b.
End of the Ka-26 helicopter rotor blade by XR	End of the Ka-26 helicopter rotor blade by NR

Future prospects

The complex radiography testing is able to take part of the qualification work of the rotor blade of the Ka-26 helicopters.

Objectives

The low energy X-ray radiography (XR) is available to verify the difference between the hydraulic balance ball of the helicopters. The balls were made from gum. The source of the X-ray radiation was a Super Liliput portable X-ray generator (140.kV; 5 mA). The imaging plate technique was used as the detector of the XR pictures.

Results

Two groups of the hydraulic balance ball of the helicopters were inspected. The first ones were the original production of the helicopter factory. The second ones were copy. Both groups were made from the same category gum. The outside geometrical dimensions of them were the same. The used parameters of the exposed pictures were 40 kV; 2 mA on 60 sec. The applied imaging plate was MS 25X20 type. The information was registered by the BAS 2500 type scanner. The evaluation work was contributed by AIDA software. The Fig. 1. shows the XR picture of the original hydraulic ball. The XR picture of the copy ball is shown in Fig. 2. On the figures the directions of the arrows are able to show the distinguishable radiuses of the material above the vulcanizations. These little differences were the cause of the splitting of the hydraulic balls.
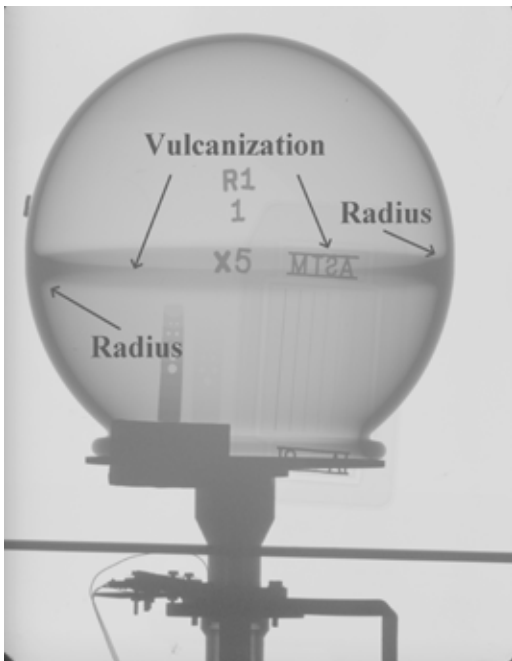
Fig.1. XR picture of the original hydraulic ball
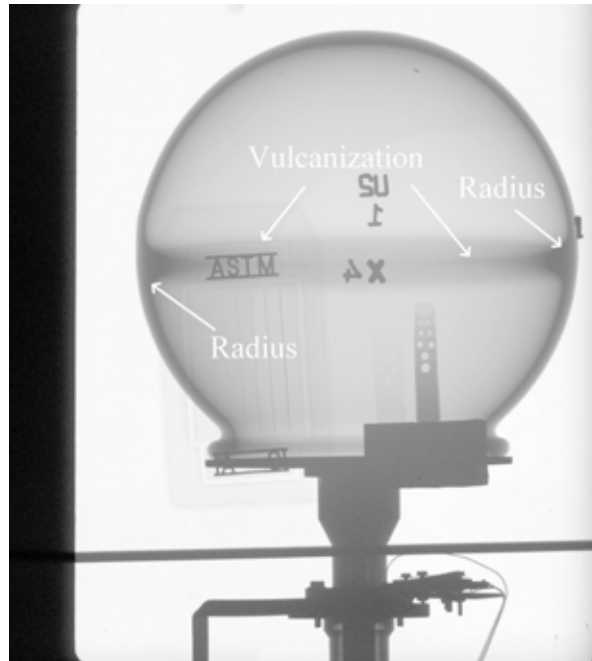
Fig. 2. XR picture of the copy hydraulic ball

Future prospects

The work was finished by the Report for the proposer.

Objectives

In another proposal (BRR 201), Prompt Gamma Activation Analysis (PGAA) of various Late Roman Iron Age to Medieval Western European iron artefacts and production remains was proposed. The aim of the PGAA experiments was to determine chemical composition - first of all P, As and Mn content - of the bulk of these precious archaeological objects. From the composition data, together with previous TOF-ND experiments at ISIS, we hope to obtain important information on early iron metallurgy.

Since all of the iron swords and knives to be analysed are heavily corroded, we proposed X-ray radiography of the objects, prior to PGAA, in order to identify points where metal is preserved.

Results

X-radiography (XR) of five archaeological iron swords and two knives was performed at the Dynamic n/γ Radiography Station at BNC. The experiments were designed and managed by Márton Balaskó and L. Horváth. The high voltage of X-ray generator and the exposure time was calculated and adjusted so as to achive the best quality images. The images were recorded on a photo-luminescent imaging plate, type MS 25X40 and processed by BAS 2500 reader and AIDA software. The experimental details are in the table. Based on the images, it was possible to identify the points worth analysing by PGAA later.

The XR picture of RH 333A sword is shown in Fig. 1.

	Object	IP number	Energy	Exposure time
1	Rh651B Knife	088	80kV, 3mA	2'
2	Rh248A Knife	088	80kV, 3mA	2'
3	Rh814A1x Sword	3093	100kV, 3mA	2'
4	Rh814A1x	3093	100kV, 3mA	2'
5	Rh333ASword	3093	90kV, 2mA	2'
6	Rh333A	3093	100kV, 2mA	2'
7	Rh660CSword	3093	100kV, 2mA	2'
8	Rh660C	3093	90kV, 2mA	2'
9	Rh796ASword	3093	85kV, 2mA	2'
10	Rh796A	3093	70kV, 2mA	2'
11	Rh534ASword	3093	90kV, 2mA	2'
12	Rh534A	3093	90kV, 2mA	2'
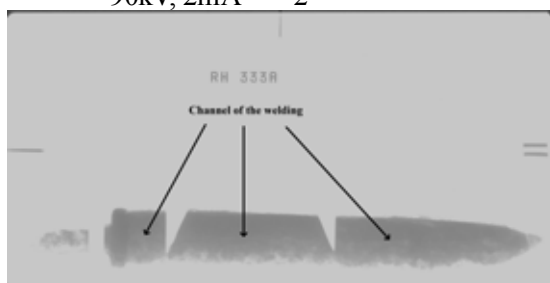
Fig. 1. XR picture of RH 333A sword

Future prospects:

The project is continued time by time as it is required by the restoration work.

B N C **Experimental Report**	*Experiment title* **Investigation of the interaction between spring and the wall of Zr tube by combined Radiography technique**	*Proposal No.* Rad-13/07, *Local contact* M. Balaskó
Principal proposer: Z. Hózer MTA KFKI AEKI *Experimental team:* M. Balaskó and L. Horváth		*Date(s) of Exp.* 05-10. 2007. *Date of Report* 01. 01. 2008.

Objectives

The versatile combination of the radiation beams gave the possibility to investigate the interaction between the spring and the wall of the Zr tube on the Dynamic Radiography station. The X-ray radiography (XR) is able to inspect the geometric distortion of the inner structure of the samples before and after the heat-treatment. The neutron radiography (NR) is able to observe the potential possibility of the efficiency of the alloying between the two parts of the mock-up after the heat-treatment. The applied X-ray source was a Super Liliput portable industrial X-ray generator (140 KeV; 5 mA). The radiography pictures were detected by MS 25X20 and ND 25X20 imaging plates using a BAS 2500 scanner to record the information. The evaluation work was contributed by the AIDA software.

Results

Some special mock-ups of the end part of a fuel element were made. The springs were made from "R" and "S" type steels were alloyed a few Mn and Si. The exposure power was 60 kV; 2mA in 30 sec for the XR
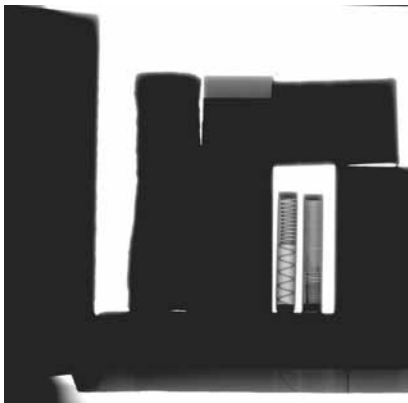
Fig. 1. XR picture of the two springs
after the heat-treatment

Fig. 2. NR picture of the two springs
after the heat-treatment

pictures. The XR picture of the two springs is shown in Fig.1. after the heat-treatment. The exposure time of the NR pictures were 60 sec using 100 mm Pb filter. The NR picture of the two springs is visible in Fig. 2. after the heat-treatment. Both radiography techniques were not able to find any geometric distortion and any disordering on the radiography pictures.

Future prospects

The project was finished by the Final Report of the OAH/NBI-ABA-96/06 contract.

B N C	Experiment title	Proposal No.
Experimental Report	**The short- and medium range structure of vitrous v-B$_2$O$_3$ glass**	PSD-1
		Local contact
		M. Fábián
Principal proposer: E. Veress *Experimental team:* M. Fábián, E. Sváb, Gy. Mészáros, SZFKI; E. Veress, Cluj		*Date(s) of Exp.* January 2006. *Date of Report* 15. 01. 2009.

Objectives

Vitreous **v-**B$_2$O$_3$ is a classical glass forming material due to its several technological applications as key component in many kinds of commercial glasses. Though the several studies gave valuable information on the structure of **v-**B$_2$O$_3$ glass, there are still important unresolved details. For example, it is generally accepted that the molecular building units are the planar 3-fold oxygen coordinated BO$_3$ groups with strong covalent bonding, however, the manner in which these units are connected to each other forming the network structure is question of debate in the literature.

The aim of this work is to gain new structural information from neutron diffraction experiment (ND) using the reverse Monte Carlo (RMC) modelling. Our ND measurement is extended up to high momentum transfer range, Q=30 Å^{-1} by combining the PSD data with those measured by the NPDF time-of flight spectrometer in Los Alamos National Laboratory [1], which made fine r-space resolution available for real space analyses.

Results

The **v-**B$_2$O$_3$ glassy sample was prepared by melt quench method, and it was isotopically enriched in ^{11}B (99.6%) in order to reduce the influence of the high neutron absorption of ^{10}B present in natural boron. By using reasonable constraints in the RMC simulation of the ND data, several important structural characteristic features have been revealed [2]. For illustration, the partial atomic pair-correlation functions are shown in Fig.1.
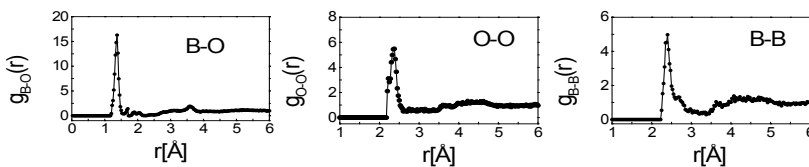
Fig. 1. Partial atomic pair-correlation functions obtained by RMC modelling for the v-B$_2$O$_3$ glass

Fig. 2. B-O network bond configuration
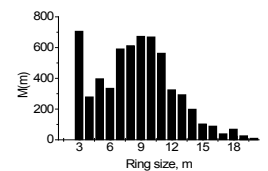
Fig. 3. Ring-size distribution

Figure 2 displays the B-O network bond configuration for 500 atoms (the RMC modelling was done for 5000 atoms). The ring size distribution, M(m), which characterizes the medium range structure of the glassy network is shown in Fig. 3 . It contains a maximum at m=3, which can be attributed to the boroxol ring (B$_3$O$_6$). The fraction of boron atoms forming boroxol ring is 12%, while the broad second maximum between 7–11-membered rings accounts for cc. 50% of the boron atoms. The tail of the distribution extends up to about 20-membered rings.

Future prospects

Publication is in progress

References

[1] Th. Proffen, S.J.L. Billinge, T. Egami, and D. Louca, *Zeitschrift für Kristallographie* **218** (2003) 132 and http://lansce.lanl.gov/lujan/instruments/NPDF/index.html

[2] M. Fábián, E. Sváb, Th. Proffen and E. Veress, subm itted to *J. Non-Cryst. Solids*

B N C **Experimental Report**	*Experiment title* **On the structure of 75Na$_2$O-25B$_2$O$_3$ glass**	*Proposal No.* PSD- 2 *Local contact* E. Sváb
Principal proposer: E. Veress *Experimental team:* M. Fábián, Gy. Mészáros ,E. Sváb, SZFKI , E. Veress, Cluj, Romania		*Date(s) of Exp.* *Jan-Febr 2006.* *Date of Report* 15. 01. 2009.

Objectives

Alkali borate glasses are classical glass forming materials due to their several technological applications as key component in many kinds of commercial glasses. For alkali borate glasses is widely accepted that the alkali ions, - in our case Na$_2$O - converts the trigonal BO$_3$ units into 4-fold oxygen coordinated tetrahedral BO$_4$ units, and the linkage of BO$_3$ and BO$_4$ forms superstructural units, however, the fine details of the network structure contains several open questions, like the fraction of BO$_3$/BO$_4$ units, the three-particle bond angle distributions, etc. The aim of our study to get new structural information on this glass.

Results

We have synthesized 75B$_2$O$_3$-25Na$_2$O glass by the conventional melt-quench technique. Neutron diffraction measurements have been performed in a relatively broad momentum transfer range, combining the data measured by the 'PSD' diffractometer (λ_0=1.069 Å) and by the time-of-flight 'NPDF' instrument [1] at the LANSCE pulsed neutron source. The structure factor has been measured over a broad momentum transfer range, 0.4-26 Å^{-1}, which made fine r-space resolution available for real space analyses. The reverse Monte Carlo (RMC) method [2] was successfully applied to calculate a possible 3-dimensional atomic configuration that is consistent with the measured structure factor. The convergence of the RMC simulation was very good and the final S$_{RMC}$(Q) matched fairly well the S$_{EXP}$(Q), as it is shown in Fig. 1.

The partial atomic pair correlation functions, nearest neighbour atomic distances, coordination number distributions, average coordination number values and the three-particle bond angle distributions have been revealed [3]. It was established that addition of 25 mol% Na$_2$O to *v*-B$_2$O$_3$ transforms 41% of the 3-fold oxygen coordinated boron atoms into 4-fold coordinated ones. The B-O peak is centred at 1.38 Å and a sub-peak appears at ~1.55 Å, these distances correspond to the B-O pairs forming BO$_3$ and BO$_4$ units, respectively. The O-O and B-B first neighbour distances are at 2.30 Å and 2.7 Å, respectively, as obtained from the partial atomic pair-correlation functions (see Fig. 2.).
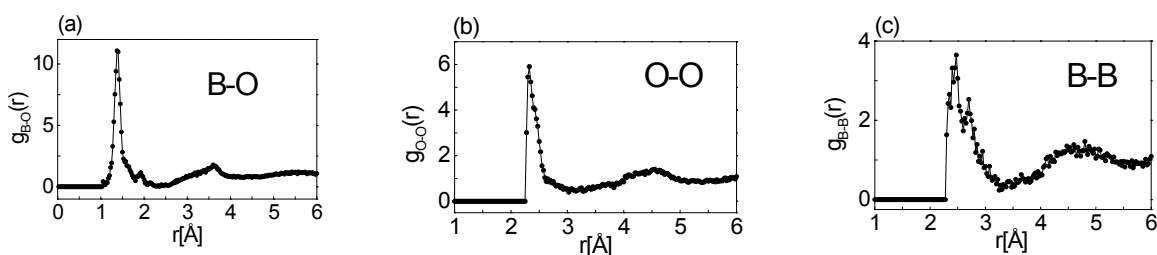
Fig. 2. Partial atomic pair-correlation functions obtained by RMC modeling.

References

[1] Th. Proffen, S.J.L. Billinge, T. Egami, D. Louca, *Z. Kristallogr.* **218** (2003) 132.
[2] R.L. McGreevy and L. Pusztai, *Molecular Simulation*, **1** (1988) 359.
[3] M. Fábián, E. Sváb, Th. Proffen and E. Veress, submitted to *J. Non-Cryst. Solids*

B N C Experimental Report	Experiment title **Diffraction measurements on sodium borosilicate glass system**	Proposal No. PSD- 3 *Local contact* M. Fábián
Principal proposer: E. Veress *Experimental team:* M. Fábián, Gy. Mészáros, E. Sváb, SZFKI; E. Veress, Cluj, Romania		*Date(s) of Exp.* April-May 2007 *Date of Report* 15. 01. 2009.

Objectives

Multicomponent alkali borosilicate glasses are generally accepted as proper High Level Waste isolating media [1], the radioactive elements become immobilized as part of the host material structure. We are involved in the research activity to synthesize new materials and to perform detailed structural study [2-4]. In the frame of this project we have prepared 3-component borosilicate glasses with the general composition of $(75-x)SiO_2 \cdot xB_2O_3 \cdot 25Na_2O$, where x= 5, 10, 15, 20 mol% and neutron diffraction measurements have been carried out with the aim to get information on the atomic structure.

Results

The glassy samples were prepared by melting the mixture of oxides in platinum crucible at 1300-1450°C, working in atmospheric conditions. The [11]B-isotope enrichment was 99.6%. Powder samples of about 3–4 g each for neutron diffraction measurements were prepared by powder milling of the quenched glasses in an agate mill. The glassy specimens were filled into vanadium scan of 8mm diameter (wall thickness 0.7mm), and they were measured by the PSD neutron diffractometer (λ_0=1.069 Å).

Correction and normalization procedures utilized to obtain the total structure factor, S(Q) from the measured pattern was described in our previous work [5]. Figure 1 shows the experimental S(Q) for the four compositions.

Future prospects

Extension of the momentum transfer range up to 30 Å^{-1} by time-of-flight neutron diffraction and by synchrotron based x-ray diffraction are underway.

References

[1] K.S.Chun, S.S. Kim and C.H. Kang, *Journal of Nuclear Materials* **298** (2001) 150.

[2] M. Fábián, E. Sváb, Gy. Mészáros, Zs. Révay, Th. Proffen and E. Veress, *J. Non-Cryst. Solids* **353** (2007) 2084.

[3] M. Fábián, E. Sváb, Gy. Mészáros, L. Kőszegi, L. Temleitner, E. Veress, *Zeitschrift für Kris. tallographie* **23** (2006) 461.

[4] M. Fábián, E. Sváb, Gy. Mészáros, Zs. Révay and E. Veress, *J. Non-Cryst. Solids* **353** (2007) 1941.

[5] E. Sváb, Gy. Mészáros, G. Konczos, S.N. Ishmaev, S.L. Isakov, A.A. Chernyshov, *J. Non-Cryst. Solids* **104** (1988) 291.

BNC _Experimental Report_	_Experiment title_ **Diffraction study of borosilicate waste glasses containing uranium**	_Proposal No._ PSD- 4 _Local contact_ M. Fábián
Principal proposer: E. Veress _Experimental team:_ M. Fábián, Gy. Mészáros, E. Sváb, SZFKI ; E. Veress, Cluj, Romania		_Date(s) of Exp._ April-May 2007. _Date of Report_ 15. 01. 2009.

Objectives

Alkali borosilicate glasses are of significant current interest as suitable materials for isolating host media for radioactive waste material storage (i.e. UO_3 or PuO_2). Structural characterization of these so called matrix (waste) glasses is essential for understanding of glass durability [1]. Here we investigate the structure of multi-component sodium borosilicate glasses added with UO_3, namely $70wt\%[(65-x) SiO_2 \cdot xB_2O_3 \cdot 25Na_2O \cdot 5BaO \cdot 5ZrO_2]+30wt\%UO_3$, where x= 5, 10, 15, 20 mol%. In these glasses SiO_2 and B_2O_3 are strong network formers; Na_2O serves as network modifier; while BaO serves both as network modifier, glass and hydrolytic stabilizers. In the course of our previous studies [1-3] we have established that addition of ZrO_2 improves the glass and hydrolytic stability due its strong charge compensating ability.

Results

The glassy samples denoted as UB5, UB10, UB15 and UB20 were prepared by melt quench technique [3]. Boron was isotopically enriched in ^{11}B (99.6%) in order to reduce the influence of the high neutron absorption of ^{10}B present in natural boron. We have performed neutron diffraction experiments using the 'PSD' instrument in the scattering vector range of Q=0.6-10 Å^{-1} and also high energy x-ray diffraction using the BW5/HASYLAB, DESY experimental station in the scattering vector range of Q= 0.5-25 Å^{-1}. A simultaneous reverse Monte Carlo simulation of the two data sets was applied to generate reliable 3-dimensional atomic configurations and, to calculate several partial atomic pair correlation functions, nearest neighbour distances and coordination number distributions. The result of RMC simulation of the neutron- and x-ray diffraction data are displayed in Fig. 1/a,b.
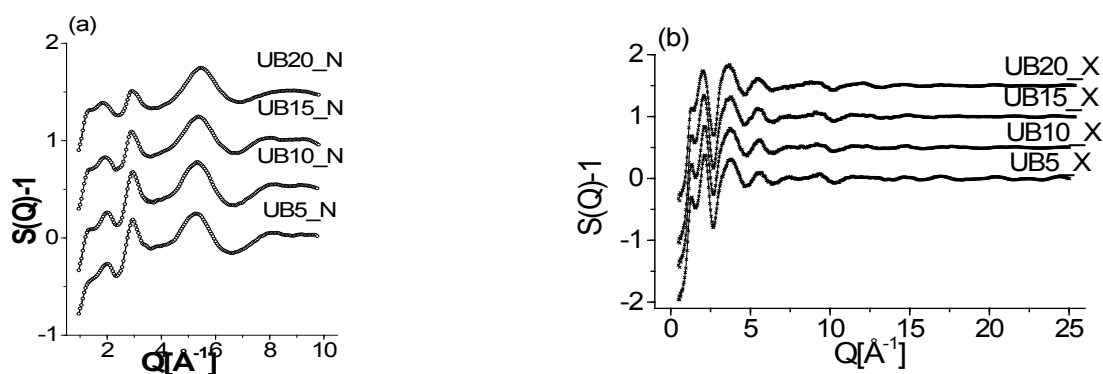
Fig. 1. a) Neutron and b) x-ray diffraction structure factors for
$70wt\%[(65-x)SiO_2 \cdot xB_2O_3 \cdot 25Na_2O \cdot 5BaO \cdot 5ZrO_2]+30wt\%UO_3$, _x=5, 10, 15, 20, experimental data (cross) and RMC simulation (line) (the curves are shifted vertically)_

Future prospects

Data treatment and publication is in progress.

References

[1] M. Fábián, E. Sváb, Gy. Mészáros, Zs. Révay, Th. Proffen and E. Veress, _J. Non-Cryst. Solids_ **353** (2007) 2084.
[2] M. Fábián, E. Sváb, Gy. Mészáros, L. Kőszegi, L. Temleitner, E. Veress, _Zeitschrift für Krist._ **23** (2006) 461.
[3] M. Fábián, E. Sváb, Gy. Mészáros, Zs. Révay and E. Veress, _J. Non-Cryst. Solids_ **353** (2007) 1941.

B N C Experimental Report	*Experiment title* **Diffraction study of Ge-Sb-S-Te chalcogenide glass system**	*Proposal No.* PSD- 5 *Local contact* M. Fábián
Principal proposer: V. Pamukchieva *Experimental team:* M. Fábián, Gy. Mészáros, E. Sváb, SZFKI; V. Pamukchieva, Sofia/Bulgaria		*Date(s) of Exp.* May2006 *Date of Report* 20. 01. 2009.

Objectives

Chalcogenide glasses have received a great deal of attention due to their transparency in the infrared region, their high refractive index and photosensitivity [1-2]. These materials are heavy anion glasses since S and Te are the main constituents of their compositions. Addition of Ge and Sb stabilizes the glassy state and cross-linking formations of the structure. Here we study the short range structure of samples with composition of $Ge_xSb_{(40-x)}S_{(60-y)}Te_y$; x= 10, 20, 27; y=10, 5.

Results

The bulk glasses were prepared by conventional melt-quenching method from 5N purity elements. Synthesizes were performed in evacuated quartz ampoules (10-3 Pa) using a rotary furnace. The ampoules were heated up to 950°C and were kept at this temperature for 24 h, rotating the furnace the melt to be homogenized. After 24 hours the ampoules were pulled out from the furnace and were quenched in air. The materials, obtained by this way, were powdered.

Neutron diffraction measurements (I=1.069Å) were performed in vanadium cans with diameter 8mm and wall thickness 0.07mm. The structure factors were revealed and reverse Monte Carlo simulation was applied for modelling the 3-dimensional atomic configuration. Figure 1 displays the experimental data and the result of RMC modelling.
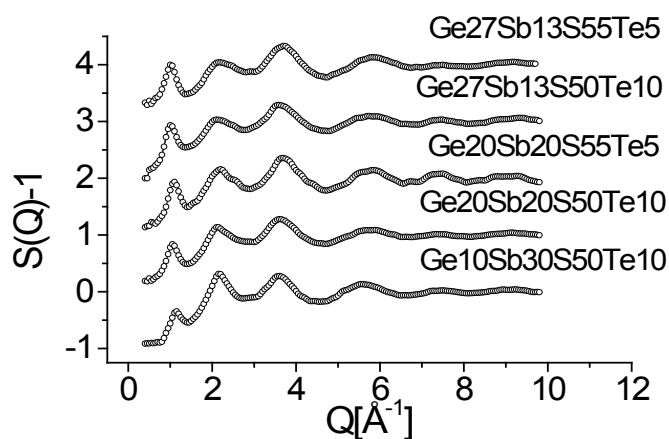
Figure 1. Neutron diffraction structure factors, experimental data (circle) and RMC simulation (solid line). (The curves are shifted vertically for clarity.)

Future prospects

Data evaluation is in progress. Neutron diffraction experiments are planned to be extended the momentum transfer range up to Qmax=30 Å-1, and also hard x-ray experiments are underway.

References

[1] N.S. Kapany R.J. Simms, *Infrared Phys.* **5** (1965) 69.
[2] J.R. Gannon, "Infrared Fibers (0.8–12 mm) I,"Proc. SPIE—*Int. Soc. Opt. Eng.* **266** (1981) 62.

Objectives

As a next step of our previous work on Ge-Sb-S-Te chalcogenide glass system (see previous PSD-5 report), we have studied the Ge-As-S-Te glassy system. The bulk glasses with composition of $Ge_xAs_{40-x}S_{50}Te_{10}$ (x=10, 20, 27) and $Ge_xAs_{40-x}S_{55}Te_5$ (x=20, 27) were synthesized by the conventional melt-quenching method. Here we present the neutron diffraction experiments performed on the PSD instrument.

Results

The powdered glasses with a weight of about 2-3 g were filled in cylindrical vanadium sample holder of 8 mm diameter, 50 mm height and 0.07 mm wall thickness. The neutron diffraction measurements were performed with a monochromatic wavelength of l_0=1.069 Å in the momentum transfer range of Q= 0.45-9.8 Å-1. For data treatment the combination of the Fourier transformation of the structure factor, S(Q) and the MCGR modelling [1] have been applied, so far. Figure 1 displays the experimental data and the result of MCGR modelling.
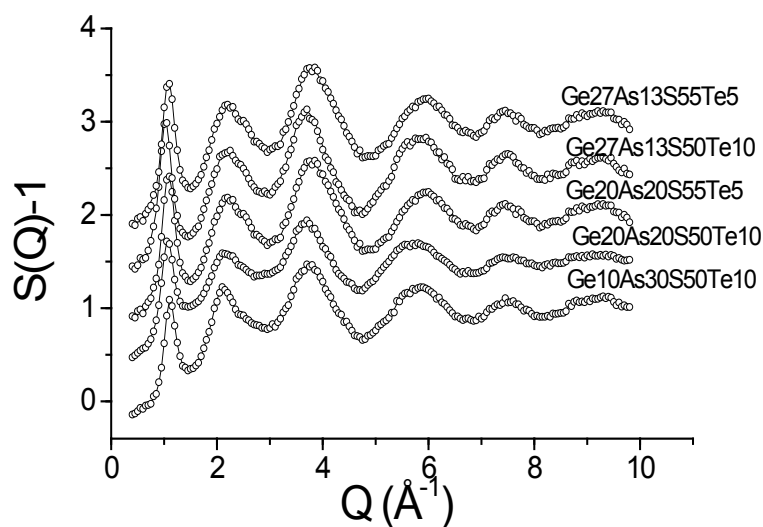
Figure 2. Neutron diffraction structure factors, experimental data (circle) and MCGR model (solid line)

Future prospects

Data evaluation is in progress. Neutron diffraction experiments are planned to be extended the momentum transfer range up to Qmax=30 Å-1, and synchrotron x-ray experiments are also underway.

References

[1] P. Zetterström, R.L. McGreevy, Physica B 276 (2000) 187.

Objectives

Amorphous chalcogenides possess interesting fundamental properties and have potential applications in optical imaging, optical recording, infrared and integrated optics, microelectronics and optical communications. Chalcogenides from the As(Sb)-Se and Ge-Se systems exhibit metastable phenomena. Our recent research interest has turned to Ge-Se system with additions of As and Te. Here we present our neutron diffraction experiments on Ge-As(Sb)-Se-Te compositions.

Results

The glassy specimens were prepared by melt-quenching technique from elements of 5N purity, the following actual compositions have been measured by neutron diffraction:

a) $Ge_xAs_{40-x}Se_{50}Te_{10}$ (x=10, 20, 27) and

b) $Ge_xSb_{40-x}Se_{50}Te_{10}$ (x=10, 20, 27).

The 3 specimens of a) series proved to be fully amorphous, while the $Ge_{10}Sb_{30}Se_{50}Te_{10}$ specimen from b) series was partly crystalline. For the amorphous specimens we have calculated the structure factor, $S(Q)$ using corrections and normalization procedure, as they are displayed in Fig. 1.a/b. The overall character of the curves is rather similar, however, the position and relative intensity of the peaks show significant differences. Note, that the intensity of the first sharp peak in $S(Q)$ increases with increasing **Ge**-content and their position shifts slightly to lower values.
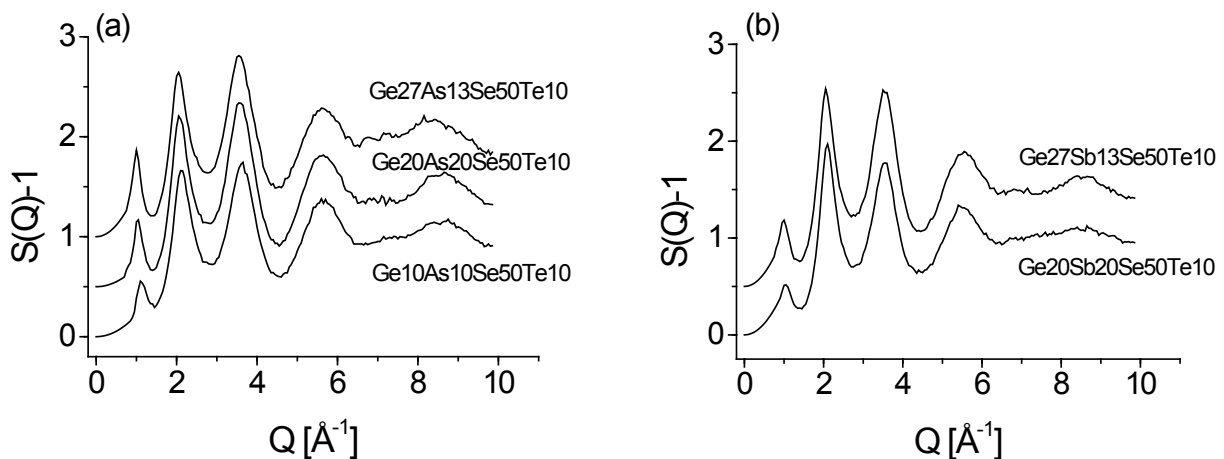
Figure 1. Neutron diffraction structure factor, $S(Q)$ of the chalcogenide glasses:
a) Ge-As-Se-Te and b) Ge-Sb-Se-Te. (The curves are shifted vertically for clarity.)

Future prospects

Data evaluation is in progress. Neutron diffraction experiments are planned to be extended the momentum transfer range up to Q_{max} =30 Å^{-1}, and synchrotron x-ray experiments are also underway.

Objectives.

Detailed knowledge concerning the structure of electrolyte solutions is of utmost importance for understanding a wide range of phenomena, from corrosion to the hydration of DNA. In general, these materials are rather difficult subjects of structural studies, due to the large number of components (at least 4: H/D, O, cation, anion). The present experiments form a part of a systematic study of Rb and Cs salt solutions, of which CsF may be made the most concentrated (up to only 1.5 water molecules per ion). Apart from the present neutron diffraction experiments, the samples have also been measured using high energy X-ray diffraction at a synchrotron source (Spring-8, Japan). Exploiting the combination of neutron and X-ray diffraction data, we wished to characterize the structure of the hydration shells in the (rather concentrated) solutions.

Results

The CsF salt, which was a commercial product (higher than 99 % purity, from Aldrich Chemicals Co.), has been dissolved in appropriate amounts of heavy water to yield solutions of concentrations of 1, 15 and 32 molar %, the last one representing near-saturation at room temperature. The liquids were contained in thin walled vanadium containers. Neutron diffraction experiments at room temperature have been carried out, applying a wavelength of 1.069 Å. Raw intensities were corrected for background and detector efficiency, after which treatment, Reverse Monte Carlo (RMC) calculations were conducted which were able to refine normalization and background corrections to the data. Figure 1 shows experimental and RMC simulated total scattering structure factors for the lowest (1 molar %) and highest (32 molar %) concentrations. (Note the rather unique 'pre-peak' emerging before the main maxium as concentration grows.)
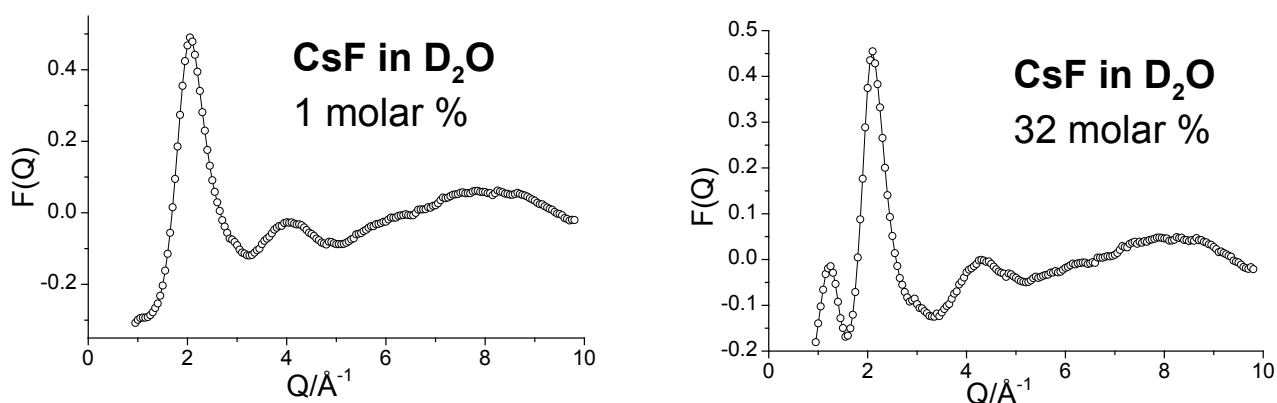
Figure 1. Experimental total scattering structure factors, F(Q),(symbols), together with their Reverse Monte Carlo fits (solid lines) of a 1 molar % (left panel) and 32 molar % (right panel) aqueous caesium fluoride.

Future prospects

The measurements, together with X-ray diffraction results, will be used for a detailed Reverse Monte Carlo study of the solutions in question.

B N C **Experimental Report**	*Experiment title* **The structure of liquids containing molecules with non-regular tetrahedral shape: methylene-iodide and dichloro-dibromo-methane**	*Proposal No.* PSD- 9 *Local contact* L. Temleitner
Principal proposer: Sz. Pothoczki *Experimental team:* Sz. Pothoczki, L. Pusztai and L. Temleitner SZFKI		*Date(s) of Exp.* *Sep 2007* *Date of Report* *21.01.2009*

Objectives.

Over the past decade, detailed investigations of liquids containing symmetric molecules have been conducted in our department. Following XCl_4-type molecules which possess perfect tetrahedral symmetry, we continued our studies of liquids containing molecules with slightly distorted tetrahedral symmetry. In the framework of the present experiments, (deuterated) methylene-iodide (CD_2I_2) and a non-hydrogenous methane derivative, dichloro-dibromo-methane (CCl_2Br_2) have been considered. The same samples have also been measured using high energy X-ray diffraction at a synchrotron source (Spring-8, Japan). Exploiting the combination of neutron and X-ray diffraction data, we wished to characterize correlations between molecular orientations in the liquids.

Results

The samples were commercial products (higher than 99 % purity, from Aldrich Chemicals Co.). They were contained in thin walled vanadium containers. Neutron diffraction experiments at room temperature have been carried out, applying a wavelength of 1.069 Å. Raw intensities were corrected for background and detector efficiency, after which treatment, Reverse Monte Carlo (RMC) calculations were conducted which were able to refine normalization and background corrections to the data. Figure 1 shows experimental and RMC simulated total scattering structure factors of both liquid CD_2I_2 and CCl_2Br_2. (It is worthwhile noting that the latter material transformed into a—as yet, unnoticed—gel-like disordered phase by the end of the measurement, at a temperature of about 291 K.)
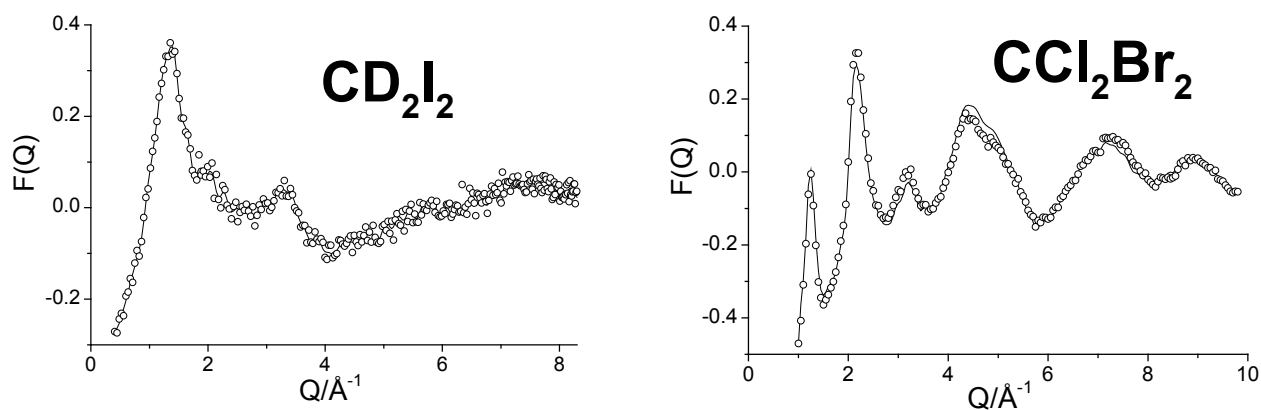
Figure 1. Experimental total scattering structure factors, F(Q),(symbols), together with their Reverse Monte Carlo fits (solid lines) of CD_2I_2 (left panel) and CCl_2Br_2 (right panel).

Future prospects

The measurements, together with X-ray diffraction results, will be used for a detailed Reverse Monte Carlo study of the materials (together with earlier results on CD_2Cl_2 and CD_2Br_2.

B N C	*Experiment title*	*Proposal No.*
Experimental Report	**Total scattering experiment on C₂Cl₆ at room temperature**	PSD- 10 *Local contact* L. Temleitner
Principal proposer: L. Temleitner *Experimental team:* L. Temleitner, Sz. Pothoczki, V. Mile and Gy. Mészáros, SZFKI		*Date(s) of Exp.* Sept 2007 *Date of Report* 23.01.2009

Objectives

Solid hexachloroethane is a model material for the class of crystals with distorted octahedral symmetry. It has three solid phases at normal pressure ([1]): up to 318 K (*Pnma*), 318-344 K (*unknown*), 344-458 K (*Im3m*). The body centered cubic phase is well studied by different models, but the structure (particularly variations of the short range order) is not yet known in detail. The aim of the present measurement was to obtain an additional, auxiliary total scattering dataset of the room temperature phase.

Results

The measurement has been carried out at 291 K with a neutron wavelength of 1.069 Å. During the measurement the sample (99%, Aldrich) was contained in a 8 mm vanadium can. Rietveld-refinement (Fig. 1) has confirmed the earlier results [1]: the structure is orthorhombic (*Pnma*) with a=11.56(2) Å, b=10.21(2) Å and c=6.43(4) Å lattice parameters. The atomic positions, together with isotropic displacement parameters, are shown in Table 1. Although the fit shown in Fig. 1 is not perfect, the RMCPOW simulation procedure (not shown), which models the Bragg and diffuse contribution together, was able to take into account anisotropic displacement of atoms.

	x	y	z	B
C(1)	0.10(1)	0.250	0.73(6)	5.2
C(2)	0.12(4)	0.250	0.03(3)	
Cl(1)	0.26(0)	0.250	0.26(0)	
Cl(2)	0.81(3)	0.250	0.98(1)	2.3
Cl(3)	0.01(0)	0.39(0)	0.75(0)	
Cl(4)	0.23(9)	0.11(2)	0.08(5)	
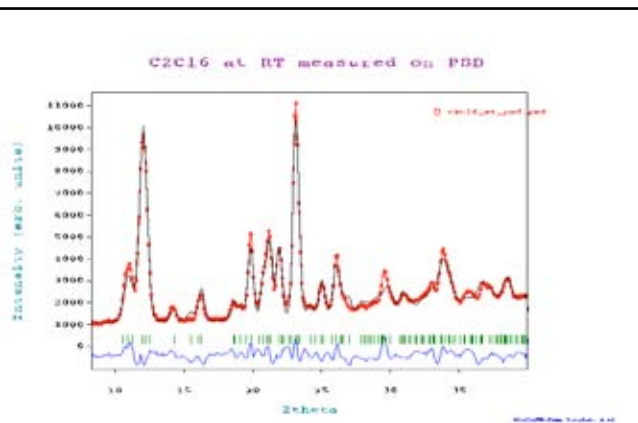
*Table 1. **Rietveld-refined positions of the C₂Cl₆** in the **Pnma** cell.*

*Figure 1. **Rietveld refinement of the neutron diffraction pattern of C₂Cl₆**, as measured on the PSD diffractometer at 291 K.*

Future prospects

This diffraction pattern will be modeled at different temperatures, in order to gather more knowledge about (the changes of) orientational correlations present in the different phases.

References

[1] Hohlwein et al., *Acta Cryst.* **B35** (1979) 2975.

		Experiment title		Proposal No.
B N C		*Experiment title* **Total scattering experiment on CDI$_3$ at room temperature**		PSD- 11 *Local contact* L. Temleitner

Objectives

Iodoform has a stable hexagonal crystalline phase at room temperature; however TSD [1] and Raman measurements [2] suggest that the local structure changes in the 240-280 K temperature region. This change might be captured by total scattering analysis, where the Bragg- and diffuse scattering contributions are recorded and interpreted. The present room temperature measurement serves as a basis for the (future) extended investigations at various temperatures by neutron and x-ray diffraction.

Results

The measurement was carried out using 1.069 Å wavelength neutrons at 292 K. During the experiment the deuterated (>99%, Aldrich) sample was contained in a 5 mm thin-walled vanadium can. The average structure is hexagonal (P6$_3$/m), with a=6.7640 Å and c=7.4962 Å lattice parameters, as obtained from Rietveld-refinement (see Fig. 1). The structure can be described by a 12 molecule unit cell (with zero displacement for each atom). The refined positions are given in Table 1. These positions serve as initial positions for the subsequent RMCPOW simulations which will focus on the study of the short range order.

	x	y	z
C	0.3217	0.6829	0.6732
D	0.2865	0.6738	0.5309
I(1)	0.0540	0.3683	0.7989
I(2)	0.3295	0.9912	0.7860
I(3)	0.6619	0.7273	0.7172
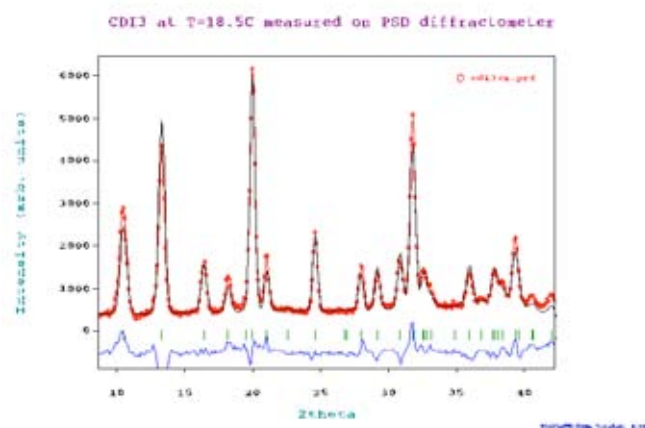
*Figure 1. **Rietveld-refinement of neutron diffraction pattern of CDI$_3$.***

*Table 1. **Rietveld-refined positions of atoms in the unit cell containing 12 rigid molecules.***

Future prospects

The measurement, together with different temperature results, will be modeled by RMCPOW for understanding (changes of) the short range order at different temperatures.

References

[1] Samoc et al., ***J. Phys. D: Appl. Phys.*** 18 (1985) 2529.
[2] Sidorov et al., ***Crystallogr. Reports.*** **45** (2000) 319

B N C **Experimental Report**	*Experiment title* **Total scattering experiments on** **crystalline Ge$_{.2}$Sb$_{.2}$Te$_{.5}$**	*Proposal No.* PSD- 12 *Local contact* L. Temleitner
Principal proposer: L. Temleitner *Experimental team:* L. Temleitner, M. Fábián, Gy. Mészáros SZFKI		*Date(s) of Exp.* Nov 2007 Jan 2008 *Date of Report* 23.01.2009

Objectives

Ge$_{.2}$Sb$_{.2}$Te$_{.5}$ is a phase change material widely used in DVD/RW for storing information. It has three solid modifications at normal pressure and room temperature: hexagonal (stable, *P-3m1*), cubic (metastable, *Fm-3m*) crystalline and an amorphous phase. The materials science interest comes from the reversibility of the phase change from cubic into amorphous phases and vice versa, while the optical reflectivities of the two phases are different. The cubic phase was studied by neutron diffraction earlier and emphasized the role of the large mobility of Ge atoms in the observed properties of this material [1]. Our previous simulation study, based on modeling X-ray scattering and the published neutron diffraction ([1]) results, could not prove this statement. We hoped that an angle dispersive neutron powder diffraction measurement could clarify this question. The stable phase has been studied by diffraction methods earlier and three different models with different occupations of Ge and Sb at the *2c* Wyckoff-site have been proposed: 100% Ge [2], 100% Sb [3], 55.9% Ge [4]. Since the neutron diffraction result is quite old, a new total scattering neutron diffraction measurement may be able to provide a better defined answer.

Results

Three measurements have been carried out, using neutrons of 1.069 Å wavelength at room temperature, on the original sample and the ones annealed at 653 and 853 K. During the measurements the sample (99% Ge$_{.2}$Sb$_{.2}$Te$_{.5}$) was contained in a 5 mm vanadium can. Unfortunately, the original sample was not fully cubic, so we later concentrated on the stable phase. The sample annealed at 853 K proved to be almost pure, so total scattering analyses could be performed by RMCPOW modeling (Fig. 1). The occupation of the Ge atoms in the *2c* Wyckoff-site was found to be between 56 and 59 % based on the best fit to diffraction data. It is in agreement with the X-ray diffraction result ([4]). The other two ([2,3]) and an additional 50% occupation models have also been tested (Fig. 1); the models proposed in [2] and [3] have been rejected.
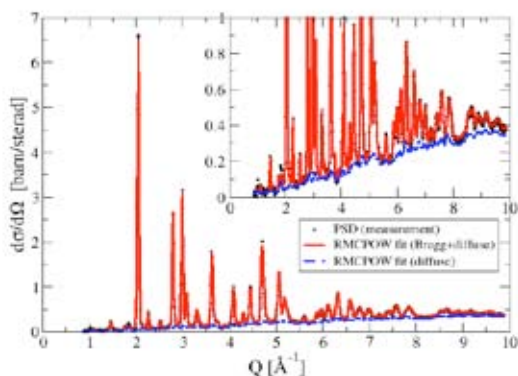
Figure 1. Best fit to data taken on stable Ge$_{.2}$Sb$_{.2}$Te$_{.5}$, using RMCPOW structural modeling.
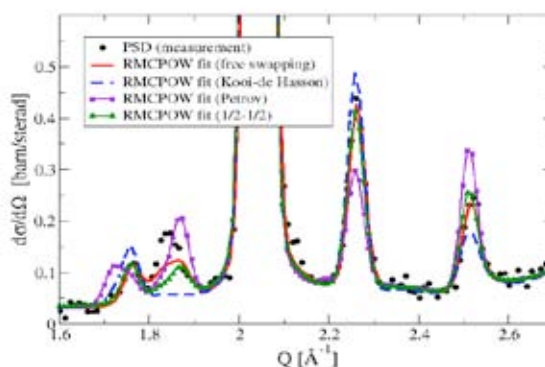
Figure 2. Testing the different occupation models by RMCPOW.

Future prospects

Results of the measurements and the corresponding simulations will be published.

References

[1] Shamoto et al., *Appl. Phys. Lett.* **86** (2005) 081904.
[2] Petrov et al., *Sov. Phys. Cryst.* **13** (1968) 339.
[3] Kooi et al., *J. Appl. Phys. Lett.* **92** (2002) 3584.
[4] Matsunaga al., *Acta. Cryst.* **B60** (2004) 685.

	Experiment title:	Proposal No.
B N C **Experimental Report**	*Experiment title:* **Neutron diffraction study of lanthanum scandium borate doped with chromium**	Proposal No. PSD- 13 *Local contact* E. Sváb
Principal proposer: E. Beregi *Experimental team:* M. Fábián, Gy. Mészáros, E. Sváb, E. Beregi SZFKI		*Date(s) of Exp.* Febr-March 2007. *Date of Report* 10. 01. 2009.

Objectives

A huntite like $LaSc_3(BO_3)_4$ (LSB) is a potential diode- pumped self-frequency-doubling laser crystal. Recently it was discovered that LSB crystal is a polymorphic compound. The purpose of this work is to prepare single phase LSB, and to find correlation between the preparation technique and the crystallographic characteristics.

Results

Single crystals $LaSc_3(BO_3)_4$ (LSB) doped with chromium (coloured light and dark green corresponding to a smaller and a larger amount of Cr) and, as reference sample pure $YAl_3(BO_3)_4$ (YAB) were grown by top-seeded high temperature solution (flux) method. The single crystals were powdered into fine grains and measured by the PSD neutron diffractometer. The neutron diffraction data are displayed in Fig. 1/a-c. The spectra for LSB-2 and YAB is similar, while that for LSB-1 is very different. Model calculations performed by Rietveld method have shown that the crystal structure of LSB-1 sample can be represented in s.g. R-3c hexagonal, while LSB-2 and YAB in s.g. R32 hexagonal,

a)   b)   c)
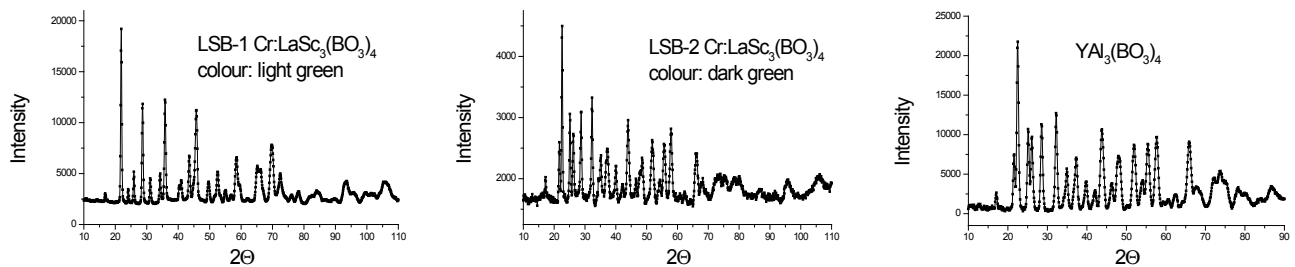
Fig.1. Neutron diffraction pattern ($\lambda=1.069\text{Å}$): a) - b) $Cr:LaSc_3(BO_3)_4$ with different Cr-content c) $YAl_3(BO_3)_4$.

a)   b)
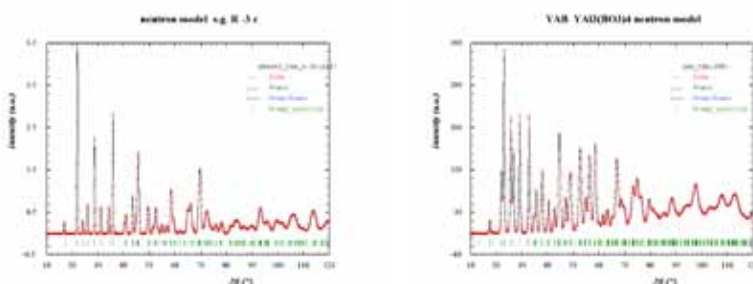
Fig. 2. Rietveld model calculation: a) s.g. R-3c with a=4.7590 Å, c= 15.3258 Å b) s.g. R32 with a=9.2756 Å, c= 7.2239 Å

Future prospects

Data treatment and publication of the results is in progress.

B N C Experimental Report	Experiment title **Effect of** *Lu and Bi* **substitution on the structure of** $YAl_3(BO_3)_4$	Proposal No. PSD- 14 *Local contact* E. Sváb
Principal proposer: E. Beregi *Experimental team:* M. Fábián, Gy. Mészáros, E. Sváb, E. Beregi, SZFKI		*Date(s) of Exp.* June 2007. *Date of Report* 10. 01. 2009.

Objectives

Yttrium aluminium borate $YAl_3(BO_3)_4$ (**YAB**) single crystals have excellent non-linear optical properties, and doped YAB crystals have important applications in laser engineering. **YAB** crystals have suitable sites for some rare-earth elements at the Y^{3+} site. The aim of this study was to investigate the effect of **Lu** and **Bi** substitution on the crystallographic parameters of $YAl_3(BO_3)_4$, and to find the correlation between the changes of optical properties and lattice distortions.

Results

Single crystals **Lu:YAB, Bi:YAB** and as reference sample pure **YAB** were grown by top-seeded high temperature solution (flux) method. The single crystals were powdered into fine grains and measured by the PSD neutron diffractometer. The crystal structure of **YAB** is rhombohedral with space group **R32**. The **Y** atoms, **Al** atoms and **B** atoms occupy trigonal prisms, octahedra, and triangles of oxygen, respectively. The Rietveld refinement of the pattern (Fig. 1) has shown that the substitution of **Y** atoms by **Lu** leaves the space group invariant.
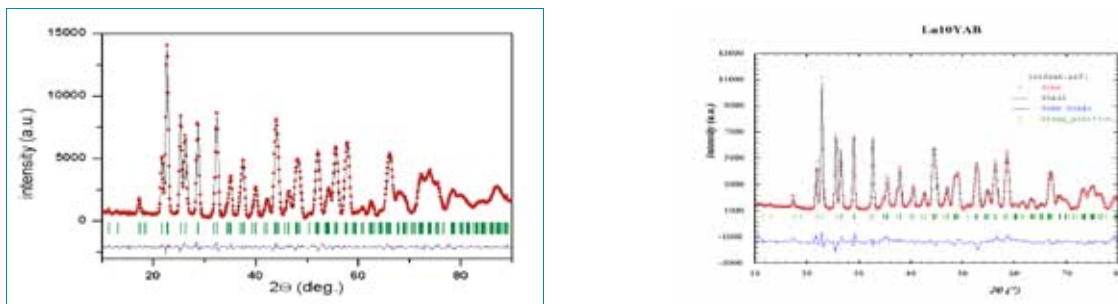
a)   b)
Fig. 1 Neutron diffraction patterns(λ=1.069Å) and Rietveld refinement in s.g. R32: a) YAB b) Lu:YAB
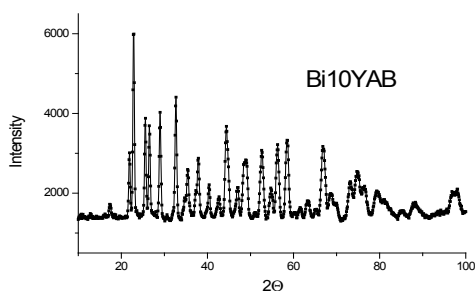
Fig. 2. Neutron diffraction pattern (λ=1.069Å) of Bi:YAB

Figure 2 shows the measured neutron diffraction spectrum for *Bi:YAB*, which reflects the characteristic features of *YAB* spectrum. From this it can be concluded that *Bi* substitution leaves also the s.g. R32 invariant.

Future prospects

Data treatment and publication of the results is in progress

Objectives

Multiferroics have been of particular interest recently both to understand the fundamental aspects of the novel mechanism that gives rise to the magnetic-ferroelectric coupling and because of the intriguing possibility of using these coupled order parameters in novel device applications. Recent "proof of principle" work has shown that it is possible to control the magnetic phase transition with an applied electric field, and control the electric polarization with an applied magnetic field. Such compounds are $BiMnO_3$, $BiFeO_3$, $BiCrO_3$, etc. All these compounds have perovskite-type structure. In this connection it is of current interest to investigate solid solutions whose end members display ferroelectric and magnetic properties. The subject of the present study are mixed oxides being solid solutions compounds already known to exhibit multiferroic properties such as phases in the systems Y-Fe-Cr-O with end member the multiferroic $YCrO_3$. We report on the structural characterization of these complex perovskites.

Results

The study was performed at room temperature on powder samples. Materials of nominal stoichiometry $YCr_{1-x}Fe_xO_3$ ($0 \leq x \leq 1$) were obtained as black polycrystalline powders following an original route of preparation by implementing a modified self-propagation combustion method. The reaction products were characterized by x-ray diffraction (XRD) for phase identification and to assess phase purity. The neutron powder diffraction (NPD) measurements were performed within the angular range 8-115o of 2θ (λ= 1.06925 Å). Thin walled cylindrical vanadium sample holders with a diameter of 5 mm were used. The crystal and magnetic structure refinements of both X-ray and neutron diffraction spectra were performed simultaneously using the Rietveld method implemented in the FullProf suite. Fig. 1a shows that the main XRD peaks are with nearly equal intensities and angular positions indicating that similarly to $YFeO_3$ and $YCrO_3$ all the members of the system are orthorhombically distorted perovskites. Correspondingly, all spectra could be indexed within the space group Pnma. Fig. 1b illustrates for $YCrO_3$ the crystal structure determination from the simultaneous refinement of the XRD and NPD patterns. The refined structural parameters are given in Table 1.
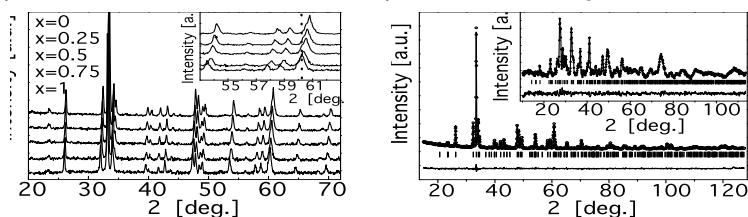
Figure 1. a) XRD patterns of the $YCr_{1-x}Fe_xO_3$ series. Inset: limited angular part with reflections 311, 321, 240 and 042; b) Full profile refinement of the XRD and NPD (inset) patterns of $YCrO_3$ at 300 K

Table 1. Positional and isotropic thermal parameters of $YCrO_3$

(lattice constants in • : a= 5.5223(5), b=7.5338(6), c=5.2415(4)).

Ion	x	y	z	B_{iso}
Y^{+3}	0.0663_4	0.25	0.9818_6	0.55_7
Cr^{+3}	0.00	0.00	0.50	0.22_8

Future prospects

The work on the refinement of the rest structures is in progress.

Objectives

In multiferroic materials the magnetic and ferroelectric orderings coexist and are coupled. Besides important implications for novel electronic devices the physics behind the expected complex magnetoelectric phenomena is of great current interest. Few multiferroic compounds with effective magnetoelectric properties are known (e.g. BiFeO3, BiMnO3, YMnO3) since proper ferroelectricity and magnetism are usually antithetic. Much of the current interest is in the so-called improper multiferroics (with magnetically induced ferroelectricity) such as RMnO3, RMn2O5 (R= rare earth) and other perovskite-like materials with frustrated magnetic interactions and noncollinear spin ordering. We studied mixed oxides Y-Fe-Cr-O (0≤x≤1) whose end member YCrO3 display intriguing magnetic and electric properties. We found the structural information for the system very limited and undertook a systematic structural and magnetic characterization of phases in the system.

Results

Materials with general formula YCr1-xFexO3 (x = 1.0, 0.875, 0.75, 0.67, 0.5, 0.33, 0.25, 0.125, 0.0) were obtained by a modified self-propagation combustion method. The neutron experiment was performed within the angular range 8-115o of 2θ (λ= 1.06925 Å). The crystal and magnetic structure refinements of both X-Ray (XRD) and neutron powder (NPD) diffraction spectra were performed simultaneously using FullProf. In both YFeO3 and YCrO3 below the Neel temperature TN=648K and 141K, respectively, the noncollinear antiferromagnetic state Γ4 (GcFbAa) is established. As exemplified on Fig. 1 we found that the G-type magnetic ordering scheme is preserved for the Fe-rich compositions. Fig. 2 gives a schematic presentation of the refined magnetic structures. The smooth changes in the unit cell volume and measured magnetic moment versus x depicted in Fig. 2a, indicate that the formation of solid solution of YCrO3 and YFeO3 occurs in the whole concentration interval.
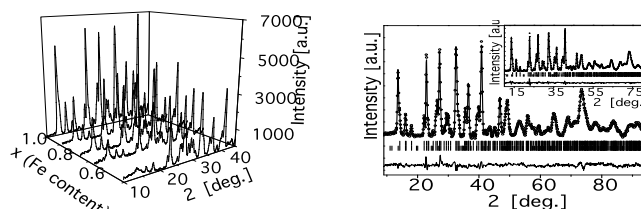
Figure 1. a) Low angle part of room temperature NPD patterns of YCr$_{1-x}$Fe$_x$O$_3$; b) Full profile refinement of the NPD patterns of YFe$_{0.875}$Cr$_{0.125}$O$_3$ and YFeO$_3$ (inset). (λ= 1.06925 Å)
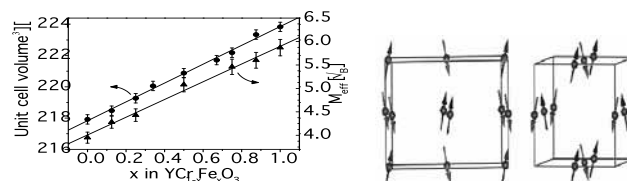
Figure 2. a) Dependence of the unit cell volume and the effective magnetic moment on Fe content, x: experimental data with error bars and linear fits; b). Schematic view of the magnetic structure at room temperature of YCr$_{1-x}$Fe$_x$O$_3$ (0.33<x<1) along a-axis and along b-axis (right).

Future prospects

S. Kovachev, D. Kovacheva, S. Aleksovska, E. Svab, K. Krezhov, to be published in JOAM

Objectives.

The substitution of the alkali earth ion by lead in the perovskites $A_{1-x}A'_xMO_3$ (A=rare earth ion or Bi, A'=alkali earth ions, M = 3d transition metal ions) is a feasible way to modify the properties. Moreover, it is interesting from structural point of view as well, since the lone electron pair of Pb^{2+} should influence strongly the configuration around the A cation. The aim of this experiment has been the evaluation of the true space group and Rietveld refinement of the crystal and magnetic structures of a novel set of lead containing transition metal oxides with general formula $Pb_{0.5}La_{0.5}Fe_{1-x}Mn_xO_3$ ($0 \leq x \leq 1.0$) and $Pb_{0.5}-xBi_xLa_{0.5}FeO_3$ ($0 < x \leq 0.25$) for which there are no data in the literature.

Results.

The study was performed at ambient temperature on powder samples. All compounds were synthesized through a specific solution combustion technique. First, X-ray powder diffraction spectra were recorded on Bruker D8 Advance (CuKα radiation, SolX detector) for sample characterization with respect to phase purity. For the neutron diffraction measurements within the angular range 8-115° of 2θ (λ= 1.06925 Å) thin walled vanadium sample holders were used. The neutron patterns were analysed using the FULLPROF program package by applying the profile matching mode followed by the full profile Rietveld refinement of the structural model. It was expected that because of the similar ion radius iron directly would replace Mn^{3+} as Fe^{3+} (S=5/2) so that the electronic structure would not be significantly influenced and that the main effect of doping should manifest itself in effective reduction of the Mn^{3+} / Mn^{4+} ratio by influencing the double exchange. Since X ray atomic scattering factors of Fe and Mn as well as of Pb and Bi are close, neutron diffraction data are crucial for elucidating the type of cationic distribution, positions of oxygen, revealing the possible magnetic structures and better understanding of crystal chemistry of these new compounds. Rhombohedral and orthorhombic space groups were found at present to describe satisfactorily most of the crystal structures. Fig.1 illustrates that Fe-doping and partial substitution of Pb for Bi produce clearly pronounced effects on the structure. Indeed, the structure analysis points to substantial lattice deformations reflected in changes in unit cell volume and cation-oxygen distances.
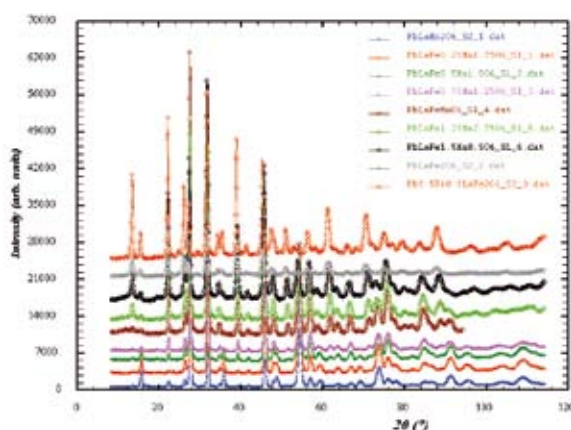
Figure 1. Full profile refinement of the neutron diffraction spectra (λ = 1.0692Å)

Future prospects

The work on the refinement is in progress.

B N C **Experimental Report**	*Experiment title* **Monitoring the chloride concentrations in the primary coolant of the Budapest Research Reactor (BRR)**	*Proposal No.* *Local contact* I. Sziklai-László
Principal proposer: Ibolya Sziklai-László, KFKI Atomic Energy Research Institute, HAS, Budapest *Experimental team:* R. Szőke, KFKI, Atomic Energy Research Institute, HAS, Budapest		*Date(s) of Exper.* *Date of Report* December 20, 2006

Objectives

The control of reactor water parameters such as conductivity, pH, radioactivity and its interrelationship with reactor circuit materials are important factors in controlling the corrosion. Another parameter that is carefully monitored and controlled in most nuclear facilities is chloride content. The reason for maintaining the chloride ion concentration at the minimum level is that several forms of corrosion are accelerated by chloride ion. The aim of this study was to measure the chloride concentrations in the primary water of the BRR and compare them with the authority limit.

Results

Corrosion causing species like chloride and I, Na, K and alkaline earth metals (Mg, Ca and Ba), soluble and insoluble corrosion products (Al, Fe, Cr, Mn, Cu, Co and other impurities: Mg, La, Sb, Ta, V and Zn) are measured in water samples of the primary circuit of the BRR. The chloride content was determined by neutron activation analysis followed by a preconcentration procedure. Water chemistry data were stored in a PC-based data storage system together with other technological parameters such as temperature, pH, conductivity, water purification system operation and flow rate. In Figure 1. the annual variation of chloride concentrations in the primary water is shown between the sampling periods of 1996-2006. Comparison of the values to the authority limit [1] shows that all data, except in one sample, were within the limitation.
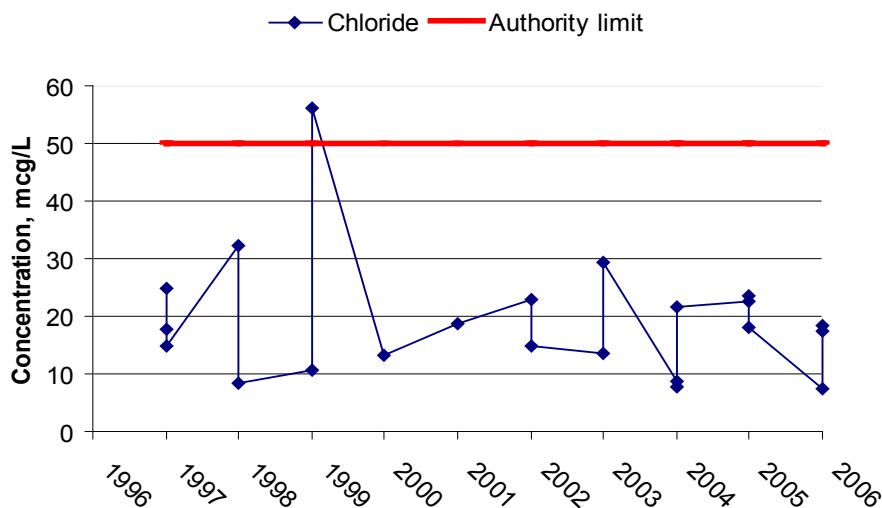
Fig. 1. Maximum concentrations of chloride in the primary coolant at the BRR between 1997-2006.

[1] Final Safety Report of the BRR, Budapest, 2004.

Future prospects

To continue data acquisition, processing and evaluation in order to build up a database for corrosion characteristics of the specimens and the measured water parameters for establishing a reliable trend analysis.

B N C Experimental Report	Experiment title **Water chemistry at the Budapest Research Reactor**	Proposal No. Local contact I. Sziklai-László
Principal proposer: Ibolya Sziklai-László, KFKI Atomic Energy Research Institute, HAS, Budapest Experimental team: R. Szőke, D. Elter, KFKI, Atomic Energy Research Institute, HAS, Budapest		Date(s) of Exper. Date of Report December 20, 2007

Objectives

In 2007, we participated in the preparation of the documentation on storage of fuel assemblies and the surveillance of coolants at Budapest Research Reactor (BRR), prepared by the Reactor Department. The water quality through measuring the concentrations of selected halogens, alkali and alkali earth metals, corrosion products in the water samples of the BRR are monitored on a routine basis. In this work, the annual variation of characteristic parameters of primary water (**PW**), fuel storage "at-reactor-pool" (**AR**) and "away-from-reactor" (**AFR**) were investigated.

Results

The fuel assemblies are stored for many years under water, therefore it is very important to measure the activity, pH, conductivity and other components of the water, in order to detect the leakage of fuel as early as possible and to decrease the speed of corrosion. The Al, Cl, Cu and Fe concentrations in water samples were determined by a pre-concentration procedure followed by neutron activation analysis. Following the comparison of measured values to the authority limits [1] it can be stated that all data were within the limitations. During 2003 and 2004, the increased activity of the AFR-pool, and the high chloride and iron concentrations, as well as the conductivity of the water were increased, due to the encapsulation procedures and to the problems occurring with the water purification system. The annual variations of the concentration levels of Al, Cl, Cu and Fe in samples of the primary water, the AR- and AFR-pools in comparison with the conductivity data are shown in Figure 1.
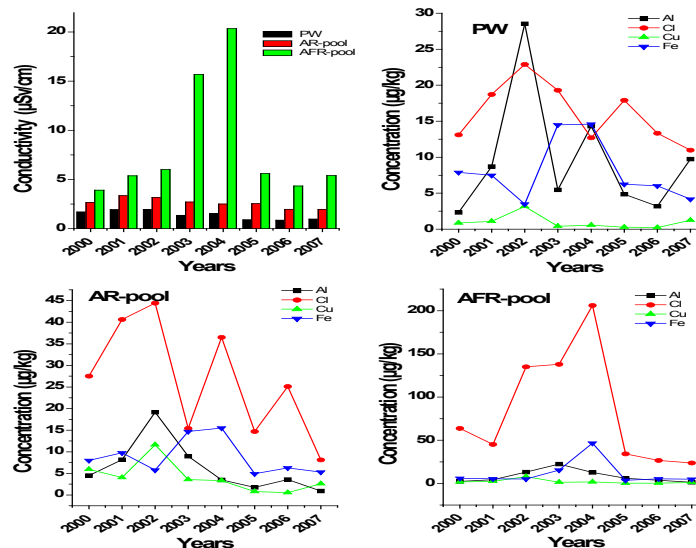
Fig. 1. Annual variation of conductivity and the concentrations of Al, Cl, Cu and Fe in PW, AR- and AFR-pool water

[1] Final Safety Report of the BRR, Budapest, 2004.

Future prospects

The work is in progress.

B N C Experimental Report	*Experiment title* **Determination of the age of uranium samples of arbitrary shape**	*Proposal No.* *Local contact* I. Sziklai-László
Principal proposer: Ibolya Sziklai-László, KFKI Atomic Energy Research Institute, HAS *Experimental team*: J. Zsigrai, C. T. Nguyen, Institute of Isotopes, HAS		*Date(s) of Exper.* 2006.07. 24.-11.20. *Date of Report* December 20, 2006.

Objective

Obtaining information on the age of nuclear material is of relevance in nuclear forensic science in order to determine the date of the production campaign of the material. This might be helpful to identify the source of the material. A non-destructive, gamma-spectrometric method for uranium age-dating, developed previously, was applied in this study for the determination of the age of VVR-SM, VVR-SM/3 fuel assemblies and broken pieces of EK-10 fuel rods of the Budapest Research Reactor.

Results

The method for age determination of uranium samples is based on measuring the daughter/parent activity ratio $^{214}Bi/^{234}U$ with high-resolution low-background gamma-spectrometry, assuming that the daughter nuclides have been completely removed during the last separation or purification of the material. ^{214}Bi is a daughter of ^{234}U, which decays through ^{230}Th to ^{226}Ra, which, in turn decays to ^{214}Bi through three short-lived nuclides. The time needed for secular equilibrium between ^{226}Ra and ^{214}Bi is about 2 weeks, so it can be safely assumed that the activities of ^{226}Ra and ^{214}Bi are equal at the time of our measurement in 2006. Therefore, using the law of radioactive decay, the activity ratio $^{214}Bi/^{234}U$ at time T after purification of the material can be calculated [1]. In order to eliminate the geometrical effects, relative efficiency calibration is used. In this way the age of uranium samples of arbitrary physical form and shape can be determined. For each fuel rod an intrinsic efficiency calibration was performed, using the peaks of ^{234}Pa and ^{234m}Pa, which are short-lived daughters of ^{238}U. Using this intrinsic efficiency curve and the count rate of the 609 keV line of ^{214}Bi, the activity ratio $^{214}Bi/^{238}U$ was calculated for each assayed fuel rod.

From the activity ratios $^{214}Bi/^{238}U$ and $^{234}U/^{238}U$ the activity ratio $^{214}Bi/^{234}U$, and thus the age of uranium samples can be calculated. The measured ages were found to agree with the ages calculated based on the date of the production of the fuel rods. In fact, the uranium age in each case is larger than the assumed age of the rods. This is, at least partially, due to the fact that the uranium material, from which the rods have been produced, had been chemically separated and enriched before the fuel production took place. We can conclude, that gamma spectroscopy can be used for age dating of realistic uranium samples of arbitrary shape, even if they cannot be dismantled, such as fuel rods.

Table 1. The age the fuel rods and the age of uranium in the rods.

Type	Identification Number	Enrichment (%)	Year of production of the fuel rod	Age of fuel rod (years)	Measured uranium age (years)
VVR-SM	28	36	1967	39	45 ± 4
VVR-SM	527	36	1968	38	40 ± 3
VVR-SM	211	36	1985	21	29 ± 4
VVR-SM/3	51	36	2000	6	< 13
EK-10	-	10	before 1967 or before 1959	39 or 47	47 ± 4

Reference

1.J. Zsigrai, C. Tam Nguyen, I. Sziklai-László: Determination of the age of uranium-bearing items of arbitrary shape. Proc. Symp. Int. Safeguards: Addressing Verification Challenges. IAEA-CN-148/161P. IAEA, Vienna, 16-20 Oct. 2006.

B N C Experimental Report	*Experiment title* **Determination of minor and trace elements in hair and skin of the mummy by INAA**	*Proposal No.* *Local contact* I. Sziklai-László
Principal proposer: Ibolya Sziklai-László, KFKI Atomic Energy Research Institute, HAS, Budapest *Experimental team*: A. Shahram Institute of Inorganic Chemistry of the University of Vienna, Austria R. Szőke, KFKI, Atomic Energy Research Institute, HAS, Budapest		*Date(s) of Exper.* *Date of Report* December 20, 2007

Objectives

After discovery in 1997 of the archaeological site "Laguna de los Condores" in Peru, a multidisciplinary project was initiated to explore the history of this site. The mummies from "Laguna de los Condores" are the only artificially prepared Chachapoya mummies known to date. Since 1998, the laboratory of the Institute of Inorganic Chemistry of the University of Vienna took part in the investigation of the "Chachapoya Inca's" culture in Peru. As part of this project, the measurement of the minor and trace elements of the hair and skin of the mummies was the main objective of these experiments.

Experiment

10-25 mg of the hair and skin samples was packed in high purity polyethylene bags and irradiated in the vertical pneumatic transfer system at the Budapest Research Reactor. The measurements were performed with high-rate gamma-ray spectrometry using the Westphal-type Loss-Free Counting module with Dual Spectrum Storage Option. For gamma spectra evaluations the HYPERMET-PC software was used. The quantitative evaluation of the measurements was based on the k0 standardization method using gold and zirconium reference comparators co-irradiated with the samples. The INAACNC program was used for concentration calculations.

Results

Al, Br, Ca, Cl, Cu, I, K, Mg, Mn, Na, S, Sc, V and Zn were determined in hair and skin samples of the mummies by instrumental neutron activation analysis. Because the external contamination is a high concern in ancient hair samples, we compared our results with the data of control hair (modern) as well as reference values. Although, we investigated only a small number of samples, our results for elements like Br, Cu, Mg, Mn, S and Zn were within the range of the literature values. Ca, K, Mg, Na and Zn levels were higher and Cu and I were lower in mummy hair, than in the control hair. We also analyzed the reference material NIES CRM No. 13 Human Hair in order to check the accuracy of the analytical method. The concentrations for elements like Ca, Mg, Mn, Na, S, Zn and V are in a good agreement with the certified values. Our results showed that comparable values were found for element Ag, K, S and Zn in hair and skin of the same mummy. Significant differences were found in skin samples for Ca, Cl Mn, S and Sc when compared to reference values. Results of the metal content of the tissue samples may have a key importance, concerning the materials used for the embalming and preserving the human and other organic remains.

Future prospects

We continue the trace element research with other hair samples collected from subjects living in the vicinity of the archeological site and compare the elemental concentrations in ancient and modern hair.

B N C **Experimental Report**	*Experiment title* **Rare-earth element distribution of volcanic rocks in the Carpathian-Pannonian Region measured by NAA**	*Proposal No.* *Local contact* Réka Szőke
Principal proposer: K. Gméling, P. Kiss, Institute of Isotopes, HAS *Experimental team:* Réka Szőke, KFKI, Atomic Energy Research Institute, HAS		*Date(s) of Exper.* 07.03.01- 03.02. *Date of Report* 2009.01.30.

Objectives

In the Carpathian Pannonian region (CPR) a wide range of volcanic rocks can be found that formed during the last 20 Ma. Formation of the volcanic area is related to the collision of the European and African plates. Subduction of an oceanic lithosphere occurred along the curvilinear belt of the present Outer-Carpathians. Termination of subduction was graded from west to east-southeast. At the Western Carpathians subduction commenced at approximately 20 Ma without coexisting volcanism and terminated at about 17 Ma, while in the Central Segment 16.5-12 Ma and absolutely terminated 13-11 Ma in the South-Eastern Segment. The Tokaji Mts. is in the transition zone of the Western- and Eastern Carpathians Volcanic Arc. Volcanism happened on a thicker continental crust, which makes the volcanic structures more complicated. Some physical volcanological study was made in this region, and numerous studies on the hydrothermally altered areas, but trace amount from a geodynamical view. Thus we measured the major oxide, the trace element, and especially the rear-earth element (REE) concentration of these rocks.

Results

The studied rock samples were previously analyzed with PGAA, which facility enables us to determine the major oxide concentrations of bulk-rocks and gives just a few trace element abundances, like B. The B data give information about relative fluid addition of the magma generation zone, does not give alone sufficient information about the formation of rocks. For further conclusions, we needed other concentrations of similarly incompatible but fluid immobile elements, which can not be measured by PGAA. Thus we measured eleven rhyolite and dacite rock samples from the Tokaji Mts. with INAA to determine the rare-earth element concentrations of these calc-alkaline volcanic rocks. Some of the trace elements can be measured by both INAA and PGAA, which also gives basis for comparison (e.g. Sm, Cl, Nd, Ni, Co, Dy) of the two nuclear analytical techniques. Geochemical data suggest the following conclusions: 1) the parent magma of acidic rocks originate from partial melting of the astenosphere due to escapement of fluids from the subducting marine sediments; 2) the Eu anomalies of the rocks suggests the presence of fractional crystallization during magma differentiation; 3) acidic melts could contaminate crustal materials to enrich in ore forming elements and volatiles at some zones only. Boron concentration of the measured calc-alkaline samples fall in the range typical of subduction related volcanic rocks. Changes in the B content refers to different degree of fluid addition, but can be influenced by fractional crystallisation as well.

The results are published in an MSc Thesis of Mr. Péter Kiss, and included in a PhD thesis of Katalin Gméling and also published in a conference abstract.

References

Kiss, P., Molnar, F., Gméling, K., Pécskay, Z. (2007): Contribution to the understanding of the acidic volcanism and its relationship to large scale hydrothermal processes an the basis of new geochemical and K-Ar age data in the Tokaj Mts. (NE-Hungary). Geology Conference in Sovata, Romania. (Abstract-poster).

Kiss, P. (2007): A Zlatá Bana vulkán (Szalánci-) és a Tokaji-hegység vulkanizmusának és hidrotermás rendszereinek összehasonlítása. Dimlomamunka, ELTE-TTK, 78.

Future prospects

We are planning to extend the B concentration and REE measurements on intrusive volcanic rocks. Results of volcanological and geochemical studies of the well exposed intrusive bodies along the Carpathians can offer better understanding of the geodynamic processes, and they could promote and supplement the previous geochemical and geophysical works. This work was supported: OTKA (K68153).

Objectives

The phosphate fertilizer industry is responsible for negative impacts on the environment and human health, giving rise to an increase in incidence rate for fluorosis, respiratory and other diseases. The target point of the project is the TURNU fertilizer plant, situated about 4 km from the town of Turnu Magurele, on the left bank of the Danube River in Romania. Environmental impact of the plant was investigated on soil and vegetation (potato, carrot and tree leaves) collected in the near and wider vicinity of the fertilizer plant.

Instrumental neutron activation analysis (INAA) based on short-lived radionuclides was applied for the determination of Al, Ca, Cl, Mg, Mn, Ti, V, and I. The concentrations of the elements in vegetables and soil samples collected in the vicinity of the plant were compared to those found in control samples.

Results

The sampled potatoes, carrots and tree leaves were air dried for about a month. Prior to drying, the external parts of the samples were rinsed with distilled water to remove the adhering particles from soil and/or atmospheric deposition. For each type of crop, a homogeneous sample was prepared by mixing the samples collected from a specific site (two pieces, in general). Masses of 150-200 g dry matter were taken and cut in small pieces and/or ground and homogenized in an agate mortar. About 50-100 mg of each sample wrapped in high purity polyethylene bags was used for INAA. IAEA-336 Lichen, IAEA-359 Cabbage and IAEA-Soil 7 were used as refrence materials.

The concentrations of Al, Cl, I, Mg, Mn, Ti, and V determined in potato and carrot samples collected in the vicinity of the fertilizer plant are given in Table 1.

Table 1. Element concentrations of vegetables from the vicinity of the Turnu fertilizer plant (in dry-weight basis).

Element	Concentration (μg/g, SD%)	
	Potato (pulp)	Carrot (pulp)
Al	180 (6)	3350 (3)
Cl	6980 (3)	8120 (4)
I	1.5 (4)	9.8 (4)
Mg	1470 (5)	9834 (3)
Mn	25 (5)	143 (4)
Ti	10 (5)	83 (4)
V	1 (6)	1.4 (5)

A decrease in the concentration of the vanadium in soils and vegetables surrounding the Turnu fertilizer plant as a function of the distance to the plant was observed. For Ca, Cl, Mg and Mn concentrations in carrot pulp, as well as for Cl in potato pulp were found to exceed the normal Romanian levels.

Remaining work

INAA based on long-lived radionuclides will be applied for the determination of Ag, As, Au, Ba, Br, Ca, Co, Cr, Cs, Fe, Hf, Hg, K, Mo, Na, Ni, Rb, Sb, Se, Sr, Ta, Th, U, Zn, and rare-earth elements.

BNC Experimental Report	Experiment title **Epiboron NAA: an option to analyze unfavorable matrices**	Proposal No. Local contact **Réka Szőke**
Principal proposer: Réka Szőke, KFKI, Atomic Energy Research Institute, HAS, Budapest *Experimental team*: Ibolya Sziklai-László, András Simonits, KFKI, Atomic Energy Research Institute, HAS, Budapest		*Date(s) of Exper.* *Date of Report* **Jan. 28, 2008**

Objectives

When applying instrumental NAA, induced activities of major components can occasionally dominate the resulting spectrum hampering the detection of trace elements in a sample to be investigated. A solution to the above mentioned problem is the application of selective irradiation using boron filters.

Results

In case of the epithermal irradiation the activities of all nuclides whose cross sections show high resonances in the epithermal region are strongly enhanced with respect to the activities of those nuclides having approximately 1/v cross section.

Table 1. Nuclear data, B ratios and improvement factors for some (n,γ) reactions of interest

Elements	Nuclear reaction	Nuclear data		B ratios	Improvement factor	
		$\bar{E}$, eV	I_0/σ_0	$R_B \pm SD(\%)$	$IF_B(Na)$	$IF_B(Sc)$
Ag	$^{109}Ag(n,\gamma)^{110m}Ag$	6.08	16.7	24.5 (3)	3.0	4.9
As	$^{75}As(n,\gamma)^{76}As$	106	13.6	6.2 (2)	6.0	9.8
Co	$^{59}Co(n,\gamma)^{60}Co$	136	1.99	44.1 (4)	2.2	3.6
Cs	$^{133}Cs(n,\gamma)^{134}Cs$	9.27	13.2	15.1 (4)	3.8	6.3
Eu	$^{151}Eu(n,\gamma)^{152}Eu$	0.448	0.87	440 (5)	0.7	1.2
	$^{153}Eu(n,\gamma)^{154}Eu$	5.8	5.66	39.6 (2)	2.4	3.9
Fe	$^{58}Fe(n,\gamma)^{59}Fe$	637	0.97	92 (2)	0.5	2.5
La	$^{139}La(n,\gamma)^{140}La$	76	1.24	69.0 (2)	1.8	2.9
Na	$^{23}Na(n,\gamma)^{24}Na$	3380	0.59	220 (6)	-	1.3
Rb	$^{85}Rb(n,\gamma)^{86}Rb$	839	14.8	4.7 (3)	6.9	11.2
Sc	$^{45}Sc(n,\gamma)^{46}Sc$	5130	0.43	589 (5)	0.6	-
Se	$^{74}Se(n,\gamma)^{75}Se$	29.4	10.8	12.7 (6)	4.2	6.8
Zn	$^{64}Zn(n,\gamma)^{65}Zn$	2560	1.91	30.4 (6)	2.7	4.4
	$^{68}Zn(n,\gamma)^{69m}Zn$	590	3.19	18.1 (3)	3.5	5.7
Zr	$^{94}Zr(n,\gamma)^{95}Zr$	6260	5.31	9.3 (2)	4.8	8.1
	$^{96}Zr(n,\gamma)^{97}Zr/^{97m}Nb$	338	251.6	1.4 (2)	12.6	20.5
U	$^{238}U(n,\gamma)^{239}U/^{239}Np$	16.9	103.4	4.4 (2)	7.0	11.5

The activation ratios were calculated for individual (n,γ) reactions using the specific activities of samples induced in bare and filtered irradiations. The improvement achieved by filtered irradiations may be expressed in terms of the so-called improvement factor:

$$IF_B = \sqrt{R_B \diamond R_B} \; ,$$

where RB(1) refers to the determinant, and RB(2) refers to the dominant interfering element.

Using the boron shield a very effective suppression (from 130 to 600 times) of strongly activating 1/v and low resonance target isotopes (i.e. 24Na, 42K, 38Cl, 46Sc, 52V ...) can be achieved. The reliability of epiboron NAA is comparable to conventional thermal neutron activation analysis, and the number of the elements that can be determined instrumentally in biological and geological materials is considerably extended.

Remaining work

This project was finished in the end of 2006.

B N C **Experimental Report**	*Experiment title* **Structure of the Water Salt Solutions of DNA** **With Sulfonated Scandium Diphthalocyanine**	*Proposal No.* *Local contact* Gy. Török.
Principal proposer: **Yu. V. Kulvelis,[1] V. T. Lebedev,[1] G. Torok,[2] and A. B. Melnikov[3]** [1] PNPI [2] St. Petersburg State University, Physical Faculty. *Experimental team:* Gy. Török (SzFKI)		*Date(s) of Exp.* 2006 *Date of Report* 2008

Objectives *(Aim of the research in some sentences)*

Phthalocyanine is a synthetic analog of porphyrins [1]. It forms complex compounds metallophthalocyanines by reactions with metal salts. Light-metal phthalocyanines were first synthesized in England in the 1930s. They proved to be very radiation-resistant and thermally stable compounds [2-5].

Recently, reactions of water-soluble cationic porphyrines with DNA have been widely studied. It was found that the nature of cationic porphyrine–DNA complexes (porphyrine intercalation or external binding) depends on the composition and nucleotide sequence in the double helix of DNA, on the structure and properties of porphyrine, and on the content ratio of porphyrine and base pairs of DNA. However, there were no publications on interactions of anionic porphyrins with DNA. The lack of interest in anionic porphyrins was explained by the fact that in solution the DNA molecule has a negative charge and should not tend to form anion complexes. The aim of this work is investigation of the interaction of sulfonated scandium diphthalocyanine with DNA.

Preliminary results indicate that DNA interacts with $ScPc_2(SO_3)_4^{4-}$ and $LuPc_2(SO_3)_4^{4-}$ and packaging of DNA molecules occurs in water salt solutions after addition of the stated dyes.

Samples and Methods

A DNA sample from the cattle spleen was used; the molecular mass of the sample was 13 MDa as determined previously by viscosimetry. Sulfonated scandium diphthalocyanine (dye) was synthesized in the form of the ammonium salt $ScPc_2(SO_3)_4(NH_4)_4$. D_2O solutions of DNA with salt additions (1 mM NH_4Cl) were studied by small angle neutron scattering, dynamic light scattering, and atomic force microscopy in the presence (or absence) of a dye.

Results   (2)
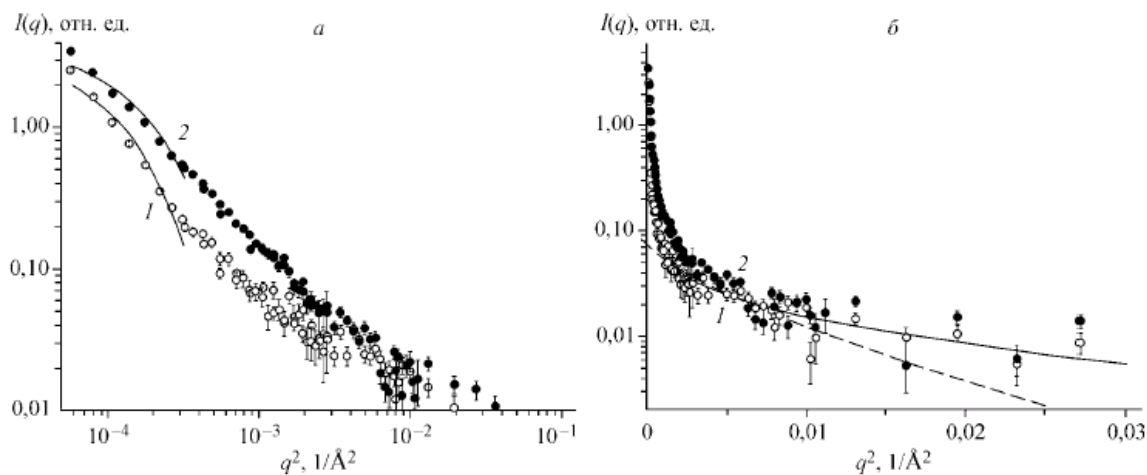
Fig. 1. *Intensity of neutron scattering of aqueous D_2O solutions of (1) DNA and (2) DNA + $ScPc_2(SO_3)_4(NH_4)_4$ as a function of q: (a) the region of small q (lines — calculation by Eq. (1)), (b) the region of large q (lines — calculation by Eq. (2)).*

The analysis of neutron scattering data indicated that the conformation of DNA changed after addition of ScPc2(SO3)4(NH4)4 to the solution.

At the lower limit of the pulse range (q 0.1 Å–1, Fig. 1) the scattering intensity $I(q)$ as a

$$I(q) = I_0 e^{-\frac{(qR_g)^2}{3}},$$

At the upper limit of the q range (q 0.1 Å–1, Fig. 1b) the intensity distribution obeys an equation

$$I(q) = \frac{A}{q} e^{-\frac{(qr_G)^2}{2}}$$
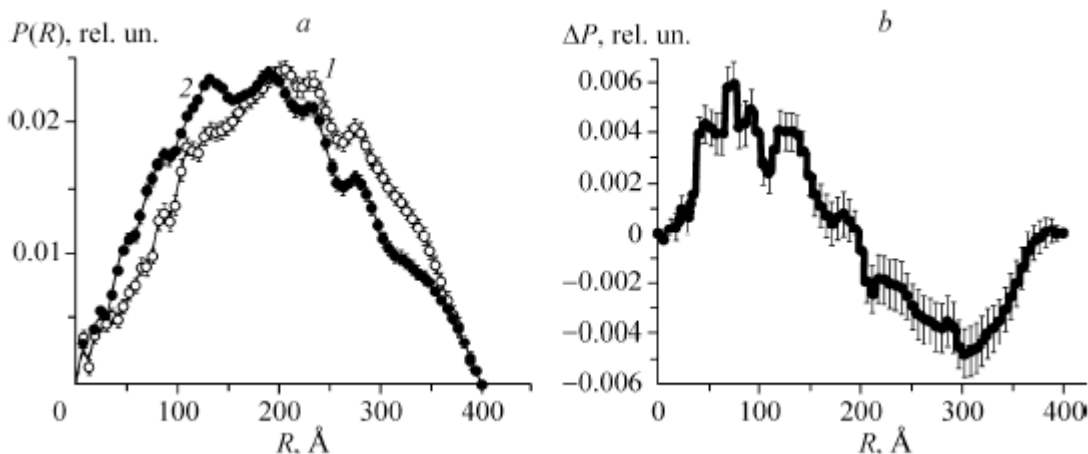
Fig. 2. Dependence of the (a) correlation functions for solutions of (1) DNA and (2)
DNA + ScPc2(SO3)4(NH4)4 and (b) difference in the correlation functions $\Delta P = P_{com} - P_{DNA}$ on the radius of correlation.

To understand how the dye affects the DNA conformation in more detail we determined the correlation function $\gamma(R) \sim \Delta\rho(0) \Delta\rho(R)-$ of both solutions (regularization method, ATSAS package). The Fig.2 shows a modified function $P(R) = \gamma(R)R^2$ which defines the averaged correlations of molecules in spherical layers relative to an arbitrary point of the molecule. The addition of $ScPc_2(SO_3)_4^4$ shifts the correlation function toward smaller distances by approximately 50 Å. The difference between the correlation functions $P = P_{com} - P_{DNA}$ is positive for R 200 Å and negative at long distances (Fig. 2b). The peaks $P(R)$ for R <200Å imply that the dye favors structuring of a strand because it lies at definite intervals, depending on its mole concentration.

Conclusions

Based on neutron and light scattering data one can draw a conclusion about complexation of sulfonated scandium diphthalocyanine with DNA in water salt solutions and DNA packaging under the action of the dye. The complex is stable over the temperature range 20-40C . Complexation of the negatively charged DNA molecules with sulfonated diphthalocyanines may be due to the formation of a double layer of ions around DNA, with the first positively charged layer of counterions attracting the negatively charged diphthalocyanine molecules. One can also assume that the conformation of DNA changes under the action of diphthalocyanines because of changes in its secondary structure, as in the case of cationic porphyrines. However, preliminary measurements of circular dichroism spectra of DNA solutions with ScPc2(SO3)4 or LuPc2(SO3)4 showed that there were no induced bands typical of the binding of cationic porphyrines with DNA in the visible region of the spectrum

The data about DNA packaging agree with the results obtained previously at 20 for solutions in light water by viscosimetry and spectrophotometry in the visible region.

References

1., G. P. Gurinovich, A. N. Sevchenko, and K. N. Solov'yov, *Spectroscopy of Chlorophyll and Related Compounds* [Russian], Nauka i Tekhnika, Minsk (1968).

2. P. Linstead, *J. Chem. Soc.*, 1016/1017 (1934).

4. J. M. Robertson, *ibid.*, 615-621 (1935).

5. J. M. Robertson, *ibid.*, 1195-1209 (1936).(1985).257 (1985).

B N C **Experimental Report**	*Experiment title* **Structural changes during monosaccharide formation**	*Proposal No.* *Local contact* Gy. Török.
Principal proposer: .　　　　　　Helena Grigoriew *Experimental team:*　Dagmara Chmielewska		*Date(s) of Exp.* 200, June 23-29 *Date of Report* 2008

Objectives *(Aim of the research in some sentences)*　The SANS measurements of the gels composed of galactose and mannose gelators with toluene, benzene and diphenyl ether as solvents were performed. The SANS answer was very weak, although we used 1 hour exposition time and repeated the measurements a couple of times. Each sample was measured in two temperatures: the first - at room temperature, as gel, and the second – at highest temperature, as sol state. However, after integration the signals from CCD detector , and subtraction the hydrogen plot from the sample plot, the remaining signal consisted only of statistic noise, without any structural features. It means that a very weak structural ordering in these materials, together with big amount of hydrogen in them, prevent to get any informative results.

..

Results *(Description of concrete results, understandable also for non-experts of the field. Insert, if possible, a typical figure)*
　Additionally, the magnetorheological polyurethane gel processed with carbonyl iron (CU) spheres was measured. The polyurethane gel was synthesized from polyether polyol with polyol and isocyanate compound.. The amount of CI spheres was equal 11.5% of volume. The curing process of the composite was carried out under magnetic field of 0.3 T Studies of such type composites structure vs electromagnetic properties was carried out, but not in the small-angle region It was found. that that the electromagnetic properties depend strongly on structure of CI spheres. The CI can be of onion –type arrangement of layers of cementite structure, or without the arrangement of ferromagnetic alfa-iron structure. Our SANS measurements showed that pure CI spheres are of onion-type arrangement, with interlayer distance of about 50nm, and after the composite curing, of alfa-iron structure.

(2)

Future prospects *(Summary of the remaining problems to be solved, basis for the continuation of the work)*

.

Objectives *(Aim of the research in some sentences)*

Use of various chemicals affect the properties of textile fibres, including strength, hydrophilicity and optical appearance (lustre). One of the many variable properties of natural wool fibres are their optical characteristics. Some fibres exhibit a very high luster, whereas other types of fibre consistently appear very dull. The mechanisms creating this optical effect are believed to lie in the arrangement of the outer layer of the individual fibres. Scanning electron microscopy (SEM) is one way of observing the fibre. Fibre structure is fairly well observed by SEM, (Fig 1.)
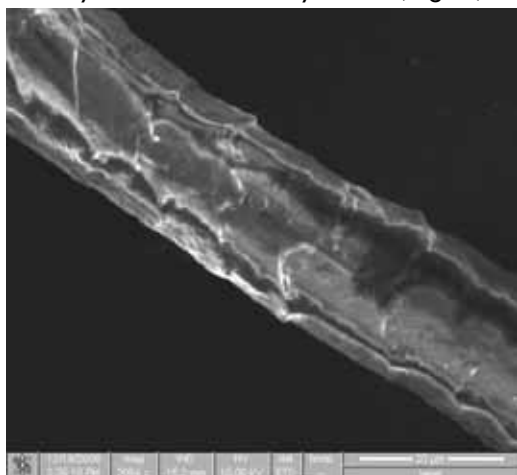
. The crystallinity within the fibres is not simple with standard techniques, such as X-ray fibre diffraction due to the small dimensions of the fibre (microns) and the need to bulk average the data. The presence of high-Z contaminants within the fibre furthermore dominates the underlying X-ray scattering from the fibre itself. Similarly the bulk atoms will be composed of similar Z to the surface, where the luster effect is expected to occur, thus limiting any contrast difference, however such a method is impractical. Since the optical effect is believed to be on the microscopic scale, the potential to observe the characteristics that control the lustrous appearance, using a technique such as small angle neutron scattering (SANS), was investigated.

Fig 1

Results *(Description of concrete results, understandable also for non-experts of the field. Insert, if possible, a typical figure)*

We report here on observations of the spectra obtained from small angle neutron scattering from natural wool fibres that exhibit a very low or very high optical lustre. Initial indicated anisotropic neutron scattering properties for the different types of wool fibre.

Xxx Hol van a 4. és 5. ábra?
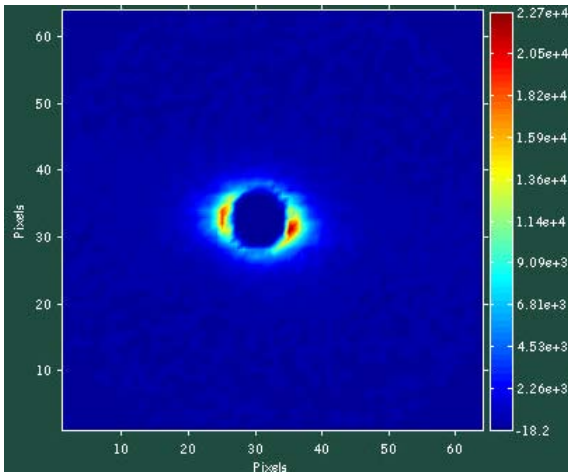
*Fig 2   SANS spectrum from dull woo*l   *Fig 3 SANS spectra for lustrous wool*
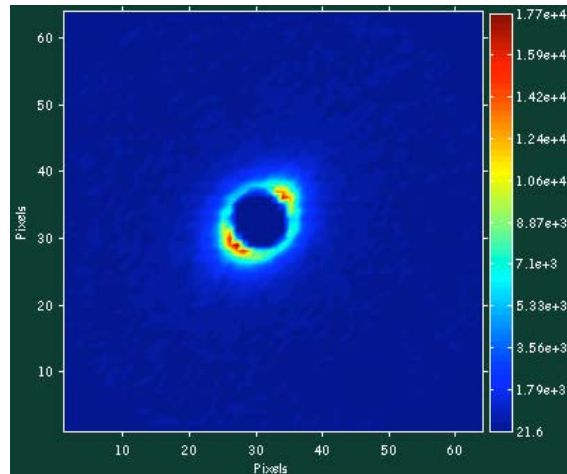
Figures 2 and 3 illustrate the 2-D scattering spectra, obtained at 11 Å, for the dull and very lustrous fibres respectively. The anisotropic nature of the spectra was analyzed by considering sectors of equal size, with high and low intensity. The data was analyzed using the open source software package GRASP-4.26.
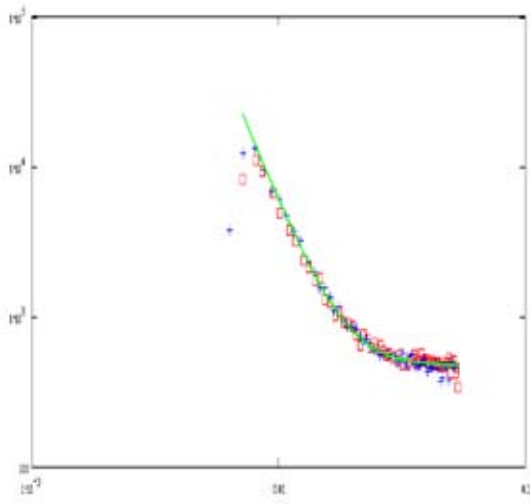
Comparison of dull and high luster in high intensity region at 7.5 A   Comparison of dull and high luster in low intensity region at 7.5 A
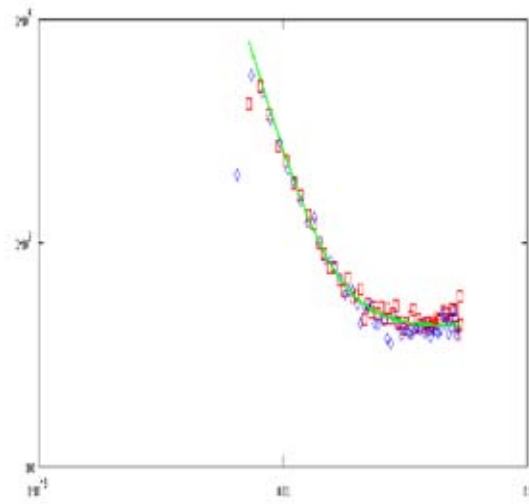
Fig 6.   *Fig 7.*

Figures 6 and 7 are comparisons of the scatter intensity versus Q^{-1} in the high and low intensity sectors respectively at 7.5 Å
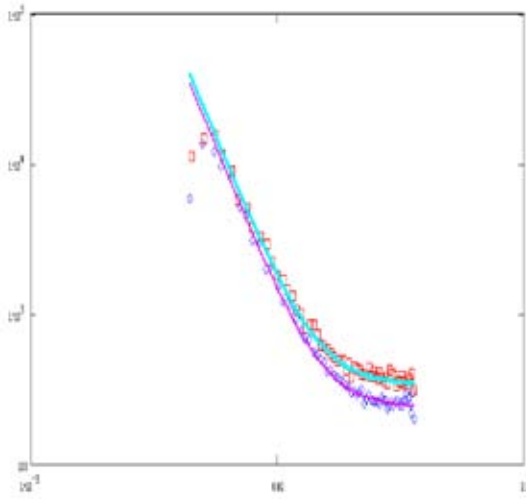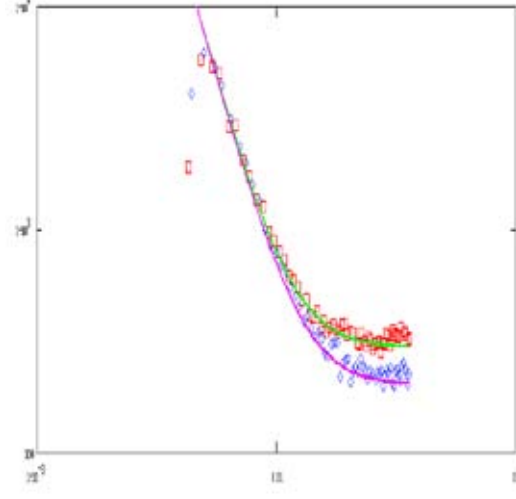
| *Fig 8.* | *Fig 9.* |

Figures 8 and 9 are the comparisons of the scatter intensity versus Q^{-1} in the high and low intensity sectors at 11.22 Å.

The curves appear to mainly follow the scattering properties exhibited by large grains, namely I proportional to Q^{-4}. Fits to the data for the high and low intensity sectors at the three wavelengths are presented for the lustrous fibres in Table 1 and for two wavelengths for the dull fibres in Table 2

Wavelength (Å)	High intensity sector	Low intensity sector
3.38	$I = 1020.+25.*10^{-5}*Q^{-4.05}$	$I = 960.+16.*10^{-5}*Q^{-3.857}$
7.51	$I = 470.+4.5*10^{-5}*Q^{-4.05}$	$I = 380.+3.5*10^{-5}*Q^{-3.88}$
11.22	$I = 239.+10^{*-5}*Q^{-4.05}$	$I = 200.+10^{-5}*Q^{-3.853}$

Table 1. Fits to the scatter intensity versus momentum transfer, Q, for lustrous fibres

Wavelength (Å)	High intensity sector	Low intensity sector
7.51	$I = 470+4.5*10^{-5}*Q^{-4.05}$	$I = 380.+3.5*10^{-5}*Q^{-3.88}$
11.22	$I = 350.+10^{-5}*Q^{-4.085}$	$I = 295.+10^{-5}*Q^{-3.853}$

Table 2. Fits to the scatter intensity versus momentum transfer, Q, for dull fibres.

Future prospects *(Summary of the remaining problems to be solved, basis for the continuation of the work)*
We need to continue this investigation in direction of surface roughness of wool fibres and to the direction of wetting mechanisms.

BNC **Experimental Report**	Experiment title **Study of Fe-oxide particle size by neutron diffraction in fresh and spent catalyst samples**	Proposal No.
		Local contact Gy. Török.

Principal proposer:
. Dr. Fejes Pál Dept. of Applied Chemistry, Szeged University
Imre Kovacs Institute of Isotopes Dept of Catalysts and surfaces

Experimental team:
 Gyula Török (SzFKI)

Date(s) of Exp. 2006
Date of Report 2008

Objectives *(Aim of the research in some sentences)*

.Various kinds of iron oxides (except hematite) are able in high dispersity to catalyse selective oxidation (SCO), or selective reduction (SCR) reactions. Therefore, these catalysts find application in the chemical industry and environmental protection. As the net result (even in SCR) is exothermic, the iron oxide particles change their structure and size by migration (of FeO.(OH) units) which leads to reduction and finally loss of activity.

From theoretical point of view and eventually in order to find experimental ways to hinder activity loss, it is of importance to study the genesis of particle size growth.

Preliminary experiments carried out on spent catalyst samples show that neutron diffraction is a promising method to study and follow the increase of iron oxide particle size in these samples. In order to check to magnetic state of magnetite (and other iron oxide components) we need to use magnetic field up to saturation. The SANS experiment can answer the questions raised above.

Results *(Description of concrete results, understandable also for non-experts of the field. Insert, if possible, a typical figure)*

We have carried out a series of small angle neutron scattering (SANS) experiments on samples in the range of momentum transfer $q=0.03-4.5nm^{-1}$ (Budapest Neutron Center "Yellow Submarine" SANS facility)[1]. at room temperature. The raw data were treated in usual procedures and normalised to the water standard. To avoid multiple scattering we used samples with thickness d = 1.mm of high transmission: in the first T_{Dia} = 0.9750/ T_{DiaF2} = 0.9603; T_{DiaF5} = 0.9676 T_{DiaF7} = 0.9487;and the second case. T_{M10} = 0.9756 T_{M10B19} = 0.9674 T_{M10C19} = 0.9704 Masses of samples were close to each other in both group.: with layer thickness d = 1. mm and (density of layers ~ 0.5   and ~0.25g/cm^3).

sample	F2 (mg)	F5 mg	F7 mg	D mg
mass	101.3	123.5	109.6	103.1
density	0.457 g/cm^3	0.557 g/cm^3	0.494 g/cm^3	0.465 g/cm^3

sample	M10	M19B	M19C
mass	59.4mg	51.0 mg	58.9mg
density	0.268 g/cm^3	0.230 g/cm^3	0.266 g/cm^3

The detailed analyze were carried out using Inverse Fourier transform (Program package ATSAS).[11]

The differences in cross sections $\Delta\sigma_{DIAFX} = d\sigma/d\Omega_{DIAFX} - d\sigma/d\Omega_{DIA}$ (when diatomaceous earth the carrier contribution was subtracted) were analysed to obtain information about inclusions of Fe2O3 The variation of scattering pattern could allow to determinate the size distribution of Fe2O3 inclusions

Samples

M10. The surface measured from isotherm measurement is 570.2m^2/g giving average void diameter 10nm.

For **diatomaceous earth** the isotherm measurement gives: 22.6 m2/g. A bimodal void structure is known with 4nm (10-15%) and 14-15nm diam (85-90%)

The scattering data (Fig.1a,Fig1b, and Fig2a,Fig2b,) at high q, i.e. in the Porod limit, $I(q) \rightarrow A/q^4+B$ gives an estimate of internal surface area of system. In Porod representation [11] the scattering curves $q^4I(q) = A+Bq^4$ gives a linear approximation with fitting parameters given in Table 2.

sample	DIA	F2	F5	F7
A	0.2887	0.8108	0.7867	1.34533
B	0.0006	-0.00138	-0.00239	0.002137
S=A/K^2*2π	97m^2/g	----	----	---

sample	M10	F19C	F19B
A	0.8082	1.2231	1.2482
B	-0.0007	0.0153	0.0159
S=A/K^2*2π	588 m^2/g	----	-

Table 2
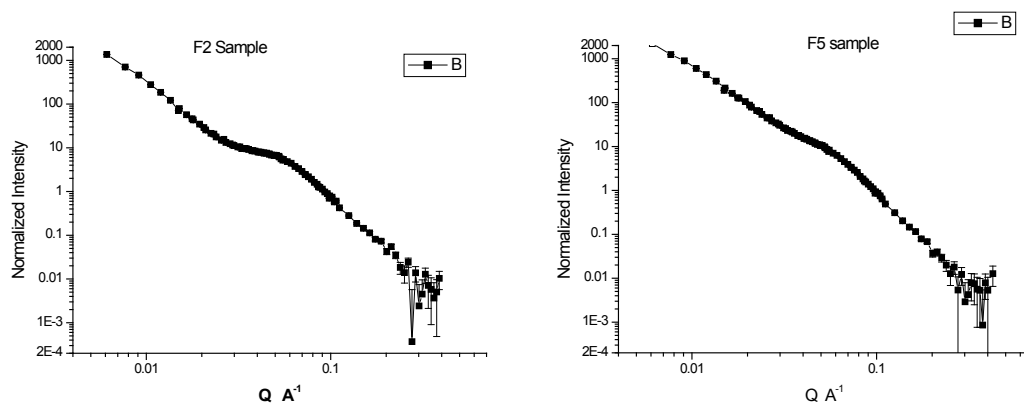
Fig.1a, The scattering patter of F2 and F5 sample
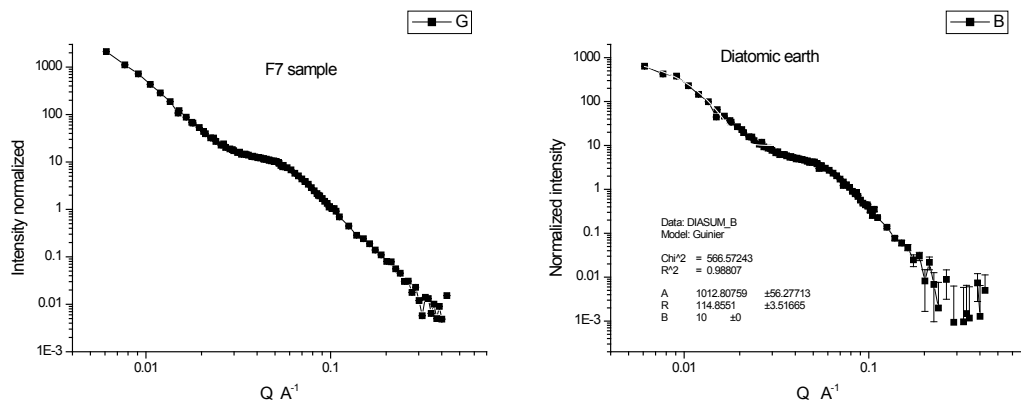
Fig.1b, The scattering pattern of F7 and of diatomic soil sample.
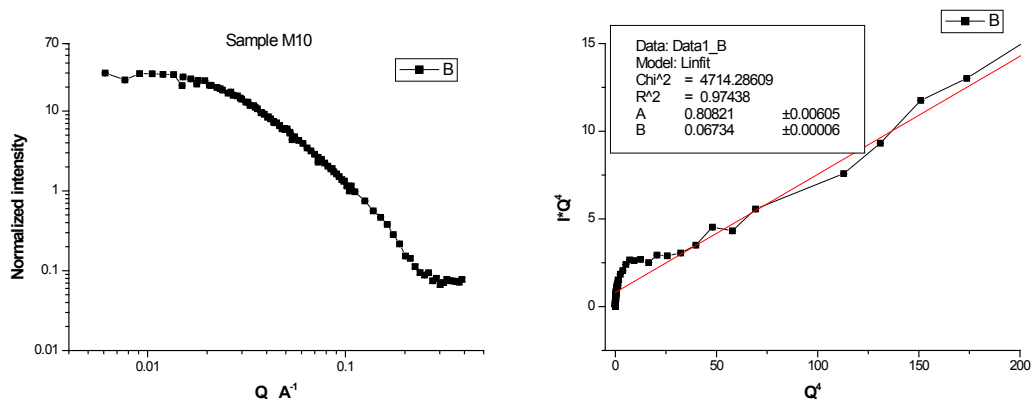
Fig.2a, The scattering pattern of M10 carrier sample in normal and Porod representation
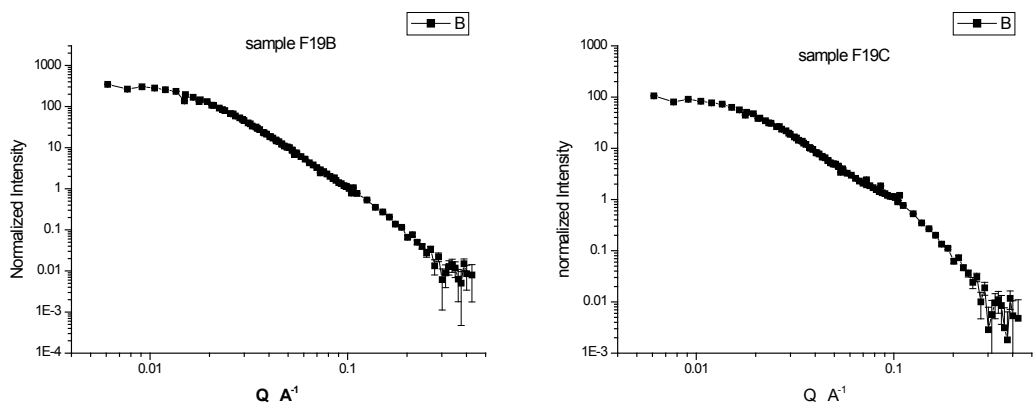
Fig.2b, The scattering pattern of F19B and f F19C   sample in normal and Porod representation

The parameter $A=2\pi K_s^2 S_t$ is proportional to the full surface area of interface (interphase boundaries, boundaries of pores and crystallites) and squared contrast factor at the interface.

In case of samples M10 and diatomic earth we have got the surfaces.

The result is in good agreement with isotherm measurement. in case of **M10 carrier**, and poor in case of diatomic earth. Here we should note that the neutron measurement gives the full surface area including the inner surface elements such as voids, dislocations cracks too, what is not measured at isothermic measurement.(BET)

From these parameters we can estimate the diameter of Fe2O3 inclusions assuming that the carrier matrix structure has not been changed substantially.

Future prospects *(Summary of the remaining problems to be solved, basis for the continuation of the work)*
Because results are in good agreement with other kind of measurements (M10) but some are different. (diatomic earth) . We cannot exclude some multiple scattering and multiple bragg refelction effects. Some part of measurement should be carefully repeated.

Objectives *(Aim of the research in some sentences)*
---Processes of self-organization of ionomers based on sulfonated PS containing ionogenic groups in the salt form (SO_3Na) in chloroform have been studied by small-angle neutron scattering. At a small content of ionogenic groups SO_3Na (1.35 mol %), the conformation of PS chains changes from coil-like to globular due to electrostatic interactions between them. An increase in the share of ionogenic groups to 2.6 mol % brings about the assembly of ionomer chains into a hollow spherical structure with the solvent inside. In the shell of a micelle, polar groups are densely packed and shielded from the solvent by nonpolar fragments of adjoining chains. At a low content of ionogenic groups in ionomers, two-thirds of macromolecules in solution are not incorporated in any structures. With an increase in the content of polar groups to 2.6 mol %, almost all chains are organized to small clusters---the stable pairs of macromolecules

Results
Sulfonated PSs containing 1.35 and 2.6 mol % of SO_3Na groups (samples 1, 2) were prepared based on PS with Mw = 115 × 103 (Mw/Mn = 1.05) (produced by anionic polymerization Chloroform of reagent grade (a density of 1.50 g/cm3) was used to prepare solutions of reagents. Polymer solutions in chloroform (a concentration of 0.5 g/dl) were prepared at room temperature over several days.
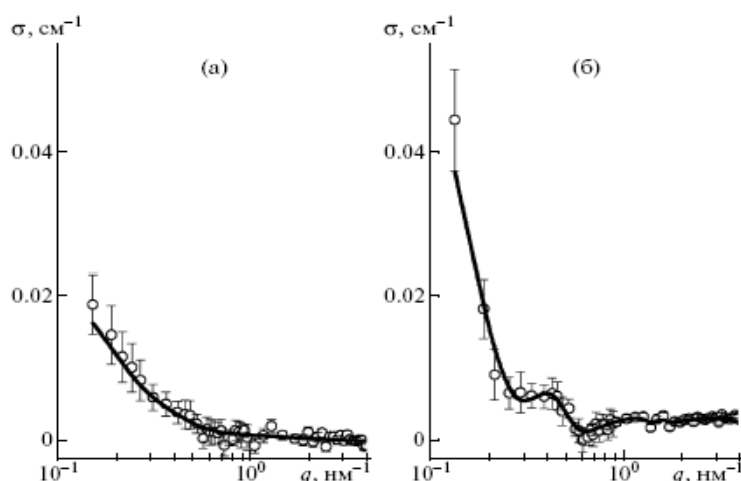
Fig 1., The cross section of neutron scattering σ as a function of momentum transfer q in solutions of sulfonated PS (samples 1, 2) in chloroform (20°C) containing (a) 1.35 and (b) 2.6 mol % SO3Na ionogenic groups. The approximating curves correspond to correlation functions γ(R)
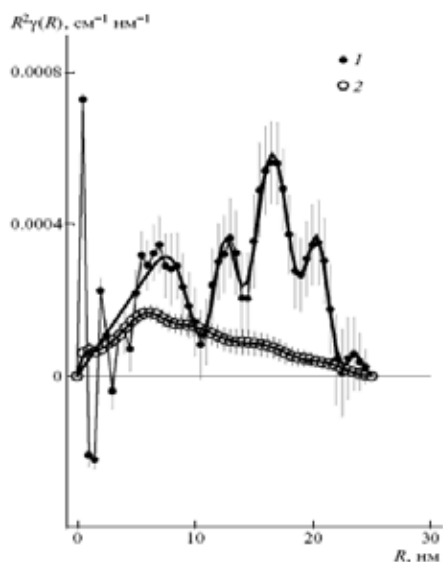
Fig. 2.
Correlation functions derived the data of neutron scattering for solutions of ionomers 1 and 2 containing (1) 1.35 and (2) 2.6 mol % SO3Na ionogenic groups as a function of radius of molecular correlations. The corresponding approximation functions are shown by the lines

Neutron scattering data indicate the enhancement of scattering at small pulses with increasing concentration of polar groups (Fig. 1). This effect can be explained by the formation of supramolecular structures of ionomers due to electrostatic interactions. This suggestion is proved by the results of Fourier transform of cross sections of scattering $\sigma(q)$ in the function of molecular correlations $\gamma(R)$ [13, 14] over the range of radii R = 0 --30 nm (Fig. 2): Function $R^2\gamma(R)$ directly reflects the spectrum of spatial correlations in the range of radii from the size of a unit to the size of macromolecules and supramolecular structures. The conformity of this spectrum (Fig. 2) with the real structure of a system is confirmed by the calculated cross sections $\sigma(q)$ based on this spectrum; the values of cross sections fit well the experimental relationships (Fig. 1). The presence of maxima on the $R^2\gamma(R)$ plots (Fig. 2) allows one to estimate the sizes and mutual correlations of particles in the system.

The sequence of models corresponds to the transition from loosened chain structures to globular and uniform dense objects. Taking into consideration the data from [12], where the collapse of ionomers with an increase in their content of ionogenic groups is described, the results of the present study correlate with these models.

. The data from Fig. 2 can be approximated by the integral correlation function

$$R^2\gamma(R) = \alpha_0 R^2 \exp(--R/R_C) + \alpha_1 R^2 \exp[--(R-R1)^2/2\,\delta_1^2\,]. \quad (5)$$

Here, the first item describes the structure of a globular particle with correlation radius R_C, whereas the second item characterizes the pair correlations of particles in solution. The table summarizes coefficients α_0 and α_1 relating correlation functions to the measured cross section (Fig. 2a) and parameters R_C, R_1, and δ_1.

Thus, based on the above evidence, the macromolecule of ionomer 1 can be represented as a spherically symmetric globule the dense nucleus has the correlation radius R_C and is surrounded shell consisting of chain fragments

As the amount of SO_3Na groups in sulfonated PS chains is increased from 1.35 to 2.6 mol % (sample 2), the structure of macromolecules changes substantially. This is evidenced by the asymmetry of the first peak (Fig. 2).

With an increase in radius to R = $R_{max}^{(1)}$, function $R^2\gamma(R)$ increases linearly; at R > $R_{max}^{(1)}$, it declines sharply. Such a character of the correlation function is typical of an object in the form of the spherical layer

For a thin layer with a small difference in the external and inner radii (R2 − R1 ! << 2R1), the correlation function is characterized by the triangular profile:

$$R^2\gamma(R) = R(R2 -- R1)/2 \quad \text{at} \quad (R2 − R1)/2 \leq R \leq 2R2 \qquad (6)$$
$$R^2\gamma(R) = 0 \text{ at } R > 2R2$$

The real thickness of the layer is determined by deviations of groups from the average position on the sphere of radius R_A. The value of radius R_1 is close to the external diameter of a macromolecule $D_E = D_A + \Delta L = 12.9 \pm 1.8$ nm. This means that macromolecules occur at the minimal distance (associated). Based on the ratio of areas under the second and first peaks (S_2, S_1) (Fig. 2), the probability (P_{D2}) of formation of chain pairs in the solution of sample 2 is $P_{D2} = S2/S1 = 0.95 \pm 0.17$. At a concentration of SO_3Na groups of 2.6 mol %, the probability of association of chains PD2 three times higher than the probability P_{D1} of binding of ionomers containing 1.35 mol % groups.

The results of this study are in agreement with the theoretical concepts and experimental data on the structural organization of strongly associating polymers in weakly polar solvents [1, 4--6]. In accordance with [1, 4--6], ionomer chains can form dense layers with ionogenic groups (multiplets) and aggregates in solution. According to theoretical predictions [5], an anisotropic disk and hollow micelles (vesicles) form in the spherical layer built up of associated ionogenic groups in the limiting case of strong segregation of polar and nonpolar chain fragments in solutions. Our data demonstrate that the internal structuring of the ionomer with a high content of SO_3Na groups (2.6 mol %) occurs via the lamellar micelle model [5].

1. A. M. Young, J. S. Higgins, D. G. Peiffer, and A. R. Rennie, Polymer **36**, 691 (1995).
2. D. I. Svergun and L. A. Feigin, @Small-Angle X-Ray and Neutron Scattering (Nauka, Moscow, 1986) [in Russian].
3. D. I. Svergun, J. Crystallogr. **25**, 495 (1992).
4. I. A. Nyrkova, A. R. Khokhlov, and M. Doi, Macromolecules **26**, 3601 (1993).
5. A. N. Semenov, I. A. Nyrkova, and A. R. Khokhlov, Macromolecules **28,** 7491 (1995).
6. A. N. Semenov, J. F. Joanny, and A. R. Khokhlov, Macromolecules **28**, 1066 (1995).

Future prospects *(Summary of the remaining problems to be solved, basis for the continuation of the work)*

B N C Experimental Report	Experiment title **Structure of possible magnetocarriers with photodithazine by SANS**	Proposal No.
		Local contact Gy. Török.

Principal proposer: Yu V Kulvelis[1], V.A. Trounov[1], V.T.Lebedev[1], D.V. Orlova[1], M,L,Gelfand[2] [1] PNPI , [2]Oncological Institute of St Petersburg Experimental team: Gy. Török (SzFKI)	Date(s) of Exp. 2006 Date of Report 2008

Objectives *(Aim of the research in some sentences)*

. Complexes of nanoscale ferromagnetic particles with Russian photosensitizer «photodithazine» have been first synthesized and studied by small-angle neutron scattering to evaluate structure and molecular characteristics of complexes as functional materials for cancer treatment. The influence of biocompatible macromolecules of pluronic on the functional properties of the synthesized complexes has also been studied. In following biomedical tests the complexes have shown a high efficiency as the compounds capable to suppress the reproduction of tumor cell culture. The results can be used in development of magnet-guided medicine for photodynamic therapy of cancer.

Results *(Description of concrete results, understandable also for non-experts of the field. Insert, if possible, a typical figure)*
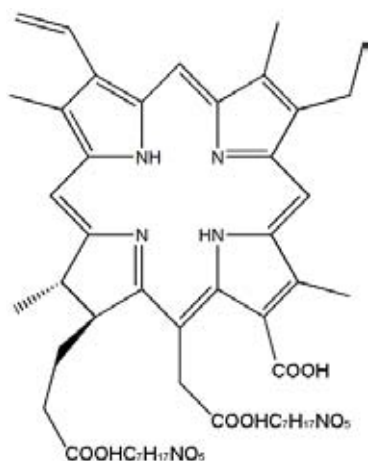
Fig. 1. Photodithazine
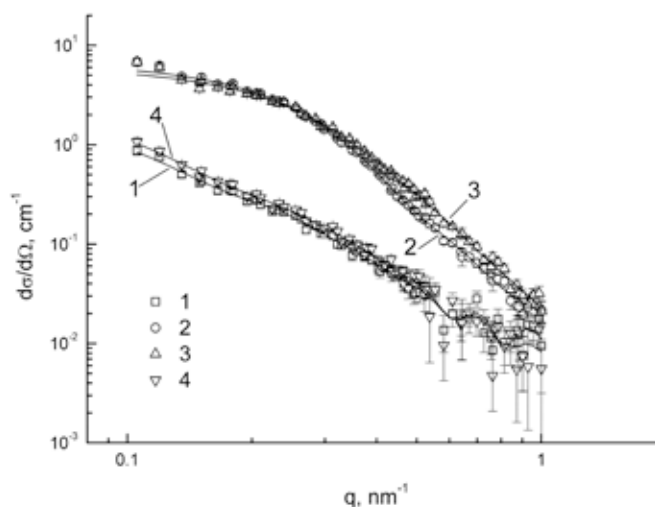
Fig 2 Scattering function samples No 1,2,3,4, vs q impulse transfer

The 4 samples of magnetic liquids with pluronics F127 and photodithazine in 90 % D_2O: has been prepared and measured:

1 – magnetic liquid, 2 –magnetic liquid with pluronic ,
3 – magnetic liquid with pluronic and and photodithazine, 4 – magnetic liquid with photodithazine.

The scattering curve at samples 1,4 (without pluronic) well described by model (2):

$$\frac{d\sigma}{d\Omega}(q) = \frac{I(0)}{(1+(qR_c)^2)^2}\{1+\sum_{i=1}^{5} A_i \frac{\sin qR_i}{qR_i}\}$$

(2)

At samples 2, 3 (with pluronic) the model (3) can be used

$$\frac{d\sigma}{d\Omega}(q) = [I_1(0)\frac{3(\sin q_1 - q_1 \cos q_1)}{(q_1)^3} + I_2(0)\frac{3(\sin q_2 - q_2 \cos q_2)}{(q_2)^3}]^2\{1+A\frac{\sin qR}{qR}\}$$

(3)

The formfactor corresponds to the magnetite spherical particle (radius r_1) and shell containing pluronic (radius r_2) and contains only one part for correlation function in space with characteristic distance R

Table 1. Chemical composition and parameters of samples 1,4

Sample	C_{magn}, %	C_{F-127},%	C_{pd}, %	I(0),cm^{-1}	R_c, nm	A_1	R_1, nm
1	2.4872	0	0	0.18(3)	2.0(2)	2.1(3)	8.0(4)
4	2.4895	0	0.0493	0.29(9)	2.5(3)	1.5(4)	7.9(7)

sample	A_2	R_2, nm	A_3	R_3, nm	A_4	R_4, nm	A_5	R_5, nm
1	2.0(4)	14.2(7)	2.3(5)	20.6(6)	2.4(6)	28.3(6)	1.3(4)	36.7(10)
4	1.4(6)	14.1(12)	1.9(7)	20.2(8)	2.0(6)	28.2(7)	0.9(4)	37.5(13)

Table2. . Chemical composition and parameters of samples 2,3 (with pluronic)

sample	C_{magn}%	C_{F-127}, %	C_{pd}, %	I_1(0),cm^{-1}	r_1, nm	I_2(0),cm^{-1}	r_2, nm	A	R, nm
2	2.4898	0.5355	0	0.53(9)	3.1(4)	1.02(7)	7.3(4)	1.77(12)	9.08(11)
3	2.4975	0.5092	0.0491	0.74(6)	3.57(19)	1.02(5)	8.0(4)	0.96(12)	9.7(3)
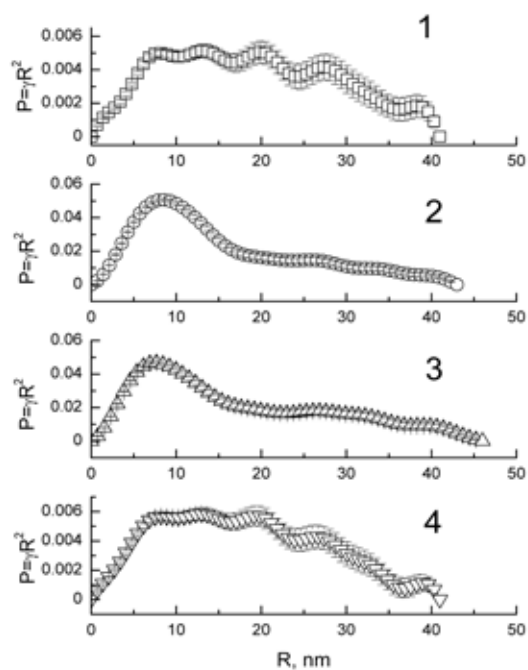
For samples 1 и 4 the correlation at distances R1 ~ 8 nm, R2 ~ 13 nm, R3 ~ 20 nm, R4 ~ 28 nm and R5 ~ 38 nm, can be observed well corresponding to Ri distances between particles (table. 1).

The structural organization of samples 2,3 similar. The neighboring magnetite particles forms clusters form ~6 particles covered by spherical shell with diam $2r_2$ ~ 15-16 нм

Such clusters forms associations from 3 (sample2) or from 2 (sample 3) what follows from parameter A showing the amount of clusters in associates: A + 1 = 2.77 ~ 3 (sample 2); A + 1 = 1.96 ~ 2 (sample 3)..The presence of photodithazine weekend the correlation between clusters and gives rise the distance between centers from 9,08 till 9,7 nm

Fig 3 The P(R) = γR^2 correlation function of samples 1-4.

Future prospects *(Summary of the remaining problems to be solved, basis for the continuation of the work)*
We shown that compleses are stabile at 20-40 C the Pluronic gives a rise of effectivity of samples in clinical tests, such complex can be used as a magnetically regulated photodiazine theraphy.

Objectives *(Aim of the research in some sentences)*

.. Diphthalocyanines of rare earths and some other elements are sandwich like compounds in which the complexing metal ion is located between two phthalocyanine molecules Sulfonated diphthalocyanines of metals are soluble in water and exhibit a clearly pronounced antiviral activity (against the influenza and Rous sarcoma viruses). The toxicity of these compounds is lower than that of Remantadin [6]. The highest values of the protection coefficient were obtained in tests of scandium and lutetium compounds [6–8].

Results *(Description of concrete results, understandable also for non-experts of the field. Insert, if possible, a typical figure)*

(2)

The heavy-water solutions of PVP in the presence of each of the porphyrins were studied using small-angle neutron scattering in the momentum transfer range q 0.01–0.30 Å$_{-1}$
. In the momentum transfer range $q < 0.1$Å$_{-1}$, the scattering intensity as a function of the momentum transfer was

approximated by the Guinier function $I(q) = I_0 e^{-\frac{(qR_g)^2}{3}}$, where $I_0=I(q0)$ is proportional to the concentration of the polymer in the solution and to the mass of scattering objects (segments) and R_G is the radius of gyration In the Guinier approximation, the radius of gyration of the PVP molecule decreases upon addition of each dye (Fig. 1).

Fig. 1. Gyration radius of (1) H2TPPS4(HCl)2 + PVP and (2) CuTPPS4 + PVP complexes in heavy water solutions as a function of the molar ratio of the components at a constant PVP concentration CPVP = 0.49 g/dl (0.044 M) and a variable concentration of porphyrins. T = 20°C.

Conclusions

The above results allow us to draw the conclusion that, in aqueous solutions, the sulfonated tetraphenylporphins H2TPPS4(HCl)2 and CuTPPS4 form complexes with a PVP molecule and that, under the effect of these porphyrins,

the PVP molecule becomes morecompact. The nature of the interaction of PVP molecules with sulfonated tetraphenylporphins can be associated with the ion–dipole interactions between theO=O dipoles of the pyrrolidone rings and negatively charged sulfo groups of the porphyrins.

These results agree with the data obtained earlier for analogous systems, namely, poly-*N*-vinylcaprolactam and DNA with sulfonated diphthalocyanines of lutetium and scandium, in which the attachment of diphthalocyanine anions to the poly-*N*-vinylcaprolactam molecule, charging of this molecule, and a decrease in the volume of DNA molecules were observed.

	Experiment title	Proposal No.
B N C **Experimental Report**	*Experiment title* **Residual stress investigation of steel welding of WWER-1000 reactor wall**	
		Local contact Gy. Török.
Principal proposer: **V.T.Lebedev, Gy.Torok, V.M.Lebedev, A.N.Lapin2, V.A.Petrov2, B.Z.Margolin2** [1] PNPI [2]Prometey *Experimental team:* Gy. Török (SzFKI)		*Date(s) of Exp.* 2006 *Date of Report* 2008

Objectives *(Aim of the research in some sentences)*

The residual stresses in a component or structure are stresses caused by incompatible internal permanent strains. They may be generated or modified at every stage in the component life cycle, from original material production to final disposal. Welding is one of the most significant causes of residual stresses and typically produces large tensile stresses whose maximum value is approximately equal to the yield strength of the materials being joined, balanced by lower compressive residual stresses elsewhere in the component.

Tensile residual stresses may reduce the performance or cause failure of manufactured products. They may increase the rate of damage by fatigue, creep or environmental degradation. Compressive residual stresses are generally beneficial, but cause a decrease in the buckling load. The investigation of stresses in the reactor wall material is exceptionally important due to the affect of reactor safety.

Results *(Description of concrete results, understandable also for non-experts of the field. Insert, if possible, a typical figure)*

(2)
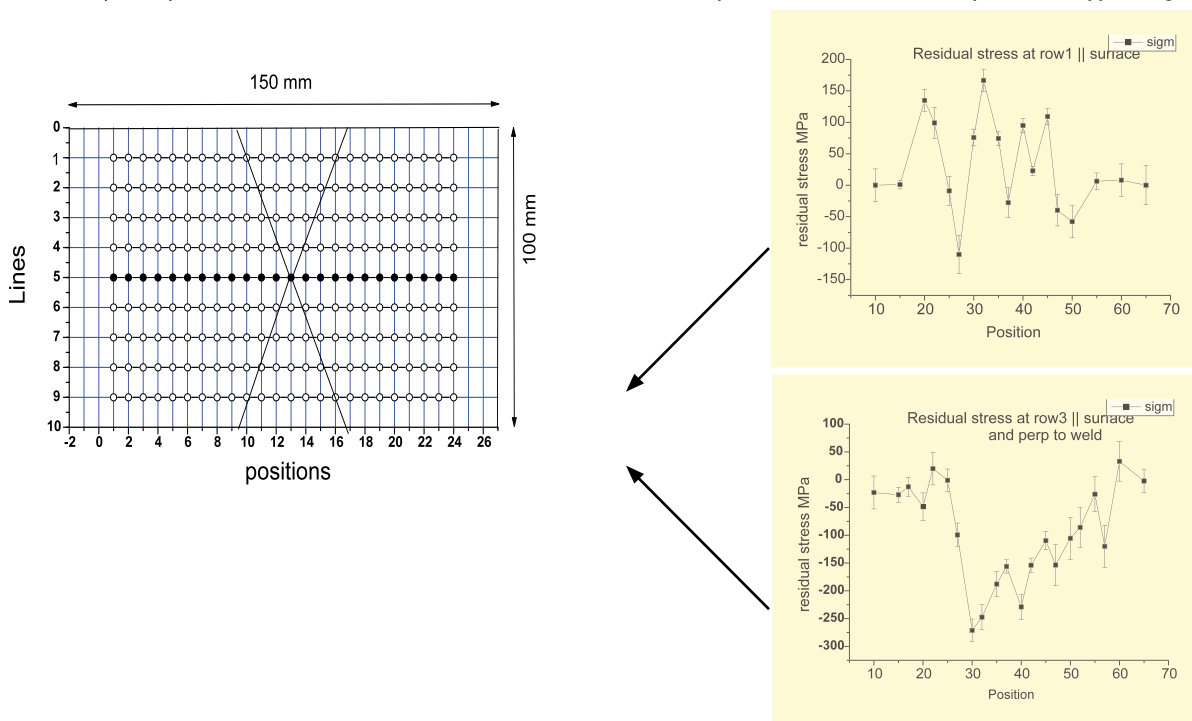
As is displayed on the pictures the welding probe has a relatively small tensile component on the surface what becomes more inside the test element. That can be relaxed further by another heat treatment. The overall stress in the sample are much less than a usual welded specimen.

B N C **Experimental Report**	*Experiment title* The Effect of Surface Oil Contamination on the Reflectivity of Neutron Supermirrors	*Proposal No.* Reflektométer *Local contact* **T Veres**
Principal proposer: Kovács-Mezei Rita *Experimental team:* T. Veres, L. Cser, L. Riecsánszky		*Date(s) of Exper.* 06.11.2007 *Date of Report* 21.01.2009

Objectives *(Aim of the research in some sentences)*

Neutron supermirrors (SM) [1] commonly used in neutron guides frequently become contaminated with oil originating from either the vacuum pumps, or their surrounding atmosphere. As a result, due to the multiple reflections the intensity at the neutron guide exit can dramatically decrease. The aim of the present experiment is to study the quantitative dependence of the surface contamination on the reflectivity.

Results *(Description of concrete results, understandable also for non-experts of the field. Insert, if possible, a typical figure)*

The oil layer (Edwards Ultragrade 19 vacuum pump oil) with thicknesses from 0.17 to 2.3 μm was deposited on the 2.5 *m* SM surface (*m* is the multiples of the critical angle of the SM compared to the natural nickel) consisting of Ni and Ti layers, coated with a 70 nm Ni layer. The SM multilayer system was prepared on a 500 mm long, 100 mm wide and 5 mm thick borofloat glass substrate. The oil was deposited from oil vapour created in a heated vessel containing vacuum-pump oil. In practice this oil is a mixture of straight-chain and branched, fully saturated hydrocarbons, and its average molecular weight according to the information from the Edwards Co. is equal to 420 which corresponds to average chemical composition $C_{30}H_{62}$. The amount of the evaporated oil on the surface of the SM was measured using a balance and optical interferometry. Reflectometry results are shown in the Figure 1.
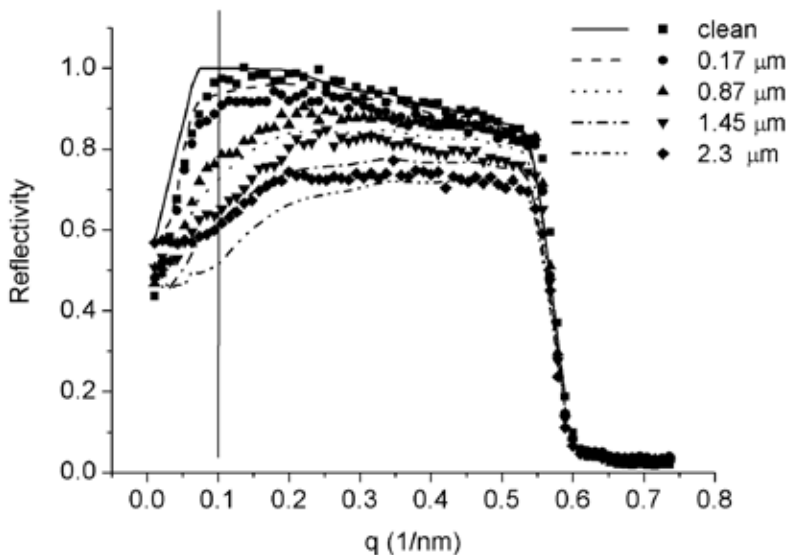
Figure 1. The reflectivity of the SM coated by oil layers of various thicknesses between 0.17 and 2.3 μm versus momentum transfer q. The points represent the experimental results. The continuous and broken lines correspond to the model calculation results taking the geometrical effects and finite resolution into account. Below the vertical line (q=0.1 nm⁻¹) the reflectivity is distorted due to the finite collimation slit and sample size.

For the model calculation, the Parratt recurrence formula (Parratt32) was applied.

Relying on the obtained results the loss of the neutron intensity was estimated for a real neutron guide by the use of VITESS program. The result is demonstrated in the Figure 2.
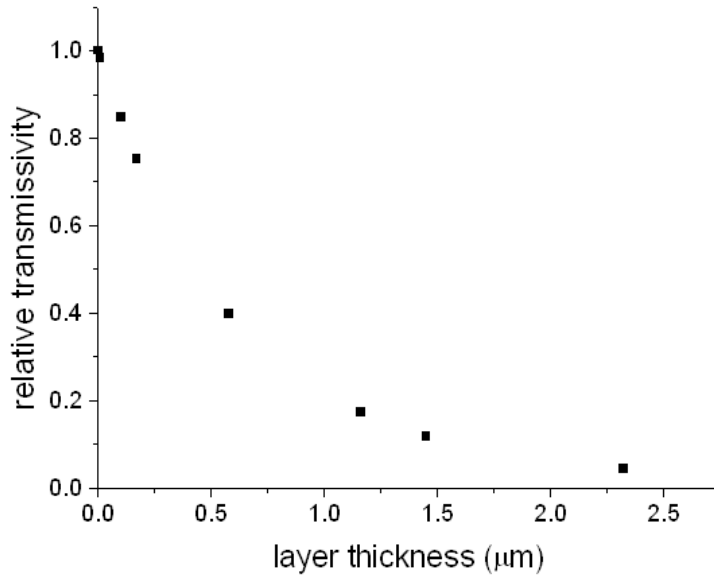
Figure 2. The calculated neutron yield at the guide exit for different thicknesses of oil contamination after multiple reflections over the flight of the 30 m long curved (r=4500 m, width 2.5cm, height 10 cm) guide normalized to unity. Unity is the transmission for a clean neutron guide. The calculation was performed at λ=0.4 nm.

As the result it was demonstrated that even moderate amount of contamination of the mirror surface may cause appreciable loss of the neutron intensity.

Future prospects *(Summary of the remaining problems to be solved, basis for the continuation of the work)*
There remain several effects for further studying and explanation. E.g.: What is the reason of rather large reflectivity at very small scattering momentum (q) transfer? Why the model calculation does not fit to the measured data in the medium q range? Finally, the VITESS model calculation will be generalized for neutron guides of various length and curvature.

References *(Published or accepted papers, research reports, conference lectures, seminars etc.)*

The results were presented at the regular open seminar of Research Institute for Solid State Physics and optics.

Objectives The TOF neutron diffractometer has been installed to the radial channel No. 1 of Budapest Reactor. To keep the short wavelength part of the flux the neutron guide has not been curved. Since the choppers are Gd coated, the application of fast neutron filter become necessary. The spectrometer will operate with a large surface 2D detector and a set of flat ^{3}He tubes. For the optimization of them, the achievable resolution has been determined on Al_2O_3 powder.

Results

The filter is made of silicon single crystal cylinders with the (111) direction in the longitudinal axis. The two pieces (14 and 16cm in length and 9cm in diameter) are fixed in two different segments of the beam shutter in Al capsules.

The gain in the signal-noise ratio is about five: at about fifty percent loss in the effective flux the number of fast neutrons has been decreased by more than a factor of ten. The effect on a normal diffraction spectrum is shown in the figure 2. The results are in very good agreement with the planed values.

For the optimization of the featured detector system (multi tube and 2D), the available resolution was tested with a pressed (10x30 mm cross-section) ^{3}He single detector at 170 degree, in the optimal orientation. The dependency of the relative peak widths on the wavelength is shown on figure 3. As it is seen, with appropriate detector system, better then 10^{-3} resolution can be achieved.

Fig.1 *The background and the beam spectra measured on vanadium without and with filters*

Fig.2 *The effect of the filters on diffraction spectra (Al_2O_3 powder)*

References Kali G, Santa Z, et al.*Installation of the high resolution TOF diffractometer at the Budapest Research Reactor* Z. Kristallogr p 165-170 Part 1 Suppl. 26 (2007)

B N C **Experimental Report**	*Experiment title* **TOF neutron diffraction measurements on Cu alloy reference samples for archaelogical investigations.**	*Proposal No.* *Local contact* Zs. Sánta
Principal proposer: Zsombor Sánta *Experimental team:* Zsombor Sánta, György Káli		*Date(s) of Exper.* March 2007 *Date of Report* 30. 01.2009

Objectives

For better calibration of the data obtained from archaeological bronze samples a seventeen binary and ternary bronze specimens were caste.(Table 1.). The compounds (Sn, Pb, Cd, Sb, Ag, Ni, P and Fe) were chosen to cover the possible contents in archaeological samples.

Results High and low resolution diffraction patterns were collected from the ingot. Cases by case different peak profiles and shifts were observed accordingly to the equilibrium phase compositions. The database will be used for faster data processing and in the determination of non-equilibrium phase compositions of the archaeological objects.
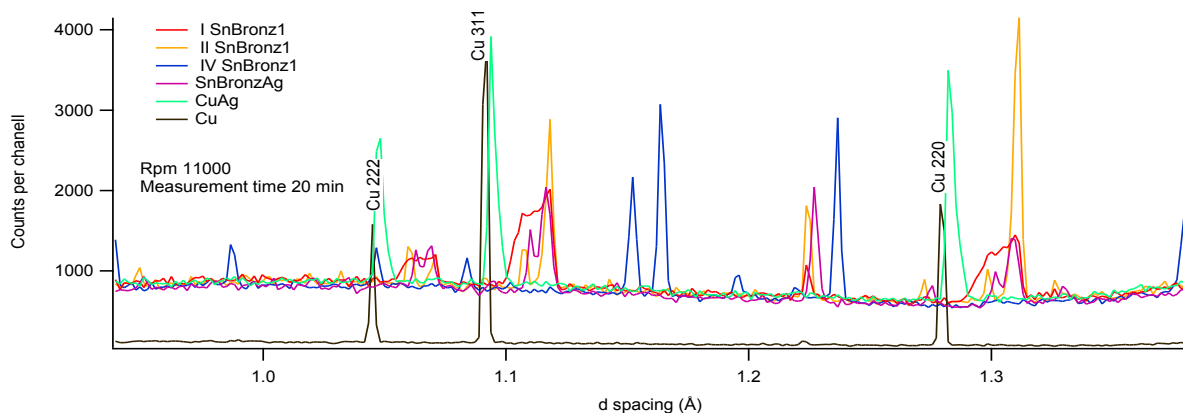
Fig 1. Diffraction spectra of ingots.

	Cu	P	Fe	Ni	Zn	Ag	Cd	Sn	Sb	Pb	Sum
SnBronze1	85							15			100
SnBronze2	73							27			100
SnBronze3	68							32			100
SnBronze4	62							38			100
PbBronze1	77									23	100
PbBronze2	61									39	100
SnPbBronze1	66							12		22	100
SnPbBronze2	61							14		25	100
SnPbBronze3	54							17		29	100
Brass1	74				26						100
CdZnBrass1	68				12		20				100
CdBronze	74						26				100
PbBronzeSb	63								6	31	100
CuAg	97					3,3					100
SnBronzeAg	68					2,9		29			100
CuNi	81			19							100
CuPFe	97	0,9	1,7								100

Table 1. Different Sn, Pb, Cd, Sb, Ag, Ni, P and Fe alloyed Cu samples. (in weight %)

Future prospects:

In collaboration with museums non-destructive investigation of different bronze objects are planed to determine the used manufacturing techniques.

References:

Archaeological bronze objects studied by neutron based methods, Conference poster:European Powder Diffraction Conference (EPDIC), 19-22 September 2008, Warsaw, Poland

B N C **Experimental Report**	*Experiment title* TOF powder diffraction on archeological bronze axes	*Proposal No.* *Local contact* ***Zsombor Sánta***
Principal proposer: ***Zsombor Sánta, T.B. Katalin*** *Experimental team:* Zsombor Sánta, György Káli		*Date(s) of Exper.* 2007 *Date of Report* 2009 01 30

Objectives

In collaboration with the Hungarian National Museum sets of nine axes and fourteen buckles were examined by Time of Flight powder diffraction (TOF). The goal of the experiment was to determine the microstructure (phase compositions, texture) of the alloys to recover the method how the presented historical objects were produced (by casting or hammering) and treated. It was supposed by archeologists that some objects were hammered from natural copper.

Results

Low and high resolution diffraction spectra were recorded from all the objects, in some cases from various parts of them. At some, sample texture analyses were done with positive results at the edges, but all pieces proved to be cast. On the high resolution patterns the shifts and the shape of the peaks are well observable, and carry information not only about the alloying degree, but the speed of cooling too. On the other hand for precise quantitative analyses preliminary data about the chemical compositions are necessary. PGAA was already performed, but those data have not been processed.
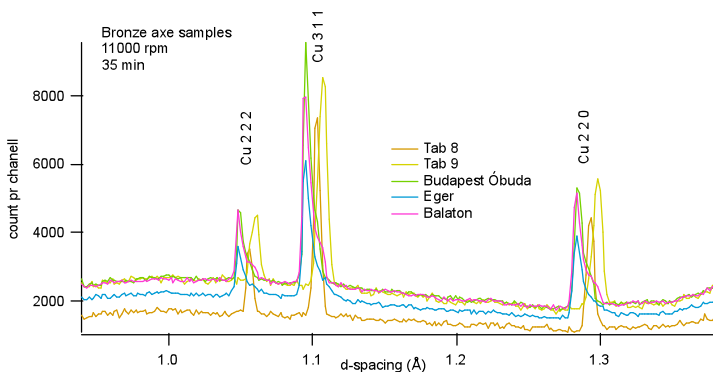
Future prospects

Collaborating with the Hungarian National Museum other archaeological bronze objects will be examined with the same purposes.

References:

Conference poster: 19-22 September 2008, Warsaw, Poland

Archaeological bronze objects studied by neutron based methods.

B N C **Experimental Report**	*Experiment title* Instrumental developments on the Time of Flight diffractometer	*Proposal No.* TOF *Local contact* *Gy. Káli*
Principal proposer: **György Káli** *Experimental team:* **GyörgyKáli, Zsombor Sánta**		*Date(s) of Exper.* *2007 September*

Objectives The TOF neutron diffractometer has been installed on the radial channel No. 1 of the Budapest Reactor. To keep the short wavelength part of the flux, the neutron guide has not been curved. Since the choppers are Gd coated, the application of fast neutron filter become necessary. The spectrometer will operate with a large surface 2D detector and a set of flat ^{3}He tubes. For the optimization of them, the achievable resolution has been determined on Al_2O3 powder.

Results

The filter is made of silicon single crystal cylinders with the (111) direction in the longitudinal axis. The two pieces (14 and 16cm in length and 9cm in diameter) are fixed in two different segments of the beam shutter in Al capsules.

The gain in the signal-noise ratio is about five: at about fifty percent loss in the effective flux the number of fast neutrons has been decreased by more than a factor of ten. The effect on a normal diffraction spectrum is shown in the figure 2. The results are in very good agreement with the planed values.

For the optimization of the featured detector system (multi tube and 2D), the available resolution was tested with a pressed (10x30 mm cross-section) ^{3}He single detector at 170 degree, in the optimal orientation. The dependency of the relative peak widths on the wavelength is shown on figure 3. As it is seen, with appropriate detector system, better then 10^{-3} resolution can be achieved.

Fig.1 *The background and the beam spectra measured on vanadium without and with filters*

Fig.2 *The effect of the filters on diffraction spectra (Al_2O_3 powder)*

References

Kali G, Santa Z, et al. *Installation of the high resolution TOF diffractometer at the Budapest Research Reactor* Z. Kristallogr p 165-170 Part 1 Suppl. 26 (2007)

B N C **Experimental Report**	*Experiment title* **Total scattering neutron diffraction experiment on C_2Cl_6 at different temperatures**	*Proposal No.* MTEST- .../07 *Local contact* L. Temleitner
Principal proposer: L. Temleitner, SZFKI *Experimental team:* L. Temleitner, L. Kőszegi SZFKI		*Date(s) of Exp.* Sept -Oct 2007 *Date of Report* 23.01.2009

Objectives

C_2Cl_6 – hexachloroethane – shows a distorted octahedral symmetry, and serves as a model of this type of materials. It has three solid modifications ([1]) at normal pressure: up to 318 K (*Pnma*), 318-344 K (*unknown*), 344-458 K (*Im3m*). The bcc phase is well studied by different crystallographic methods, but the structure (and changes of the short range order) has not been known in detail yet. The aim of this set of experiments was to provide total scattering diffraction patterns at different temperatures (at least one in each phase) and determine the average structure of the intermediate phase under normal conditions. For achieving this latter goal, high resolution is required.

Results

The measurement has been carried out at 291 K with low and at 332+/-1 K with the maximal possible resolution on the MTEST diffractometer using 1.433 Å neutrons. During the measurement the sample (99%, Aldrich) was contained in a 8 mm vanadium can. At 332 K a vanadium furnace was used. Although the ordered-intermediate phase transition was observed, unfortunately, the type of the lattice could not be determined. The total diffraction pattern of the room temperature data has been modeled by RMCPOW simulation using a 4x4x4 crystallographic unit cell, as a preliminary study, before using a larger supercell. The present simulation used the previously determined lattice parameters ([1]).
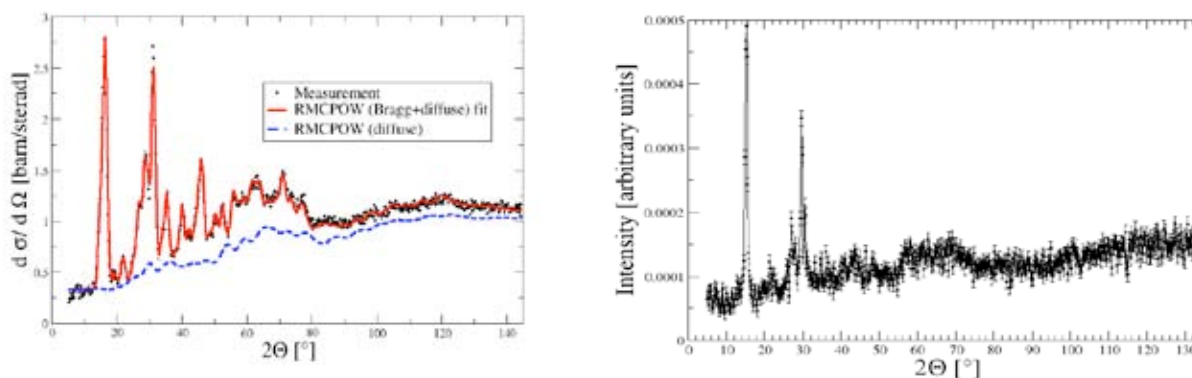
Figure 1. Measured differential cross-section (dots) of C_2Cl_6 at 291 K (left) and at 332 K (right). The room temperature total diffraction pattern was modeled by RMCPOW simulation (Bragg+diffuse: solid line; diffuse: dashed line).

Future prospects

These patterns will be modeled (using RMCPOW) together with X-ray diffraction data. After the determination of the average structure of the intermediate phase from other sources, the 331 K dataset will also be used.

References

[1] Hohlwein et al., *Acta Cryst.* **B35** (1979) 2975.

B N C **Experimental Report**	*Experiment title* **Total scattering experiment on stable** **Ge.₂Sb.₂Te.₅**	*Proposal No.* MTEST- 1/2008 *Local contact* L. Temleitner
Principal proposer: L. Temleitner, SZFKI *Experimental team:* L. Temleitner, L. Kőszegi SZFKI		*Date(s) of Exp.* Jun-Jul 2008 *Date of Report* 23.01.2009

Objectives

$Ge_2Sb_2Te_5$ is a phase change material used in DVD-RW for storing information. It has three solid modifications; one of them is the stable hexagonal phase (*P-3m1*). Three different models have been proposed, characterized by different occupations of Ge and Sb at the *2c* Wyckoff-site: 100% Ge [1], 100% Sb [2] and 55.9% Ge [3]. In our earlier measurement on the PSD diffractometer it was found that the best fit is very close to the last model ([3]). However, this result is based on comparing the model and experimental data in the 1.6-2.7 $Å^{-1}$ range, where the differences between the models are most significant. Unfortunately, the intensities are very low there and blurred by small amount of impurities contained in the sample. The last problem might be solved by better resolution.

Results

The measurement has been carried out with 1.435 Å wavelength at room temperature using a powder sample annealed at 853 K for several hours. During the measurements the sample (99% $Ge_2Sb_2Te_5$) was contained in a 5 mm vanadium can and rotated along its cylindrical axis. For this measurement the high resolution mode was employed, focusing on the 1.6-2.0 $Å^{-1}$ range, because the fit was worst here between measurement and model. In this range the pattern obtained from PSD is reproduced well by the MTEST one (Fig. 1), but the improved resolution has not separated the peaks. Although beyond 2.2 $Å^{-1}$ the proportion of the two peaks are differs from the PSD data, the uncertainty of the measured intensities are too big. The results of the measurement at PSD are confirmed.
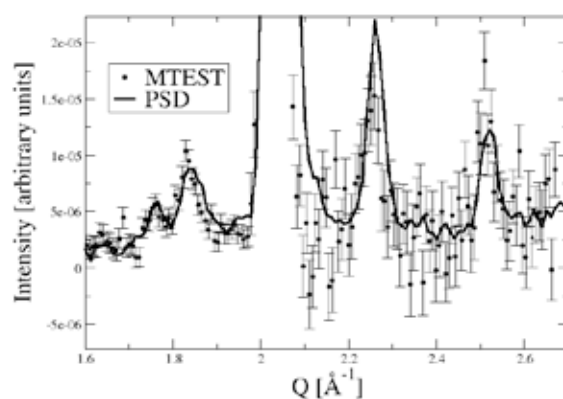
Figure 1. Comparison of the corrected powder diffraction patterns are measured on MTEST and on PSD.

Future prospects

Results of the measurement will be written up and published in the near future.

References

[1] Matsunaga al., *Acta. Cryst.* **B60** (2004) 685.
[2] Petrov et al., *Sov. Phys. Cryst.* **13** (1968) 339.
[3] Kooi et al., *J. Appl. Phys. Lett.* **92** (2002) 3584.

B N C **Experimental Report**	*Experiment title* Neutron holographic measurement on Ammonium Chloride (NH$_4$Cl)	*Proposal No.* TAST *Local contact* *Márton Markó*
Principal proposer: *Márton Markó* *Experimental team:* László Cser, Gerhard Krexner, Gyula Török		*Date(s) of Exper.* Jan. 2007 *Date of Report* Febr. 2009

Objectives *(Aim of the research in some sentences)*

Neutron holography is a relatively new measurement technique for three dimensional visualization of the close neighbourhood of a special atom of a crystal lattice. In this measurement we continued a neutron holographic measurement on the ammonium-clhoride single crystal where there is more than one detector atom in the unit-cell.

Results *(Description of concrete results, understandable also for non-experts of the field. Insert, if possible, a typical figure)*

In the previous measurement we made holographic measurement using the internal source method, where the nucleus of the H-atom acted as a point-like source of neutrons. In the present measurement we used the internal detector method. In this case the proton (the nucleus of H-atom) acts as a point like detector of neutrons. In this case the inelastic scattering on the slightly bounded ammonium-ion causes no distortion effect.

The measurement was done on the 8th vertical thermal neutron cannel of the BRR, at the TAST instrument. The incoherently scattered neutrons were detected by a single ^{3}He-filled counter tube. The scattering angle was at 12° what is much smaller than the scattering angle of the first bragg peak. In this measurement we did not use the analyzer crystal. The optimal resolution of the measurement (to see the first H neighbours of the H atom at 1.68 Å distance) is 5.43°. To achieve this resolution we have put the detector to the place of the monochromator crystal 60cm far from the sample, and for avoiding the background we have applied an extra collimator between the monochromator house and the sample. It was a Cd tube coated with 1cm thick boronated plastic against the high energy neutrons. In this case we could suppress the background under 1 cnt/sec. The wavelength of the beam was 1Å. The omega table was at 90 degree (the Eulerian Cradle was parallel to the beam). We have moved only the Chi and Phi angles of the cradle. The measurement was done using 3° steps in the φ-χ-plane, in the χ angle from 0° to 60°, in the φ-angle from 0° to 357°. In the reconstructed image it is clearly seen the first neighbour N atoms, and the first neighbour H atoms. The H can occupy 8 positions in the unit cell, that is why one see 8 N neighbours and 12 H neighbours.
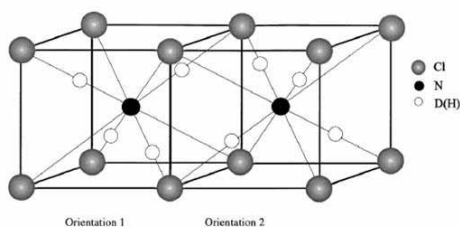
Fig. 1.: The two possible unit cell of the NH4Cl single crystal
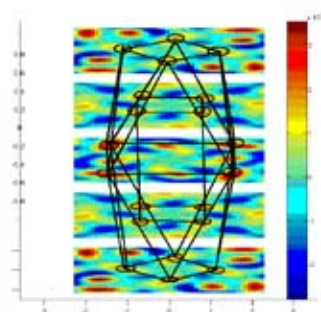
Fig. 2.: The 8 first N neighbour, and the 12 first H neighbour of the H atom

Future prospects *(Summary of the remaining problems to be solved, basis for the continuation of the work)*

References *(Published or accepted papers, research reports, conference lectures, seminars etc.)*

B N C Experimental Report	*Experiment title* **Study on radiation resistance of CCD cameras**	*Proposal No.* BIBE 2/2007 *Local contact* J. Pálfalvi
Principal proposer: Dr.G. Kocsis, KFKI RMKI, Dept. of Plasma Physics, Budapest *Experimental team:* J. Pálfalvi, T. Pazmandi, KFKI-AEKI, G. Kocsis, KFKI RMKI, G. Por, BME NTI, Budapest		*Date(s) of Exper.* From 02.05,2007 To 20.11.2007 *Date of Report* 24.04.2008

Objectives

To study the optical appearance of the plasma in fusion experiments at KFKI RMKI Plasma Physics Department the test of the radiation resistance of a CCD camera became necessary. The Biological Irradiation Facility of the BRR was selected for the purpose having a variable neutron beam

Results

A commercially available and a specially made CCD WEB video camera were tested in the new irradiation cavity (Fig. 1.) having the neutron spectrum as shown in Fig. 2. Following observations were made: (1) if the camera was switched on during the exposure the number of the blind pixels increased with time. (2) Some of the pixels recovered after exposure, but many remained blind. (3) After delivering !67 Gy (absorbed dose in water), the camera became radioactive, in 5 cm distance from the objective the gamma dose rate was more than the maximum range of the measuring device (~1.2 mGy/h). The disintegration curve (Fig. 3) indicate the presence of several short lived isotopes with different half lives. The presents of gold plated electronic elements were well recognizable (^{198}Au with 2.7 days half life, emitting 412 keV photons) by gamma spectrometry.
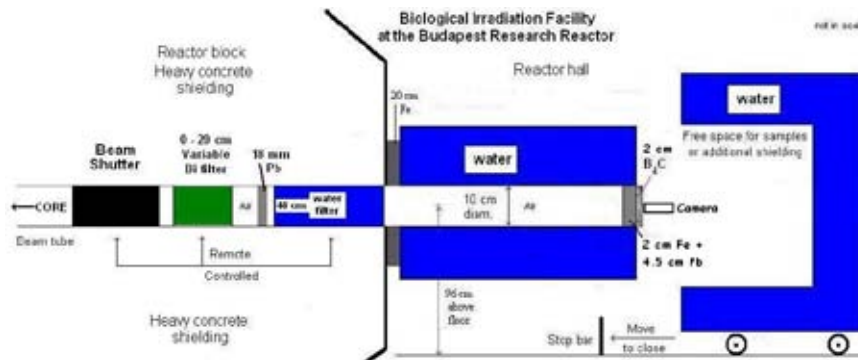
Fig. 1. The schematic view of the experimental arrangement.

The leakage neutron spectrum from the core contains a large percent of low energy neutrons below 10 keV (open circles in Fig.2). A combination of Bi, Fe, Pb and B_4C materials applied as filters eliminates the low energy neutrons and shifts the energy peak slightly downward (diamond in Fig.2) meanwhile decreases the gamma radiation and the activation of the sample to be exposed.
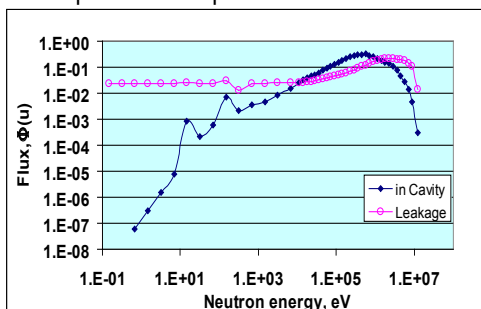
Fig. 2. Neutron spectra   Fig. 3. Time dependence of disintegration
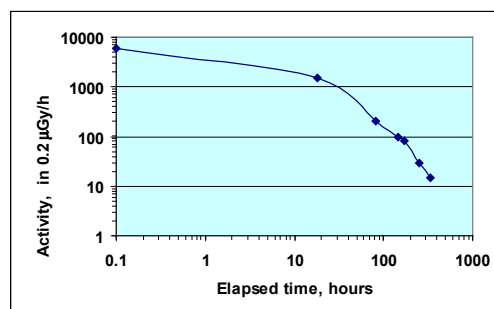
Objectives

The IAEA has been supporting for a long time the development of methods which enable the radiobiologists to study the sequence of the complete genome of those plants considered as foodstuff. It was recognised that the application of the fast neutron deletion mutagenesis is an encouraging possibility if it is coupled with a well established neutron micro dosimetry.

Results

The arabidopsis, sunflower and cassava seed exposures were carried out at the Biological Irradiation Facility (BIF) of the BRR. Fast neutrons (spectrum is a solid line in Fig. 1) produce mostly protons (shown as circles) by the H(n,n') p recoil reaction in a hidrogeneous material as seed cells. The effectiveness of the production depends on the H (water) content of the seeds, which is determined by evaporation method. The neutron spectrum has been shaped by adequate internal and external beam filters in such a way that the proton spectrum falls in the energy interval of 0.01 and 1 MeV where the energy deposition of the protons is the highest and the range is small that all the protons are absorbed within a cell The neutron dose measurements are based on the same recoil reaction using solid state nuclear track detectors which are evaluated by a locally developed image analyser and software. The dose rate dependence on internal Bi filter thickness in the irradiation cavity (collimator) is shown in Fig. 2.
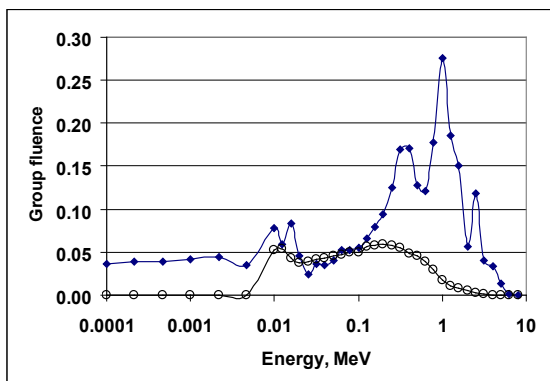
.A new reverse genetics method has been developed by the Maxygen Co. to identify and isolate deletion mutants for targeted plant genes. Deletion mutant libraries were generated using fast neutron exposures at the BRR. DNS samples extracted from the libraries were screened for mutants by polymerase chain reaction. The complete genoms of arabidopsis and sunflower plants were obtained first time.

B N C **Experimental Report**	*Experiment title* **Investigation of neutron detection sensitivity of solid state nuclear track detectors (SSNTD) used for space dosimetry.**	*Proposal No.* BIBE 2/2006 *Local contact* J. Pálfalvi

Principal proposer:
    J. Pálfalvi, KFKI-AEKI, Budapest
Experimental team:
    J. Pálfalvi, J. Szabo and B. Dudas, KFKI-AEKI, Budapest
		Date(s) of Exper.
		From 04.01.2006
		To 31 08. 2007.
		Date of Report
		08.10.2007

Objectives

The aim of the research was to study the neutron detection sensitivity of solid state nuclear track detectors type TASTRAK in the energy range of 0.1 and 10 MeV, where the maximum neutron flux had been observed by Si detectors on board of the International Space Station (ISS).

Results

The exposures were carried out at the Biological Irradiation Facility of the BRR, applying two different internal Bi filters. The neutron spectra at the irradiation position were calculated from the core leakage spectrum by the MCNP4B code (see the figure below). The leakage spectrum (marked by diamonds) is normalized to 1 neutron, the spectra filtered by 10 cm (open circles) and 15 cm Bi (rectangles) are normalized to 10^6 source neutrons.

After chemically treating the SSNTDs the evaluations were done by a home made image analyser, investigating the distributions of various track parameters. It was found that the inverse track diameter distributions were well correlated with the linear energy transfer (LET) spectra of the recoil protons generated by the H(n,n')p reaction inside the detector material ($C_{12}H_{18}O7$).

An appropriate conversion function was deduced to obtain the LET spectrum from the diameter distribution. The function depends on the chemical treatment (etching in an alkaline solution), therefore two standard conditions were established to achieve the detection of protons between 0.12 and 8 MeV (or expressing it in LET: between 10 and 100 keV/μm). The lower limit depends also on the resolution of the image analyser. The method has been successfully applied for the evaluation SSNTDs exposed on the ISS and also on The Foton-M2 biosatellite.

References

- J. K. Pálfalvi, Yu. Akatov, J. Szabó, L. Sajó-Bohus and I. Eördögh. Detection of Primary and Secondary Cosmic Ray Particles Aboard the ISS Using SSNTD Stacks, Rad. Prot. Dos. V. 120, pp. 427-432/ 2006.
- J. K. Pálfalvi, J. Szabó, B. Dudás. Neutron Detection on the Foton-M2 Satellite by a Track Etch Detector Stack. Rad. Prot. Dos. V. 126. pp. 590-594/2007.
- M. Hajek, T. Berger, N. Vana, M. Fugger , J. K. Pálfalvi, J. Szabó, I. Eördögh, Y.A. Akatov, V. V. Arkhangelsky, V. A. Shurshakov. Convolution of TLD and SSNTD measurements during the BRADOS-1 experiments onboard ISS (2001). Rad. Meas. V 43, pp. 1231-1236/2008.
- K. Pálfalvi, J. Szabó, B. Dudás, I. Fehér and I. Eördögh. Cosmic Ray Detection on the Foton-M2 Satellite by a Track Etch Detector Stack. Advances in Space Research. V 42, pp. 1030-1036/2008.
- Fehér, I. and Pálfalvi, J. K., Depth Dose Distribution Measurements on the Foton-M2 Bio-satellite by TLD Technique. Advances in Space Research. V 42, pp. 1037-1042/2008.
- J. Szabó, J.K. Pálfalvi, B. Dudás, Yu. Akatov, I. Eördögh. Cosmic ray detection on the ISS by a 3 axes track etch detector stack and the complementary calibration studies. Rad. Meas. V. 43, pp. 688-693/2008.

4, INSTRUMENTS

4.1. SMALL-ANGLE NEUTRON SCATTERING SPECTROMETER "YELLOW SUBMARINE"

Instrument responsible: Noémi SZÉKELY

The Small-Angle Neutron Scattering (SANS) diffractometer "Yellow Submarine" is installed on the cold neutron guide No. 2, with a 4x4 cm^2 cross-section. The beam is monochromatized by a multidisk type velocity selector, the rotation speed can be tuned between 700 and 7000 rot/min. The covered a Q-range is between 0.003 Å^{-1} and 0.5 Å^{-1} allowing density composition and magnetization fluctuations in materials to be measured on a length scale from 5 Å to 1400 Å. The width of the transmitted wavelength distribution can be varied between 12% and 30% by changing the angle between the selector axis and the direction of the neutron beam according to the requirements of the given measurement. The beam intensity is monitored by a fission chamber placed at the end of the neutron guides. The beam is collimated using a 5 m long collimation system allowing the optimization of flux and resolution for different sample-to-detector distances. The scattered neutrons are detected by a 64 x 64 cm^2 two dimensional position sensitive detector filled with BF$_3$ gas. The pixel size is 1cm x 1cm. The detector has been made by LETI, Grenoble, France.

Sample environment

In most of the experiments the samples are placed in an automatic sample changer having 6 positions. It can be thermostated from an external bath between -10 and 100 °C with an accuracy of $\pm$ 0.5 °C. The sample holder can be changed to an electromagnet (up to 1.8 T) with thermostated sample position.

Data aquisition

The control and data acquisition electronics and software have been made in the Laboratoire Léon Brillouin, Saclay, France. The primary data treatment can be done with the software package made in the LLB, it includes the regrouping of the two-dimensional scattering patterns depending on the type of scattering (isotropic –*Regiso, Paresu* or anisotropic - *PXY*), background subtraction, correction for transmission and normalization to standard samples, usually to 1 mm water.

*Table: Characteristic parameters of the SANS instrument **Yellow Submarine:***

Monochromator:	Mechanical velocity selector (Reference: L. Rosta: Physica B 174 (1991) 562)
Incident wavelength:	3 – 25 Å
Wavelength spread:	Adjustable between 12 – 30%
Transferred momentum range:	0.003 - 0.5 Å^{-1}
Neutron flux at the guide exit:	5*10^7 n/cm^{2}s
Sample-to-detector distance:	Continuously adjustable between 1.3 m and 5.5 m
Detector:	2D, 64 x 64 cm^2, filled with BF$_3$ gas
Sample environment	Thermostated sample changer, electromagnet
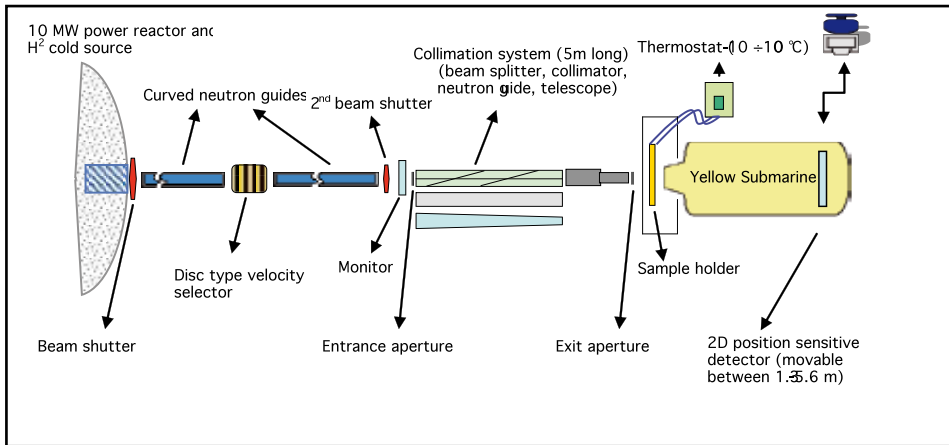
Scheme of the SANS diffractometer
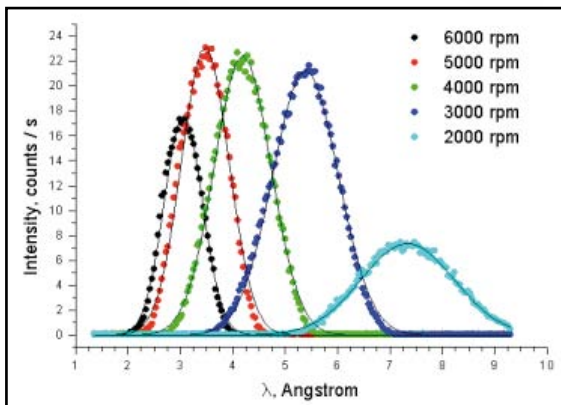
The wavelength distribution of transmitted neutrons by the selector.
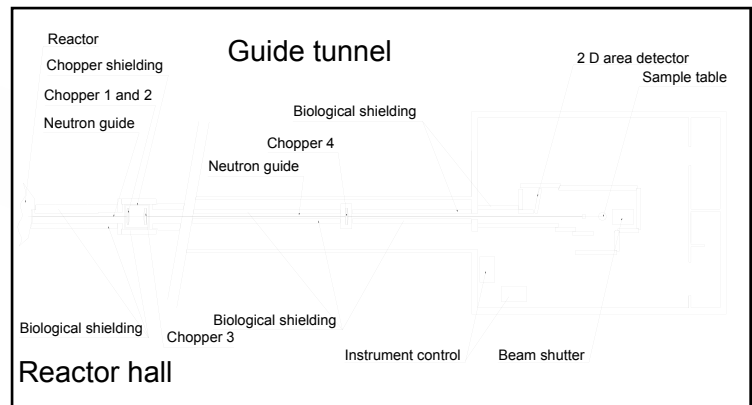
Figure 1. Layout of the TOF diffractometer at the Channel No.1 of BRR

4.2. NEUTRON CAPTURE GAMMA-RAY FACILITIES

Two instruments are located at the end position of neutron guide NV1. The prompt gamma activation analysis (PGAA) facility serves for non-destructive analysis of elemental composition by observing neutron-capture prompt gamma rays. The neutron induced prompt gamma-ray spectroscopy (NIPS) facility has been designed for a large variety of experiments involving nuclear reaction-induced prompt and delayed gamma radiations, including γ-γ-coincidences or neutron radiography, tomography, as well as PGA Imaging.

The neutron guides have been replaced for $2\theta_c$ supermirror guides, which increased the flux significantly (1.5×10^8 cm^{-2} s^{-1} at the PGAA system in vacuum).

The experimental area is a 3×5 m^2 place, backed by the rear wall of the guide hall (see Figure 1). The pneumatic beam shutter at the end of the guide lets the neutrons enter the 3 m long evacuated aluminium tube extending across the experimental area, down to the beam stop at the rear wall of the guide hall. The guided beam is divided into two beams of smaller diameter by appropriate collimators. At present, the upper beam is used for PGAA measurements. A neutron absorber beyond the PGAA target chamber stops the upper beam, while the lower beam passes through underneath, to the NIPS station.

The PGAA target chamber is at 1.5 m distance from the end of the guide. It is possible to maintain vacuum, or gaseous atmosphere in the sample box, to decrease the background induced by the neutrons. Besides, a horizontally placed neutron absorber layer prevents scattering from the lower beam to the PGAA sample. The targets are suspended on a thin aluminium frame by thin Teflon strings.

The NIPS station is at a further 1 m distance from the PGAA station along the beam tube, and is shielded with lead bricks to minimize the background radiation originated from the other measurement. The section of the aluminum tube including the NIPS sample chamber is narrow enough, so that several detectors can be placed close to the sample.

All three sections of the aluminum tube system can be easily removed and put back if necessary. This is essential when samples larger then the target chamber are to be investigated. For special experiments a beam chopper is also provided
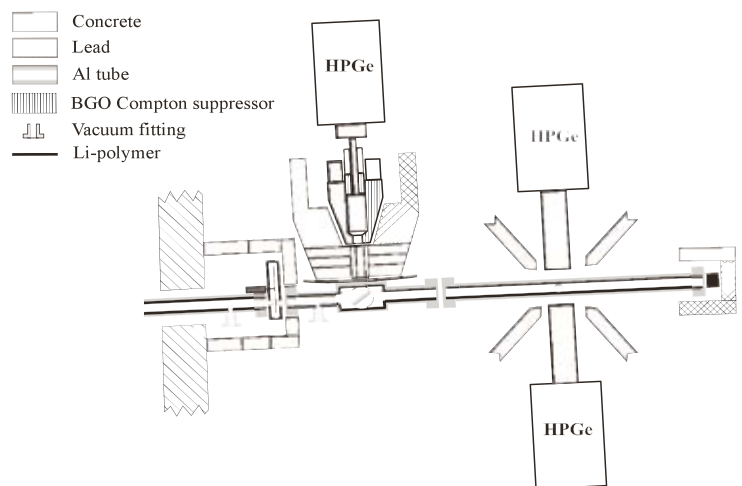
Thanks to the upgraded neutron guide system the thermal-equivalent neutron fluxes at the PGAA and NIPS sample positions became 3–4-times higher: 1.5×10^8 cm^{-2} s^{-1} and 7×10^7 cm^{-2}s^{-1}, respectively. Both beams are individually collimated to a cross-section of 2×2 cm^2 or 1×1 cm^2. The neutron flux profile at the PGAA sample position is plotted in Figure 2.
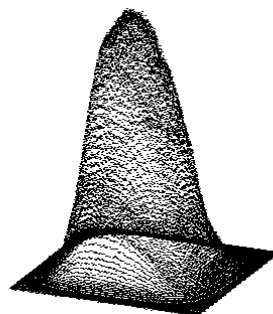
Figure 2. Neutron flux profile at the sample position of the PGAA facility

The PGAA facility
Instrument responsible: Zsolt RÉVAY

When a nucleus captures a neutron, the binding energy of the neutron is emitted promptly in the form of gamma radiation. This radiation is characteristic, in that the energies of the gamma photons are specific to the nucleus, while their numbers are proportional to the quantity of that nuclide. By analysing the energy spectrum of the emitted prompt gamma radiation, the isotopic and elemental contents of the irradiated sample can be determined. This is the essence of the prompt gamma activation analysis method.

The basic instrument of the PGAA facility consists of an n-type high-purity germanium (HPGe) main detector with closed-end coaxial geometry, and a BGO scintillator guard detector annulus surrounded by a 10 cm thick lead shielding. The whole system is positioned on a table, which can be moved in either direction. By removing the three lead disks comprising the front side of the detector shielding, the HPGe main detector can be placed as close as 12 cm to the target. (For an even closer geometry one can use the bare detector to approach the sample to 3 cm.)

The BGO annulus and the catchers around the HPGe detects most of the scattered gamma photons. Connecting the HPGe and the BGO in anticoincidence mode Compton-supressed spectra can be acquired. With appropriate electronic gating, the HPGe-BGO gamma spectrometer can be also be used in annihilation-pair mode, in order to simplify the spectra at high energies. A 16k personal computer-based multichannel analyser collects the data. A schematic drawing of the HPGe-BGO detector assembly is shown in Figure 3. The main parameters of the PGAA system are collected in Table 1.

Table 1. Main specifications of the PGAA facility

Beam tube:	NV1 guide, end position
Distance from guide end	1.5 m
beam cross section:	$1\times1cm^2$, $2\times2cm^2$, $25mm^2$, $5mm^2$, 1mm slit
Thermal-equivalent flux at target:	$\approx1.5\times10^8$ cm^{-2}s^{-1} (in vacuum)
Vacuum in target chamber (optional):	≈1 mbar
Target chamber Al-window thickness	0.5 mm
Form of target at room temperature:	Solid, powder, liquid, gas in pressure container
Target packing at atmospheric pressure:	sealed FEP Teflon bag or vial
Activity of target after irradiation:	negligible
Largest target dimensions:	$4\times4\times10$ cm^3
γ-ray detector	n-type coax. HPGe, with BGO shield
Distance from target to detector window:	230 mm
HPGe window:	Al, 0.5 mm
Relative efficiency:	27% at 1332 keV (^{60}Co)
FWHM:	2.1 keV at 1332 keV (^{60}Co)
Compton suppression enhancement:	≈5 (1332 keV) to ≈40 (7000 keV)
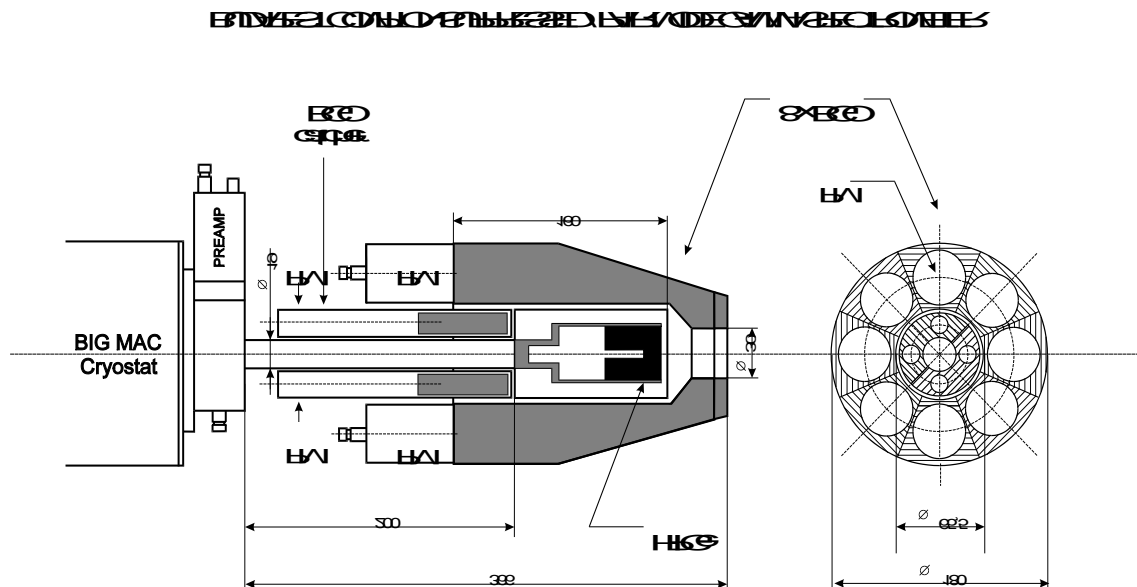
Figure 3. Cross-sectional view of the HPGe-BGO gamma spectrometer

The system is carefully calibrated at the beginning of every semester for counting efficiency and non-linearity [2, 3].

Data acquisition and analysis

The original CANBERRA S100 type single-input, PC-based multichannel analyzer (MCA) that was used to collect the PGAA spectra has been replaced with a Canberra AIM (Acquisition Interface Module). The gamma spectra are collected in a PC using the Canberra Genie software.

The extremely complex γ-ray spectra are evaluated using Hypermet-PC [4, 5]. A series of measurements has been performed at the PGAA facility using the thermal beam in order to create a prompt γ-ray catalogue suitable for both qualitative and quantitative analysis. The new gamma-ray energy and intensity data are highly accurate, thanks to the precise energy calibrations and standardisation procedures applied throughout [6]. A program written in the form of an Excel Macro is used for the chemical analysis, that compares the spectroscopic data library and the measured areas of the characteristic peaks [7].

Thanks to the new cold neutron source and the improvements made to the neutron guide system, the neutron flux has been substantially increased at the PGAA station as well. The approximate detection limits are shown in the next Table.

Table 2. Minimum achievable detection limits for the elements at the Budapest PGAA facility (assuming 100 000 sec measuring time and a matrix with lowest possible background).

Z	El	E (keV)	σ_γ	DL (µg)	Z	El	E (keV)	σ_γ	DL (µg)
1	H	2223.248	0.3326(7)	0.3			3033.896(6)	0.0179(3)	150
		6250.243(3)	0.000519(7)	190	14	Si	3538.966(22)	0.1190(20)	24
3	Li	2032.30(4)	0.0381(8)	18			4933.889(24)	0.1120(23)	25
		980.53(7)	0.00415(13)	170			2092.902(18)	0.0331(6)	100
		1051.90(7)	0.00414(12)	170	15	P	636.663(21)	0.0311(14)	100
4	Be	6809.61(3)	0.0058(5)	160			3899.89(3)	0.0294(10)	110
		3367.448(25)	0.00285(22)	300			6785.504(24)	0.0267(15)	120
		853.630(12)	0.00208(24)	400	16	S	840.993(13)	0.347(6)	10
5	B	477.595(3)	716.0(25)	0.00150			5420.574(24)	0.308(7)	10
6	C	4945.301(3)	0.00261(5)	500			2379.661(14)	0.208(5)	15
		1261.765(9)	0.00124(3)	1000	17	Cl	1951.1400(20)	6.33(4)	0.6
		3683.920(9)	0.00122(3)	1000			1959.346(4)	4.10(3)	0.9
7	N	1884.821(16)	0.01470(18)	100			517.0730(10)	7.58(5)	0.5
		5269.159(13)	0.0236(3)	60	18	Ar	167.30(20)	0.53(5)	8
		5297.821(15)	0.01680(23)	80			4745.3(8)	0.36(4)	11
8	O	870.68(6)	1.77E-04(11)	9000			1186.8(3)	0.34(3)	12
		2184.42(7)	1.64E-04(7)	9800	19	K	770.3050(20)	0.903(12)	4
		1087.75(6)	1.58E-04(7)	10 000			1158.887(10)	0.1600(25)	24
9	F	1633.53(3)	0.0096(4)	200			7768.919(14)	0.117(7)	30
		6600.175(16)	0.00096(3)	2000	20	Ca	1942.67(3)	0.352(7)	11
		583.561(16)	0.00356(12)	500			6419.59(5)	0.176(5)	23
10	Ne	2035.67(20)	0.0245(25)	80			4418.52(5)	0.0708(18)	60
		350.72(6)	0.0198(4)	100	21	Sc	147.011(10)	6.08(9)	0.7
		4374.13(6)	0.01910(22)	110			142.528(8)	4.88(7)	0.9
11	Na	472.202(9)	0.478(4)	5			216.44(4)	2.49(4)	2.5
		90.9920(10)	0.235(3)	10	22	Ti	1381.745(5)	5.18(12)	0.9
		874.389(6)	0.0760(11)	30			6760.084(14)	2.97(9)	1.6
12	Mg	585.00(3)	0.0314(11)	80			341.706(5)	1.840(21)	3
		3916.84(3)	0.0320(11)	80	23	V	1434.10(3)	4.81(10)	1.1
		2828.172(25)	0.0240(8)	100			125.082(3)	1.61(4)	3
13	Al	1778.92(3)	0.232(4)	12			6517.282(19)	0.78(4)	7
		7724.027(4)	0.0493(15)	60	24	Cr	834.849(22)	1.38(3)	4

Z	El	E (keV)	σ$_\gamma$	DL (μg)	Z	El	E (keV)	σ$_\gamma$	DL (μg)
		8884.36(5)	0.78(5)	7			195.602(4)	0.434(14)	18
		749.09(3)	0.569(9)	9	36	Kr	881.74(11)	20.8(3)	0.4
25	Mn	846.754(20)	13.10(4)	0.4			1213.42(12)	8.28(17)	1.0
		212.039(21)	2.13(3)	2.5			1463.86(6)	7.10(8)	1.2
		7243.52(9)	1.36(3)	4	37	Rb	556.82(3)	0.0913(24)	90
26	Fe	7631.136(14)	0.653(13)	9			555.61(3)	0.0407(10)	210
		7645.5450(10)	0.549(11)	10			487.89(4)	0.0494(12)	170
		352.347(12)	0.273(3)	20	38	Sr	1836.067(21)	1.030(18)	9
27	Co	229.879(17)	7.18(8)	0.8			898.055(11)	0.702(10)	12
		277.161(17)	6.77(8)	0.9			850.657(12)	0.275(4)	30
		6706.01(3)	3.02(6)	2.0	39	Y	6080.171(22)	0.76(4)	12
28	Ni	8998.414(15)	1.49(3)	4			776.613(18)	0.659(9)	13
		464.978(12)	0.843(10)	7			202.53(3)	0.289(7)	30
		8533.509(17)	0.721(13)	8	40	Zr	934.4640(10)	0.125(5)	70
29	Cu	278.250(14)	0.893(15)	7			1405.159(3)	0.0301(10)	300
		7915.62(4)	0.869(20)	7			560.958(3)	0.0285(5)	320
		7637.40(4)	0.54(7)	12	41	Nb	99.4070(10)	0.196(9)	50
30	Zn	1077.335(16)	0.356(5)	18			255.9290(20)	0.176(3)	50
		115.225(18)	0.167(3)	40			253.115(5)	0.1320(19)	70
		7863.55(7)	0.1410(19)	50	42	Mo	778.221(10)	2.02(6)	5
31	Ga	834.08(3)	1.65(5)	4			849.85(3)	0.43(3)	22
		145.14(3)	0.466(7)	15			847.603(11)	0.324(9)	30
		690.943(24)	0.305(4)	23	43	Tc	172.02(7)	16.60(11)	0.6
32	Ge	595.851(5)	1.100(24)	7			223.34(6)	1.490(17)	7
		867.899(5)	0.553(12)	13			590.770(20)	1.296(11)	8
		608.353(4)	0.250(6)	30	44	Ru	539.538(15)	1.53(13)	7
33	As	559.10(5)	2.00(10)	4			475.0950(20)	0.98(9)	10
		165.0490(10)	0.996(16)	8			686.907(17)	0.52(5)	20
		6810.898(8)	0.56(3)	40	45	Rh	180.87(3)	22.6(15)	0.5
34	Se	613.724(3)	2.14(5)	4			97.14(3)	19.5(4)	0.5
		238.9980(10)	2.06(3)	4			51.50(3)	16.0(4)	3
		6600.690(21)	0.623(20)	13	46	Pd	511.843(20)	4.00(4)	3
35	Br	245.203(4)	0.80(3)	10			717.356(22)	0.777(9)	14
		271.374(3)	0.462(7)	17			616.192(20)	0.629(9)	17

Z	El	E (keV)	σ_γ	DL (µg)	Z	El	E (keV)	σ_γ	DL (µg)
47	Ag	198.72(4)	7.75(13)	1.4			4766.10(5)	0.113(8)	120
		117.45(8)	3.85(7)	3			475.04(4)	0.082(7)	170
		657.50(10)	1.86(5)	6	59	Pr	176.8630(20)	1.06(4)	13
48	Cd	558.32(3)	1860(30)	0.006			1575.6(5)	0.426(12)	40
		651.19(3)	358(5)	0.03			126.8460(20)	0.307(15)	50
		805.85(3)	134.0(18)	0.08	60	Nd	696.499(10)	33.3(23)	0.4
49	In	272.9660(20)	33.1(24)	0.3			618.062(19)	13.4(3)	1.1
		186.2100(20)	26.6(18)	0.4			814.12(3)	4.98(12)	3
		1293.54(15)	131(3)e	0.09	62	Sm	333.97(4)	4790(60)	0.003
50	Sn	1293.591(15)	0.1340(21)	90			439.40(4)	2860(150)	0.005
		1171.28(6)	0.0879(13)	140			737.44(4)	597(8)	0.025
		1229.64(6)	0.0673(13)	180	63	Eu	89.847(6)	1430(30)	0.010
51	Sb	564.24(4)	2.700(4)	5			221.30(8)	73(3)	0.21
		121.4970(10)	0.40(9)	30			963.390(12)	183(16)	0.08
		282.6500(10)	0.274(7)	40	64	Gd	181.931(4)	7200(300)	0.0022
52	Te	602.729(17)	2.46(16)	5			79.5100(10)	4010(100)	0.004
		722.772(25)	0.52(4)	24			944.174(10)	3090(70)	0.005
		645.819(20)	0.263(22)	50	65	Tb	153.6870(20)	0.44(5)	40
53	I	133.6110(10)	1.42(10)	9			178.881(3)	0.42(8)	40
		442.901(10)	0.600(10)	21			97.503(3)	0.50(6)	30
		153.011(3)	0.209(14)	70	66	Dy	184.257(4)	146(15)	0.11
54	Xe	667.79(6)	6.7(5)	2.0			538.609(8)	69.2(19)	0.23
		772.72(4)	1.78(14)	10			496.931(5)	44.9(11)	0.4
		536.17(9)	1.71(24)	8	67	Ho	136.6650(20)	14.5(7)	1.1
55	Cs	176.4040(20)	2.47(4)	5			116.8360(10)	8.1(4)	2.0
		205.615(3)	1.560(25)	9			426.012(5)	2.88(15)	6
		307.015(4)	1.45(3)	9	68	Er	184.2850(10)	56(5)	0.30
56	Ba	627.29(5)	0.294(6)	50			815.9890(20)	42.5(15)	0.4
		818.514(12)	0.212(4)	60			284.6560(20)	13.7(12)	1.2
		1435.77(4)	0.308(7)	90	69	Tm	204.45(10)	8.72(19)	2.0
57	La	1596.21(4)	5.84(9)	20			149.7180(10)	7.11(12)	2.4
		218.225(22)	0.78(3)	18			144.48(10)	5.96(11)	3
		288.255(5)	0.73(3)	19	70	Yb	514.868(7)	9.0(9)	1.9
58	Ce	661.99(5)	0.241(15)	60			639.261(9)	1.43(17)	12

Z	El	E (keV)	σ_γ	DL (µg)	Z	El	E (keV)	σ_γ	DL (µg)
		5266.3(4)	1.4(6)	12			332.985(4)	2.580(25)	8
71	Lu	150.392(3)	13.8(4)	1.3			521.161(5)	0.338(10)	60
		457.944(15)	8.3(3)	2.1	79	Au	411.8	94.0(10)	0.21
		761.564(20)	2.60(9)	7			214.9710(10)	9.0(12)	2.2
72	Hf	213.439(7)	29.3(7)	0.06			247.5730(10)	5.56(8)	4
		214.3410(20)	16.3(3)	1.3	80	Hg	367.947(9)	251(5)	0.08
		303.9880(20)	3.38(9)	5			5967.02(4)	62.5(15)	0.3
73	Ta	270.4030(20)	2.60(6)	7			1693.296(11)	56.2(16)	0.4
		173.2050(20)	1.210(25)	15	81	Tl	347.96(8)	0.361(10)	60
		402.623(3)	1.180(23)	15			5641.57(12)	0.316(7)	60
74	W	145.79(3)	0.970(21)	19			873.16(8)	0.168(4)	120
		5261.68(6)	0.86(4)	21	82	Pb	7367.78(7)	0.137(3)	150
		685.73(4)	3.24(7)	6			6737.62(10)	0.00691(19)	3000
75	Re	207.853(4)	4.44(21)	4			6729.38(9)	0.00320(10)	6500
		63.5820(20)	8.0(14)	10	83	Bi	4171.05(9)	0.0171(22)	1200
		155.041(4)	7.16(25)	5			4054.57(6)	0.0137(18)	1500
76	Os	186.7180(20)	2.08(5)	9			319.78(4)	0.0115(14)	1800
		155.10(4)	1.19(3)	16	90	Th	472.30(10)	0.165(8)	140
		557.978(5)	0.84(3)	23			968.78(9)	0.132(6)	180
77	Ir	351.689(4)	10.9(4)	1.8			3473.00(8)	0.057(3)	400
		328.448(14)	9.1(3)	2.1	92	U	4060.35(5)	0.186(3)	130
		226.2980(20)	4.0(4)	5			1279.01(10)	0.200(10)	120
78	Pt	355.6840(20)	6.17(6)	3			6395.16(15)	0.0032(4)	7500

The NIPS facility

Instrument responsible: Tamás BELGYA

The NIPS facility is located after the PGAA facility at the end position of the neutron guide NV1. The NIPS facility is designed for a large variety of experiments, including study of nuclear reactions induced by slow neutrons, γ-γ-coincidences or any other idea. The beam is led through a narrow tube of 5×5 cm² cross section. This enables to place detectors very close to the target, while the detector protection is still maintained. At present two coaxial HPGe detectors (23 and 13% relative efficiency) and one planar HPGe detector, as well as one NaI(Tl) scintillation detector and two BaF₂ fast scintillators are available for prompt γ-γ coincidence measurements.

The main specifications are listed in Table 3. A typical setup for gamma-gamma-coincidence experiments can be seen in Figure 6.

Table 3. Main specifications of NIPS facility

Beam tube:	NV1 guide, end position
Distance from guide end	2.6 m
Neutron beam cross section:	2.5×2.5 cm^2
Thermal-equivalent flux at target:	≈7×10^7×cm^{-2}s^{-1}
Vacuum in target chamber (optional):	≈1 mbar
Target chamber windowless	-
Form of target at room temperature:	Solid, powder, liquid, gas in pressure container
Target packing at atmospheric pressure:	sealed FEP Teflon bag or vial
Activity of target after irradiation:	negligible
Largest target dimensions:	1.5×1.5×3.5 cm^3
Distance from target to detector window:	minimum 2.5 cm
γ-ray detector No.1	n-type coax. HPGe
HPGe window:	carbon
Relative efficiency:	13% at 1332 keV (^{60}Co)
FWHM:	1.8 keV at 1332 keV (^{60}Co)
γ-ray detector No 2.	n-type coax. HPGe
HPGe window:	Al, 0.5 mm
Relative efficiency:	23% at 1332 keV (^{60}Co)
FWHM:	1.9 keV at 1332 keV (^{60}Co)
γ-ray detector No 3.	Planar HPGe
HPGe window:	Be, 0.5 mm
FWHM:	0.6 keV at 122 keV (^{57}Co)

Figure 6. A typical setup for gamma-gamma-coincidence experiments
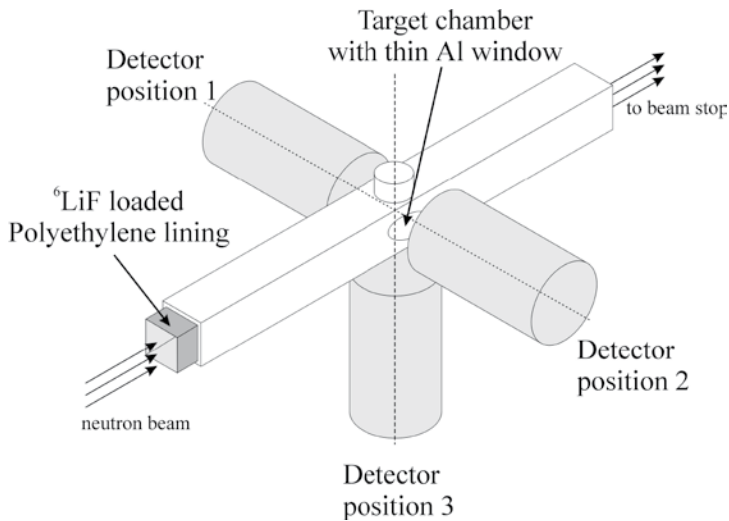
Multiparameter data acquisition is supported by a multiplexer-based sytem shown in Figure 7. The intelligent multiplexer consists of programmable modules. The master module coordinates the operation of the box and communicates with the PC, while the ADC outputs are connected to individual modules. Singles spectra and multiparameter data can be collected at the same time. The throughput of the system in multiparameter mode is around 0.5 Mbytes/s. The homemade communication software runs on a PC under DOS.

Figure 7. Programmable Multichannel Data Acquisition system

The advantage of the setup that its neutron tube can be replaced with shorter one to accommodate a variety of setups. One example is given in Figure 8 which was built to serve prompt gamma ray imaging and neutron tomography (PGAI/NT) [8].
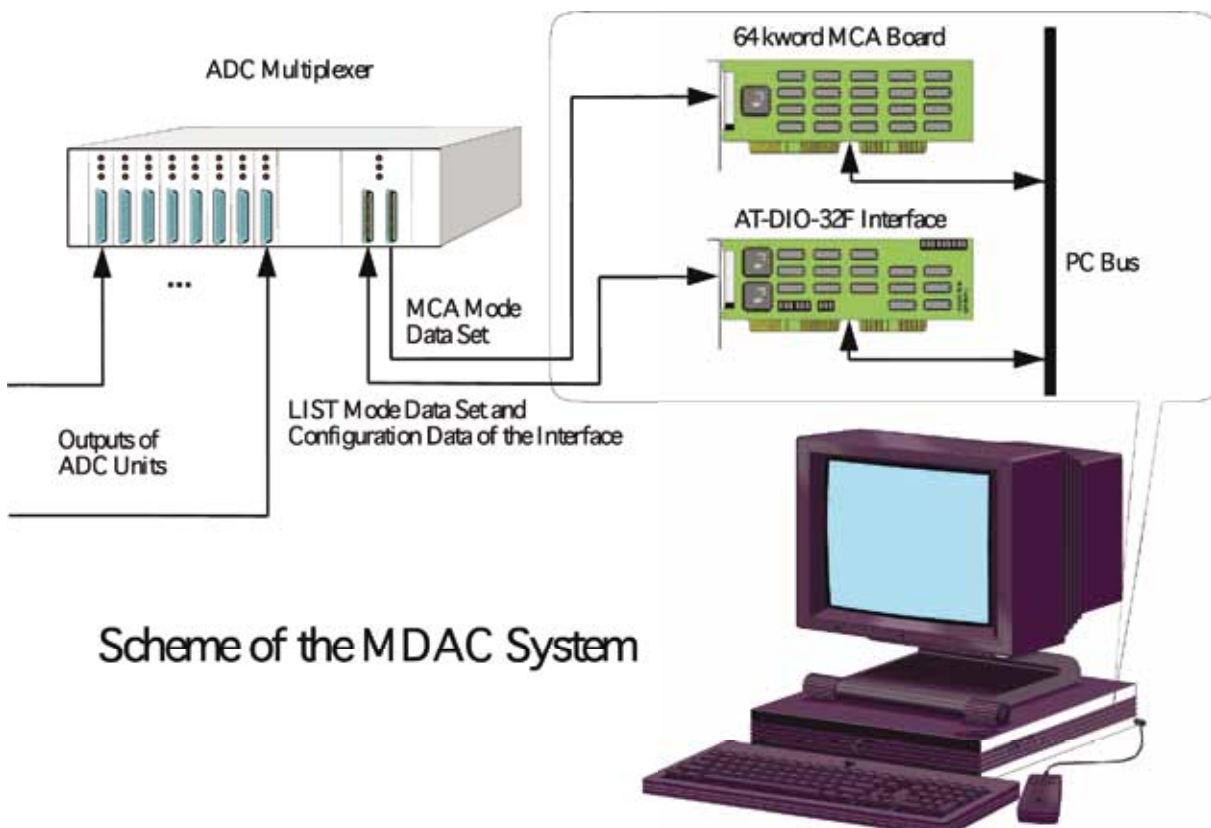
Scheme of the MDAC System

Figure 8. PGAI/NT setup at the NIPS station

In the past few years new three different Digital Signal processor electronics have been acquired. They provide a wide variety of electronic setups too.
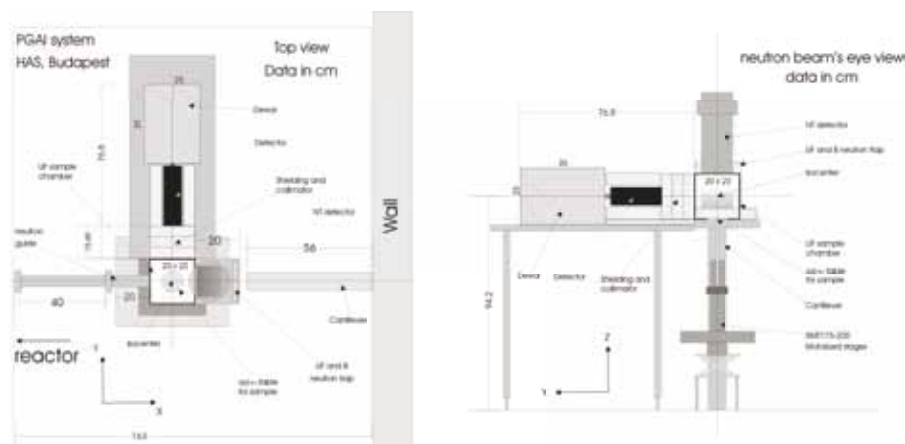
References

1. Zs. Révay, T. Belgya, L. Szentmiklósi, Z. Kis: **Recent developments in prompt gamma activation analysis in Budapest**, J. Radioanal. Nucl. Chem. 278 (2008) 643.

2. G.L. Molnar, Z. Révay, T. Belgya, **Wide energy range efficiency calibration method for Ge detectors,** Nucl. Instrum. Meth. A 489 (2002) 140.

3. B. Fazekas, Zs. Révay, J. Östör, T. Belgya, G. Molnár, A. Simonits: **A new method for determination of gamma-ray spectrometer nonlinearity** Nucl. Instr. Meth. A422 (1999) 469.

4. B. Fazekas, J. Östör, Z. Kis, G. L. Molnár, A. Simonits: **The new features of Hypermet-PC**, in: Proc. 9th International Symposium on Capture Gamma-Ray Spectroscopy and Related Topics, Budapest, Hungary, October 8-12, (G. Molnár, T. Belgya, Zs. Révay Eds.) Springer Verlag, Budapest/Berlin/Heidelberg, 1997, p. 774.

5. Zs. Révay, T. Belgya, G.L. Molnár, J. Radioanal. Nucl. Chem., 265 (2005) 261.

6. Zs. Révay, R.B. Firestone, T. Belgya, G.L. Molnár: **Catalog and Atlas of Prompt Gamma Rays in Handbook of Prompt Gamma Activation Analysis with Neutron Beams**, (G.L. Molnár ed.), Kluwer Academic Publishers, Dordrecht/Boston/New York, 2004, pp. 173–364.

7. Zs. Révay: **Calculation of uncertainties in prompt gamma activation analysis,** Nucl. Instrum. Meth A 564 (2006) 688.

8. Belgya, T., Z. Kis, L. Szentmiklósi, Z. Kasztovszky, G. Festa, L. Andreanelli, M.P. De Pascale, A. Pietropaolo, P. Kudejova, R. Schulze, and T. Materna, **A new PGAI-NT setup at the NIPS facility of the Budapest Research Reactor.** J. Radioanal. Nucl. Chem., **278**(3), (2008) p. 713-718.

4.3. DYNAMIC RADIOGRAPHY STATION
Instrument responsible: Márton BALASKÓ

Neutron radiography utilizes transmission to obtain information on the structure and/or inner processes of a given object. It is used for various non-destructive test measurements. A dynamic radiography station has been built out visualize and analyse the flow of fluids, the evaporation and the condensation processes in closed metal objects, tube systems and other types of dynamic events.

Main parameters of the dynamic radiography station:

- Thermal channel: No. 2

„A"   In the conventional arrangement:

- Complex pin-hole type collimator for neutron and gamma radiation with a collimation ratio of L/D = 170
- Neutron flux at the objects position: 10^8 n$\times$cm$^{-2}\times$sec^{-1},
  behind of CD an In filter: 6×10^6 n$\times$cm$^{-2}\times$sec^{-1}
- Gamma intensity: ~ 8,5 Gy/h
- X-ray energy: 50-300 keV; 5 mA
- Variable beam diameter, with a maximum of 150 mm at the object position.
  Maximum surface for investigation: 700×1000 mm^2
- Maximum weight of the investigated object: 250 kg

„B"   In the extended inspection area (for study of helicopter rotor blades)

- Maximum beam diameter: 185 mm
- Maximum surface: for investigation9750×700 mm^2
- Maximum weight of the investigated object: 200 kg
- Practicable to study, the efficiency of the moisture condition of the inspected objects, by a Moistening module is driven by a High pressure water pump
- Converters (radiation into light): for neutron radiography NE 426 scintillation screen with resolution of 100 μm; for gamma and X-ray radiography NaCs single crystal with resolution of 200 μm, or ZnS screen with resolution of 100 μm
- Variable filters: Cd, In
- Detection of the radiography image: low-light-level TV camera with a light sensitivity of 10^{-4} lux, imaging cycle is 40 msec, and a double cooled CCD camera (756 x 580 pixel), 10 bit.
- Radiography image is visualised on monitor, stored by S-VHS video recorder and DVD recorder and for further quantitative analysis a Quantel image processing system is used with Sapphire V.0.5 software, and an Iman β version software.
- Conventional film technique is used: by X-ray or gamma radiation
  or by neutron radiation with transfer method
  [In and Dy (100 μm) foils]
- Photo-luminescent Imaging Plates technique used by X-ray radiation or by neutron
  radiation with transfer method BAS
  IP-SR 20×25 and IP-SR 20x40
  [In and Dy (100 μm) foils]
  The evaluation of exposed IP-s are by BAS
  2500 reader unit used an AIDA picture
  reconstruction software.

Unique feature of the dynamic radiography station :

Our radiation sources give a possibility to study semi-simultaneously or simultaneously the
investigated objects by neutron-, gamma- and X-ray radiography to use the all advantages of the complementary features of the
different radiations.
Simultaneously application other non-destructive inspection as vibration diagnostics and acoustic emission. For example to
observe the secondary events of the supercritical water (SCW). The Fig.1 shows the sketch of the combined investigation of the
events of SCW.
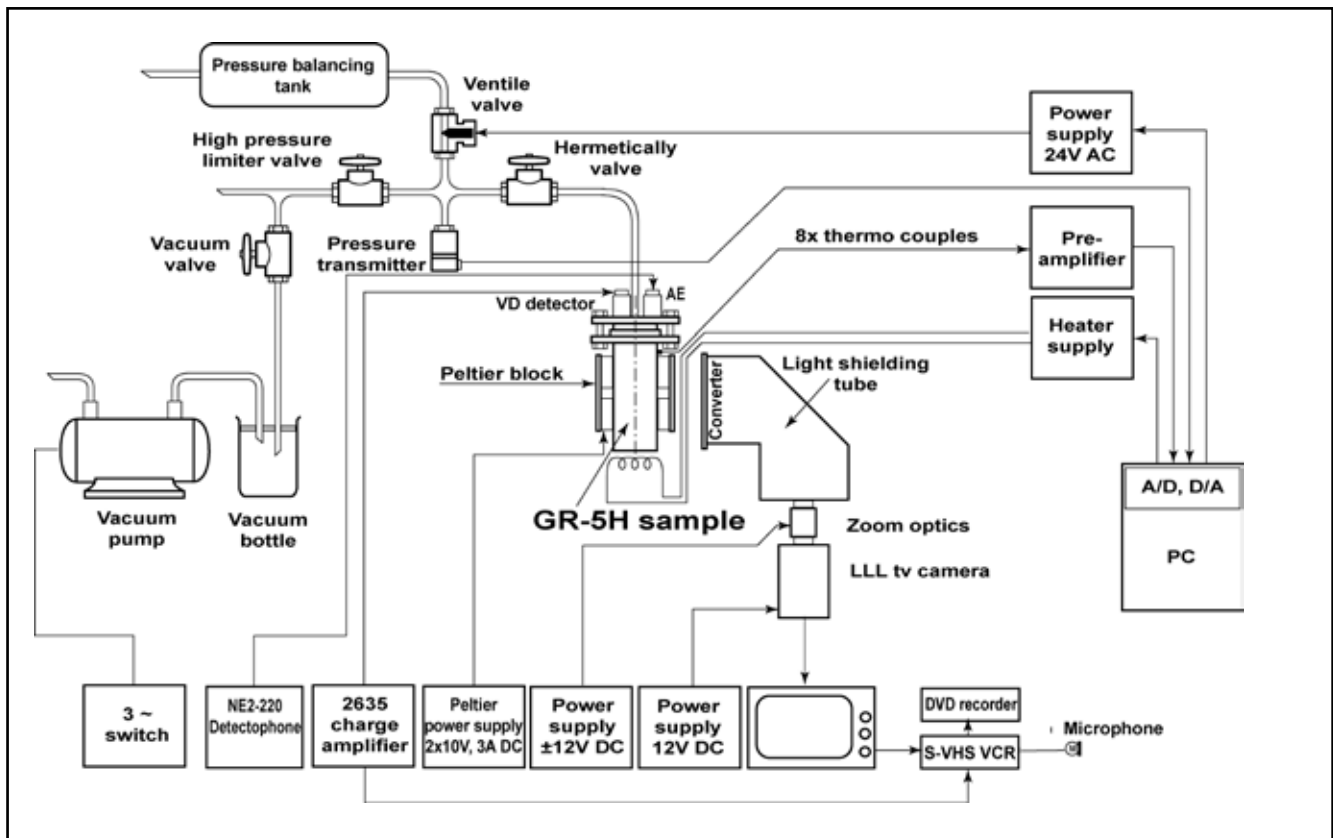
Fig.1. sketch of the combined investigation of the events of SCW.

The arrangement has a water cooled double Peltier block to freeze the water during the evacuation of the sample holder
above the water level. After the evacuation the hermetical valve is closed and water injected in the high pressure area. This
area contains a pressure transmitter for measuring the pressure when the temperature is increased above 200 °C and contains
a remote control ventilating valve which is able to stabilize the pressure independent from the temperature. Additional this last
element can make a situation for modelling of a loss-of-coolant type accident. Over 200 °C the hermetical valve is opened.
Naturally the Peltier block is moved away before the heating procedure is started. The limit of the temperature 500 °C and the
limit of the pressure is 40 MPa at the SCW measurements.

4.4. High Resolution TOF powder diffractometer

Instrument responsible: György KÁLI

The **high resolution time-of-flight powder diffractometer** (TOF) at BNC has been installed to a radial thermal neutron beam in a new guide-hall in collaboration with the Hahn-Meitner-Institut. According to Monte-Carlo simulation results [2-3] it was expected that this type of instrument can outperforms a conventional crystal monochromator powder diffractometer at continuous reactor source in the **resolution range of Δd/d =1–5×10⁻³**. The other advantage to apply TOF monochromatisation to neutron diffractometry on a continuous source is the variable resolution and intensity. A full diffraction spectrum can be gained within a variable bandwidth with ultrahigh resolution or with high intensity at conventional resolutions.

The **monochromator system** consists of a fast double and the two single choppers and a straight neutron guide with 2.5x10 cm cross section at the end. The double chopper is designed for a maximum speed of 12000 rpm. While in high resolution mode the very short - 10µs – neutron pulse and the 25m total flight path allows us to obtain a diffractogram with an accuracy of 10^{-3}Å (at back scattering mode) in a single measurement on **polycrystalline materials**, in low resolution mode **liquid diffraction** can be performed at good neutron intensity **up to 15Å^{-1}** scattering vector. As it was expected, the beam was contaminated with epithermal and fast neutrons because the straight guide is directed on the centre of the zone and the gadolinium coated chopper disks are transparent for them. Temporary silicon filters was applied with which the signal-noise ratio had been increased by a factor of 5-10.

The double disk **chopper** (Ch1 and Ch2) has two windows: a 1.5° opening for short pulses (10 µs) and a 15° window for long variable pulses (20–200 µs), and can be operated in parallel or counter rotating mode. The latter option is used to produce very short pulses at high speed. To minimize the opening time the neutron beam is reduced from 25 to 10 mm width at the position of the pulse choppers using a 4.5m **compressor neutron guide** section before and a same decompressor after them (see Figure1). Ch3 limits crosstalk between different pulses and Ch4 prevents frame overlap.

The instrument is working in **back scattering mode** to reach the best possible resolution. Until the planned detector (a 60x100 cm² 2D detector) reach completion, a box of four ³He tube is used with a 2.5MHz event recording board. Because of the much smaller surface, the box is placed closer (2m) to the sample opposite to the designed (3m). To achieve the maximum resolution the **2D position sensitive detector** will be applied in combination with a **bank of 32** pieces 6 mm thick pressed **³He tubes** . The **data are acquisited** in so called list or **time stamping** mode: all the event on the detector, the chopper signs and optionally changes in the sample environment are registered with the time passed since the starting of the experiment. In this mode many uncertainties can be filtered out during the treatment and re-treatments.

References

H. J. Bleif, D. Wechsler and F. Mezei, 2000, *Physica B:*, V276-278, p 181-182

J. A. Stride, F. Mezei, H. -J. Bleif and C. Guy.,1997 *Physica B:*, V 234-236, p. 1157-1159,.

J. Peters, H.-J. Bleif, Gy. Káli, L. Rosta and F. Mezei, 2006, *Physica B:*, 385-86 1019-1021

Káli Gy., Sánta Zs., et al. 2006 *Proceedings of EPDIC10 Zeitschrift für Kristallographie*;
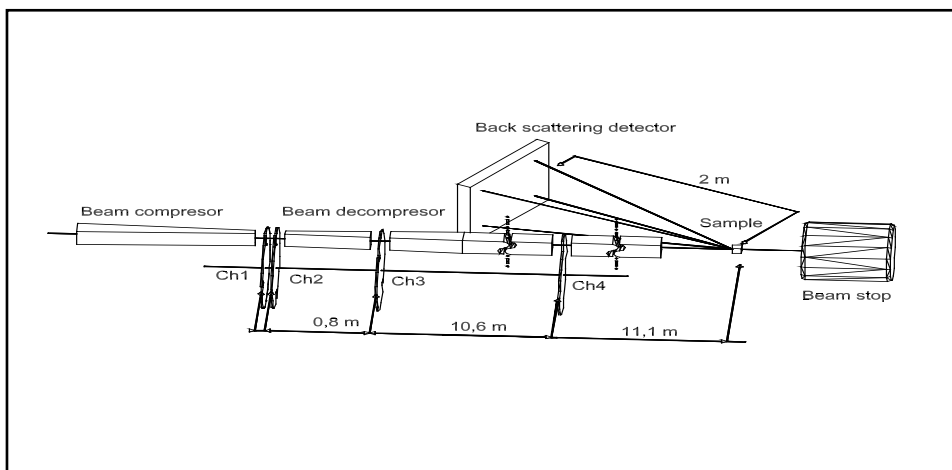
Figure1. Instrument Layout

Total flight path from chopper 1	L=25 m
Wavelength range	0.07-0.45 nm
Bandwidth in single experiment$\Delta \lambda$	from 0.4 nm to 0.08 nm (200 Hz)
Resolution $\Delta d/d$	1×10^{-3} at d=0.15 nm
Straight neutron guide cross section	25x100 mm^2
Coating	Supermirror NiTi, m=2
Beam flux at opened windows	4×10^7 neutron/s/cm^2
Pulse length	10-1000 µs
Max. speed for the double chopper	12000 rpm

Table1. Main parameters
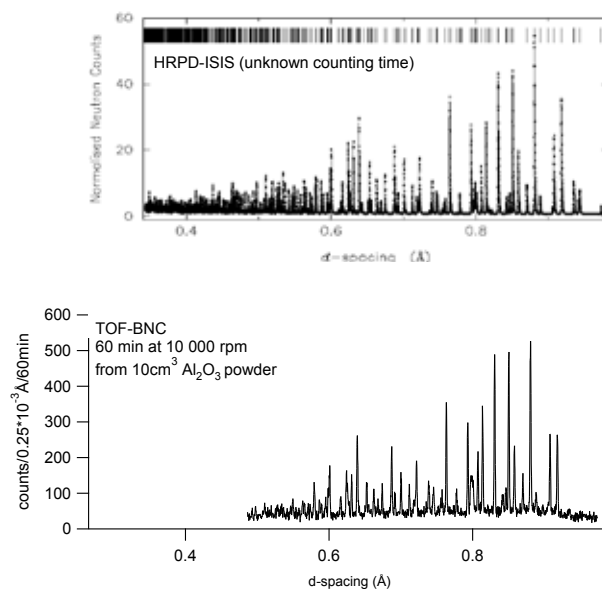
Figure2. A typical spectra in comparison wit HRPD at ISIS

Instrument team:

Gy. Káli, Zs. Sánta (Budapest Neutron Centre)

4.5. TRIPLE-AXIS SPECTROMETER

Instrument responsible: Márton MARKÓ

A triple-axis spectrometer has been designed for structural and dynamical studies of condensed matter. Because of the limited number of other operational equipment the triple axis spectrometer is used in a multi purpose regime, e.g. high resolution diffractometry, strain analysis, reflectometry, quasielasctic and inelastic scattering. We have a polarization setup on this spectrometer too.

The spectrometer is installed on a curved (4200m) neutron guide at a 19 m position from the beam port exit. The guide is 1.5 Θc boron glass and is coated NiTi multilayer

The monochromatic beam is provided by a 90mm high focusing multi- blade pyrolithic graphite monochromator.

The movable part of the monochromatic shielding has a chain type construction. Changing the incident wavelength the hole chain is driven by the monochromator-sample arm. This construction automatically provides the most effective shielding near the detector area. (see Fig 1.). We could achieve very low background conditions (1 neutron/300s).

The beam divergence is determined by thin film soller type mylar collimators coated with GdO.

A two dimensional position sensitive detector in medium resolution mode were installed .and the efficiency of data collection has been raised 40 times in quasielastic mode.

The spectrometer is to be developed into the RITA-type spectrometer. For the polarization option, we use a mirror assembly as a polarizer and analyzer. Heussler crystals are foreseen in a future .

Main parameters of the spectrometer :

Beam tube :	neutron guide No.1
Monochromator :	pyrolitic graphite 90x80 mm (24min mosaicity)
Analyser :	pyrolitic graphite 50x90 mm (24min mosaicity), or Ge monocrystal (15min mosaicity)
Collimations :	interchangeable 45′, 30′, 15′
Range of monochromator angle:	$36° < 2\Theta < 126°$
Range of scattering angle :	$-120° < 2\Phi < 70°$
Range of analyser angle :	$-40° < 2\Theta < 120°$
Range of crystal orientation :	$0° < 2\Theta < 360°$
Angular resolution :	$0.01°$
Flux at specimen :	2×10^6 n/cm^2/.sec
Beam size :	25×90 mm^2
Momentum transfer :	$0 – 2.7$ Å^{-1}
Energy transfer :	$0 - 9$ meV
Characteristic resolution at 3.3 Å	$120\text{-}150$ μeV
Sample environment :	cryostat (liq. N2) , magnet up to.2T, max scattering angle 100 deg furnace up to 1000°C, Thermostat (-20°C-100°C)

Control and data collection : IBM-AT compatible computer

Schematic arrangement of the triple axis spectrometer

DETECTOR

Size of primary beam 25X100 mm

Monochromator 90x75 mm

Monochromator (PG) -Sample 1600 mm

Sample Analyzer 750 mm

Analyzer detector 800 mm

Analyzer size 50x100 mm

Size of detector 190x190 mm

Beam divergence before monochromator: horizontal 24-30 min

Vertical divergence when focussing to sample 100min

The arrangement of measurement

The 190x190mm area detector
equipped to the spectrometer.

Acoustic phonon on PG crystal, Peaks left and right
are correspond the energy gain and loss process
The middle is the gain+loss two phonon process

Acoustic branch measurement on Heussler crystal due to rotation of sample .The central peak corresponds to the incoherent scattering and zero energy exchange. The form of phonon branch corresponds to the cosine function according to the impulse transfer in Z direction.

4.6. REACTOR-NEUTRON ACTIVATION ANALYSIS

R. Baranyai, I. L. Sziklai_László, R. Szőke, A. Simonits

KFKI Atomic Energy Research Institute

In spite of advanced nuclear analytical methods developed in the past two decades (PIXE, XRF, etc.) classic (n,γ) reactor neutron activation analysis (RNAA) is still preserving its role as a "workhorse" for the vast amount of analytical work. Combined with computerized high resolution gamma-ray spectrometry, RNAA offers mostly non-destructive, multi-element routine analysis needed in such areas as environmental monitoring, geochemistry, medicine and technological processes. Among its favourable characteristics negligible matrix effects, excellent selectivity and high sensitivity are worth mentioning (for about 75 elements less than 0.01 μg can be determined)

Instrumentation

Besides more than 40 vertical channels operated by the reactor staff, a pneumatic sample transfer system is also available at the Budapest Research Reactor. (Figure 1.)
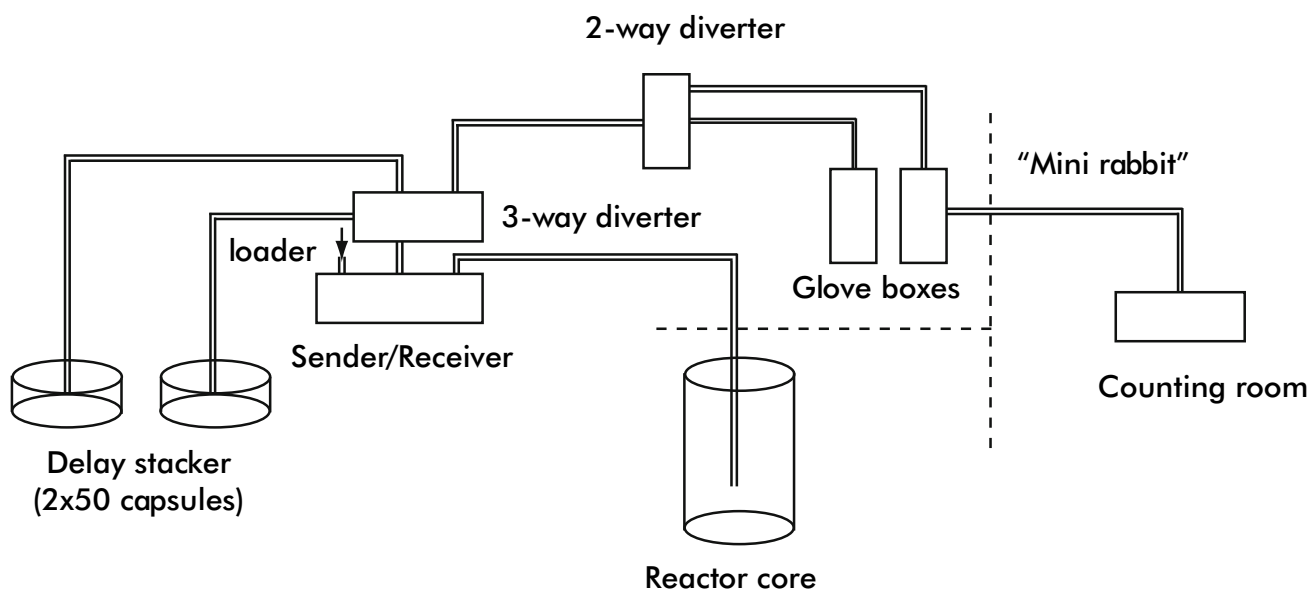
Figure 1. Schematic diagram of the multi-purpose pneumatic transfer system

The rather sophisticated but very versatile system includes:

- **Sender/Receiver Station** permitting capsule injection and programmable capsule transfer between the irradiation position and the station
- **Tubing system** (50 m long flexible polyprophylene) with photo detectors along the capsule pathway to control capsule position and speed
- **Aluminium irradiation end** (~5 m) equipped with a large variety of sensors to monitor capsule arrival at the irradiation position, cooling gas flow, humidity, temperature, etc.
- **Delay Stacker** (2 x 50 capsules) for decay of short-lived isotopes before counting
- **Drop-out Stations** for sample manipulation before counting
- **"Mini Rabbit" system** to transport radioactive samples to the counting room

The "rabbit" system operates by compressed air (2 bar). Capsules made of polyethylene can be cooled during irradiation with CO_2 in order to extend the irradiation period (over 20 minutes at present). The whole system is PC-controlled and the developed acquisition software allows a simple and user-friendly operation.

In the "B" vertical pneumatic tube, thermal neutron flux variation along the axis of the irradiation capsule is less than 5 %. As a rule, small samples and monitors are packed in 10 mm height x 8 mm dia. polyethylene vials in which less than 0.5 % flux inhomogenity can be expected during irradiation.

Neutron flux parameters have been measured with the "Bare Triple- Monitor" method using Zr foil, as well as Al-0.1%Au and Al-0.1% Lu wires. As seen in Table 1., channel "B" is fairly well thermalized (f≈40) and when representing the epithermal flux distribution with the $1/E^{1+\alpha}$ function, the α-value is positive.

MEASURED NEUTRON FLUX PARAMETERS IN THE PNEUMATIC TUBE "B"					
(Lattice position: 310-311-266, Date: 04-NOV-1997)					
$\Phi_s = n_{cd} \times v_0$ "subCd flux" [n/cm²×s]	f=Φ_s/Φ_{epi} flux ratio	Φ_{fast} [n/ cm²s]	α	T_n [°C]	NOTES
6.0×10^{13}	36	$1.1 \ 10^{12}$	0.033	57*	Primary coolant temp: 50 °C

Instrumental, multielement neutron activation analysis makes perhaps the most stringent demands on the applied gamma-ray spectrometry. The measured spectra are often very complex, containing more than hundred peaks with many multiplets. Consequently, the importance of the quality of the applied hardware as well as the flexibility of the evaluation software can not be overemphasized.

In NAA practice, unknown samples are usually irradiated first for only a few minutes to "scan" possible major components and to gather information for planning the subsequent long irradiation. Short-time NAA usually results in "hot" samples with a number of fast-decaying isotopes (^{28}Al, ^{52}V, ^{49}Ca, ^{38}Cl etc.). A good quality spectrometer should, therefore, maintain spectrum quality at high and variable incoming rates while properly correcting all kind of pulse losses (dead time, pulse pile-up) to preserve the accuracy of quantitative analysis as well.

The block diagram of one of the three gamma-ray spectrometers is shown in Figure 2. All the setups incorporate now Westphal's Loss-Free Counting (LFC) modules with dual spectrum storage option.

Recently, conventional amplifiers and ADCs have been replaced with their digital counterparts (CI 2060) or with a standalone digital spectrum processor (DSpec**PLUS**) in order to improve system characteristics (long time spectrum stability, rate-dependent resolution, etc.)
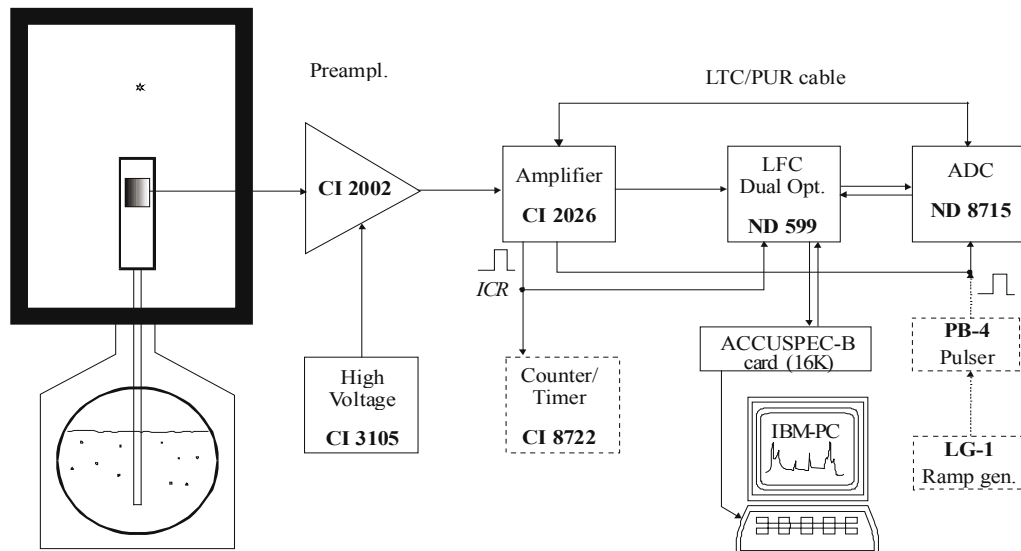
Figure 2. A gamma-ray spectrometer equipped with Dual Spectrum LFC module

Performance tests of the above mentioned gamma-ray spectrometers are carried out regularly. Sometimes factory engineers are consulted to check a built-in module (such as an ADC). For testing system parameters at high and varying counting rates, special homemade and certified isotopes should be made available. In Figures 3 and 4 some test results are shown.
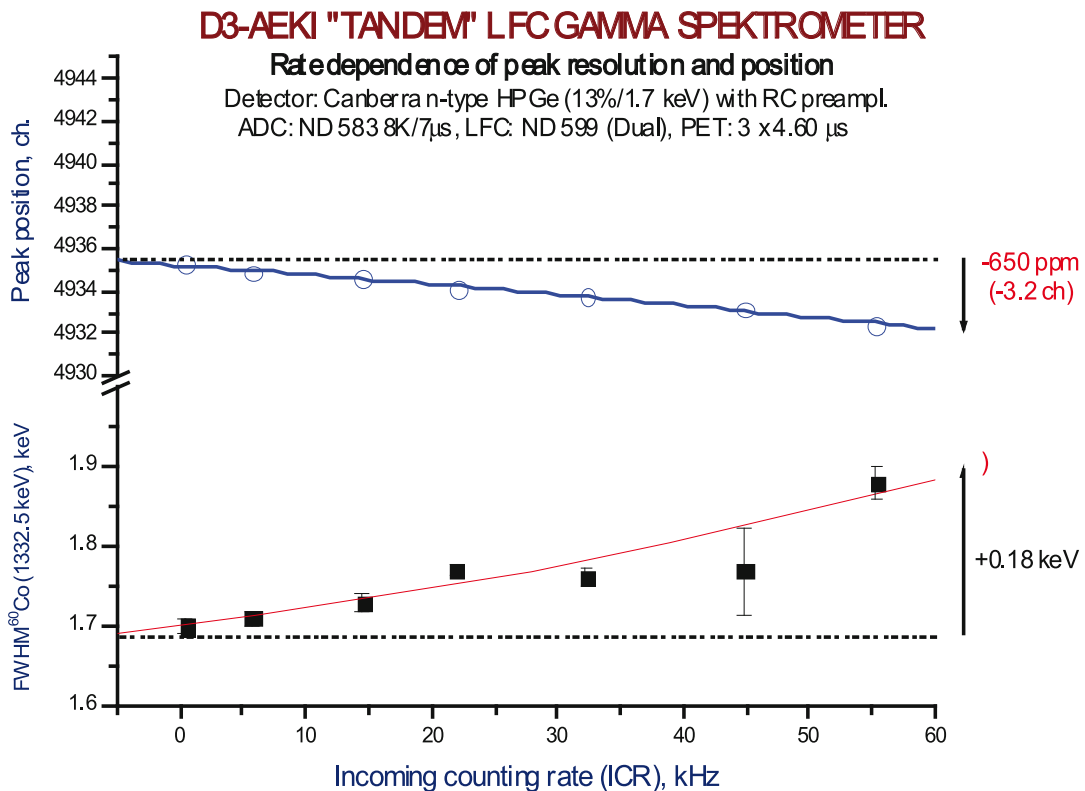
Figure 3a. Peak centroid and resolution stability of AEKI detector D3 coupled to a conventional setup (amplifier + ADC) comprising a Dual LFC module
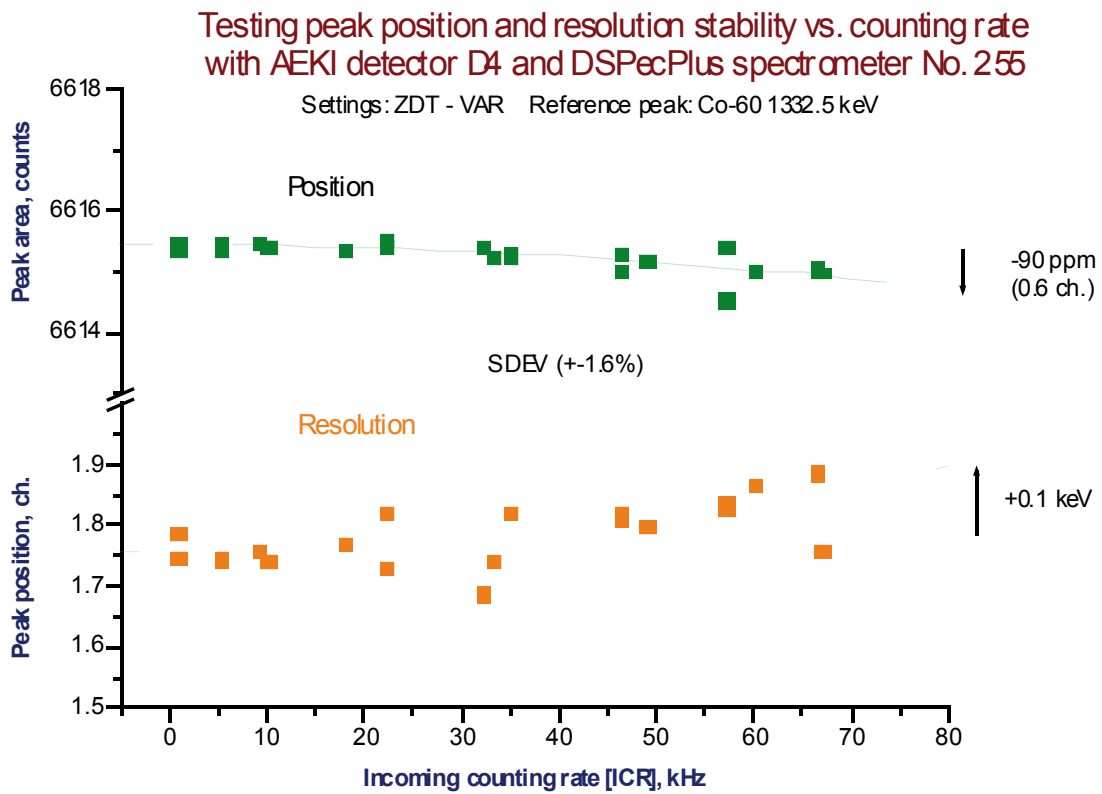
Figure 3b Peak centroid and resolution stability vs. counting rate of D4-AEKI detector with DSpec^Plus
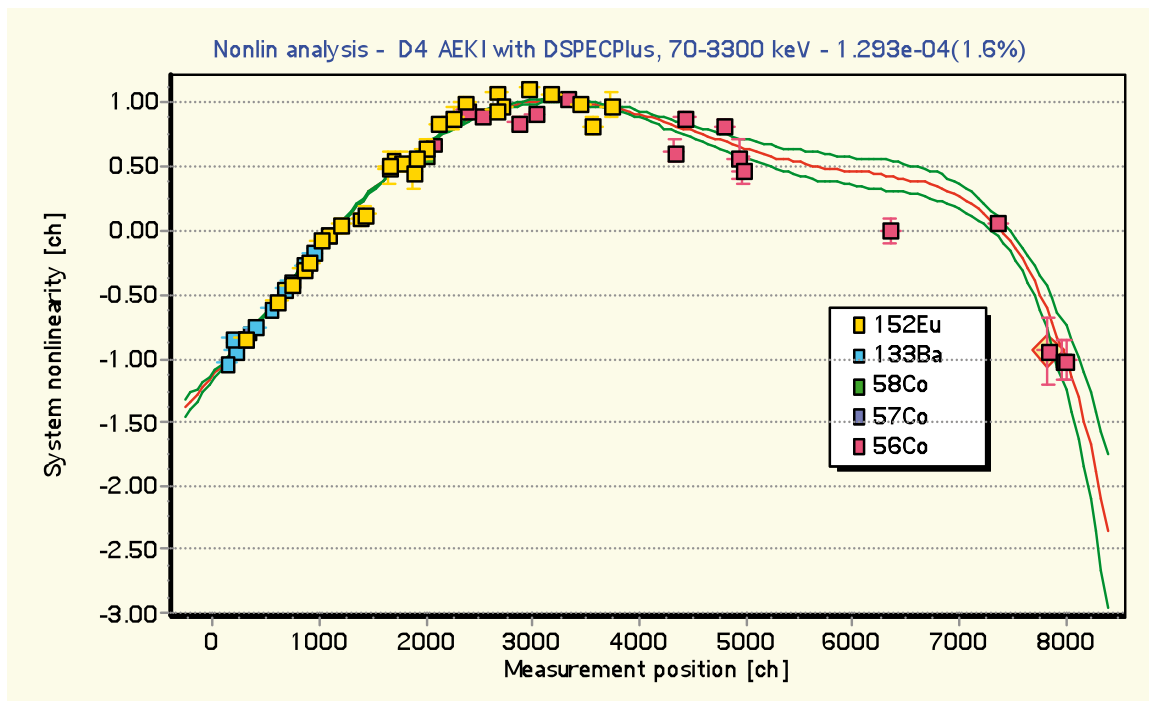
Figure 4. System nonlinearity with D4 detector and DSpec^Plus.

The recorded "tandem" spectra are evaluated with the program Hypermet-PC Ver. 5.0 which is fully compatible with the KAYZERO/SOLCOI program package used for concentration calculation.

Developments and applications

One important aspect of routine activation analysis is the simplification of the applied standardization procedure. A new method using compound nuclear constants (i. e. so called k_0-factors determined experimentally with high accuracy) was developed to eliminate standard preparations and errors originating from randomly selected nuclear data. In the course of a two decade co-operating research with the INW Gent University (Belgium), k_0-values and related nuclear data are now established for 140 (n,γ) reactions and the method is now operational in more than 50 NAA laboratories world-wide. In view of its large nuclear data library and its complex algorithms it was but logical that a computer code KAYZERO/SOLCOI was developed at DSM Research (The Netherlands) for k_0-NAA. In a framework of an EU COPERNICUS project the method is now tested and verified by analysing European multielement standard reference materials in five NAA laboratories. The latest compilation of recommended nuclear data for use in k_0-NAA is published in the Atomic Data and Nuclear Data Tables (Vol. 85 (2003) 47-67)

The INAA method described above was applied to study the concentration distributions of typical toxic heavy metals in small amounts of industrial type air particulate fractions. Generally, toxic components are distributed in two forms in the particulates, e.g. in a matrix involved form and in a surface deposited form of which the latter one can be considerably enriched. Within the scope of this project enrichment rates of about 18 toxic elements have been investigated in function of the sampling temperature.

The trace element content of vegetation growing inside the fertilizer plant and in the vicinity was investigated by neutron activation analysis method. We determined the degree of elemental enrichment in different plant species (carrot, potato) and soil samples collected on the premises of the plant and in some control area. Our results show that area is exposed to the emissions of the phosphate fertilizer industry. The specific pollutants emitted into the air by fertilizer plant are Sr, Cd, La, Ce, Sm, Tb, Yb, U and Th.

The nutritional importance of trace elements has grown rapidly during the last years mainly because of a better understanding of their biological functions. For determination of low concentration levels of Se INAA is very expedient a sensitive multielement technique which is valuable for both homogeneity testing and certification analyses due to its high precision and accuracy. INAA procedure using the ^{75}Se isotope was developed and the activation, decay and measuring scheme was optimized to the needs of the food samples and applied for the determination of Se levels in basic food ingredients. In addition the selenium state and its changes with age in children and adults living in three geographical regions of Hungary were studied

A nondestructive analytical method was developed to monitor the activity of the primary coolant of the Budapest Research Reactor. The activity of radionuclides in water and gas samples taken from the primary circuit have been measured for more than four years to monitor the technological parameters of the research reactor during normal operation. In the primary water samples 7 noble gas nuclides (Kr, Xe), 12 corrosion (activation) products (Cr, Mn, Co, Fe, etc.), fission iodine and 8 other fission products and impurities (La, Sb, Ta, etc.) as well as radioactive components in the gas samples were determined routinely by high resolution gamma-ray spectrometry.

A non-destructive neutron activation analytical method was also developed for analysis of wear-components in liquid oil samples. More than 20 elements were determined and their enrichment rate studied in used lubricating oils from aircraft engines.

Epithermal neutron activation analysis (ENAA) was introduced to analyse geological and biological samples. The major advantage offered by epithermal neutron activation analysis is the substantial reduction of interfering matrix activities. Consequently, a number of important nuclides (^{75}As, ^{197}Au, ^{111}Cd, ^{100}Mo, ^{121}Sb, ^{124}Sn, ^{238}U) can be determined instrumentally with minimum delay.

Instrument responsible: Rózsa BARANYAI

4.7. MTEST diffractometer

László Kőszegi

Research Institute for Solid State Physics and Optics

MTEST diffractometer is installed on the 6th axial thermal channel of the reactor. A sapphire single crystal is used, deep inside the beam shutter, to avoid the epithermal neutrons. Low efficiency fission chamber monitor and a BF3 single detector serve the data collections.

MTEST diffractometer has been equipped with air cushions to achieve the necessary flexibility for a continuously variable wavelength. CAMAC-based electronics serves the movement's control.

The Instrument is already under operation since 01. 01. 2002.

MTEST is conceived for those kind of research which needs higher resolution difractometry that was available earlier in Budapest. **Cu(111)**, **Cu(200)**, **Ge(111)**, **Ge(220)** and **Heusler** crystals are available for producing monochromatic beams.

This variety makes possible to choose the wavelength between **0.065-0.35 nm.**

2*10⁶ neutron/(cm²*sec) at the sample table at **0.133 nm**.

The instrument is installed mostly for internal strain-stress measurements but the four-circle goniometer makes also the chance for texture measurements as well.
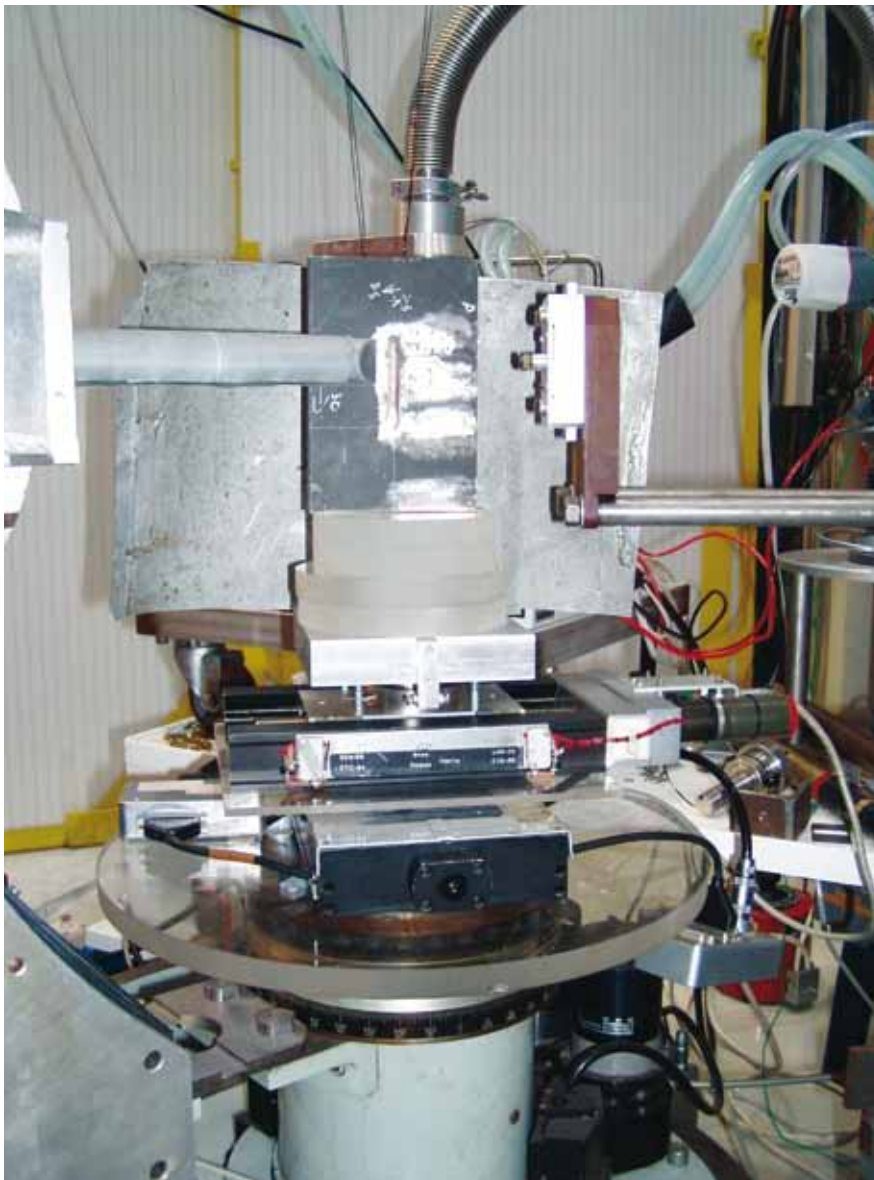
The diffraction spectra can be measured up to **144°.**

Different slits and variable slit-sample distances are for the neutron beam tailoring.

With the collimation we can go down to **12'**.

Positioning the sampling volume, beyond the automatic rotations.

Automatic X, Y sample displacements. **Manual Z** displacement.

Automatic sample changer is available for **4** samples. (not together with the automatic XY movements)

For special needs a vacuum-furnace (**RT-1000°C**) can also be placed on the sample table.

Economise the measuring time a sample changer with four positions is also available. A PC using special software that makes also possible to construct measuring sequences controls the whole instrument. Picture shows the automatic XY option. The figure shows the scheme of whole instrument where the main parameters of the freedom of movements are indicated.

**Instrument responsible:
László KŐSZEGI**

Figure 1.

a. Top - view of the whole system

Sapphire
single crystal

Reactor

Detector

Thermal neutrons
channel No.6.

Monochromator

Shieldings

Air cushions

75°

15°

**MTEST
Diffractometer**

Sample and its rotation

141°

2Θ movement (from 0° to 141°)
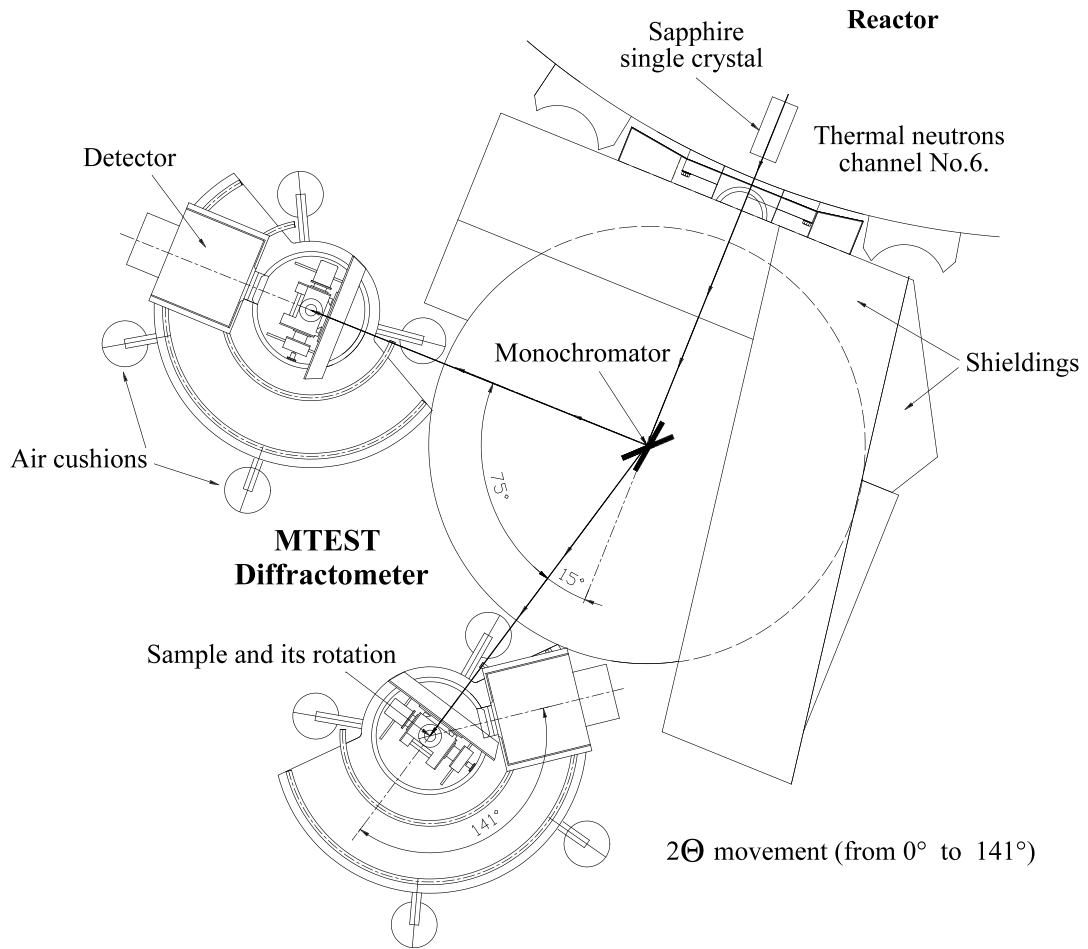
b. Side - view of the 4 - circle diffractometer

Tilting (from -13° to +38°)

Detector

38°

13°

Sample position

Sample table

Connection to the
monochromator
shielding
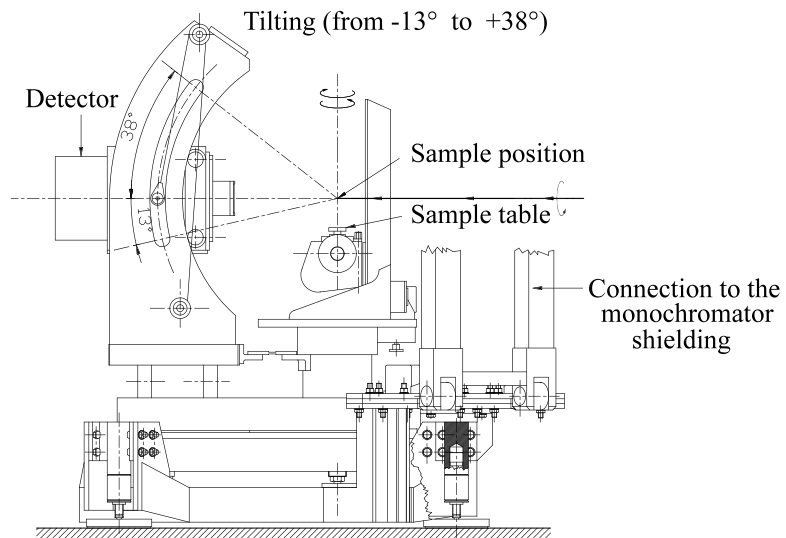
4.8 PSD - NEUTRON DIFFRACTOMETER

Erzsébet Sváb and Margit Fábián
Research Institute for Solid State Physics and Optics

The PSD neutron diffractometer is suitable for atomic structure investigations of amorphous materials, liquids and crystalline materials where the resolution requirements are not high. It is a 2-axis diffractometer equipped with a linear position sensitive detector system. The detector assembly is mounted on the diffractometer arm and it spans a scattering angle range of 25° at a given detector position. The entire diffraction spectrum can be measured in five steps.

Table 1. Characteristic features of the PSD diffractometer for two actual arrangements

Channel	thermal, 9T tangential	
Primary collimation	Soller-type (50', 20', 15')	
Take-off monochromator angle facility	$-5° < 2\Theta_M < 45°$	
Monochromator and mosaicity	Cu(111), 16'	Cu(220), 20'
Monochromatic wavelength	1.069 Å	0.66 Å
Resolution, $\Delta d/d$	$1.2 \cdot 10^{-2}$	$2.4 \cdot 10^{-2}$
Flux at the sample position	10^6 ncm^{-2}s^{-1}	10^5 ncm^{-2}s^{-1}
Beam size at the specimen	10 mm×50 mm	
Scattering angle, 2θ	$5° < 2\Theta < 110°$	
Momentum transfer interval, Q	0.6-9.2 Å^{-1}	0.8-15.8 Å^{-1}
Monitor counter	fission chamber	
Detector system	- 3 linear position sensitive ^{3}He detectors - the detector assembly spans 25° scattering angle at a given position	
Data collection	Xilinx preprogrammed unit	
Data transfer and control	PC-AT with Eagle I/O card and special instrumental control card	
Remote control and file transfer	Windows programme package	

Kiril KREZHOV scientist, user

Detector assembly

Goniometer with sample can

Erzsébet VERESS scientist, user

Figure 2. Photographs taken at the PSD neutron diffractometer

Instrument responsible: Erzsébet Sváb

5, EDUCATION

The PGAA group regularly accepts tranees from the International Atomic Energy Agency. We participate in the arrangement of the biennial Central European Neutron School. Our laboratory leads laboratory practices for chemist and chemical engineer students from the Budapest Technical University and from the Eötvös University. Our colleagues continuously supervise MS and PhD students working on their theses in our laboratory.

Graduate and postgraduate courses

2006-07 Disorder in condensed phases (L. Pusztai, ELTE)

Laboratory practice and seminars

2006 - Radiation protection laboratory practices (L. Temleitner, BME)

2006 - Environmental protection laboratory practices: radiation aspects (L. Temleitner, BME)

2006-07 Experimental physics classroom practical course (Sz. Pothoczki, BME)

Diploma works

2006 - Sz. Pothoczki (BME): Investigation of the structure of molecular liquids by neutron diffraction and Reverse Monte Carlo simulation (Supervisor: L. Pusztai)

Ph.D. students

Z. Somogyvári (BME): Magnetic and atomic structure investigations by neutron diffraction (Supervisor: E. Sváb)

L. Temleitner (BME): Diffraction and computer simulation studies of disordered molecular systems (Supervisor: L. Pusztai)

I. Harsányi (ELTE): The structure of aqueous electrolyte solutions (Supervisor: L. Pusztai)

M. Fábián (ELTE): The structure of borosilicate glasses (Supervisor: E. Sváb)

Sz. Pothoczki (BME): Investigation of the structure of molecular liquids by neutron diffraction and computer simulation (Supervisor: L. Pusztai)

V. Mile (ELTE): Diffraction and computer simulation studies of structural disorder in molecular liquids and solids (Supervisor: L. Pusztai)

Dissertations, PhD

2006 - I. Harsányi: Investigation of the structure of aqueous electrolyte solutions using computer simulation methods, Ph.D. Theses, ELTE (Supervisor: L. Pusztai)

2007 - L. Temleitner: Investigation of structural disorder by neutron diffraction and computer simulation, Ph.D. Theses, BME (Supervisor: L. Pusztai)

Awards

2006 - Sz. Pothoczki (BME): 1st prize and the Dean's Award, Young Researcgers' Conference (Supervisor: L. Pusztai)

Lectures

Education is one of the missions of our research reactor centre. Traditionally, the research laboratories at the Budapest Neutron Centre play an important role in graduate and professional training, performed at various levels and different frameworks from informal popular public communications to high level professional international training.

We consider as an important part of our education programme the widening and improvement of the public acceptance and knowledge on the operation of our research reactor and the application of nuclear techniques to the various basic and applied research problems as well as commercial activities performed at our centre. One of the means for this public information is that BNC is open for visitors every last Friday of a month. Upon preliminary registration organised groups can visit the reactor and the research facilities. In this way we receive many tens of visitors groups from school classes to professional company groups.

In the frame of the national university training programmes, basically our senior scientists conduct special courses on neutron scattering for condensed matter, activation analysis as well as on nuclear physics at the Budapest Technical University (BME), Eötvös Loránd University (ELTE), Gödöllő Szent István University, Miskolc University (ME), Veszprém University (VE). In connection with the above activity, practical/hands-on "laboratory training" is regularly performed on the BNC diffractometers, triple axis spectrometers, prompt gamma activation analysis stations, small angle neutron scattering device as well as at the radiography stations for the students of the above universities.

Several university masters and Ph.D. thesis works are performed at the BNC laboratories each year. In the period of 2006-2007 three diploma/masters works were prepared for students of the BME, and ELTE. 11 Ph.D. works are under preparation.

At international level our training programme is run also by various means. Graduate and PhD students are received regularly for 1 - 4 months training in neutron research for materials science, nuclear data treatment, computing etc. These students arrive from various universities as well as from foreign establishments e.g. Universities of Angers, Cluj, St Petersburg, Moscow.

6. EVENTS (workshops, meetings)

Conferences

3rd Reverse Monte Carlo Conference and Tutorial; Hotel Normafa, Budapest; 26-30 September 2006; organised by László Pusztai (Department of Neutron Physics). 44 participants (28 from abroad). Proceedings volume has been published in Journal of Physics: Condensed Matter. **Vol 19.**

APPENDIX

7. EXPERIMENTAL STATIONS OF THE BNC

Acronym	Instrument	Current status	Responsible person phone: +361 392 2222 /EXT, e-mail
PSD	Powder diffractometer	scheduled, **EU7**	Erzs□bet SV B /1418 svab@szfki.hu
MTEST	Materials test diffractometer	scheduled, **EU7**	László KŐSZEGI /1469 koszegi@szfki.hu
SANS	Small angle scattering spectro-meter with XY detector	scheduled, **EU7**	L szl—ROSTA /3520 rosta@szfki.hu No□mi SZ KELY/1682 szekely@szfki.hu
ATHOS	Three-axis spectrometer on neutron guide	scheduled, **EU7**	Gyula T R K/1439 torok@szfki.hu
TAST	Three-axis spectrometer on a thermal beam	Scheduled, **EU7**	M rton MARK /1416 Marko@szfki.hu
PRFM	Neutron reflectometer	installed, being tested	Tam s VERES /1738 veres@szfki.hu
DNR/SNR	D y n a m i c / s t a t i c radiography	scheduled, **EU7**	M rton BALASK /1434 balasko@aeki.kfki.hu
BIO	Biological irradiations	scheduled, **EU7**	J—zsef P LFALFI /1495,1671 palfalvi@aeki.kfki.hu
PGAA	Prompt activation analysis	scheduled, **EU7**	Zsolt R VAY /3143 revay@iki.kfki.hu
NIPS	Neutron Induced P r o m p t - G a m m a Spectroscopy	Scheduled, **EU7**	Tam s BELGYA /32-34 belgya@iki.kfki.hu
TOF	T i m e - o f - f l i g h t diffractometer	installed, being tested	Gy□rgy K LI/1439 kali@szfki.hu
BAGIRA	Controlled temper-ature irradiation rig	scheduled	kos HORV TH /3628 horvath@aeki.kfki.hu
RNAA	Fast-rabbit system and activation analysis	scheduled, **EU7**	R—zsa BARANYAI /1256 baranyai@aeki.kfki.hu

Information: László ROSTA scientific programme coordinator
phone: +361 3922222/3520, fax: +361 3959165, e-mail: rosta@szfki.hu

8. PUBLICATIONS

Articles

1.	M. Balask—A. Kuba, A. Nagy, A. Tan cs and B. Schillinger, Comparision Radiography and Tomography Possibilities of FMR II.(20MW) and Budapest (10MW) Research Reactor, Conf. Proc. of WCNR-8, Gaithersburg, USA. October 16-19, 2006. (10).

2.	M. Balaskó, L. Kőszegi and J Dombovári, Study of Museum Object by Neutron-, Gamma-, X-ray Radiography and Neutron Diffraction, Conf. Proc. of WCNR-8, Gaithersburg, USA. October 16-19, 2006. (27).

3.	M. Balask—G. Endr zi, Gy. Tarnai, Gy. Moln r, Z. Vigh and E. Sv b, Reference measurements of defects in helicopter rotor blades by neutron- and X-ray radiography, vibration diagnostics and ultrasound, Conf. Proc. of WCNR-8, Gaithersburg, USA. October 16- 19, 2006. (63).

4.	M. Balask—E. Sv b, Z. Kiss, A. Tan cs, A. Nagy and A. Kuba, Study of the inner structure of a damaged control rod by neutron- and X-ray radiography and discrete tomography, Conf. Proc. of WCNR-8, Gaithersburg, USA. October 16- 19, 2006. (64).

5.	M. Balaskó, L. Horváth, Á. Horváth, L. Kammel, P. Tóth, and G. Endrőczi "INVESTIGATION OF THE BEHAVIOUR OF SUPERCRITICAL WATER IN THE MODEL OF 4TH GENERATION NUCLEAR REACTOR BY COMBINED NDE METHODS Ó Proc 6th International Conference on NDE in Relationto Structural Integrity for nuclear and Pressurised Components, Edited by EC Directorate-general Joint Research Centre, EUR 23356 EN- 2008, Budapest, 8-10 October 2007, 441-448 , (2008).

6.	M. Balaskó, I. Benkovics, L. Horváth, S. Tőzsér, +A. Kuba, Z. Kiss, A. Tanács, A. Nagy, and E. Sváb COMBINED NDE METHODS IN THE INSPECTION OF THE DAMAGED CONTROL RODSÓProc 6th International Conference on NDE in Relationto Structural Integrity for nuclear and Pressurised Components, Edited by EC Directorate-general Joint Research Centre, Budapest, 8-10 October 2007, 449-458, (2008).

7.	Balaskó M. és Sváb E. "Komplex digitalis radiográfia alkalmazása a budapesti kutató reactor szabályz—rdj nak vizsg lat banÓ Proc. V. Roncsol smentes Anyagvizsg l—konferencia s ki ll't s, Eger 2007. március 6-9, előadás CD és publikálás alatt az Anyagvizsgálok lapjában (2007).

8.	Balask—M., Horv th L., Vigh Z. s Pog cs s I. Kompozit szerkezetek tanulm nyoz sa Komplex, Digitális Radiográfiával", Proc. V. Roncsolásmentes Anyagvizsgáló konferencia, Eger 2007. március 6-9, előadás CD és publikálás alatt az Anyagvizsgálok lapjában, (válogatás 2008.) 21-25 old.

9.	Tóth P., Balaskó M. és Sváb E. "Korrózió és lerakodás vizsgálata nagy átmérőjű szigetelt és szigeteletlen cs ve k eset benÓ Proc. V. Roncsol smentes Anyagvizsg l—konferencia, Eger 2007. m rcius 6-9, előadás CD és publikálás alatt az Anyagvizsgálok lapjában (2007).

10.	Hózer Z. at al. – Balaskó M. " A rugó szerepe a fűtőelemek sérülésében", kutatási jelentés, AEKI –FRL 2007-266-01/02, 53 oldal

11.	Z. H—zer, at al. – M.Balask— CODEX-CT-1 experiment: Quenching of fuel bundle after long term oxidation in hydrogen rich steamÓ, Res.Report 2007 (submitted).

12.	M. Balask— Summary and Contribution to the practical work at the Radiography Station of the Budapest research reactorÓ, spec. publication, 4th Central European Training Scholl on Neutron Scattering 23-27 April 2007., 30 p.

13.	J. K. P lfalvi, Yu. Akatov, J. Szab—L. Saj—Bohus and I. E d gh. Detection of Primary and Secondary Cosmic Ray Particles Aboard the ISS Using SSNTD Stacks, Rad. Prot. Dos. V. 120, pp. 427-432, 2006.

14.	Alsecz, J. Os n, J. P lfalvi, V. Groma, S. T th and G. Falkenberg. Study of the oxidation state of arsenic and uranium in individual particles from uranium mine tailings, Hungary. Accepted. Proceedings of the 11th International Conference on Environmental Remediation and Radioactive Waste Management, September 2-6, 2007, Oud Sint-Jan Hospital Conference Center, Bruges, Belgium. Proceeding No.: ICEM07-7354.

15.	P lfalvi, J., Szab—J. s Dud s B. AEKI: exobiológiai programokban. Műszaki Szemle, 50/3, 38-39, 2007.

16. Szab—Julianna, Dud s Be ta □3 P lfalvi J—zef: Az Űrállomás Fantomja. Kozmikus sugárzás mérése űrséta közben. Természet Világa, 138/7, 323-325, 2007.

17. Szab—J., P lfalvi, J. □3 Dud s B. Az AEKI kozmikus sugárzás vizsgálatai a Nemzetözi Űrállomáson. Műszaki Szemle, 50/11, 45-47, 2007.

18. J. K. P lfalvi, J. Szab—B. Dud s. Neutron Detection on the Foton-M2 Satellite by a Track Etch Detector Stack. Rad. Prot. Dos. V. 126. No. 1-4, pp. 590-594, 2007.

19. M. Hajek, T. Berger, N. Vana, M. Fugger , J. K. P lfalvi, J. Szab— J. E□d□th, Y.A. Akatov, V. V. Arkhangelsky, V. A. Shurshakov. Convolution of TLD and SSNTD measurements during the BRADOS-1 experiments onboard ISS (2001). Rad. Meas. V 43, pp. 1231-1236, 2008.

20. J. K. P lfalvi, J. Szab—B. Dud s, I. Feh□ and I. E□d□th. Cosmic Ray Detection on the Foton-M2 Satellite by a Track Etch Detector Stack. Advances in Space Research. V 42, pp. 1030-1036, 2008.

21. S. Miljanic, M. Ranogajec-Komor, S. Blagus, J. K. Palfalvi, T. Pazmandi, S. Deme, and P. Szanto. Response of Radiophotoluminescent Dosimeters to Neutrons. Rad. Meas. V. 43. pp. 1068-1071, 2008.

22. J. Szab—J.K. P lfalvi, B. Dud s, Yu. Akatov, I. E□d□th. Cosmic ray detection on the ISS by a 3 axes track etch detector stack and the complementary calibration studies. Rad. Meas. V. 43, pp. 688-693, 2008.

23. Feh□, I. and P lfalvi, J. K., Depth Dose Distribution Measurements on the Foton-M2 Bio-satellite by TLD Technique. Advances in Space Research. 42, pp. 1037-1042, 2008.

24. Dudás Beáta, Szabó Julianna, Pálfalvi József. Passzív Űrdozimetria Magyar Részvétellel. Hiradastechnika, V. 63. pp. 30-34, 2008/4.

25. I. Sziklai-László, R. Szőke, I. Kovács, N. Adányi, D. Majchrzak, M. Á. Cser: Natural antioxidant vitamin and trace element intakes in healthy and asthmatic Hungarian adolescents. Metal Ions in Biology and Medicine, Vol. **9**, 485-489 (2006)

26. 2. J. Zsigrai, C. Tam Nguyen, I. Sziklai-L szl—Determination of the age of uranium-bearing items of arbitrary shape. Proc. Symp. Int. Safeguards: Addressing Verification Challenges. IAEA-CN-148/161P. IAEA, Vienna, 16-20, Oct. 2006.

27. R. Szőke, B. Alföldy, I. Sziklai-László, I. Balásházy, W. Hofmann: Size Distribution, Chemical Composition and Pulmonary Deposition of Hungarian Biosoluble Fibrous Glasses. Inhal. Toxicol. **19**, 325-332 (2007)

28. L. Pusztai, R.L. McGreevy*; On the structure of simple molecular liquids $SbCl_5$ and WCl_6; *J. Chem. Phys.*; **125,** 044508/1-7, 2006

29. P. J—vri, L. Pusztai; Structural changes in liquid selenium with increasing temperature; *J. Mol. Liq.*; **129,** 115-119, 2006

30. I. Hars nyi, L. Pusztai, J.-C. Soetens*, Ph. A. Bopp*; Molecular dynamics simulations of aqueous RbBr-solutions over the entire solubility range at room temperature; *J. Mol. Liq.*; **129,** 80-85, 2006

31. K. Saksl*, P. J—vri, H. Franz*, Q.S. Zeng*, J. F. Liu*, J.Z. Jiang*; Atomic structure of $Al_{89}La_6Ni_5$ metallic glass; *J. Phys.: Condens. Matter*; **18** 7579-7592, 2006

32. I. Kaban*, P. J—vri, W. Hoyer*, R.G. Delaplane*, A. Wannberg*; Structural studies on Te-rich Ge-Te melts; *J. Phys.: Condens. Matter*; **18** 2749-2760, 2006

33. U. Hoppe*, R.K. Brow*, B. C. Tischendorf*, P.J—vri, A.C. Hannon*; Structure of GeO_2-P_2O_5 glasses studied by x-ray and neutron diffraction**;** *J. Phys.: Condens. Matter*; **18** 1847-1860, 2006

34. Z. Somogyv ri*, E. Sv b, K. Krezhov*, L.F.Kiss, D. Kapt s, I. Vincze, E. Beregi, F. Bour e*; Non-collinear magnetic order in a Sc-substituted barium- hexaferrite; *J Magn Magn Mat.*; **304**, e775-e777, 2006

35. M. Fábián, E. Sváb, Gy. Mészáros, L. Kőszegi, L. Temleitner, E. Veress*; Structure study of borosilicate matrix glasses; *Zeitschrift fr Kristallographie;* **Suppl.23**, 461-466, 2006

36.   D. Kapt s, E. Sv b, Z. Somogyv ri*, G. Andre*, L.F. Kiss, J. Balogh, L. Bujdos—T. Kem hy, I. Vincze; Incommensurate antiferromagnetism in FeAl$_2$: Magnetic, M sbauer, and neutron diffraction measurements, *Phys. Rev.;* **B73**, 012401, 2006

37.   J—vri P, Saksl* K, Pryds* N, Lebech* B, Bailey* NP, Mellerg rd* A, Delaplane* RG, Franz* H; Atomic structure of glassy $Mg_{60}Cu_{30}Y_{10}$ investigated with EXAFS, x-ray and neutron diffraction, and reverse Monte Carlo simulations; *Phys. Rev. B;* **76,** 054208/1-8, 2007

38.   Hars nyi I, J—vri P, M z ros Gy, Pusztai L, Bopp* PA; Neutron and X-ray diffraction studies of aqueous rubidium bromide solutions; *J. Mol. Liq*; **131-132**, 60-64, 2007

39.   Arai* T, Pusztai L, McGreevy* RL; Polyanions in molten KPba   paradox explained?; *J. Phys: Condens. Matter;* **19**, 335202/1-10, 2007

40.   Temleitner L, Pusztai L; Orientational correlations in liquid, supercritical and gaseous carbon dioxide; *J. Phys: Condens. Matter;* **19**, 335203/1-12, 2007

41.   Pothoczki Sz, Pusztai L, Kohara* S; The structure of liquid iodomethane, CH_3I/CD_3I; *J. Phys: Condens. Matter;* **19**, 335204/1-9, 2007

42.   Gabrys* BJ, Pusztai L, Pettifor* DG; On the structure of liquid phosphorous tribromide (PBr_3); *J. Phys: Condens Matter;* **19**, 335205/1-10, 2007

43.   Temleitner L, Pusztai L, Schweika* W; The structure of liquid water by polarized neutron diffraction and reverse Monte Carlo modelling; *J. Phys: Condens. Matter;* **19**, 335207/1-12, 2007

44.   Hars nyi I, Pusztai L; Hydration of ions in aqueous RbCl solutions; *J. Phys: Condens. Matter;* **19**, 335208/1-12, 2007

45.   Gereben* O, Pusztai L, McGreevy* RL; Development of the time-dependent reverse Monte Carlo simulation, RMC*t*; *J. Phys: Condens. Matter;* **19**, 335223/1-22, 2007

46.   F bi n M, J—vri P, Sv b E, M z ros Gy, Proffen* Th, Veress* E; Network structure of 0.7SiO$_2$-0.3Na$_2$O glass from neutron and x-ray diffraction and RMC modelling, *J. Phys: Condens. Matter;* **19**, 335209/1-11, 2007

47.   J—vri P, Kaban* I, Steiner* J, Beuneu* B, Sch ps* A, Webb* A, Wrong bonds in sputtered amorphous $Ge_2Sb_2Te_5$; *J. Phys: Condens. Matter;* **19,** 335212/1-9, 2007

48.   Gruner* S, Kaban* I, J—vri P, Kehr* M, Hoyer* W, Delaplane* RG, Popescu* M; Atomic structure of $As_{25}Si_{40}Te_{35}$ glass; *J. Phys: Condens. Matter;* **19**, 335210/1-9 , 2007

49.   K.13. Gereben* O, J—vri P, Temleitner L, Pusztai L; A new version of the RMC++ Reverse Monte Carlo programme, aimed at investigating the structure of covalent glasses; *J. Optoel. Advanced Mater.*; **9**, 3021-3027, 2007

50.   F bi n M, Sv b E, M z ros Gy, R vay* Zs, Proffen* Th, Veress* E; Network structure of multi-component sodium borosilicate glasses by neutron diffraction; *J. Non-Cryst. Solids*; **353,** 1941-1945, 2007

51.   F bi n M, Sv b E, M z ros Gy, R vay* Zs, Veress* E; Neutron diffraction study of sodium borosilicate waste glasses containing uranium; *J. Non-Cryst. Solids*; **353,** 2084-2089, 2007

52.   Petkova* T, Petkov* P, J—vri P, Kaban* I, Hoyer* W, Sch ps* A, Webb* A, Beuneu* B; Structural studies on AsSe-A gI glasses; *J. Non-Cryst. Solids*; **353,** 2045-2051, 2007

53.   Kaban* I, Hoyer* W, Il inskii* A, Shpak* A, J—vri P; Temperature-dependent structural changes in liquid $Ge_{15}Te_{85}$; *J. Non-Cryst. Solids*; **353** 1808-1812, 2007

54.   Hoppe* U, Brow* RK, Tischendorf* BC, Kriltz* A, J—vri P, Sch ps* A, Hannon* AC; Structure of titanophosphate glasses studied by X-ray and neutron diffraction; *J. Non-Cryst. Solids*; **353** 1802-1807, 2007

55.   Kaban* I, J—vri P, Hoyer* W, Welter* E; Determination of partial pair distribution functions in amorphous $Ge_{15}Te_{85}$ by simultaneous RMC simulation of diffraction and EXAFS data; *J. Non-Cryst. Solids*; **353,** 2474-2478, 2007

56.   Kaban* I, Gruner* S, Hoyer* W, J—vri P, Delaplane* RG, Wannberg* A; Experimental and RMC simulation study of liquid Cu_6Sn_5; *J. Non-Cryst. Solids*; **353**, 3027-3031, 2007

57.   Sv b E, F bi n M, Veress* E, Proffen* Th; Short- and intermediate range order in borosilicate waste glasses; *Acta Cryst*.; **A63**, s58-5, 2007

58.   Voinov, A.V., S.M. Grimes, U. Agvaanluvsan, E. Algin, T. Belgya, C.R. Brune, M. Guttormsen, M.J. Hornish, T. Massey, G.E. Mitchell, J. Rekstad, A. Schiller, and S. Siem, *Level density of Fe-56 and low-energy enhancement of gamma-strength function*. Phys. Rev. C, (74), (2006) p. 014314.

59.   Szentmikl—ś, L., Z. R☐vay, R. Chobola, P. Mell, S. Szak cs, and I. K sa, *Characterization of CaSO4-based dosimeter materials with PGAA and thermoluminescent methods*. Journal of Radioanalytical and Nuclear Chemistry, **267**(2), (2006) p. 415-420.

60.   Szentmikl—ś, L., Z. R☐vay, and T. Belgya, Measurement of partial gamma-ray production cross-sections and k0 factors for radionuclides with chopped-beam PGAA. Nucl. Instr. and Methods A, **564**, (2006) p. 655-661.

61.   Rogante, M., F. Milazzo, and Z. Kasztovszky, Comparative analysis of Iron Age bronze archaeological objects from a Picenum necropolis of Centre Italy with Prompt Gamma Activation Analysis. Il Nuovo Cimento, (2006) p.

62.   R☐vay, Z., T. Belgya, G.L. Moln r, H. Rausch, and T. Braun, *The analysis Of C-60 and C-70 fullerenes by prompt gamma neutron activation*. Chemical Physics Letters, **423**(4-6), (2006) p. 450-453.

63.   R☐vay, Z., Calculation of uncertainties in prompt gamma activation *analysis*. Nuclear Instruments & Methods in Physics Research Section a- Accelerators Spectrometers Detectors and Associated Equipment, **A 564**(4-6), (2006) p. 688-697.

64.   Marschall, H.R., R. Altherr, T. Ludwig, A. Kalt, K. Gm☐ling, and Z. Kasztovszky, *Partitioning and budget of Li, Be and B in high-pressure metamorphic rocks*. Geochimica et Cosmochimica Acta, **70**(18), (2006) p. 4750-4769.

65.   Kasztovszky, Z., D. Visser, W. Kockelmann, E. Pantos, A. Brown, M. Blaauw, P. Hallebeek, J. Veerkamp, W. Krook, and H.M. Stuchfield, *Combined Prompt Gamma Activation And Neutron Diffraction Analyses Of Historic Metal Objects And Limestone Samples*. Il Nuovo Cimento, (2006) p.

66.   Kasztovszky, Z. and T. Belgya, *From PGAA to PGAI: from bulk analysis to elemental mapping*. Archeometriai Műhely, **III**(2), (2006) p. 16-21.

67.   Kasztovszky, Z. and T. Belgya, Non-Destructive Investigations of Cultural Heritage Objects with Guided Neutrons. Archeometriai Műhely, **III**(1), (2006) p. 12-17.

68.   Kasztovszky, Z. and T. Belgya, A kultur lis ☐☐ks☐g t rgyi eml☐keinek roncsol smentes vizsg lata neutronnyal bbal: az Ancient Charm projekt. Term☐szet Vil ga, **137.**(10.), (2006) p. 452-454.

69.   Hillers, M., R. Altherr, T. Ludwig, H.P. Meyer, H.R. Marschall, Z. Kasztovszky, and K. Gm☐ling, *Lithium, beryllium and boron in I-type granitoids from the Aegean Sea, Greece*. Geochimica et Cosmochimica Acta, (2006) p. accepted.

70.   Belgya, T., Improved accuracy of gamma-ray intensities from basic principles for the calibration reaction 14N(n,g)15N. Physical Review C, **74**, (2006) p. 024603-1-8.

71.   Bal zsi, C., F. W☐ber, Z. K☐v☐r, Z. Shen, Z. K—nya, Z. Kasztovszky, Z. V☐rtesy, L.P. Bir—, J. Kiricsi, and P. Arat—, *Application of carbon nanotubes to silicon nitride matrix reinforcements*. Current Applied Physics, **6**(2), (2006) p. 124-130.

72.   Assuncao, M., M. Fey, A. Lefebvre-Schuhl, J. Kiener, V. Tatischeff, J.W. Hammer, C. Beck, C. Boukari-Pelissie, A. Coc, J.J. Correia, S. Courtin, F. Fleurot, E. Galanopoulos, C. Grama, F. Haas, F. Hammache, F. Hannachi, S. Harissopulos, A. Korichi, R. Kuntz, D. LeDu, A. Lopez-Martens, D. Malcherek, R. Meunier, T. Paradellis, M. Rousseau, N. Rowley, G. Staudt, S. Szilner, J.P. Thibaud, and J.L. Weil, *E1 and E2 S factors of C-12(alpha,gamma(0))O-16 from gamma-ray angular distributions with a 4 pi-detector array*. Physical Review C, **73**(5), (2006) p.

73.   Teschner, D., Z. Révay, J. Borsodi, M. Hävecker, A. Knop-Gericke, R. Schlögl, D. Milroy, D.S. Jackson, D. Torres, and P. Sautet, *Understanding Palladium Hydrogenation Catalysts: When the Nature of the Reactive Molecule Controls the Nature of the Catalyst Active Phase*. Angewandte Chemie, **47**, (2008) p. 1-6.

74.   Teschner, D., J. Borsodi, A. Wootsch, Z. Revay, M. Havecker, A. Knop-Gericke, S.D. Jackson, and R. Schlogl, *The roles of subsurface carbon and hydrogen in palladium-catalyzed alkyne hydrogenation*. Science, **320**(5872), (2008) p. 86-89.

75.   Szentmiklósi, L., Z. Révay, T. Belgya, A. Simonits, and Z. Kis, *Combining prompt gamma activation analysis and off-line counting*. J. Nucl. Radioanal. Chem., **278**(3), (2008) p. 657-660.

76.   Szentmiklósi, L., Z. Kis, T. Belgya, Z. Kasztovszky, P. Kudejova, T. Materna, and R. Schulze, A new PGAI-NT setup and elemental imaging experiments at the Budapest Research Reactor, in NRC7 - SEVENTH INTERNATIONAL CONFERENCE ON NUCLEAR AND RADIOCHEMISTRY: Budapest, Hungary 24-29 August 2008, (2008) p. 1-5.

77.   Revay, Z., T. Belgya, L. Szentmiklosi, Z. Kis, A. Wootsch, D. Teschner, M. Swoboda, R. Schlogl, J. Borsodi, and R. Zepernick, *In situ determination of hydrogen inside a catalytic reactor using prompt gamma activation analysis*. Analytical Chemistry, **80**(15), (2008) p. 6066-6071.

78.   Révay, Z., T. Belgya, L. Szentmiklosi, and Z. Kis, *Recent developments and applications at the prompt gamma activation analysis facility at Budapest*. J. Nucl. Radioanal. Chem., **278**(3), (2008) p. 643-646.

79.   Revay, Z., *Prompt gamma activation analysis of samples in thick containers*. Journal of Radioanalytical and Nuclear Chemistry, **276**(3), (2008) p. 825-830.

80.   Perry, D.L., G.A. English, R.B. Firestone, K.N. Leung, G. Garabedian, G.L. Molnar, and Z. Revay, *Analyses of oxyanion materials by prompt gamma activation analysis*. Journal of Radioanalytical and Nuclear Chemistry, **276**(1), (2008) p. 273-277.

81.   Pelletier, L., O. Müntener, A. Kalt, T.W. Vennemann, and T. Belgya, Emplacement of ultramafic rocks into the continental crust monitored by light and other trace elements: An example from the Geisspfad body (Swiss-Italian Alps). Chem. Geology, **255**, (2008) p. 143-159.

82.   Pamukchieva, V., A. Szekeres, E. Svab, M. Fabian, Z. Revay, and L. Szentmiklosi, Spectroscopic ellipsometric determination of the optical constants of chalcogenide films of the Ge-Sb-S-Te system, in Fifteenth International Summer School on Vacuum, Electron and Ion Technologies. IOP Publishing, (2008) p. 012054.

83.   Németh, K., Pécskay, Z., U. Martin, K. Gméling, F. Molnár, and S. Cronin, Hyaloclastites, peperites and soft-sediment deformation textures of a shallow subaqueous Miocene rhyolitic dome-cryptodome complex, Pálháza, Hungary. In: Structure and Emplacement of High-Level Magmatic Systems N. Journal of Geological Society, **302**, (2008) p. 63-86.

84.   Manescu, A., F. Fiori, A. Giuliani, N. Kardjilov, Z. Kasztovszky, F. Rustichelli, and B. Straumal, *Non-destructive compositional analysis of historic organ reed pipes*. Journal of Physics-Condensed Matter, **20**(10), (2008) p. 104250.

85.   Krticka, M., R.B. Firestone, D.P. McNabb, B. Sleaford, U. Agvaanluvsan, T. Belgya, and Z.S. Revay, *Thermal neutron capture cross sections of the palladium isotopes*. Physical Review C, **77**(5), (2008) p. 054615.

86.   Kovacs-Mezei, R., T. Krist, and Z. Revay, *Non-magnetic supermirrors produced at Mirrotron Ltd*. Nuclear Instruments & Methods in Physics Research Section a-Accelerators Spectrometers Detectors and Associated Equipment, **586**(1), (2008) p. 51-54.

87.   Kis, Z., T. Belgya, L. Szentmiklósi, Z. Kasztovszky, P. Kudejová, and R. Schulze, *Prompt Gamma Activation Imaging on 'black boxes' in the 'ANCIENT CHARM' project*, in *Archaeometriai Műhely*. HNM: Budapest, (2008) p. 41-60.

88.   Kasztovszky, Z., K. T. Biró, A. Markó, and V. Dobosi, Prompt gamma activation analysis for non-destructive characterization of chipped stone tools and raw materials. J. Nucl. Radioanal. Chem., **278**(2), (2008) p. 293-298.

89. Kasztovszky, Z., Z. Kis, T. Belgya, W. Kockelmann, S. Imberti, G. Festa, A. Filabozzi, C. Andreani, A. Kirfel, K. T. Biró, K. Dúzs, Z. Hajnal, P. Kudejova, and M. Tardocchi, *Prompt gamma activation analysis and time of flight neutron diffraction on 'black boxes' in the 'Ancient Charm' project*. J. Nucl. Radioanal. Chem., **278**(3), (2008) p. 661-664.

90. Kasztovszky, Z., K.T. Biro, A. Marko, and V. Dobosi, Cold neutron prompt gamma activation analysis - A non-destructive method for characterization of high silica content chipped stone tools and raw materials. Archaeometry, **50**, (2008) p. 12-29.

91. Firestone, R.B., M. Krticka, D.P. McNabb, B. Sleaford, U. Agvaanluvsan, T. Belgya, and Z. Revay. New methods for the determination of total radiative thermal neutron capture cross sections. in Compound-Nuclear Reactions and Related Topics, 22-26 Oct. 2007: AIP conf. Proc., (2008) p. 26-29.

92. English, G.A., R.B. Firestone, D.L. Perry, J.P. Reijonen, K.N. Leung, G.F. Garabedian, G.L. Molnar, and Z. Revay, Prompt gamma activation analysis (PGAA) and short-lived neutron activation analysis (NAA) applied to the characterization of legacy materials. Journal of Radioanalytical and Nuclear Chemistry, **277**(1), (2008) p. 25-29.

93. Canella, L., P. Kudejova, R. Schulze, N. Warr, A. Türler, J. Jolie, Z. Revay, and T. Belgya, First experiments at the new PGAA facility at the research reactor FRM II, in NRC7 - SEVENTH INTERNATIONAL CONFERENCE ON NUCLEAR AND RADIOCHEMISTRY: Budapest, Hungary 24-29 August 2008, (2008) p. 1-4.

94. Borella, A., T. Belgya, E. Berthoumieux, N. Colonna, C. Domingo-Pardo, J.C. Drohe, F. Gunsing, S. Marrone, T. Martinez, C. Massimi, P.M. Mastinu, P.M. Milazzo, P. Schillebeeckx, G. Tagliente, J. Tain, R. Terlizzi, and R. Wynants. *Measurements of the branching ratio of the 209Bi(n,g)210gBi/210mBi reactions at GELINA*. in *International Conference on Nuclear Data for Science and Technology*. Niza, France, 2007: EDP Sciences, (2008) p. 563-566.

95. Belgya, T., P. Schillebeeckx, and A. Plompen. *Thermal neutron capture cross section measurements using a cold neutron beam*. in *Neutron Measurements, Evaluations and Applications*. Prague, Czech Republic, 16-18 October 2007: European Communities, 2008, (2008) p. 31-34.

96. Belgya, T. and K. Lazar, *First experiments on a new in-beam Mossbauer spectroscopy station at the Budapest Research Reactor*. Journal of Radioanalytical and Nuclear Chemistry, **276**(1), (2008) p. 269-272.

97. Belgya, T., Z. Kis, L. Szentmiklósi, Z. Kasztovszky, P. Kudejova, R. Schulze, T. Materna, G. Festa, and P.A. Caroppi, *First elemental imaging experiments on a combined PGAI and NT setup at the Budapest Research Reactor*. J. Radioanal. Nucl. Chem., **278**(3), (2008) p. 751-754.

98. Belgya, T., Z. Kis, L. Szentmiklósi, Z. Kasztovszky, G. Festa, L. Andreanelli, M.P. De Pascale, A. Pietropaolo, P. Kudejova, R. Schulze, and T. Materna, *A new PGAI-NT setup at the NIPS facility of the Budapest Research Reactor*. J. Radioanal. Nucl. Chem., **278**(3), (2008) p. 713-718.

99. Belgya, T., O. Bouland, G. Noguere, A. Plompen, P. Schillebeeckx, and L. Szentmiklosi. *The thermal neutron capture cross section of 129I*. in *International Conference on Nuclear Data for Science and Technology*. Niza, France, 2007: EDP Siences, (2008) p. 631-634.

100. Belgya, T., New gamma-ray intensities for the N-14(n,gamma)N-15 high energy standard and its influence on PGAA and on nuclear quantities. Journal of Radioanalytical and Nuclear Chemistry, **276**(3), (2008) p. 609-614.

101. Szentmiklosi, L., Z. Revay, and T. Belgya, *An improved beam chopper setup at the Budapest PGAA facility*. Nucl. Instr. and Methods B, **263**, (2007) p. 90-94.

102. Szentmiklósi, L., K. Gméling, and Z. Révay, *Fitting the boron peak and resolving interferences in the 450-490 keV region of PGAA spectra*. Journal of Radioanalytical and Nuclear Chemistry, **271**(2), (2007) p. 447-453.

103. Szentmiklósi, L., T. Belgya, G.L. Molnár, and Z. Révay, *Time resolved gamma-ray spectrometry*. Journal of Radioanalytical and Nuclear Chemistry, **271**(2), (2007) p. 439-445.

104. Rogante, M., G. De Marinis, Z. Kasztovszky, and F. Milazzo, Comparative analysis of iron age bronze archaeological objects from a picenum necropolis of centre Italy with Prompt Gamma Activation Analysis. Nuovo Cimento Della Societa Italiana Di Fisica C-Geophysics and Space Physics, **30**(1), (2007) p. 113-122.

105. Revay, Z., R.K. Harrison, E. Alvarez, S.R. Biegalski, and S. Landsberger, *Construction and characterization of the redesigned PGAA facility at The University of Texas at Austin*. Nuclear Instruments & Methods in Physics Research Section a-Accelerators Spectrometers Detectors and Associated Equipment, **577**(3), (2007) p. 611-618.

106. Revay, Z., Comparison of the analytical sensitivities for non-1/v elements in different neutron beams. Nucl. Instrum. & Methods B, **263**, (2007) p. 79-84.

107. Kasztovszky, Z., D. Visser, W. Kockelmann, E. Pantos, A. Brown, M. Blaauw, P. Hallebeek, J. Veerkamp, W. Krook, and H.M. Stuchfield, *Combined prompt gamma activation and neutron diffraction analyses of historic metal objects and limestone samples*. Nuovo Cimento Della Societa Italiana Di Fisica C-Geophysics and Space Physics, **30**(1), (2007) p. 67-78.

108. Kasztovszky, Z., Application of prompt gamma activation analysis to investigate archaeological ceramics. Archeometriai Műhely, **II**, (2007) p. 49-54.

109. Harangi, S., H. Downes, M. Thirlwall, and K. Gméling, Geochemistry, Petrogenesis and Geodynamic Relationships of Miocene Calc-alkaline Volcanic Rocks in the Western Carpathian Arc, Eastern Central Europe. Journal of Petrology, **48**(12), (2007) p. 2261-2287.

110. Harangi, S., H. Dowmes, M. Thirlwall, and K. Gmeling, Geochemistry, petrogenesis and geodynamic relationship of Miocene calc-alkaline volcanic rocks in the Western Carpathian Arc, Eastern Central Europe. J. Petrology, **48**(12), (2007) p. 2261-2287.

111. Gmeling, K., K. Nemeth, U. Martin, N. Eby, and Z. Varga, *Boron concentrations of volcanic fields in different geotectonic settings*. Journal of Volcanology and Geothermal Research, **159**(1-3), (2007) p. 70-84.

112. Gmeling, K., Z. Kasztovszky, L. Szentmiklosi, Z. Revay, and S. Harangi, Boron concentration measurements by prompt gamma activation analysis: Application on miocene-quaternary volcanics of the Carpathian-Pannonian Region. Journal of Radioanalytical and Nuclear Chemistry, **271**(2), (2007) p. 397-403.

113. Gmeling, K., S. Harangi, Z. Kasztovszky, Z. Pecskay, A. Simonits, and Vc, *Inferences for the style of subduction in the Carpathian-Pannonian region based on boron signatures*. Geochimica Et Cosmochimica Acta, **71**(15), (2007) p. A331-A331.

114. Gméling, K., S. Harangi, and Z. Kasztovszky, A bór geokémiai szerepe szubdukciós zónákban (A bór geokémiai változékonysága a Kárpát-Pannon térségben. Földtani Közlöny, **137**(4), (2007) p. 557-580.

115. Firestone, R.B., A. Westc, J.P. Kennettd, L. Beckere, T.E. Bunchf, Z.S. Revayg, P.H. Schultzh, T. Belgya, D.J. Kennetti, J.M. Erlandsoni, O.J. Dickensonj, A.C. Goodyeark, R.S. Harrish, G.A. Howardl, J.B. Kloostermanm, P. Lechlern, P.A. Mayewskio, J. Montgomeryj, R. Poredap, T. Darrahp, S.S. Que Heeq, A.R. Smitha, A. Stichr, W. Toppings, J.H. Wittkef, and W.S. Wolbachr, *Evidence for an extraterrestrial impact 12,900 years ago that contributed to the megafaunal extinctions and the Younger Dryas cooling*. PNAS, **104**(41), (2007) p. 16016-16021.

116. Fabian, M., E. Svab, G. Meszaros, Z. Revay, and E. Veress, *Neutron diffraction study of sodium borosilicate waste glasses containing uranium*. Journal of Non-Crystalline Solids, **353**(18-21), (2007) p. 1941-1945.

117. Fabian, M., E. Svab, G. Meszaros, Z. Revay, T. Proffen, and E. Veress, *Network structure of multicomponent sodium borosilicate glasses by neutron diffraction*. Journal of Non-Crystalline Solids, **353**(18-21), (2007) p. 2084-2089.

118. Algin, E., A. Schiller, A. Voinov, U. Agvaanluvsan, T. Belgya, L.A. Bernstein, C.R. Brune, R. Chankova, P.E. Garrett, S.M. Grimes, M. Guttormsen, M. Hjorth-Jensen, M.J. Hornish, C.W. Johnson, T. Massey, G.E. Mitchell, J. Rekstad, S. Siem, W. Younes, and Pc, *Bulk properties of iron isotopes*. Physics of Atomic Nuclei, **70**(9), (2007) p. 1634-1639.

119. Aksenov* VL, Avdeev* MV, Tropin* TV, Korobov* MV, Kozhemyakina* NV, Avramenko* NV, Rosta L; Formation of fullerene clusters in the system C60/NMP/water by SANS; *Physica B;* **385-386** (2006) 795-797

120. Alm sy L, Len A, Mark—M, R□falvi E; The effective wavelength in SANS experiment using mechanical velocity selector; *Zeitschrift fr Kristallographie;* **S23**, 211-216, 2006

121. Avdeev* MV, Aksenov* VL, Balasoiu* M, Garamus* VM, Schreyer* A, T□□k Gy, Rosta L, Bica* D, V□k s* L; Comparative analysis of the structure of sterically stabilized ferrofluids on polar carriers by small-angle neutron scattering; *Journal of Colloid and Interface Science*; **295**, 100-107, 2006

122. Avdeev* MV, Tropin* TV, Aksenov* VL, Rosta L, Garamus* VM, Rozhkova* NN; Pore structures in shungites as revealed by small-angle neutron scattering; *Carbon* **44** (2006) 954-961

123. Cser L, Krexner* G, Mark—M, Prem* M, Sharkov* I, T□□k Gy; Atomic resolution neutron holography (Present status and future prospects); *Physica B;* **385-386**, 1197-1199, 2006

124. Cser L, Krexner* G, Mark—M, Sharkov* I, T□□k Gy; Instrumental distortion effects in atomic resolution neutron holography; *Physica B;* **385-386**, 1200-1202, 2006

125. Cser L, T□□k Gy, Krexner* G, Mark—M, Sharkov* I; Direct observation of local distortion of crystal lattice with picometer accuracy using atomic resolution neutron holography; *Phys Rev Lett;* **97**, 255501/1-4, 2006

126. Füzi J; Dynamic vector hysteresis modeling; *Physica B;* **372**, 396-400, 2006

127. Füzi J; Analytical hysteresis model; *Physica B;* **372**, 393-395, 2006

128. Füzi J; Magnetic characteristics of dipole clusters; *Physica B;* **372**, 239-242, 2006

129. Füzi J; Neutron beam phase space mapping; *Physica B;* **385-386**, 1253-1255, 2006

130. Füzi J, Dávid* E, Kozlowski* T, Lewis* P, Messing* G, Mezei* F, Penttila* S, Rosta L, Russina* M, T□□k Gy; Neutron optical imaging study of neutron moderator and beam extraction system; *Physica B; Physica B;* **385-386**, 1315-1317, 2006

131. Knaapila* M, Alm sy L, Garamus* VM, Pearson* C, Pradhan* S, Petty* MC, Scherf* U, Burrows* HD, Monkman* AP; Solubilization of polyelectrolytic hairy-rod polyfluorene in aqueous solutions of nonionic surfactant; *J Phys Chem B;* **110**, 10248-10257, 2006

132. Knaapila* M, Garamus* VM, Dias* FB, Alm sy L, Galbrecht* F, Charas* A, Morgado* J, Burrows* HD, Scherf* U, Monkman* AP; Influence of solvent quality on the self-organization of archetypical hairy-rods - branched and linear side chain polyfluorenes: Rigid rods versus "beta sheets" in solution; *Macromolecules;* **39**, 6505-6512, 2006

133. Krakovsky* □□ O P i V□/ □□3 O H W O J; Structure and swelling behaviour of hydrophilic epoxy networks investigated by SANS; *Polymer;* **47**, 218-226, 2006

134. Lebedev* VT, T□□k Gy; Effect of anomalous particles diffusion damping in ferrofluid near Curie temperature; *Romanian Reports in Physics;* **58**, 249-254, 2006

135. Lebedev* VT, T□□k Gy, Nazarova* OV, Panarin* EF, Orlova* DN, Pavlov* GM; Hierarchy of structural organization of fullerene-containing polyvinylformamide in solutions; *Fullerenes, Nanotubes and Carbon Nanostructures;* **14** (2-3), 321-326, 2006

136. Perera* A, Sokolić* F, Alm sy L, Koga* Y; Kirkwood-Buff integrals of aqueous alcohol binary mixtures; *J of Chemical Physics;* **124**, 124515/1-9, 2006

137. Peters* J, Bleif* HJ, K li Gy, Rosta L, Mezei* F; Performance of TOF powder diffractometers on reactor sources; *Physica B;* **385-386**, 1019-1021, 2006

138. Rogante* M, Lebedev* VT, Kralj* S, Rosta L, T□□k Gy; Neutron techniques for welding project methods development in nuclear/traditional industrial application; *Multidiscipline Modeling in Materials and Structures;* **2**, 419-433, 2006

139. Rosta L, Füzi J, Hom nyi* L; Benchmark testing of a multiblade neutron velocity selector; *Physica B;* **385-386**, 1283-1286, 2006

140. Schmiedel* H, Alm sy L, Klose* G; Multilamellarity, structure and hydration of extruded POPC vesicles by SANS; *European Biophysics Journal with Biophysics Letters;* **35**, 181-189, 2006

141. T k Gy, Lebedev* VT, Bica* D, V k s* L, Avdeev* MV; Concetration and temperature effect in microstructure of ferrofluids; *Journal of Magnetism and Magnetic Materials;* **300**, e221-e224, 2006

142. T k Gy, Lebedev* VT, Bica* D, V k s* L, Avdeev* MV; Concetration and temperature effect in microstructure of ferrofluids; *Romanian Reports in Physics;* **58**, 279-285, 2006

143. T k Gy, Len A, Rosta L, Balasoiu* M, Avdeev* MV, Aksenov* VL, Ghenescu* I, Hasegan* D, Bica* D, V k s* L; Interaction effects in non-polar and polar ferrofluids by small-angle neutron scattering; *Romanian Reports in Physics,* **58**, 255-261, 2006

144. Zamponi* M, Wischnewski* A, Monkenbusch* M, Willner* L, Richter* D, Likhtman* AE, Kali G, Farago* B; Molecular observation of constraint release in polymer melts; *Phys Rev Letters;* **96**, 238302/1-4, 2006

145. Trounov* VA, Sokolov* AE, Lebedev* VT, Smirnov* OP, Kurbakov* AI, Van den Heuvel* J, Batyrev* E, Yuryeva* TM, Plyasova* IM, T k Gy; Detection of Hydrogen-copper clustering in Zn_1Cu_xO compounds using neutron scattering methods; *Physics of the Solid State*; **48**, 1291-1297, 2006

146. Zemlyanaya* EV, Kiselev* MA, Zbytovska* J, Alm sy L, Aswal* VK, Strunz* P, Wartewig* S, Neubert* RHH: Numerical analyses of the structure of unilamellar vesicles based on small angle scattering data; *Crystallography Reports;* **51**, S1, 22-26, 2006

147. Len A; A kisszögű neutronszórás archeometriai alkalmazási lehetőségei; *Archeometriai Műhely* - elektronikus foly—rat, Magyar Nemzeti Mz eum*; Possible Applications of Small Angle Neutron Scattering in Archaeometry; *Archaeometry Workshop* - e-journal published by the Hungarian National Museum; (www.ace.hu/am/index.html); **2006/2**, 27-31, 2006

148. Sánta Zs; Nagyfelbontású repülési idő diffraktométer a Budapesti Neutron Központban; *Archeometriai Műhely* - elektronikus foly—rat, Magyar Nemzeti Mz eum*; High Resolution Time of Flight Diffractometer at the Budapest Neutron Centre; *Archaeometry Workshop* - e-journal published by the Hungarian National Museum; (www.ace.hu/am/ index.html); **2006/2**, 22-26, 2006

149. Aksenov* VL, Avdeev* MV, Kyzyma* OA, Rosta L, Korobov* MV; Age effect of solution C_{60}/N-methilpyrrolidone on the cluster structure in the system C_{60}/N-methilpyrrolidone/water; *Crystallography reports* **52** (2007) 523-527

150. Alm sy L, Len A, Sz kely NK, Plestil* J; Solute aggregation in dilute aqueous solutions of tetramethylurea; *Fluid Phase Equilibria,* **257** (2007) 114-119

151. Avdeev* MV, Aksenov* VL, Rosta L; Pressure induced changes in fractal structure of detonation nanodiamond powder by small-angle neutron scattering; *Diamond Related Mater* **16** (2007) 2050-2053

152. Avdeev* MV, Bica* D, V k s* L, Marinica* O, Balasoiu* M, Aksenov* VL, Rosta L, Garamus* VM, Schreyer* A; On the possibility of using short chain length mono-carboxylic acids for stabilization of magnetic fluids; *J Magn Magn Mater* **311** (2007) 6-9

153. Ficker* T, Len A, Chmelk* R, Lovicar* L, Martisek* D, Nemec* P; Fracture surfaces of porous materials; *EPL* **80** (2007) 16002; www.epljournal.org; doi: 10.1209/0295-5075/80/16002

154. Ficker* T, Len A, Nemec* P; Notes on hydrated cement fractals investigated by SANS, *J Phys D: Appl Phys* **40** (2007) 4055.4059

155. Khokhryakov* AO, Avdeev* MV, Kyzyma* OA, Len A, Bulavin* LA, Aksenov* VL; Colloidal structure and nature of stabilization of nonmodified fullerene water solutions; *Crystallography reports* **52** (2007) 532-537

156. Khokhryakov* AO, Kyzyma* OA, Bulavin* LA, Len A, Avdeev* MV, Aksenov* VL; Colloidal structure and nature of stabilization of nonmodified fullerene water solutions; *Crystallography reports* **52** (2007) 487-491

157.   Kulvelis* YM, Lebedev* VT, Török Gy, Klyubin* VV; Complexes of Poly-N-Vynilpirrolidone with Sulfonated Tetraphenylporphyrins (in Russian); *Kristallographya* **52** no3 (2007) 492-495

158.   Kulvelis* YM, Lebedev* VT, Török Gy, Klyubin* VV; Complexes of Poly-N-Vynilpirrolidone with Sulfonated Tetraphenylporphyrins; *Crystallography Reports* **52** no3 (2007) 515-518

159.   Kulvelis YV, Lebedev VT, Török Gy, Melnikov AB; Structure of the water salt solutions of DNA with sulfonated scandium diphthalocyanine; *Journal of Structural Chemistry* **48** no 4 (2007) 740-746

160.   Lebedev* VT, Vinogradova* LV, Török Gy; Structural Features of Star Shaped Fullerene (C60) Containing Polystyrenes: Neutron Scattering Experiments, *Polymer Science Ser A* **50**, (10) (2007) 1090-1097

161.   Székely NK, Rosta L; Determination of Coherently Forward Scattered Intensity from SANS Measurements of Binary Liquids Mixtures Without Resorting to Structural Models; *J. Optoelectronics and Advanced Materials,* **9** (2007) 544-546

162.   Székely NK, Almásy L, Jancsó* G; Small-angle neutron scattering and volumetric studies of dilute solutions of N,N'–dimethylethyleneurea in heavy water; *Journal of Molecular Liquids* **136** (2007) 184-189

163.   Székely NK, Almásy L, Rădulescu* A, Rosta L; SANS Study of Aqueous Solutions of Pentanediol and Hexanediol; *J Appl Cryst.,* **40** (2007) s307-s311

164.   Trounov* VA, Lebedev* VT, Grushko* YS, Sokolov* AE, Ivanova* II, Rybakov* VB, Yuryeva* TM, Ivanchev* SS, Török Gy; Some Capabilities of Neutron Methods in the Investigation of Materials and Components of Equipments in Hydrogen Power Engineering (in Russian); *Kristallographya* **52** no3 (2007) 536-544

165.   Trounov* VA, Lebedev* VT, Grushko* YS, Sokolov* AE, Ivanova* II, Rybakov* VB, Yuryeva* TM, Ivanchev* SS, Török Gy; Some Capabilities of Neutron Methods in the Investigation of Materials and Components of Equipments in Hydrogen Power Engineering; *Crystallography Reports* **52** no3 (2007) 512-520

166.   Trounov* VA, Lebedev* VT, Sokolov* AE, Grushko* YS, Török Gy, Van den Heuvel* J, Batyrev* E, Yuryeva* TM, Plyasova* LM; Investigation of Hydrogen Capacity of Composites Based on ZnOCu (in Russian); *Kristallographya* **52** no3 (2007) 496-500

167.   Trounov* VA, Lebedev* VT, Sokolov* AE, Grushko* YS, Török Gy, van den Heuvel* C, Batyrev* E, Yuryeva* TM, Plyasova* LM; Investigation of Hydrogen Capacity of Composites Based on ZnOCu; *Crystallography Reports* **52** no3 (2007) 474-478

Conference Proceedings

1.   K. Krezhov*, D. Tzankov*, D. Kovacheva*, R. Puzniak*, A. Wisniewski*, E. Svab and M. Mikhov*; Bismuth substitution for rare earth and charge/orbital ordering related structural effects in some half hole-doped manganites, General Conf. of the Balkan Physics Union (BPU-6), August 21-26, 2006, Istambul, invited

2.   M. Fábián, E. Veress*, Ioan Bratu*, E.Culea*, Emil Indrea*, E. Sváb; New borosilicate glasses developed as host media for actinides immobilization, Int. Conf.of the Chemical Societies of the South-East European Countries (ICOSECS 5 -), Ohrid-Macedonia, September 2006

3.   Ioan Bratu*, E. Indrea*, E.Culea*, M. Fábián, E. Veress*, E. Sváb; Structural characterization of and Ce^{3+}/Ce^{4+} redox equilibrium in simulated HLW borosilicate glasses, 5th Int. Conf. on Inorganic Materials, Ljubljana, September 22-26, 2006

4.   E. Beregi, I. Földvári, E. Sváb, Gy. Mészáros, P. Solarz*, G. Dominiak-Dzik*; Effect of Er^{3+} concentration on the structure and spectroscopic properties of Er:YAB crystals, 6th Int. Conf. on Crystal-physics, Chernogolovka, Russia, November, 21-24, 2006

5.   M. Fábián, E. Sváb, E. Veress* and Th. Proffen*; Structure study of multi-component borosilicate waste glasses from high Q neutron diffraction measurement and RMC modelling, 4th European Conference on Neutron Scattering, 25-29 June 2007, Lund, Sweden, Abstract Booklet p346

6. M. Fábián, E. Sváb, Th. Proffen*; Radioactive Waste stored in borosilicate glasses, International Atomic Agency Meeting, 17, May 2007, Budapest

7. D. Tzankov*, K. Krezhov, D. Kovacheva*, R. Puzniak*, A. Wiśniewski*, E. Sváb, F. Bourée*, M. Mikhov*; Magnetic and transport properties of Bi0.5Sr0.5FexMn1−xO3, AIP Conf. Proc. , ed American Inst of Physics, 899(1) (2007) 263-264

8. K. Krezhov*; Charge order and magnetoresistivity in a perovskite family of bismuth based manganites, IEEE Proceedings of 3rd Intern. Conf. on Recent Advances in Space Research Technologies, RAST2007, Istanbul, Turkey, June 14-17, 2007, invited, 6 pages

9. S. Kovachev*, D. Kovacheva*, S. Aleksovskac*, E. Svab, K. Krezhov*; Neutron and X-ray diffraction investigation of the solid solution system YCrO3 - YFeO3 with potential multiferroic properties, 6th PSI Summer School on Condensed Matter Research on Correlated Electron Materials, August 18-25, 2007, Zuoz, Switzerland (extended abstract) Oral and Poster Presentation

10. K. Krezhov*, S. Kovachev*, D. Kovacheva*, E. Svab, F. Bourée*, G. André*, M. Mikhov*; Effects of doping on the charge, orbital and spin ordering in a family of half hole doped bismuth manganites (Bi,RE)0.5(Ca,Sr)0.5FexMn1-xO3 (Re=La, Nd, Ho, Yb, Tm), NMI3 W-07-I_106, Workshop on"Neutron Scattering in Strongly Correlated Electron Systems" October 25 – 28, 2007, Physik Department E21, Technische Universitat München, Munich, Germany

11. V. Pamukchieva*, A. Szekeres*, E. Svab, M. Fabian and Zs. Revay; Spectral ellipsometric determination of the optical constants of multicompoment chalcogenide films of Ge-Sb-S-Te system, 16th International School on Vacuum, Electron and Ion Technologies (VEIT) 2007, 17-22 Sept., Sozopol, Bulgaria

12. Zöldföldi, J., S. Richter, Z. Kasztovszky, and J. Mihály, *Where does Lapis Lazuli come from?* Proceedings of 34th International Symposium on Archaeometry, (2006) p. 351-361.

13. Zöldföldi, J., F. Pintér, B. Székely, H. Taubald, K. T. Biró, Z. Mráv, M. Tóth, M. Satir, Z. Kasztovszky, and G. Szakmány. *Provenance Studies on Roman Marble Fragments in the Hungarian National Museum, Budapest,.* in *34th International Symposium on Archaeometry*. Zaragoza, (2006) p. 353-361.

14. Visser, D., Z. Kasztovszky, P. Hallebeek, and J. Veerkamp. *Comparative archaeometric study of Dutch antique lead-tin spoons from Amsterdam (1350-1775 AD) by prompt gamma activation analysis, neutron time of flight diffraction and X-ray fluorescence spectroscopy.* in *36th International Symposium on Archaeometry*. 2-6 May, 2006, Quebec City, Canada, (2006) p. poster.

15. Taubald, H., K. T. Biró, Z. Kasztovszky, and M. Balla. *Early Neolithic pottery and its environment in Hungary.* in *36th International Symposium on Archaeometry*. 2-6 May, 2006, Quebec City, Canada, (2006) p. poster.

16. T. Biró, K. and Z. Kasztovszky. *Further studies on grey flint samples.* in *36th International Symposium on Archaeometry*. 2-6 May, 2006, Quebec City, Canada, (2006) p. poster.

17. Szentmiklósi, L., Z. Révay, and T. Belgya. *Recent improvements in methodology at the Budapest PGAA facility.* in *BNC ISAC Meeting*. Budapest, (2006) p.

18. Szentmiklósi, L., Z. Révay, and T. Belgya. *Besugárzás utáni számlálás: a PGAA kiegészítő módszere.* in Őszi Radiokémiai Napok. Siófok, (2006) p.

19. Szentmiklósi, L., *Időfüggő folyamatok alkalmazása a prompt-gamma aktivációs analízisben*, Budapesti Műszaki és Gazdaságtudományi Egyetem, (2006)

20. Rogante, M., F. Milazzo, and Z. Kasztovszky. *Comparative analysis of Iron Age bronze archaeological objects from a Picenum necropolis of Centre Italy with Prompt Gamma Activation Analysis.* in *Research Infrastructures for Cultural Heritage*. Italy, (2006) p.

21. Révay, Z., T. Belgya, Z. Kasztovszky, L. Szentmiklósi, and K. Gméling. *Prompt gamma aktivációs analízis és alkalmazásai.* in *Analitikai Ankét*. Budapest, (2006) p.

22. Revay, Z., *Prompt gamma activation analyisis at Budapest*, CNEA, (2006), p.

23. Revay, Z., *Prompt gamma activation analysis and its applications atBudapest.*, Texas University, (2006), p.

24. Revay, Z., *Analytical data library for prompt gamma activation analysis*, Lawrence Livermore National Laboratory, (2006), p.

25. Revay, Z. *Prompt Gamma Activation Analysis of samples in thick containers*. in *Methods and applications of radioanalytical chemistry (MARC VII)*. Kona, USA, (2006) p.

26. Perry, D.L., G.A. English, R.B. Firestone, J.P. Reijonen, K.-N. Leung, G.F. Garabedian, G.L. Molnar, and Z. Revay. *CHARACTERIZATION OF LEGACY MATERIALS BY PROMPT GAMMA ACTIVATION ANALYSIS (PGAA) AND SHORT-LIVED NEUTRON ACTIVATION ANALYSIS*. in *Methods and applications of radioanalytical chemistry (MARC VII)*. Kona, USA, (2006) p.

27. Németh, K., Z. Pécskay, U. Martin, K. Gméling, F. Molnár, and S. Cronin. *Peperites and soft sediment deformation textures of a shallow subaqueous Miocene rhyolitic cryptodome and dyke complex,*, (2006) p.

28. Kasztovszky, Z., D. Visser, W. Kockelmann, E. Pantos, A. Brown, M. Blaauw, P. Hallebeek, J. Veerkamp, W. Krook, and H.M. Stuchfield. *Combined Prompt Gamma Activation And Neutron Diffraction Analyses Of Historic Metal Objects And Limestone Samples*. in *Research Infrastructures for Cultural Heritage Worksop*. Italy, (2006) p.

29. Kasztovszky, Z. and K.T. Biró. *Fingerprinting carpathian obsidians by PGAA, first results on geological and archaeological specimens*. in *34th International Symposium on Archaeometry*. Zaragoza, (2006) p. 301-308.

30. Gméling, K., Z. Pécskay, A. Simonits, and E. Panczyk. *Variation of boron content through time and space in Miocene volcanic rocks of the Tokaj Mts (Hungary*. in *International Conference Neogene Magmatism of the Central Aegean and Adjacent Areas: Petrology, Tectonics, Geodynamics, Mineral Resources and Environment, (NECAM 2006)*. Greece, (2006) p.

31. Gméling, K., S. Harangi, and Z. Kasztovszky. *Boron variation in the South-Eastern Segments of the Neogene Carpathian-Pannonian volcanic area*. in *International Conference Neogene Magmatism of the Central Aegean and Adjacent Areas: Petrology, Tectonics, Geodynamics, Mineral Resources and Environment, (NECAM 2006)*. Greece, (2006) p.

32. Belgya, T., Z. Revay, and L. Szentmiklosi. Determination of Thermal Neutron Capture Cross Sections Using Cold Neutron Beams at the Budapest PGAA and NIPS Facilities. in 12th International Symposium on Capture Gamma-Ray Spectroscopy and Related Topics. September 4-9, 2005 University of Notre Dame, Indiana, USA: AIP Melville, New York, (2006) p. 300-306.

33. Belgya, T. and P. Schillebeeckx. *Cold neutron capture in the lead region*. in *American Chemical Society 231 meeting, Contemporary Frontiers in Nuclear Structure*. 26-30, March, 2006, Atlanta, Georgia, USA, (2006) p. Invited talk.

34. Belgya, T. and K. Lázár. *First experiments on a new in-beam Mössbauer spectroscopy station at the Budapest Research Reactor*. in *Seventh Int. Conf Methods and Applications of Radioanalytical Chemistry*. Kaliua-Kona, Hawai'i, USA, (2006) p. Poster.

35. Belgya, T. and Z. Kasztovszky, *Half thickness for gamma radiation and for thermal neutrons in various materials*, (2006) p. 1-18.

36. Belgya, T. *Determination of thermal neutron capture cross sections using cold neutron beams at the Budapest PGAA-NIPS facilities*. in *Workshop On Nuclear Data Evaluation for Reactor applications organized by CEA and NEA*. CEA Cadarache Château, France, 9 – 11 October, 2006, (2006) p. talk.

37. Belgya, T. *ANCIENT CHARM WP2, Progress Report*. in *2nd Ancient Charm meeting*. 26-28 April 2006, Villa Mondragone, Rome, Italy, (2006) p. talk.

38. Belgya, T. *First year plan for ACIENT CHARM*. in *ANCIENT CHARM Kick-off meeting*. 20-21 January 2006 Milton Hill Hotel, Abingdon, Oxfordshire, UK, (2006) p. talk.

39. Belgya, T. *Institute of Isotopes, HAS, Research and Development Present and Future Collaborations with EC JRC*. in *ROUND TABLE: Promoting collaboration between the JRC and Hungarian organisations in Science and Technology-related areas*. 10, March, 2006, Budapest, Hungary, (2006) p. Seminar.

40. Belgya, T. *Determination of thermal neutron capture cross sections using cold neutron beams*. 13, April, 2006, 88-inch Cyclotron, Berkeley, California, USA, (2006) p. Seminar.

41. Belgya, T. *Research at the PGAA-NIPS Facility of the Budapest Research Reactor*. 11, April, 2006, Lawrence Livermore Nat. Lab., Livermore, California , USA, (2006) p. Seminar.

42. Belgya, T. *New gamma-ray intensities for the 14N(n,g)15N high energy standard and its influence on PGAA and on nuclear quantities*. in *Seventh Int. Conf Methods and Applications of Radioanalytical Chemistry*. 3-7, April, 2006, Kaliua-Kona, Hawai'i, USA, (2006) p. Poster.

43.   Weil, J.L., T. Belgya, and H.-F. Wirth. The 99Tc(n,g)100Tc cross section, 99Tc(d,p)100Tc and the 100Tc decay scheme and neutron binding energy. in International Conference on Nuclear Data for Science and Technology. Niza, France, 2007: EDP Sciences, (2008) p. 611-614.

44.   Révay, Z., T. Belgya, and R.B. Firestone. Determination of Thermal Neutron Capture Cross-sections at Budapest PGAA Facility. in VII. Latin American Symposium on Nuclear Physics and Applications. Cusco, Peru: AIP, Conf. Proc., (2007) p. 445-448.

45.   Visser, D., Z. Kasztovszky, J. Blair, J. Bayliss, M.H. Stuchfield, and S. Badham. *Non-destructive element analyis of medieval English brass letters*. in *37th International Symposium on Archaeometry*. Siena, Italy, 12-16 May 2008, (2008) p. Poster.

46.   Tari, E., V. Kulcsár, D. Mérai, R. Patay, K. Bodnár, E. Horváth, J. Kalmár, A. Kőrösi, F. Molnár, N. B., S. Pánczél, B. Péterdi, and V. Szilágyi. *Pressed towards new approaches: A Late Sarmatian pottery centre at Üllő (M0)*. in *36th Annual Conference on Computer Applications and Quantitative Methods in Archaeology – On the Road to Reconstructing the Past*. Budapest, Hungary, 2-6 April 2008, (2008) p. Talk.

47.   Szilágyi, V., H. Taubald, K. T. Biró, P. Csengeri, J. S. Koós, M. Tóth, and G. Szakmány. *Bükk pottery - Master craftsmen of the Stone Age*. in *37th International Symposium on Archaeometry*. Siena, Italy, 12-16 May 2008, (2008) p. Poster.

48.   Szilágyi, V., H. Taubald, K. T. Biró, P. Csengeri, J. S. Koós, M. Tóth, and G. Szakmány. *Bükki kerámia – A kőkorszak mestereinek műalkotása*. in *Archeometriai Műhely* Magyar Nemzeti Múzeum, Budapest, Hungary, 3. Nov. 2008, (2008) p. Talk.

49.   Szilágyi, V., G. Szakmány, T. Heinrich, M. Balla, and Z. Kasztovszky. *Az eredetazonosítás lehetőségei módosított természetes üledékekben (régészeti kerámiákban) műszeres geokémiai módszerekkel (INAA, PGAA, XRF)* in Őszi Radiokémiai Napok. Hajdúszoboszló, Hungary, 2008. október 29-31, (2008) p. Talk.

50.   Szilágyi, V., G. Szakmány, J. Gyarmati, and M. Tóth. *A geokémiai értelmezés jelentősége a régészeti kerámiák eredetvizsgálatában – bolíviai inka korú leletek alapján*. in „A geokémiai interpretáció jelentősége az archeometriai kutatásban" c. előadói nap. Budapest, Hungary, 19 Nov. 2008, (2008) p. Talk.

51.   Szentmiklósi, L., Z. Kis, T. Belgya, Z. Kasztovszky, P. Kudejová, T. Materna, and R. Schulze. *A new PGAI-NT setup and elemental imaging experiments at the Budapest Research Reactor*. in *NRC7 - Seventh International Conference on Nuclear and Radiochemistry*. Budapest, Hungary, 24-29 Aug. 2008, (2008) p. Talk.

52.   Szentmiklosi, L., T. Belgya, Z. Révay, and Z. Kis. *Fejlesztések a Budapesti PGAA-NIPS berendezésen 2006-2008*. in Őszi Radiokémiai Napok. Hajdúszoboszló, Hungary, 29-31 Oct. 2008, (2008) p. Talk.

53.   Schnabel, C., K. Wilcken, K. Gméling, L. DiNicola, S. Freeman, and F.M. Stuart. *Determination of chlorine concentrations in carbonate and whole rock samples with prompt-gamma activation analysis (PGAA) and isotope dilution AMS*. in *The 11th International Conference on Accelerator Mass Spectrometry*. Rome, Italy, 14-19 Sept. 2008, (2008) p. Poster.

54.   Révay, Z. *In situ prompt gamma aktivációs analízis MTA – doktori értekezés elővédése*. in Őszi Radiokémiai Napok. Hajdúszoboszló, Hungary, 29-31 Oct. 2008, (2008) p. Talk.

55.   Péterdi, B., G. Szakmány, K. Judik, G. Dobosi, and Z. Kasztovszky. *Petrographical and geochemical investigation of grinding stones from Üllő 5. site, Pest County, Hungary*. in *37th International Symposium on Archaeometry*. Siena, Italy, 12-16 May 2008, (2008) p. Poster.

56.   Pantos, M., K. Exell, W. Kockelmann, Z. Kasztovszky, M. Morlidge, M. Ellis, and B. Bilsborrow. *Mineralogical characterisation of limestone from the Great Pyramids and limestone quarries along the Nile*. in *X International Congress of Egyptologists*. Rhodes, Greece, 22-29 May 2008, (2008) p. talk.

57.   Pantos, M., K. Exell, W. Kockelmann, Z. Kasztovszky, M. Morlidge, M. Ellis, and B. Bilsborrow. *Mineralogical characterisation of limestone from the Great Pyramids and limestone quarries along the Nile*. in *Synchrotron Radiation in Art and Archaeology*. Barcelona, Spain, 22-24 October 2008, (2008) p. talk.

58.   Massaferro, G.I., K. Gméling, N. Németh, and M.J. Haller. *First Boron systematics approach in the Cenozoic extra-Andean basaltic volcanism in Patagonia*. in *XVII Argentine Geological Congress*. San Salvador de Jujuy, 7-10 October 2008, (2008) p. Poster.

59.   Kocsonya, A., A. Váradi, I. Fórizs, I. Kovács, Z. Kasztovszky, and Z. Szőkefalvi-Nagy. *Colourants and their provenance of a late medieval glass goblet found in Eger (Hungary)* in *37th International Symposium on Archaeometry, 12-16 May 2008*. Siena, Italy, (2008) p. Poster.

60.   Kocsonya, A., A. Váradi, I. Fórizs, I. Kovács, Z. Kasztovszky, and Z. Szõkefalvi-Nagy. *Mit árulnak el a színezõanyagok egy mûtárgy eredetérõl? Egy késõközépkori üvegkehely mûszeres analitikai vizsgálata* in

Archeometriai Műhely. Magyar Nemzeti Múzeum, Budapest, Hungary, 3 Nov. 2008, (2008) p. Talk.

61.   Kis, Z., L. Szentmiklosi, T. Belgya, Z. Kasztovszky, W. Kockelmann, G. Festa, A. Kirfel, P. Kudejova, R. Schulze, K. T. Biró, K. Dúzs, Z. Hajnal, and D. Visser. "FEKETE DOBOZOK" RADIOGRÁFIÁVAL KOMBINÁLT PGAA ÉS NEUTRONDIFFRAKCIÓS MÉRÉSEI AZ ANCIENT CHARM PROJEKT KERE-TÉBEN. in *Archeometriai Műhely*. Magyar Nemzeti Múzeum, Budapest, Hungary, 3 Nov. 2008, (2008) p. Talk.

62.   Kis, Z., L. Szentmiklosi, T. Belgya, and Z. Kasztovszky. *Műtárgyak roncsolásmentes vizsgálata neutronokkal az EU-Ancient Charm projektben*. in Őszi Radiokémiai Napok. Hajdúszoboszló, Hungary, 29-31 Oct. 2008, (2008) p. Talk.

63.   Kis, Z., T. Belgya, L. Szentmiklósi, Z. Kasztovszky, P. Kudejová, and R. Schulze. *Prompt Gamma Activation Imaging on 'black boxes' in the 'ANCIENT CHARM' project*. in *Archaeometriai Műhely*. Magyar Nemzeti Múzeum, Budapest, 3 Nov. 2008, (2008) p. Talk.

64.   Kasztovszky, Z. and J. Kunicki-Goldfinger. *Applicability of Prompt Gamma Activation Analysis to glass archaeometry*. in *37th International Symposium on Archaeometry, 12-16 May 2008*. Siena, Italy, (2008) p. Poster.

65.   Kasztovszky, Z., K.T. Biró, A. Markó, and V. Dobosi. *Pattintott kőeszközök nyersanyagainak roncsolásmentes vizsgálata prompt gamma aktivációs analízissel* in *A geokémiai interpretáció jelentősége az archeometriai kutatásban c. előadói nap, 19 Nov. 2008*. Budapest, (2008) p. Talk.

66.   Kasztovszky, Z., K.T. Biró, and K. Gherdán. *Application of PGAA To Investigate Archaeological Pottery*. in *3rd RCM for IAEA CRP on "Applications of nuclear analytical techniques to investigate the authenticity of art objects", 2008, Nov 3-7*. Cuzco, Peru, (2008) p. Talk.

67.   Kasztovszky, Z. *Prompt Gamma Activation Analysis at the Budapest Research Reactor – methodology and applications in archaeometry, geology and materials sciences* in *Italian-Hungarian TéT, 16 September 2008*. Genova, Italy, (2008) p. Talk.

68.   Kasztovszky, Z. *How can Prompt Gamma Activation Analysis help in characterisation of chipped stone artefacts? – Horvát-Magyar TéT*. in *Archeometria Műhely, 30 May 2008*. Hungarian National Museum, Budapest, (2008) p. Talk.

69.   Gméling, K., Z. Pécskay, and K. Birkenmajer. *Boron in hypabyssal andesite intrusions, Pieniny Mts., West Carpathians, Poland*. in *IAVCEI 2008 Congress*. Reykjavik, Iceland, 17-22 Aug. 2008, (2008) p. Talk.

70.   Gméling, K., S. Harangi, and Z. Kasztovszky. *A bór geokémiai szerepe szubdukciós zónákban*. in *Erdélyi Magyar Műszaki Tudományos Társaság, Bányászati, Kohászati és Földtani Konferencia*. Nagyszeben, Románia, 3-6 April 2008, (2008) p. talk.

71.   Gherdán, K., V. Szilágyi, and Z. Kasztovszky, *An example of archaeometrical usage of Prompt Gamma Activation Analysis: chemical characterization of Early Bronze Age pottery from two archaeological sites of Vörs, Western Hungary*, in *7th International Conference on Nuclear and Radiochemistry*: Budapest, Hungary, 24-29 August 2008, (2008) p. Poster.

72.   Friedel, O., B. Bradák, G. Szakmány, V. Szilágyi, and K. T. Biró. *Archaeometrical processing of polished stone artefacts of the Ebenhöch-collection (Hungarian NAtional Museum, Budapest, Hungary)*. in *37th International Symposium on Archaeometry*. Siena, Italy, 12-16 May 2008, (2008) p. Poster.

73.   Crandell, O.N. and Z. Kasztovszky. *The use of PGAA to aid in distinguishing between sources of jasper*. in *37th International Symposium on Archaeometry*. Siena, Italy, 12-16 May 2008, (2008) p. Poster.

74.   Belgya, T., E. Uberseder, D. Petrich, and F. Käppeler. *Thermal neutron capture cross section of 22Ne*. in *13th Int. Symp. on Capture Gamma-Ray Spectroscopy and Relatrd Topics*. Cologne, Germany, 25-29 August 2008, (2008) p. talk.

75.   Belgya, T., Z. Kis, L. Szentmiklosi, Z. Révay, Z. Kasztovszky, P. Kudejova, R. Schulze, and J. Jolie. *Együttműködés az FRM-II PGAA csoportjával*. in Őszi Radiokémiai Napok. Hajdúszoboszló, Hungary, 29-31 Oct. 2008, (2008) p. Talk.

76.   Belgya, T., Z. Kasztovszky, and Z. Révay. *Archaeometry research with PGAA at the Budapest Research Reactor*. in *6th International Conference on Isotopes (6ICI)*. Seoul, Korea, 12-16 May 2008, (2008) p. Invited talk.

77.   Belgya, T., Z. Kasztovszky, Z. Kis, L. Szentmiklósi, W. Kockelmann, G. Festa, A. Kirfel, P. Kudejová, R. Schulze, K. T. Biró, K. Dúzs, Z. Hajnal, and D. Visser. *Radiography driven Prompt Gamma Activation Analysis and Neutron Diffraction measurements on Black Boxes designed for the 'Ancient Charm' Project*. in *37th International Symposium on Archaeometry*. Siena, Italy, 12-16 May 2008, (2008) p. Poster.

78.   Belgya, T., Z. Kasztovszky, Z. Kis, and L. Szentmiklósi. *Műtárgyak roncsolásmentes vizsgálata neutronokkal – az EU-Ancient Charm projekt*. in *XXXIII. Nemzetközi Restaurátor Konferencia*. Budapest, Hungary, 8-11 April 2008, (2008) p. talk.

79.   Belgya, T. *Research at the Budapest PGAA-NIPS facilities*. in *Hanaro Reactor*. Dageon city, Korea, 14 May 2008, (2008) p. Seminar.

80.   Astalos, C. and Z. Kasztovszky. *Prompt gamma activation analysis on stone tools and geological raw materials from North-western Romania* in *37th International Symposium on Archaeometry,12-16 May 2008*. Siena, Italy, (2008) p. Poster.

81.   Weil, J.L., T. Belgya, and H. Wirth. *100Tc decay scheme and the 99Tc(n,g)100Tc capture cross section*. in *International Conference on Nuclear Data for Science and Technology*. Nice, France, 22-27 April, 2007: AIP Conference series, (2007) p. in print.

82.   Szentmiklósi, L., Z. Révay, T. Belgya, A. Simonits, and K. Gméling. *Neutronos elemanalitikai módszerek: mit tanulhatunk egymástól?* in *MKE Centenáriumi Vegyészkonferencia*. Sopron, (2007) p.

83.   Szentmiklósi, L., Z. Révay, T. Belgya, and A. Simonits. *Combining PGAA and off-line counting to lower the detection limits*. in *12th International Conference Modern Trends in Activation Analysis*. Tokyo, Japan, 16-21 Sept. 2007, (2007) p. Poster.

84.   Révay, Z., T. Belgya, L. Szentmiklosi, Z. Kasztovszky, K. Gméling, Z. Kis, and R.B. Firestone. *Recent developments and applications at the prompt gamma activation analysis facility at Budapest*. in *12th International Conference Modern Trends in Activation Analysis*. Tokyo, Japan, 16-21 Sept. 2007, (2007) p. Invited talk.

85.   Kasztovszky, Z., K. T. Biró, A. Markó, and V. Dobosi. *Prompt Gamma Activation Analysis for non-destructive characterisation of chipped stone tools and raw materials*. in *12th International Conference Modern Trends in Activation Analysis*. Tokyo, Japan, 16-21 Sept. 2007, (2007) p. poster.

86.   Kasztovszky, Z., K. T. Biró, and K. Gherdán. *Régészeti kerámiák vizsgálata prompt gamma aktivációs analízissel*. in *Archeometria Műhely*. Nemzeti Múzeum, Budapest, 2007 márc. 7, (2007) p. előadás.

87.   Kasztovszky, Z., Z. Kis, T. Belgya, W. Kockelmann, G. Festa, A. Filabozzi, C. Andreani, A. Kirfel, K.T. Biró, K. Dús, Z. Hajnal, P. Kudejova, and A.C. Collaboration. *Prompt gamma activation analysis and time of flight neutron diffraction on 'black boxes' in the 'ancient charm' project*. in *12th International Conference Modern Trends in Activation Analysis*. Tokyo, Japan, 16-21 Sept. 2007, (2007) p. Poster.

88.   Gméling, K., S. Harangi, Z. Kasztovszky, and P. Z. *Inferences for the style of subduction in the Carpathian-Pannonian region based on boron signatures*. in *Geochim. Cosmochim. Acta, Goldschmidt Conference Abstract, Volume 71, 15, Supplement , A331 (absztrakt-poszter)*: Geochim. Cosmochim. Acta, Goldschmidt Conference Abstract, Supplement, (2007) p. A331, poster.

89.   Belgya, T., Z. Kis, L. Szentmiklosi, Z. Kasztovszky, P. Kudejová, R. Schulze, T. Materna, G. Festa, P.A. Caroppi, and A.C. Collaboration. *First elemental imaging experiments on a combined PGAI and NT setup at the Budapest research reactor*. in *12th International Conference Modern Trends in Activation Analysis*. Tokyo, Japan, 16-21 Sept. 2007, (2007) p. talk.

90.   Belgya, T., Z. Kis, L. Szentmiklosi, Z. Kasztovszky, G. Festa, L. Andreanelli, M.P. De Pascale, A. Pietropaolo, P. Kudejová, R. Schulze, T. Materna, E.P. Cippo, and A.C. Collaboration. *A new PGAI and NT setup at the NIPS facility of the Budapest research reactor*. in *12th International Conference Modern Trends in Activation Analysis*. Tokyo, Japan, 16-21 Sept. 2007, (2007) p. Poster.

91.   Belgya, T., O. Bouland, G. Noguere, A. Plompen, P. Schillebeeckx, and L. Szentmiklósi. *The thermal neutron capture cross section of 129I*. in *International Conference on Nuclear Data for Science and Technology*. Nice, France, 22-27 April, 2007: AIP Conference series, (2007) p. in print.

92.   Füzi J; Vector hysteresis model for magnetic field computation; In: *Proceedings CD, 12th IGTE Symposium on Numerical Field Calculation in Electrical Engineering, Graz, Austria;* Ed: Bíró O; 513-518, 2006

93.   Füzi J; Ferroresonant circuit simulation with dynamic hysteresis model; In: *Proceedings CD, 12th IGTE Symposium on Numerical Field Calculation in Electrical Engineering, Graz, Austria;* Ed: Bíró O; 75-78, 2006

94.   Füzi J; Vector Hysteresis model based on micromagnetic analogy; In: *Proceedings CD, 12th IGTE Symposium on Numerical Field Calculation in Electrical Engineering, Graz, Austria;* Ed: Bíró O; 69-74, 2006

95.   Heaton* ME, Rogante* M, Len A; A feasibility study for a SANS investigation of a heat cured and laser machined organic resin microturbine as used for airflow sensing; In: *Proceedings of the International Conference on Materials-Energy-Design*; MED06 Dublin, Institute of Technology, Ireland, 2006

Books, Book chapters

1.   Temleitner L, Pusztai L; Investigation of the structural disorder in ice Ih using neutron diffraction and Reverse Monte Carlo modelling; Physics and Chemistry of Ice; Ed. W. F. Kuhs (Royal Society of Chemistry Publishing, Cambridge, UK); pp. 593-600, 2007

Cser L, Study of upgrading of the small angle neutron scattering device at the research reactor of the ITN nuclear and technological institute, *IAEA-TECDOC;* **1486**, 39-52, 2006

Defended PhD Theses

1.   Szentmiklósi L., *Időfüggő folyamatok alkalmazása a prompt gamma aktivációs analízisben*, Budapesti Műszaki és Gazdaságtudományi Egyetem, (2006)